UNIVERSITY OF Southampton

University of Southampton Research Repository
ePrints Soton

Copyright © and Moral Rights for this thesis are retained by the author and/or other copyright owners. A copy can be downloaded for personal non-commercial research or study, without prior permission or charge. This thesis cannot be reproduced or quoted extensively from without first obtaining permission in writing from the copyright holder/s. The content must not be changed in any way or sold commercially in any format or medium without the formal permission of the copyright holders.

When referring to this work, full bibliographic details including the author, title, awarding institution and date of the thesis must be given e.g.

AUTHOR (year of submission) "Full thesis title", University of Southampton, name of the University School or Department, PhD Thesis, pagination

http://eprints.soton.ac.uk

UNIVERSITY OF SOUTHAMPTON

FACULTY OF MEDICINE, HEALTH AND LIFE SCIENCES

School of Biological Sciences

DECONTAMINATION OF PRIONS, PRION-ASSOCIATED AMYLOID AND INFECTIVITY FROM SURGICAL STAINLESS STEEL – IMPLICATIONS FOR THE RISK OF IATROGENIC TRANSMISSION OF CJD

By

ROBERT HOWLIN

Thesis submitted for the degree of Doctor of Philosophy

September 2009

ABSTRACT

FACULTY OF MEDICINE, HEALTH AND LIFE SCIENCES

SCHOOL OF BIOLOGICAL SCIENCES

Doctor of Philosophy

DECONTAMINATION OF PRIONS, PRION-ASSOCIATED AMYLOID AND INFECTIVITY FROM SURGICAL STAINLESS STEEL – IMPLICATIONS FOR THE RISK OF IATROGENIC TRANSMISSION OF CJD

By Robert Howlin

The physicochemical nature of the infectious agent in prion diseases creates a significant challenge for decontamination services. It has been shown to be both resistant to standard methods of decontamination, used to inactivate viruses and bacteria, and to associate avidly with surgical stainless steel. Moreover, the pathophysiology of the variant, iatrogenic and sporadic forms of Creutzfeldt-Jakob Disease (CJD) suggests deposition of the infectious agent across a wide range of extraneural, lymphoid tissues, as well as in the skeletal muscle and blood. Coupled with the potential for asymptomatic carriers, there is a significant risk of iatrogenic transmission of CJD through both neurosurgical procedures and standard surgery.

This PhD study was undertaken in order to improve methods of instrument decontamination and to evaluate prion detection techniques and their applicability for the assessment of prion inactivation and removal. The project has provided relevant, critical assessment of hospital decontamination procedures, in addition to guidance on how working protocols should be improved to provide a cleaner and safer end product for the patient. Moreover, laboratory studies have been performed to evaluate current methods of prion decontamination in the context of hospital procedures for instrument reprocessing. Challenges faced by sterile service departments, such as soil drying and surface degradation, have been addressed and their impact on the risk of iatrogenic transmission of prions has been investigated. Critically, the use of a fluorescent amyloid fluorophore for the detection of prion-associated amyloid as a marker for disease permitted the investigation of the role of amyloid in infectious disease under denaturing conditions. Correlation of this detection technique with the identification of PrP^{res} by Western blot and infectious disease suggested that, whilst fluorescent detection of prion-associated amyloid was more sensitive than Western blot, PrP^{res} detection was more specific relative to infectivity. Improved fluorophores, with greater sensitivity, have been evaluated which will enhance *in situ* detection of prions in the future.

LIST OF CONTENTS

FIGURES AND TABLES

FIGURES

TABLES

DECLARATION OF AUTHORSHIP

I, …ROBERT HOWLIN…..,

declare that the thesis entitled

DECONTAMINATION OF PRIONS, PRION-ASSOCIATED AMYLOID AND INFECTIVITY FROM SURGICAL STAINLESS STEEL – IMPLICATIONS FOR THE RISK OF IATROGENIC TRANSMISSION OF CJD.

and the work presented in the thesis are both my own, and have been generated by me as the result of my own original research. I confirm that:

- this work was done wholly or mainly while in candidature for a research degree at this University;
- where any part of this thesis has previously been submitted for a degree or any other qualification at this University or any other institution, this has been clearly stated;
- where I have consulted the published work of others, this is always clearly attributed;
- where I have quoted from the work of others, the source is always given. With the exception of such quotations, this thesis is entirely my own work;
- I have acknowledged all main sources of help;
- where the thesis is based on work done by myself jointly with others, I have made clear exactly what was done by others and what I have contributed myself;
- parts of this work have been published as: See Publications List

Signed: …….

Date:……28/09/09…….

ACKNOWLEDGMENTS

Firstly, thanks go to Professor Bill Keevil for his supervision during my PhD. I would also like to thank Dr Nancy Khammo and Dr Gerry McDonnell from STERIS Ltd whose help and guidance throughout the project has been invaluable.

Several sections of this work have been very much collaborative efforts between myself and various people and I can not thank these people enough for their contributions towards this project. The involvement of Dr Guillaume Fichet and Dr Emmanuel Comoy from the CEA and their work, advice and their friendship is very much appreciated. Thanks also go to Dr Jean-Philippe Deslys for his help and eagerness to be involved in meetings regarding this project. I am also grateful for the help and contributions of John Harrison and the SSD staff at The North Hampshire and Basingstoke Hospital towards the instrument work undertaken in this PhD. A great many thanks must go to Dr Ian Lipscomb who was not only invaluable in getting me started in the lab and in the supervision of this project before he left the department, but also his eagerness to contribute towards Chapter 5 and the analysis of wire surface degradation is much appreciated. I also wish to thank Dr Ganesan, Dr Franks and Chris Ryan for synthesising the thiazole analogues and giving me access to them for my work.

A great many thanks are also due to everyone, both past and present, at the EHU for making it such an enjoyable and friendly place to work. Special thanks go to Kate Harris, Becky Collin, Hannah Pinchin and Arinder Sihota for being my volunteers in several of the experiments and Dr Sandra Wilks for her running of the lab and willingness to help no matter how busy she is. Thanks also to Jenny Warner for her help and friendship throughout both of our projects. Many thanks also to Dr Jeremy Webb, Dr Luanne Hall-Stoodley and Dr Saul Faust for their support during the write up.

Ultimately, all my gratitude and appreciation goes to my friends (both now scattered around the UK and in Southampton) and my family, especially my mum, dad and brother for their love and encouragement. This work is dedicated to them and to Anastasia whose help, love and support over the last few years has been immense. Thank you.

This work was funded by the BBSRC (BBS/S/M/2005/12416) and STERIS Ltd.

PUBLICATIONS

Howlin, R. P., Harrison, J., McDonnell, G. & Keevil, C. W. (2008). What's on your device? *Medical Device Decontamination* **12**, 16-21.

Storr, M., Harrison, J., **Howlin, R. P**., & Keevil, C. W. (2008). Oils well that ends well. *The Clinical Services Journal* **7**, 66-68.

Howlin, R. P., Harrison, J., Secker, T. & Keevil, C. W. (2009). Acquisition of proteinaceous contamination through the handling of surgical instruments by hospital staff in sterile service departments. *Journal of Infection Prevention* **10**, 106-111.

Howlin, R. P., Khammo, N., Secker, T., McDonnell, G. & Keevil, C. W. (2010). Application of a fluorescent dual stain to assess decontamination of tissue protein and prion amyloid from surgical stainless steel during simulated washer-disinfector cycles. *Journal of Hospital Infection*. In Press.

Howlin, R. P., Fichet, G., Comoy, E., Deslys, J. P., McDonnell, G. & Keevil, C. W. (2010). Comparison of *in vitro* and *in vivo* methods of detecting prion infectivity. *Journal of Microbiological Methods*. Submitted.

LIST OF ABBREVIATIONS

28d	2-(4'-Dimethylaminophenyl)-6-Methyloxybenzothiazole
A/V/T	Alanine/Valine/Threonine
Ab	Antibody
AFM	Atomic Force Microscopy
A/R/R	Alanine/Arginine/Arginine
ARQ	Alanine/Arginine/Glutamine
BASE	Bovine Amyloidotic Spongiform Encephalopathy
BSE	Bovine Spongiform Encephalopathy
BTA-1	2-(4'-Methylaminophenyl) Benzothiazole
cBSE	classical Bovine Spongiform Encephalopathy
CEA	Commissariat à l'Énergie Atomique
CJD	Creutzfeldt-Jakob Disease
CWD	Chronic Wasting Disease
DIC	Differential Interference Contrast Microscopy
DMSO	Dimethyl sulfoxide
DOH	Department of Health
DY	Drowsy (strain of Transmissible Mink Encephalopathy)
EDIC/EF	Episcopic Differential Interference Contrast coupled with Epi-Fluorescent microscopy
EUE	Exotic Ungulate Encephalopathy
FAE	Follicle-Associated Epithelium
fCJD	familial Creutzfeldt Jakob Disease
FDC	Follicular Dendritic Cells
FFI	Fatal Familial Insomnia
FSE	Feline Spongiform Encephalopathy
GALT	Gut-Associated Lymphoid Tissue
GPI	Glycosyl-phosphatidylinositol anchor
GSS	Gerstmann-Sträussler-Scheinker syndrome

HR	Hydrophobic region
Htt	Huntington
HY	Hyper (strain of Transmissible Mink Encephalopathy)
i.c.	Intra-cerebral
i.p.	Intra-peritoneal
iCJD	Iatrogenic Creutzfeldt Jakob Disease
kDa	Kilo daltons
LD_{50}	Lethal dose, 50 %
LRS	Lymphorecticular System
MBM	Meat-and-Bone Meal
MM	Methionine homozygous
mRNA	messenger Ribonucleic Acid
MV	Methionine Valine heterozygous
MW	Molecular weight
NaOCl	Sodium Hypochlorite
NaOH	Sodium Hydroxide
NBH	Non-Infected Brain Homogenate
NHS	National Health Service
NMR	Nuclear Magnetic Resonance
OR	Octapeptide Repeat
PBS	Phosphate Buffered Saline
PET	Positron emission tomography
PK	Proteinase K
PMCA	Protein Misfolding Cyclic Amplification
PRNP	Prion protein gene
PrP^{27-30}	Prion Protein 27-30 fragment
PrP^{c}	cellular Prion Protein
PrP^{res}	Pathological conformer of the prion protein
R/H/L	Arginine/Histidine/Leucine
R/H/Q/K	Arginine/Histidine/Glutamine/Lysine
Rec.MoPrP	Recombinant Mouse Prion Protein
SAF	Scrapie Associated Fibrils

sCJD	sporadic Creutzfeldt Jakob Disease
SEAC	Spongiform Encephalopathy Advisory Committee
sFI	sporadic Fatal Insomnia
SSD	Sterile Service Department
ThT	Thioflavin T
TME	Transmissible Mink Encephalopathy
TSE	Transmissible Spongiform Encephalopathy
UK	United Kingdom
vCJD	variant Creutzfeldt Jakob Disease
VHP	Vaporised Hydrogen Peroxide
VRQ	Valine/Arginine/Glutamine
VV	Valine Valine homozygous

CHAPTER 1

INTRODUCTION TO PRION DISEASES

1.1. INTRODUCTION

Transmissible spongiform encephalopathies (TSEs) or prion diseases are a collection of severe and uniformly terminal neurodegenerative disorders affecting many mammalian species (Table 1). The central concept behind prion disease propagation and pathogenesis is the posttranslational conversion of the normal, host encoded cellular protein, PrP^{c}, to an abnormal isoform PrP^{res} as set out by the protein-only hypothesis (Prusiner, 1982; Prusiner, 1998). This transition involves conformational changes in the absence of covalent modification, conferring PrP^{res} with partial resistance to proteolytic degradation and detergent insolubility (McKinley *et al.*, 1983; Weissmann, 2004). The protein-only hypothesis states that it is the pathological conformer PrP^{res}, devoid of nucleic acid, that is responsible for and potentially the sole component of transmissible disease.

1.2. THE PRIONOPATHIES AND THEIR EPIDEMIOLOGY

Although relatively rare when compared to neurological disorders such as Alzheimer's and Parkinson's disease, Creutzfeldt-Jakob disease (CJD) is the most common human TSE (Prusiner, 1998). Aetiologically, human prion diseases can be grouped into three categories: sporadic, acquired and inherited (Collinge, 1999). The majority of cases (~ 85 %) are sporadic, with sporadic CJD the most prevelant. Countries carrying out surveillance report a $0.6 – 1.2 \times 10^{6}$ incidence rate, with equal occurrence in males and females (Ladogana *et al.*, 2005). Cases with a genetic predisposition, inherited as an autosomal dominant trait, such as fatal familial insomnia (FFI) or familial CJD (fCJD) account for around 15 % of the total reported cases. Acquired cases, including kuru, variant and iatrogenic forms of CJD (vCJD and iCJD, respectively) are thought to be relatively infrequent in the general population (Wadsworth *et al.*, 2008a).

Sporadic CJD was the first classified prionopathy. Described in 1921 by German neurologists Hans Gerhard Creutzfeldt and Alfons Maria Jakob, they reported the case of a 22 year old woman presenting with dementia, tremors, spasticity, ataxia and possibly myoclonus (Belay, 1999). To this date the aetiology of sCJD remains unclear with no exogenous or endogenous causes identified.

Table 1 Prion diseases in mammals

Prion Disease*	Host	Mechanism of pathogenesis	Year recognised
Kuru	Humans (Forè people)	Infectious; consumption of prion-contaminated tissue during ritualistic cannibalism	1957
sCJD	Humans	Unknown; Spontaneous conversion of PrP^{c} to PrP^{res}; Somatic mutations	1921
vCJD	Humans	Infectious; Consumption of BSE-infected meat products	1996
fCJD	Humans	Genetic; Heritable mutations in PRNP gene	1924
iCJD	Humans	Infectious; Exposure to prion-contaminated surgical instruments, dura mater grafts, blood transfusion, human growth hormone therapy	1974
PSPr	Humans	Unknown; Infection; Spontaneous; Genetic	2008
FFI	Humans	Genetic; Heritable mutations in PRNP gene	1986
sFI	Humans	Mechanism unclear; somatic mutations or spontaneous conversion of PrP^{c} to PrP^{res}; spontaneous	1997
GSS	Humans	Genetic; Heritable mutations in PRNP gene	1936
Scrapie	Sheep, Goat	Infectious; Ingestion or contact with scrapie-infected animals, secretions or tissues from infected animals or contaminated environment	1732
Atypical scrapie	Sheep, Goat	Unknown; Spontaneous	1998
BSE	Cattle	Infectious; Consumption of prion-infected feed	1985
Atypical BSE	Cattle	Unknown; Spontaneous	2004
CWD	Deer, Moose, Elk	Unknown; Infectious; Spontaneous; Contact or ingestion of CWD-infected secretions	1967
FSE	Cat, Ocelot, Cheetah, Lion Asiatic golden cat, Tiger, Puma	Infectious; Consumption of BSE-infected feed	1990
EUE	Kudu, Gemsbok. Nyala, Oryx, Eland	Infectious; Consumption of BSE-infected tissue	1986
TME	Mink	Infectious; Consumption of prion-infected feed	1965

*sCJD, vCJD, fCJD & iCJD (sporadic, variant, familial & iatrogenic Creutzfeldt-Jakob disease respectively); PSPr (Proteinase Sensitive Prionopathy); FFI (fatal familial insomnia); sFI (sporadic fatal insomnia); GSS (Gerstmann-Sträussler-Scheinker syndrome); BSE (bovine spongiform encephalopathy); CWD (chronic wasting disease); FSE (feline spongiform encephalopathy); EUE (exotic ungulate encephalopathy); TME (transmissible mink encephalopathy).

Kuru represents the only human epidemic of a prionopathy to date. The disease was isolated within the Forè linguistic group of the Eastern Highlands of Papua New Guinea and, to a lesser extent, neighbouring tribal groups into which the Forè intermarried (Gajdusek & Zigas, 1957; Will, 2003). Molecular and neuropathological data from transmission studies suggest that kuru originated from the chance transumption of an individual with sCJD and was propagated through cannibalistic mortuary feasts, undertaken as a mark of respect and mourning (Wadsworth *et al.*, 2008b; Whitfield *et al.*, 2008). In mortuary rituals, the consumption of internal organs, including the brain, was undertaken by the women and children but rarely by males older than six or eight, which would explain the grouping of disease primarily in the young tribal women and children (Whitfield *et al.*, 2008). In excess of 2,700 cases of kuru have been identified since 1957 within a total population of 36,000 people (Will, 2003). There is no evidence of vertical transmission of disease as children born after the cessation of endocannibalism in 1956 and those born after 1959 to mothers incubating the disease were unaffected (Collinge *et al.*, 2006).

Kuru represented the first demonstration of the transmission of a prionopathy by the oral route but was not the last (Gajdusek *et al.*, 1966; Gajdusek *et al.*, 1967). The large-scale epidemic of bovine spongiform encephalopathy (BSE) throughout the United Kingdom in the late eighties and nineties cost the British government four billion pounds. An estimated 180,000 cattle were confirmed as carriers of the disease and slaughtered, with a further one to three million likely to have been infected but destroyed before showing symptoms (Smith & Bradley, 2003). The peak of the outbreak came in 1992 when 37,280 cases were confirmed and others documented in twenty four countries worldwide (data from World Organisation for Animal Health). The initial cause of the BSE epidemic is unknown but was propagated in British cattle by the use of BSE-contaminated meat-and-bone meal (MBM), a high protein supplement feed produced by the rendering of waste material from mixed species. The termination of MBM feed in cattle farming had a dramatic effect on the rate of BSE incidence suggesting that, unlike scrapie which is endemic in UK herds, BSE transmission does not occur horizontally.

As a result of the noted similarity of neuropathological lesions in BSE and scrapie several hypotheses suggest that BSE arose from the survival of scrapie or BSE-adapted scrapie to the MBM rendering process, although studies have demonstrated inactivation of the infectious agent in BSE and scrapie under rendering procedures (Taylor *et al.*, 1995; Taylor *et al.*, 1997; Wells *et al.*, 1987). Moreover, whilst transmission of BSE to sheep has been successful through oral challenge, the BSE strain is biologically and molecularly distinct from

scrapie strains (Bruce, 2003; Foster *et al.*, 1994). In addition, under the confines of this hypothesis, it is unclear why BSE did not present in UK cattle prior to 1985 given that MBM has been used in cattle farming since the 1920s and that scrapie has been endemic in the UK over several hundred years. However, it has been noted that, in addition to the expansion of the UK sheep population, which may have increased the general incidence of scrapie, rendering procedures had been altered in the late 1970s and early 1980s, corresponding with the known incubation period of BSE (~ 5 years) and its emergence in 1985 (Wilesmith *et al.*, 1988; Wilesmith *et al.*, 1991). Alternatively, it is plausible that BSE originated sporadically at an initially low frequency, although there is no direct evidence to support this theory.

In 1996 a new variant form of CJD (vCJD) was classified, confirming BSE as a zoonosis and creating widespread public health concern (Will *et al.*, 1996). Biochemical and histopathological data confirmed that vCJD was manifested in humans as a result of the transmission of BSE prions through consumption of infected meat products (Figure 1) (Bruce *et al.*, 1997; Collinge *et al.*, 1996; Hill *et al.*, 1997).

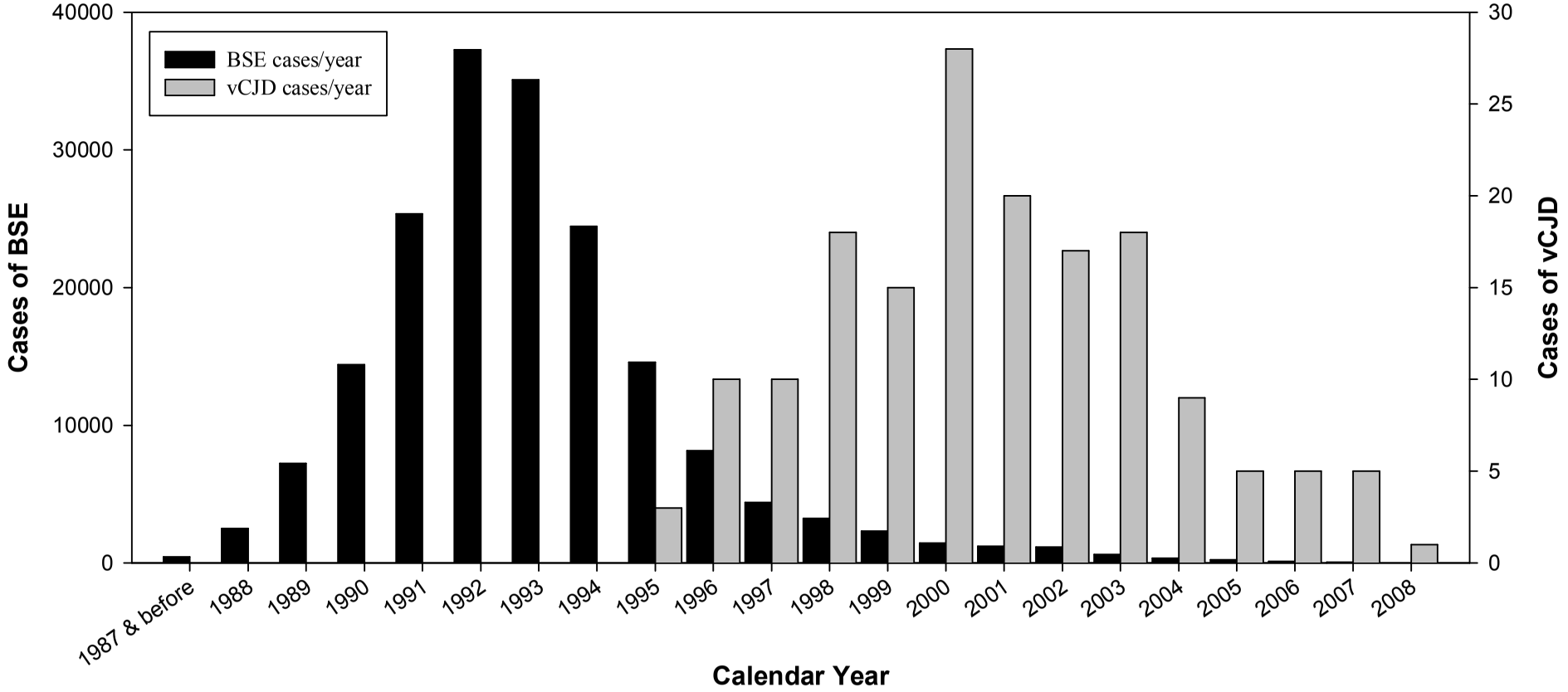

Figure 1 Cases of the zoonotic Bovine Spongiform Encephalopathy (BSE) in cattle and variant Creutzfeldt-Jakob disease (vCJD) in humans arising from the consumption of BSE-contaminated meat-products. Cases are documented by year of death of the infected individual. Data obtained from World Organisation for Animal Health and UK Creutzfeldt-Jakob Disease Surveillance Unit.

Reviews of archival material have been unable to isolate a case with a neuropathological appearance similar to vCJD prior to 1996 (Budka *et al.*, 2002). For example, variant CJD can be separated pathologically from kuru by a markedly increased prion protein load in all areas of the central nervous system (CNS) such as frontal cortex, basal ganglia, thalamus and cerebellar molecular layers, with the exception of the cerebellar granular layer (McLean, 2008). In areas such as the basis pontex, spinal gray matter and substantia gelatinosa where levels of prion protein deposition are low in vCJD, they remain substantially increased relative to kuru. Studies on the transmission characteristics and neuropathology of vCJD have also highlighted distinct similarities between BSE and vCJD but not sCJD in transgenic mice expressing the bovine prion protein (Scott *et al.*, 1999). Variant CJD can be distinguished from sporadic CJD by a number of characteristics, primarily age of death; an average of 28 years old in vCJD relative to 65 years old in sCJD (Murray *et al.*, 2008). Moreover, the disease duration is typically longer in vCJD (13 months against 4 months in sCJD) and, whilst there is an overlap in characteristics, vCJD cases are typically clinically homogenous relative to sCJD which is classically more contrasting (Spencer *et al.*, 2002). In vCJD early clinical course is largely dominated by psychiatric symptoms such as anxiety, insomnia or withdrawal within the first 4 months. In contrast, neurological symptoms such as headache, tiredness, sleep or appetite disturbance, depression, altered personality and nervousness often predate the main illness in sCJD (Kubler *et al.*, 2003). However, this is complicated by the fact that approximately 12 % of sporadic CJD patients are reported for epidemiology studies based on psychiatric evaluation and around 35 % of vCJD cases have been reported with neurological symptoms, primarily memory loss and constant pain (Collins *et al.*, 2004a; Kubler *et al.*, 2003; Spencer *et al.*, 2002). Moreover, with regards to patient age, seven cases of sCJD have been reported in teenagers in the United States of America and Canada, as well as France, Germany, Poland and two in the United Kingdom (Berman *et al.*, 1988; Brown *et al.*, 1985; Kulczycki *et al.*, 1991; Monreal *et al.*, 1981; Murray *et al.*, 2008; Petzold *et al.*, 2004). Conversley, the first documented case of vCJD in Japan was diagnosed recently in a 48 year old male (Shinde *et al*., 2009)

In 2008 there were 25 reported cases of BSE in the United Kingdom (data from World Organisation for Animal Health) and a decline in total cases of between 25 – 45 % a year has been observed since 1992 (Smith & Bradley, 2003). To date, 164 cases of vCJD have been reported, with a further 4 cases still alive but diagnosed clinically without neuropathological examination (data from UK Creutzfeldt-Jakob Disease Surveillance Unit). The peak incidence

was in 2000 when 28 cases were identified and recorded numbers have decreased year on year since then with 5 cases in 2005, 2006 and 2007 and only a single case reported in 2008. However, as the incidence of BSE and vCJD decline, chronic wasting disease (CWD) continues to undergo a dramatic spread in both game-farmed and wild cervid populations in North America. Previously this disease has been demonstrated in Rocky Mountain elk *(Cervus elaphus nelsoni*), mule deer (*Odocoileus hemionus*), white-tailed deer (*Odocoileus virginianus*) and Shira's moose (*Alces alces shirasi*) in North America, Canada and Korea (Baeten *et al.*, 2007; Kim *et al.*, 2005; Spraker *et al.*, 1997). However, international surveillance remains limited, with the exception of a testing program in Germany (Schettler *et al.*, 2006). This is of particular concern given that CWD demonstrates a particularly high rate of transmission, with a >10 % incidence in several wild deer populations in the states of Colorado and Wyoming (Manson *et al.*, 2006). Moreover, up to 79 % of a captive population have previously demonstrated subclinical incubation of CWD in the absence of symptoms upon clinical presentation of a single individual (Keane *et al.*, 2008). Chronic wasting disease also represents a particularly difficult disease to control, particularly in wild cervid populations, without impacting significantly on the surrounding ecosystem. Whilst the mechanism of pathogenesis is unknown, epidemiological evidence has suggested a horizontal mode of transmission through direct animal-to-animal contact or through oral exposure to prion-infected blood, urine, saliva, faeces or fatty tissue (Safar *et al.*, 2008; Race *et al*., 2009). However, evidence suggests that infectivity in fatty tissues, urine and saliva is low, as demonstrated by a lack of detectable PrP^{res} by the Western blot method, in addition to incomplete transmission and prologued incubation times in experiments involving transgenic mice expressing the cervid PrP gene (Race *et al*., 2009; Haley *et al*., 2009). It also remains unclear as to the extent of inter-species transmission of CWD. Studies have demonstrated the presence of CWD infectivity in skeletal muscle and, as a result, there can be no doubt that predators or scavengers have been exposed to the disease, in addition to humans given the extent of hunting and venison consumption in North America (Angers *et al.*, 2006). However, analysis of 812 tissue samples from mammalian scavengers in the CWD-affected area of Wisconsin suggests that cross-species transmission is rare, with none of the samples positive for PrP^{res} as confirmed by Western blot (Jennelle *et al*., 2009). The transmission of CWD to humans is also considered unlikely (Raymond *et al.*, 2000). Twenty-seven patients have presented with CJD and admitted to regular consumption of venison although no molecular, biochemical or histopathological data indicates the emergence of a new prion disease (Belay *et al.*, 2004; Kong *et al.*, 2005). Given the environmental contamination as a precursor to CWD

transmission, it can also be expected that domestic ruminants may be exposed to CWD if areas of grazing overlap. Importantly, however, CWD has not been successfully transmitted to species other than to those within the cervidae family through oral inoculation. Moreover, sheep and cattle indicate a poor susceptibility through intra-cerebral (i.c.) inoculation in the case of mule deer CWD (Hamir *et al.*, 2005; Hamir *et al.*, 2006). Howoever, other studies have demonstrated highly successful transmission of white-tailed deer CWD to cattle and, conversely, BSE to European red deer (*Cervus elaphus elaphus*) through i.c. inoculation with clinical signs and pathology similar to CWD (Dagleish *et al.*, 2008; Hamir *et al.*, 2007).

In addition to current concerns surrounding CWD, atypical forms of BSE and scrapie have recently been identified which should halt any urges to relax surveillance measures despite the hazards surrounding classical BSE (cBSE) having been perceived to have passed. Atypical scrapie (Nor-98) was first identified in the United Kingdom in 2002, although retrospective analysis has identified a single case in 1989 (Benestad *et al.*, 2003; Bruce *et al.*, 2007). Initially considered a different form of classical scrapie, Nor-98 is now known to be clearly distinguishable from classical scrapie and BSE. Accumulation of the prion protein is observed primarily in the cerebellum and cerebral cortex rather than the brain stem targeted in classical scrapie (Gavier-Widen *et al.*, 2004). Western blot analysis also demonstrates an additional small molecular weight (10-12 kDa) prion protein fragment following digestion by proteinase K, including a C- and N-terminal truncated form of the prion protein (Gavier-Widen *et al.*, 2004; Klingeborn *et al.*, 2006). Following the beginning of large scale surveillance of prion diseases in small ruminants, the incidence rate of Nor-98 has increased in a large number of European countries, in addition to the Falklands Islands and North America (Benestad *et al.*, 2008; Buschmann *et al.*, 2004; DeBosschere *et al.*, 2004; Epstein *et al.*, 2005; Gavier-Widen *et al.*, 2004; Onnasch *et al.*, 2004; Orge *et al.*, 2004; Seuberlich *et al.*, 2007).

Atypical BSE exists in two forms, identified recently in Europe and North America as a consequence of cBSE testing (Biacabe *et al.*, 2004;Casalone *et al.*, 2004). These forms are designated bovine amyloidotic spongiform encephalopathy (BASE, also known as BSE-L) and BSE-H; so called because of the higher and lower electrophoretic positions of the prion protein isoforms. The cause of these subtypes of BSE is unknown but they may represent a form of sporadic BSE. Of particular concern is BASE which, in addition to a different molecular profile of the prion protein, also demonstrates amyloid plaque deposition and is largely asymptomatic (Comoy *et al.*, 2008; Kong *et al.*, 2008). Serial passages of BASE into nontransgenic mice resulted in a neuropathological and molecular disease phenotype identical to cBSE infected mice suggesting an intrinsic capability of BASE to evolve towards the

classical strain of disease (Capobianco *et al.*, 2007). Although yet to be clarified, this potentially suggests sporadic generation of a cattle strain of prions which may have mutated through passage in an intermediary host, such as sheep, with the end product a bovine stable form of classical BSE.

Most recently, a new prionopathy has been described in 11 patients previously diagnosed with sporadic CJD. Designated proteinase-sensitive prionopathy (PSPr), it represents a novel, relatively rare form of human prion disease and is thought to account for 3 % of all sCJD cases (Gambetti *et al.*, 2008). The authors of the study identifying PSPr concede that it may be even more prevalent as some cases may be classified as non-Alzheimer's dementia. Clinically it is characterised by a relatively short disease duration (mean: 20 months) and a rather non-specific phenotype involving progressive dementia and ataxia, with a number of cases also displaying Parkinsonism, consisting of tremors, rigidity, hypokinesia and postural instability. It can be further distinguished from known prionopathies based on the type of spongiform degeneration, the immunostaining pattern and the presence of prion-associated amyloid microplaques in the cerebellum, cerebrum and, less frequently, in the white matter. However, of particular interest is the detection of an abnormal form of the prion protein which, in several brain regions, was almost exclusively sensitive to degradation by the protease proteinase K (PK). Detectable protease resistant PrP or PrP^{res} produced a distinct electrophoretic profile, clearly distinguishing PSPr from sporadic CJD and sporadic fatal familial insomnia (sFI) (Gambetti *et al.*, 2008). Whilst investigations into the transmissibility of PSPr are underway, this new disease, coupled with atypical forms and recent studies into existing diseases, expands the entire nature of what is known regarding prion diseases.

1.3. PRNP AND THE CELLULAR PRION PROTEIN

The prion protein gene (PRNP) is a small single-copy gene found on the short arm of chromosome 20 in humans and 2 in mice (Collinge, 1997). In humans, wild-type PRNP consists of two exons (three in mice), one of which is short and untranslated, the other considerably larger incorporating the 759 nucleotide open reading frame (ORF) for the prion protein (Collinge, 1997; Gacia *et al.*, 2006).

The cellular prion protein (PrP^{c}) is highly conserved among mammals (Collinge, 2001). It is present in a wide range of tissues including the heart and skeletal muscle. High levels of expression are observed in the CNS and at varying concentrations on cells of the

lymphohaematopoietic system. These include haematopoietic stem cells, dendritic cells, follicular dendritic cells, monocytes, macrophages, microglia, granulocytes, lymphocytes (both T and B cells), erythrocytes, platelets, $CD34^+$ and several groups of lymphoid precursors (Burthem *et al.*, 2001; Dodelet & Cashman, 1998; Isaacs *et al.*, 2006; Li *et al.*, 2001; Liu *et al.*, 2001; Zhang *et al.*, 2006). In the CNS, particularly elevated levels of this protein and its mRNA are found in neocortical and hippocampal neurons, spinal motor neurons and cerebellar Purkinje cells, with particularly wide subcellular distribution observed throughout cytoplasmic organelles, central and nerve muscle synapses, in addition to secretory granules of epithelial cells (Fournier *et al.*, 2000; Harris, 1999; Sales *et al.*, 1998). PrP^c possesses a half life in the body of around six hours. During much of this time it associates with specialized membrane domains enriched with cholesterol and glycosphingolipids known as lipid rafts, following which it is transferred to clathrin-coated pits where it is subjected to endocytosis and recycling (DeMarco & Daggett, 2005; Taylor & Hooper, 2006; Westergard *et al.*, 2007).

Encoded by PRNP, the human PrP^c protein is synthesised as a 253 amino acid polypeptide chain (Collinge, 1997; Collins *et al.*, 2004b). After targeting to the endoplasmic reticulum, the first 22 amino acids are cleaved on initiation of translation and an initial core glycan is added to one or both of the glycosylation sites available (Asn-181 and Asn-197) (DeMarco & Daggett, 2005; Zahn *et al.*, 2000). A disulfide bond is then formed between the cysteine residues 179 and 214 providing structural stability to the C-terminus followed by addition of a C-terminal glycosylphosphatidylinositol (GPI)-anchor attached at residue 230 (Ronga *et al.*, 2006). Following further structural alterations to the glycans in the Golgi apparatus, PrP^c is inserted into the plasma membrane (Figure 2).

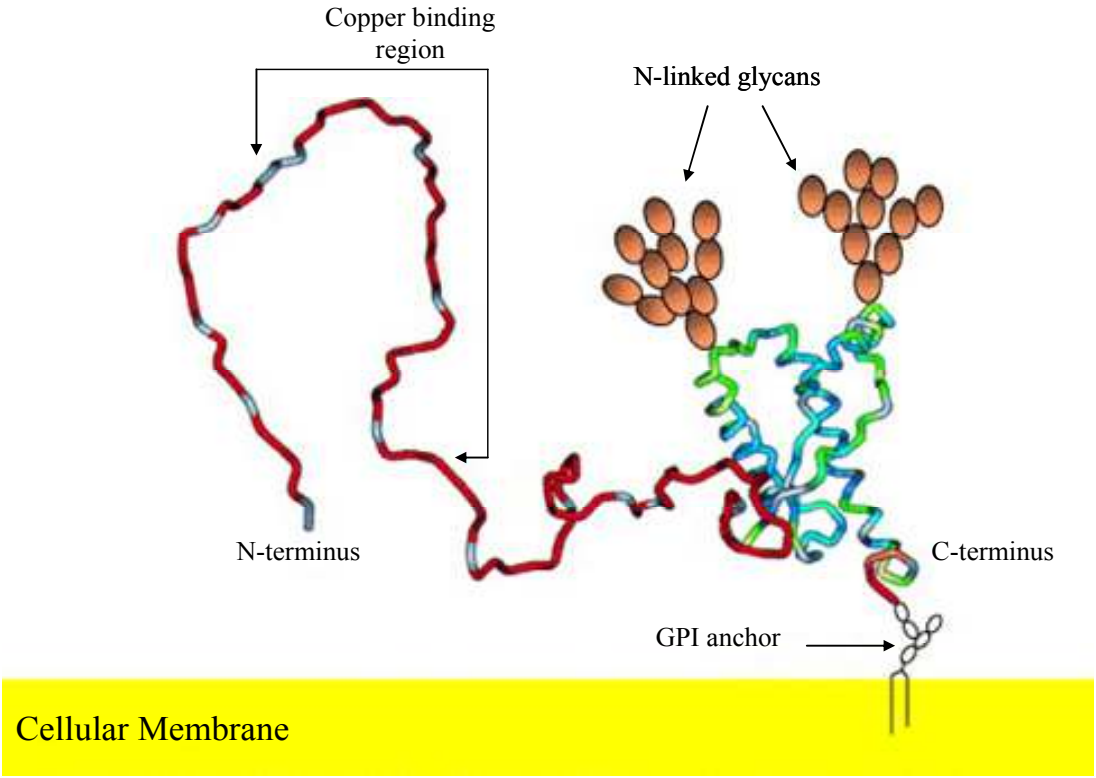

Figure 2 Orientation of PrP^c following insertion into the cellular membrane showing the flexible N-terminus and globular C-terminus with the GPI anchor attached at residue 230 and glycans at residues 181 and 197. Adapted from Pinheiro, 2006.

Although structural studies have yet to provide a precise, high resolution structure of PrP, nuclear magnetic resonance (NMR) studies have shown that, common to all species, the prion protein possesses a globular C-terminus domain. This region of the protein includes three α-helical regions: H1 consisting of residues 143-153, H2 encompassing residues 171-192 and H3 of residues 199-226, the latter two of which are linked by the disulphide bond and two N-linked glycosylation sites (Norstrom & Mastrianni, 2006). Western blot analysis demonstrates three major PrP bands corresponding to the occupation of either two, one or zero glycosylation sites. Glycosylation is thought to be important as a signal for correct intracellular trafficking and possibly for targeting of PrP^c to specific sites within the CNS (DeArmond *et al.*, 1997; DeArmond *et al.*, 1999). Two short antiparallel β-strands consisting of residues 128-130 and 160-162 are also contained within the C-terminal domain (Figure 3).

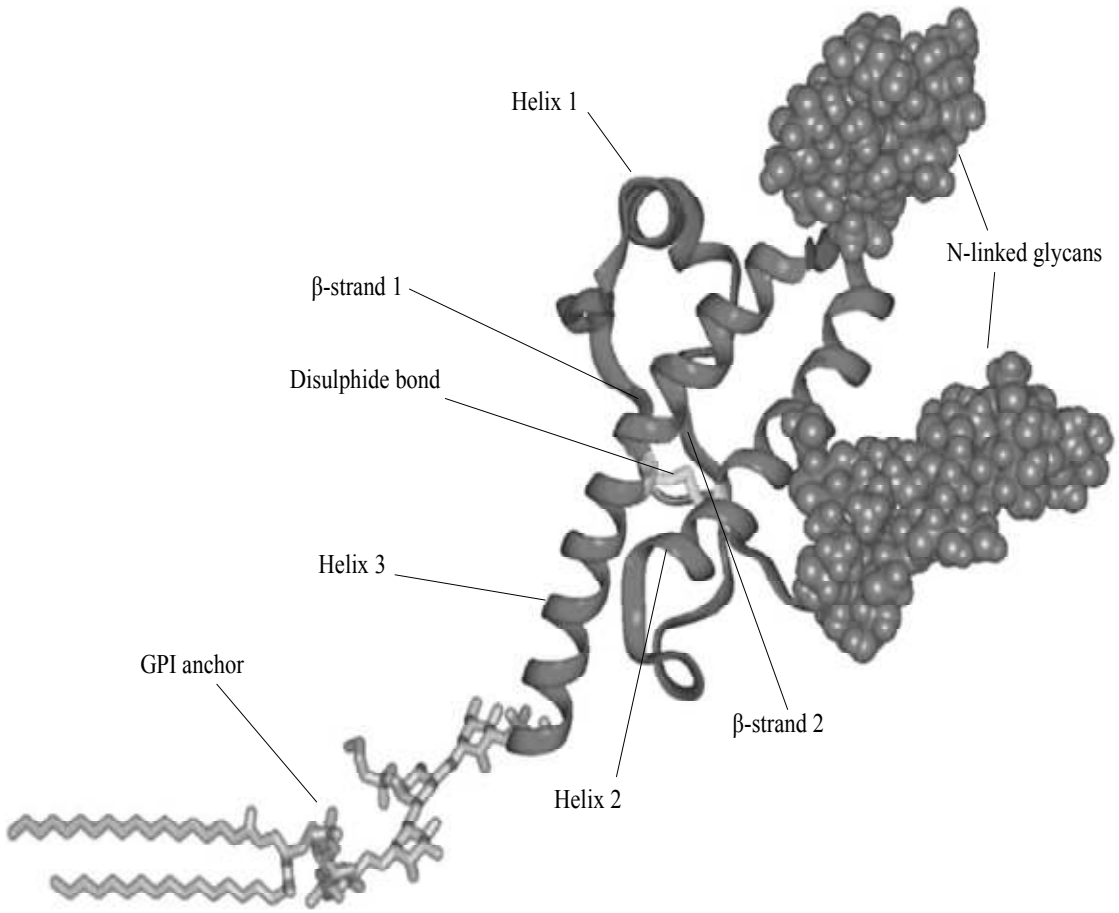

Figure 3 Proposed 3D structure of the C terminus of the human prion protein, residues 125-230 indicating the glycosylphosphatidylinositol (GPI)-anchor, Helix 1, 2 and 3, β-strands 1 and 2 and occupation of the two N-linked glycosylation sites at residues 181 and 197. Adapted from Collinge, 2005.

PrP^c also possesses a flexible, unstructured N-terminus which spans residues 23-124, encompassing a highly conserved octapeptide repeat (OR) region located between residues 51 and 95 (Collinge, 2005; Zidar *et al.*, 2008). It is mutations in the OR region, leading to the accumulation of additional repeats, which are associated with forms of inherited prion disease, potentially involving inhibition of microtubule polymerization along the pathway to cell death (Dong *et al.*, 2008). The N-terminal region also contains a polybasic N-terminal motif KKRP (residues 23-26) which is critical for endocytosis through interaction with the transmembrane adapter protein (Taylor *et al.*, 2005). Deletion of the polybasic region results in accumulation of PrP^c within the cellular membrane. Also within the N-terminal domain is a residue sequence of amino acids 104-135 comprising a short stop transfer effector (STE), a hydrophilic sequence (residues 104-111) and residues 112-135 designated a putative transmembrane segment (TM) for its hydrophobic nature. The TM segment contains a sorting

signal which, in addition to or in conjunction with signals from the GPI anchor, has been implicated in the correct trafficking of PrP^c to lipid rafts in the basolateral membrane of polarised cells (Kaneko *et al.*, 1997). As a result, the AV3 mutation which alters the TM region is known to misroute the cellular prion protein to the apical membrane (Sorgato & Bertoli, 2006). The final structure of PrP^c consists of around 3 % β-structure and 42 % α-helices (Pan *et al.*, 1993).

1.3.1. The Normal Physiological Function(s) of PrP^c

Several physiological functions for PrP^c have been suggested but, as of yet, none confirmed or completely defined. This is somewhat surprising given that PRNP was first decoded in 1985 and the physiology of a prion protein knockout mouse homozygous for PrP null alleles ($PRNP^{0/0}$) was described in 1992 (Basler *et al.*, 1986; Bueler *et al.*, 1992). This is largely a result of the fact that $PRNP^{0/0}$ mice appear to behave and develop normally showing no overt phenotype (Bueler *et al.*, 1992). The only immediately evident alteration in normal physiology is a resistance to prion disease. Inoculation of $PRNP^{0/0}$ mice with scrapie brain homogenate does not elicit a disease phenotype and no subclinical replication of the infectious agent is detected (Bueler *et al.*, 1993; Sailer *et al.*, 1994; Weissmann *et al.*, 1994). However, subtle alterations in synaptic physiology, more specifically in $GABA_A$ mediated synaptic inhibition, abnormal circadian rhythms and sleep patterns, in addition to deficits in spatial learning and long term potentiation, have since been described (Collinge, 1997; Criado *et al.*, 2005; Manson *et al.*, 1995; Tobler *et al.*, 1996). The molecular bases of these changes remain undefined and, as a consequence, the changes may be a result of the variability in genetic background of laboratory murine strains.

Importantly, $PRNP^{0/0}$ murine models and several $PRNP^{0/0}$ neural cell lines have demonstrated an increased susceptibility to oxidative stress (Brown *et al.*, 1997; Brown *et al.*, 2002; Choi *et al.*, 2007; Klamt *et al.*, 2001; Wong *et al.*, 2001). This has led to the suggestion of a neuroprotective role for the cellular prion protein. The over-expression of PrP^c in cultured neurons, some mammalian cell lines and a yeast system has been shown to rescue cells from apoptosis whereby the N-terminal domain is largely implicated (arra-Mehrpour *et al.*, 2004; Dupiereux *et al.*, 2008; Kuwahara *et al.*, 1999; Li & Harris, 2005; Sorgato & Bertoli, 2006). Critically, the octapeptide repeat region has been demonstrated to possess a pivotal role in neuroprotection. Divalent copper ions bind to the N-terminal region of the protein in the OR which consists of four tandem repeats possessing the 8 amino acid sequence Proline-Histidine-

Glycine-Glycine-Glycine-Tryptophan-Glycine-Glutamine (PHGGGWGQ) (Del *et al.*, 2007). These repeats can bind up to four Cu^{2+} ions with a high affinity in the fmol/L and μmol/L range. The stoichiometry of Cu^{2+} binding to the octapeptide repeats has been demonstrated to be heavily buffer and pH dependent with two copper ions bindings to the OR region at pH 6 and four at pH 7.4 (Whittal *et al.*, 2000). Consequently, PrP^c may function as Cu^{2+} transporter, conveying ions to Cu^+-specific intracellular trafficking proteins or transferring the divalent ions from the extracellular space to the endosome.

The ability of PrP^c to bind Cu^{2+} would imply a potential to inhibit the oxidative properties of copper through prevention of the ions interaction with water and the generation of radicals such as hydroxyl. Importantly, in the presence of copper the N-terminal region reverts from an unstructured to a more structured state which may confer antioxidant properties to the protein in a similar manner to superoxide dismutase (SOD) (Collins *et al.*, 2004b). As such PrP^c may be either directly involved in detoxifying reactive oxygen species (ROS) or indirectly through the upregulation of other proteins such as Cu-Zn SOD (Westergard *et al.*, 2007). Whilst this is an enticing hypothesis, PrP^c has not demonstrated contributions to SOD activity *in vivo* although concerns over the biological availability of copper-bound PrP^c under experimental conditions have been raised (Haigh & Brown, 2006; Hutter *et al.*, 2003). Interestingly, studies have suggested that copper toxicity may occur through mechanisms which are dependent and also independent of oxidative stress, the latter also inhibited by expression of the cellular prion protein (Haigh & Brown, 2006).

The hypothesis of a neuroprotective role has been supported by data demonstrating an increased mortality in $PRNP^{0/0}$ mice subjected to several *in vivo* models of chemically-induced seizure, a likely consequence of hyper-excitability leading to excitotoxicity (Walz *et al.*, 1999). Neuronal excitability and excitotoxic neuronal cell death are features of glutamate-activated N-methyl-D-aspartate (NMDA) receptor activity and $PRNP^{0/0}$ mice exhibit increased and prolonged NMDA-evoked currents through an increase in functional NMDA receptors containing the NR2D subunit (Khosravani *et al.*, 2008; Mody & MacDonald, 1995). Normal functionality can be rescued through over-expression of exogenous PrP^c and, as such, has led to the conclusion that PrP^c may mediate its neuroprotective role by virtue of its ability to inhibit the NR2D subunit, thus preventing glutamate excitotoxicity. It has also been noted that PrP^c is upregulated during the early stages of focal cerebral ischemia, potentially as an early adaptive response, with the extent of upregulation dependent on lesion severity (Weise *et al.*, 2004). Critically, $PRNP^{0/0}$ mice have demonstrated increased neuronal damage following ischemic stroke. The mice display an increased infarct size of up to 200 % relative to wild-

type mice, which can be protected against following over-expression of PrP^c through adenovirus-mediated gene targeting in rodent models (McLennan *et al.*, 2004; Shyu *et al.*, 2005; Spudich *et al.*, 2005). Further studies have suggested that the anti-apoptotic phosphatdylinositol 3-kinase/Akt pathway may be impaired (Weise *et al.*, 2006). This consequently results in reduced post-ischemic phospho-Akt expression leading to enhanced post-ischemic caspase-3 activation and increased neuronal injury following a simulation of transient and permanent cerebral ischemia. Transgenic mice lacking the octapeptide region (C4/- mice) which are subjected to controlled ischemia display an infarct size identical to PRNP knockout mice and three times larger than wild-type mice (Mitteregger *et al.*, 2007). Functionality can not be rescued in the knockout mice through introduction of C4/- suggesting that the N-terminal OR region plays a crucial role in PrP^c physiology and protection against oxidative stress.

Another function of the OR region appears to be linked to the sequence similarity with the Bcl-2 homology domain 2 (Sorgato & Bertoli, 2006). Bcl-2 is an anti-apoptotic factor capable of rescuing neurons from death through its direct interaction with Bax (Kurschner & Morgan, 1995). Interestingly, both Bcl-2 or PrP^c over-expression has been shown to overcome serum deprivation-induced toxicity in $PRNP^{0/0}$ neuronal cells (Kuwahara *et al.*, 1999). Subsequent studies were able to abolish the protective role exerted by PrP^c in Bax mediated cell injury through removal of the octapeptide repeat region (Bounhar *et al.*, 2001). However, the difference in cell location of PrP^c and Bcl-2 suggests rather than interacting directly with Bax, PrP^c may influence a pathway such as the Ca^{2+} metabolism of the mitochondria which involves Bax. Mitochondrial permeability transition, which is affected by both Bax and misregulation of Ca^{2+} metabolism, has been demonstrated to trigger the activation of caspases and subsequently lead to apoptosis (Sorgato & Bertoli, 2006). Later studies have observed mitochondrial irregulation in neuronal cultures devoid of PrP^c (Miele *et al.*, 2002). Importantly, transgenic mice expressing a deletion of the flexible N-terminal tail of PrP^c between residues 32-134 (thereby encompassing the OR region) develop ataxia, degeneration of cerebellar granule cells and demonstrate vacuolation of white matter in the brain and spinal cord leading to death within 3 months (Li *et al.*, 2007a). Deletion of a 21 amino acid sequence of residues 105-125 outside the OR region in the N-terminal region also shows severe neurodegeneration but fatality is observed at 1 week following birth (Li *et al.*, 2007b). While Bax deletion is shown to delay the onset of clinical illness and slow apoptosis, it offers no protection against white matter degeneration in Tg 32-134 mice. Subsequent Bax deletion in the Tg 105-125 mice has no affect on neuropathology or clinical phenotype suggesting that a

Bax related pathway mediates initial neurotoxic actions of Tg 32-134 but that neurodegeneration induced by Tg 105-125 involves Bax-independent pathways.

The theory that PrP^c may not possess any inherent, direct biological activity itself but may modify the functionality of other proteins has led to extensive efforts to classify PrP^c binding proteins or receptor candidates. However, it is not clear whether any of the PrP^c-receptor proteins identified thus far possess an *in vivo* functional pathway in which the cellular prion protein is involved. PrP^c has been shown to bind with the carboxy-terminal decapeptide region of the laminin γ-1 chain of the 37-kDa/67-kDa laminin receptor, an interaction important for both neuronal adhesion and extension and maintenance of neurites, as well as the neural cell adhesion molecule (NCAM) (Graner *et al.*, 2000; Santuccione *et al.*, 2005). Both cis and trans interactions between NCAM and PrP^c at the neuronal surface allow for recruitment of NCAM into lipid rafts therefore allowing the downstream activation of fyn kinase, an enzyme involved in NCAM mediated neurite outgrowth. This has been shown to be ablated in NCAM-deficient and PrP^c–deficient neurons and also by PrP^c antibodies indicating a potential involvement of the cellular prion protein in nervous system development. Transgenic mice lacking the central domain comprising the charge cluster (residues 95-110) and the hydrophobic core (residues 112-134) demonstrate potent neurotoxic effects with widespread central and peripheral neuropathy with myelin damage rather than neuronal loss the primary cause of lethality (Baumann *et al.*, 2007). Consequently, rather than inducing an entirely different disease, this form of PrP^c appears to aggravate symptoms caused by the loss of wild-type PrP^c function suggesting myelin integrity represents an important physiological role for which residues 94-134 are important. It is also postulated that since laminin is known to be abundant in the hippocampus, a region of the brain whose known role is in memory and function, that PrP^c may have a function in memory formation. This is consistent with the observed defects in spatial learning and long term potentiation and the increased excitability of hippocampal neurons in $PRNP^{0/0}$ knockout mice, in addition to the subcellular localisation of PrP^c at the synapses (Colling *et al.*, 1996; Colling *et al.*, 1997; Fournier *et al.*, 2000). Interestingly, it has been demonstrated that infusion of mice with anti-PrP^c antibodies impairs short- and long-term memory retention (Coitinho *et al.*, 2003; Martins & Brentani, 2002). This has also been observed in $PRNP^{0/0}$ and $PRNP^{+/+}$ mice which exhibit significant impairment, not only in memory, but also in locomotor activity and an increase in anxiety-related responses suggesting a role in age-related behavioural defects (Rial *et al*., 2009).

The interaction, either directly or indirectly, of PrP^c with the heat-shock protein 60 (Hsp 60) has raised the questions of whether PrP^c may participate in Hsp 60-dependent signal

transduction, which has been demonstrated to contribute to the establishment of a *Brucella abortus* infection, a gram-negative bacterium which replicates within macrophages vacuoles (Watarai *et al.*, 2003). Cellular prion protein–knockout macrophages have demonstrated a decreased internalization of *B. abortus* as a consequence of disruption of the receptor-ligand interaction between macrophage PrP^c and the Hsp60 of *B. abortus*. Further studies have also given weight to the suggestion that PrP^c may have a role in signal transduction. Glockshuber *et al* (1998) noted that the C-terminal domain of PrP^c possesses similarities to membrane anchored signal peptidases. Tyrosine-128 and Histidine-177 of PrP^c were demonstrated to align precisely with the active site residues within the catalytic domain of the rat signal peptidase. Critically, however, this has not been demonstrated functionally. In addition, the cross-linking of the cellular prion protein with $F(Ab)_2$ antibody fragments activates intra-cellular tyrosine kinase in a calveolin-1-dependent binding mechanism in the 1C11 cell line, particularly in neurites (Mouillet-Richard *et al.*, 2000). However no further studies have been able to verify or reproduce this signal transduction event in other cell lines.

Given the wide cellular expression on cells of the lymphohaematopoietic system it is also conceivable that PrP^c may be involved in aspects of immunological response or neuroinflammation. There is data to support this theory and PrP^c has been implicated in T cell activation, macrophage phagocytosis and T cell-dendritic cell interaction (Ballerini *et al.*, 2006; de Almeida *et al.*, 2005; Mabbott *et al.*, 1997). Moreover, there is evidence to suggest PrP^c may be involved in T-cell mediated neuroinflammation as a more aggressive disease onset and prolonged neuroinflammation was observed in a $PRNP^{0/0}$ -T cell mouse model during the course of experimental autoimmune encephalomyelitis (Tsutsui *et al.*, 2008). Cellular prion protein expression on haematopoietic stem cells (HSCs) has also demonstrated that HSCs from $PRNP^{0/0}$-bone marrow in lethally irradiated mice exhibit impaired self-renewal following serial transplantation (Zhang *et al.*, 2006).

1.4. THE PATHOLOGICAL PRION PROTEIN

It is widely accepted that the precursor to prion disease is a post-translational process, occurring after PrP^c has been inserted into the plasma membrane whereby the cellular prion protein is converted into a pathological conformer known as PrP^{sc} or PrP^{res} which is only detectable in prion disease states. This conversion can be initiated by mutations (sCJD) or

interaction of the cellular and pathogenic isoform of the prion protein (iCJD and vCJD). No transfer of genetic material is required for this transformation to occur (Scott, 2006).

Key to the understanding of the mechanism of disease is the concept that the primary amino acid sequences of both PrP^{c} and PrP^{res} are identical and that PrP^{res} generation is a result of post-translational modifications in conformational structure with no changes in mRNA transcript levels (Aguzzi & Heppner, 2000; Collinge, 2005; Collins *et al.*, 2004b; Hosszu *et al.*, 2005). The structural alteration results in an increase in β-sheet content of the protein from 3 %, to 43 %, accompanied by a small decrease in α-helix from 42 % to 30 % (Table 2). The disulphide bond linking H2 and H3 between residues 179-214 is thought to be maintained in the PrP^{res} structure although contrasting data on this fact exists (Caughey & Lansbury, 2003; Turk *et al.*, 1988). Consequently a profound change in physicochemical property of the prion protein is observed with PrP^{res} demonstrating extreme resistance to heat, radiation and various enzymes. Treatment with the protease proteinase K produces a proteolytically resistant core, with the loss of residues 23 to ~89 (Prusiner *et al.*, 1983). Designated PrP^{27-30}, due to its molecular weight in kilodaltons (kDa), this N-terminally truncated form of PrP^{res} retains its high β-sheet content and is proposed to be fully infectious, with the ability to assemble into prion rods which have the properties of amyloid fibrils (Baskakov *et al.*, 2002a; McKinley *et al.*, 1983; McKinley *et al.*, 1991a; Pan *et al.*, 1993). The pathological form of the prion protein is also highly insoluble in non-denaturing solvents and, supposedly, neurotoxic although the direct role of PrP^{res} in disease remains unclear (Prusiner, 1998).

Table 2 Secondary structure, in relation to α-helix and β-sheet content, of the known isoforms of PrP.

Isoform	α-helix (%)	β-sheet (%)
PrP^{c}	42	3
PrP^{res}	30	43
PrP^{27-30}	21	54

1.4.1. The Site of PrP^{res} Conversion

The specific site of the conversion process is difficult to ascertain. The pathological form of the prion protein is poorly immunoreactive unless treated with denaturing substances which result in disruption to cellular morphology (Harris, 1999). Expression of PrP^{c} is necessary for neuronal damage and scrapie propagation within the CNS (Brandner *et al.*, 1996). Cellular prion protein depleted neurons adjacent to an infected $PRNP^{+/+}$ graft do not

incur damage, implying that interaction of PrP^{c} with PrP^{res} at the cell surface is necessary for disease pathogenesis. Consequently, misfolding may occur at the cell surface with several studies suggesting that the lipid rafts into which PrP^{c} is inserted following synthesis and trafficking to the cell surface play an important role in the conversion process (Pinheiro, 2006). Recombinant transmembrane forms of PrP^{c} not associated with lipid rafts prevent the development of PrP^{res} (Kaneko *et al.*, 1997). In addition, cholesterol depletion redistributes PrP^{c} outside of the lipid rafts and decreases PrP^{res} formation in cell lines (Bate *et al.*, 2004; Taraboulos *et al.*, 1995). However, it is known that PrP^{res} accumulates intracellularly thus suggesting that while interaction occurs at the cell surface, conversion occurs within the cell following endocytosis (Taraboulos *et al.*, 1990). It is important to note that conversion *in vitro* is frequently observed within a pH range of 4-7, such as may be encountered within the endosomal compartment (Borchelt *et al.*, 1992). Electron microscopic evidence and studies using scrapie infected neuroblastoma (ScN2a) and hamster brain (ScHaB) cells suggest conversion may occur along the endocytic pathway or within late-endosome-like organelles or lysosomes, some of which contain acid phosphatase (Arnold *et al.*, 1995; Mayer *et al.*, 1992; McKinley *et al.*, 1991b; Taraboulos *et al.*, 1992). However, as PrP^{res} is not degraded within the lysosomes, beyond truncation of the N-terminus, it is logical to suggest that PrP^{res} formation must occur prior to contact with lysosomal proteases (Caughey *et al.*, 1991).

1.4.2. Important Molecular Structures in the Conversion of PrP^{c} to PrP^{res}

A precise tertiary structure of PrP^{res} or $PrP^{27\text{-}30}$ remains undetermined due to their insolubility and propensity to form large, heterogeneous aggregates which are difficult to analyse by high resolution methods. Consequently, isolation of specific residues involved in the conversion process, through interaction with PrP^{res} or which undergo misfolding themselves, is considerably difficult and often relies on fragment peptide studies from a variety of species, analysed in a variety of cellular or animal models.

Conflicting data exists over the role of the N-terminal domain in misfolding and prion replication. The fact that the N-terminal residues 23-89 are removed upon proteinase K treatment to produce $PrP^{27\text{-}30}$ would appear to suggest that these residues are not critical for prion replication. Indeed, the N-terminal region encompassing residues 23-89 has been demonstrated to be superfluous for prion replication in murine neuroblastoma cells (Fischer *et al.*, 1996; Rogers *et al.*, 1993). However, a further deletion of the first 113 residues of the N-terminus has been demonstrated to reduce PrP^{res} formation and, in addition, produced an

altered protease resistant product as identified by the presence of additional protease K cleavage sites (Lawson *et al.*, 2001). However, the location of membrane-bound PrP^{c} would appear to suggest that the N-terminus could potentially interact with PrP^{res} (Figure 2) (Martins *et al.*, 2002). Moreover, residues 89-175 (including the final 35 residues of the N-terminus) have been suggested to be able to adopt a β-helical formation (Govaerts *et al.*, 2004). A synthetic peptide of residues 109-122 has also been shown to acquire a β-sheet structure (Gasset *et al.*, 1992). Another peptide consisting of residues 106-126, thereby encompassing the N-terminal residues of the TM region and its hydrophobic core AGAAAAGA consisting of residues 112-119, has demonstrated formation of prion-associated amyloid plaques, similar in structure to those found in CJD and GSS brains and toxicity in primary brain cells (De *et al.*, 1994; Forloni *et al.*, 1993; Jobling *et al.*, 1999; Tagliavini *et al.*, 1993). Cellular prion protein mutants lacking the TM domain or part of it are not converted to PrP^{res} (Muramoto *et al.*, 1996). As a generalisation it would appear that the N-terminal up to and including residue 89 is not required for conversion with the remaining residues (90-124) possessing the potential to convert to a β-sheet structure and be actively involved in the conversion process to some extent. However, Cu^{2+} has demonstrated *in vitro* inhibition of conversion of PrP^{c} into amyloid fibrils suggesting a complex role for copper in prion pathogenesis, mediated by the N-terminus and the OR region (Bocharova *et al.*, 2005b). Cells expressing PrP^{c} with deletion of the OR region do not produce PrP^{res} (Sakudo *et al.*, 2008). Moreover, N-terminal deletion mutations of recombinant PrP (recPrP) of residues 51-90 and 32-121 decrease pressure stability and increase thermal lability of the protein. These effects are exacerbated as the N-terminal is shortened and the process is not reversible suggesting that this region may affect stability and the 3D organisation of recombinant murine PrP (Cordeiro *et al.*, 2005). This may be a result of the loss of residues 88 and 98 which data suggests may play a prominent role in nucleation (Sun *et al.*, 2007).

A significant body of data supports the notion that the C-terminus undergoes structural transition, retaining infectivity and protease resistance (Sorgato & Bertoli, 2006). Recombinant murine PrP (rec.MoPrP) of residues 89-230 containing neither the N-linked glycans nor the GPI anchor elicits a disease phenotype suggesting these structures are not required for infectivity (Legname *et al.*, 2004). However, it is unknown whether these structures may influence the efficiency of PrP^{res} formation (Collinge *et al.*, 1996). Subsequent studies have suggested several loci within the C-terminal domain which may be involved in β-structure propagation. A proposed model based on the electron crystallography of prion rods isolated from rodent brain material suggests that H2 and H3 remain intact and linked by the

disulphide bond (Norstrom & Mastrianni, 2006). Conversely, the N-terminal to H2 segment encompassing residues 89-175 (thereby including H1) has been suggested to be able to adopt a β-helical formation and appears to rearrange into a left-handed β-helix structure where H1 protrudes out as a loop adjacent to neighbouring prion molecules (Govaerts *et al.*, 2004; Norstrom & Mastrianni, 2006; Wille *et al.*, 2002). Whether H1 undergoes rearrangement itself is disputed (Watzlawik *et al.*, 2006). However, it has previously been postulated that the central domain, specifically residues 96-167, is involved in the interaction with PrP^{res} (Telling *et al.*, 1995). Consequently, H1 appears to be in an ideal position to influence prion replication. C- and N-terminal neighbouring residues of H1 have been demonstrated to be important in the conversion process (Kocisko *et al.*, 1995). Interestingly, H1 is an unusually hydrophilic α-helix structure where most of the charges are situated on the outer face of the helix away from the globular domain. Prion molecules lacking H1 are resistant to conversion in cell lines which have been chronically infected with prions (Vorberg *et al.*, 2001). However, it is unclear whether this may be a result of an interference with protein trafficking and complex glycosylation which are known to affect the misfolding process. Neutralization of the charges in the N-terminal residues of 143-146 but not the C-terminal residues 147-151 of H1 permits the conversion to PrP^{res} whilst complete reversal of charge orientation leads to the production of a PrP^{c} molecule unable to undergo conversion (Norstrom & Mastrianni, 2006). Importantly, the charge substitutions did not alter the secondary structure or the protein expression levels on the cell surface.

Studies involving monomeric sheep PrP^{c} have identified further loci which may participate in the β-sheet transition. The first involves residues 129-131, which form part of the intra-molecular β-sheet with residues 161-163. Deletion of the beta-strands has been shown to inhibit PrP^{res} formation (Vorberg *et al.*, 2001). In contrast to other studies described above, the second is thought to involve residues 188-204, involving the C-terminal residues of H2 and the first six residues of H3, which modelling has suggested has the capacity to act as an α-helix to β-sheet switch (Haire *et al.*, 2004). Critically, this has been demonstrated in other studies which indicate that residues 172-224, including H2 and H3, may adopt a β-sheet conformation, potentially as part of an intermediate structure (Dima & Thirumalai, 2004). Significantly, it has been suggested that structural change involving the H2 region could potentially promote β-sheet mediated transition (Tizzano *et al.*, 2005). The first three turns of H2 are closely associated with H3 whereby the glycosyl moiety on the Asn-181 residue provides efficient stabilisation of the region. However, residues 190-195 situated apart from

the last helix and H3 and could facilitate further transition to a β-sheet structure and hence aggregation (Ronga *et al.*, 2006).

1.4.3. Evidence for an Auxiliary factor in Prion Conversion

Several studies suggest that a co-factor may be involved in the misfolding of PrP^{c} to PrP^{res}. Cell-based or animal systems demonstrate maintenance of infectivity and the successful conversion of PrP^{c} to PrP^{res} (Fichet *et al.*, 2004; Ma & Lindquist, 2002). However, conversion in a cell-free system is significantly harder to achieve, requiring chemical denaturants and high temperatures under non-physiological conditions (Baskakov, 2007b; Caughey *et al.*, 1995; Legname *et al.*, 2004). Critically, studies have demonstrated that a broad variety of proteins which are unrelated to human disease can be refolded into β-sheet rich, amyloid-like conformations under induced conditions which destabilise their native state (Chiti *et al.*, 1999; Chiti *et al.*, 2000; Gross *et al.*, 1999; Ramirez-Alvarado *et al.*, 2000). As a result it would appear that the ability to form a β-sheet rich amyloid structure is not a protein-specific property unique to individual proteins but may be a general feature of polypeptide chains (Guijarro *et al.*, 1998). The accompanying infectivity surrounding PrP^{res} is therefore likely to be an intrinsic property of the protein itself and efficient conversion achievable only within a cellular environment.

Telling *et al*., (1995) investigated the mechanism behind the conversion process in transgenic mice expressing either human (TgHuPrP) or chimeric prion protein genes. Upon inoculation with brain extracts from fCJD or sCJD human patients, TgHuPrP mice were resistant to human prions and susceptibility was restored upon ablation of the murine PrP gene. In contrast, chimeric mice were fully susceptible to human prions, arguing that a species-specific macromolecule was involved, designated protein X. It is hypothesised that protein X forms a binary complex with PrP^{c} through interaction with prion residues between 96-197 (Telling *et al.*, 1995).

The designation of protein X as a protein is misleading. The possibility that the auxiliary factor is a cholesterol, glycosphingolipid, phospholipid or the membrane surface itself can not be excluded (Kaneko *et al.*, 1997). As a consequence of the fact that conversion is likely to require at least partial unfolding of PrP^{c}, protein X may encompass a cofactor which either destabilises the native state or stabilises the transition state (Baskakov, 2007b). Suggested molecules have included double stranded DNA, RNA and the zwitterionic phospholipid palmitoyl-oleoyl phosphatidylglycerol (POPG) (Adler *et al.*, 2003; Cordeiro *et*

al., 2001; Critchley *et al.*, 2004; Deleault *et al.*, 2003; Re *et al.*, 2008). Interestingly, a pH dependent association between the lipid membrane and PrP^{c} has also been recognised which suggests that the native structure of PrP^{c} is maintained at a neutral pH with unfolding and oligomerisation occurring at pH 5 suggesting that membrane-association may have a stabilising effect on the prion protein (Re *et al.*, 2008).

1.4.4. Mechanism(s) of PrP^{res} Misfolding

Two current theories are suggested to explain the mechanism behind the generation of PrP^{res}: a "refolding" or template-directed model or the nucleation-polymerisation/"seeding" model. In the former, the conversion of PrP^{c} to PrP^{res} is kinetically controlled, whereby the interaction of PrP^{res} with PrP^{c} overcomes a high activation energy barrier preventing spontaneous conversion. This induces the conformational change and subsequent replication occurs through dimerisation (Cohen *et al.*, 1994; Roostaee *et al*., 2009). The latter model suggests a reversible, thermodynamic equilibrium state between PrP^{c} and PrP^{res} balanced in favour of PrP^{c} (Jarrett & Lansbury, Jr., 1993). Stabilisation of the PrP^{res} conformational form can only be achieved following interaction with an aggregated-PrP^{res}-containing structure or "seed" through a nucleation-dependent polymerization process thus recruiting monomeric PrP^{res} molecules into amyloid fibers. Fragmentation of the amyloid increases the number of seeds for further recruitment and replication of PrP^{res} (Figure 4).

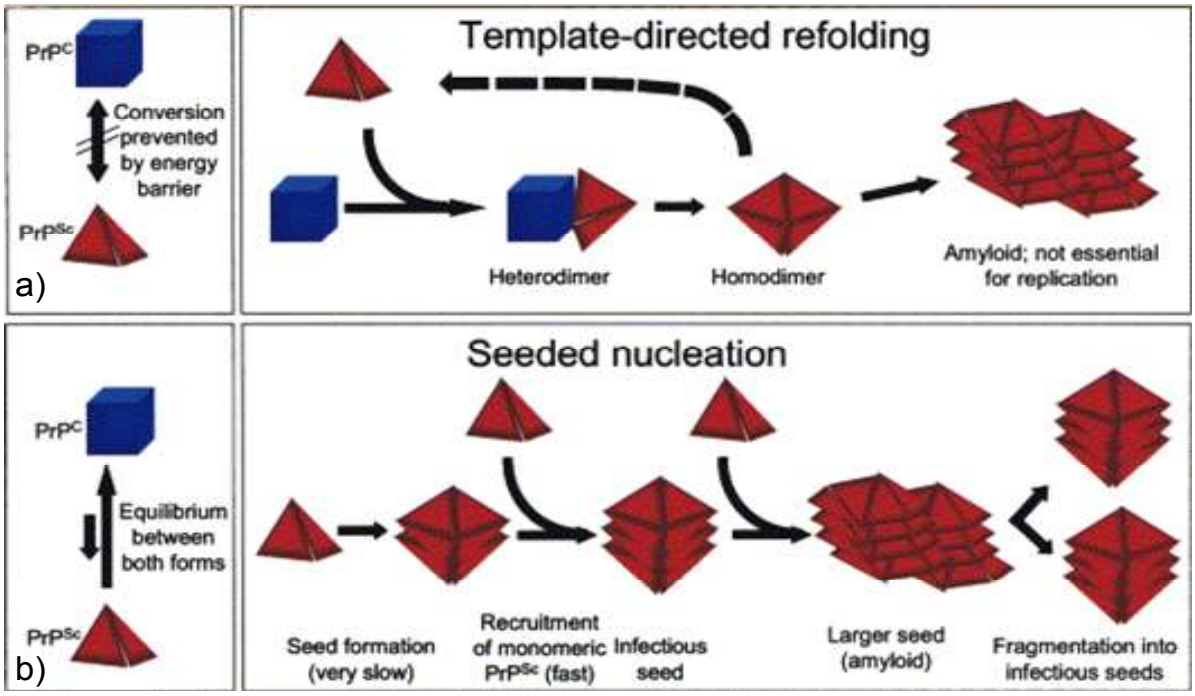

Figure 4 Diagrammatic representation for the suggested models of the conformational conversion of PrP^{c} to PrP^{res}. a) The "refolding" or template-directed model and b) The "seeding" or nucleation-polymerisation model. Taken from Aguzzi & Polymenidou, 2004.

Cell-free conversion studies have demonstrated that aggregates of PrP^{res} are capable of initiating conversion of PrP^{c} to its pathological isoform (Bessen *et al.*, 1997; Kocisko *et al.*, 1996). Importantly, the protein misfolding cyclic amplification (PMCA) technique functions on the basis of a seeding mechanism. Conceptually analogous to the polymerase chain reaction (PCR), PMCA amplifies minute concentrations of existing PrP^{res} through incubation with excess PrP^{c}. Sonication is used to fragment the generated aggregates to produce smaller seeding units which undergo further rounds of amplification in the presence of PrP^{c} thereby augmenting the initial PrP^{res} signal (Castilla *et al.*, 2005a; Castilla *et al.*, 2005b; Saa *et al.*, 2006a). Generation of infectivity has been achieved using this technique from an initial $1x10^{-12}$ dilution of scrapie brain homogenate (Saa *et al.*, 2006b). In addition, data has indicated that the β-sheet rich isoform of recombinant murine PrP is thermodynamically more stable than the native α-helical state and that transition is indeed separated by a large energetic barrier (Baskakov *et al.*, 2001; Baskakov *et al.*, 2002b). Refolding of the C-terminus is also thought to be rapid (170 μs) further suggesting a nucleation-elongation mechanism (Wildegger *et al.*, 1999). However, one caveat of the nucleation-polymerisation model is that if a thermodynamic equilibrium between PrP^{c} and PrP^{res} exists, albeit in favour of the PrP^{c}

conformation, monomeric PrP^{res} could not represent the infectious agent as it would be ubiquitous.

1.4.5. Aggregation, Fragmentation and Replication of PrP^{res}

Following misfolding of the native cellular prion into the predominantly anti-parallel β-sheet secondary structure of PrP^{res}, the prion protein readily polymerises into insoluble fibrous protein aggregates known as amyloid fibres with characteristic green birefringence upon fluorescent labelling with Congo red dye under polarised light (Prusiner *et al.*, 1983). Fibrils are known to be ordered such that the β-strands lie perpendicular to the fibrillar axis, with approximately 4.8 Å between two neighbouring strands (Baskakov, 2007a). Moreover, whilst the 3D orientation of PrP^{res} within an amyloid fibre has not been described, it is predicted that a single PrP^{res} molecule occupies approximately 1.2 nm of a fibres length (Anderson *et al.*, 2006). An immunoconformational assay published by Novitskaya *et al*., (2006) suggests that once in a fibrillar structure, region 159-174 and 224-230 of the PrP globular domain are buried within the structure and resistant to denaturation. Residues 132-156 were only accessible under partially denaturing conditions and residues 95-105 towards the N-terminal are solvent accessible. Critically, however, electron microscopy and 3D reconstruction suggests that amyloid fibrils display a range of assemblies (Figure 5). Fibres have been shown to differ in their number and the packing arrangement of protofibrils, in addition to helical twists within and between fibrils (Jimenez *et al.*, 2001; Jimenez *et al.*, 2002). This has also been demonstrated by Anderson *et al*., (2006) whereby full length murine prion fibrils varied with respect to the number of constitutive filaments and the style in which they were assembled as visualised *in vitro* by atomic force microscopy (AFM). Fibrillar morphology changed even within individual filaments suggesting multiple mechanisms of assembly that are inter-convertible and thermodynamically equivalent. The morphology of fibrils obtained *in vitro* was similar to scrapie-associated fibrils (SAF) obtained from scrapie-infected brains (Anderson *et al.*, 2006). Higher order amyloid plaque morphology is known to vary between diseases as a consequence. Kuru plaques characteristically consist of a stellate core with few or no dystrophic neurites (Hainfellner *et al.*, 1995; Liberski, 2004). In GSS, multicentric plaques consisting of numerous different sizes and shapes are a typical feature in the CNS (Liberski & Budka, 1995).

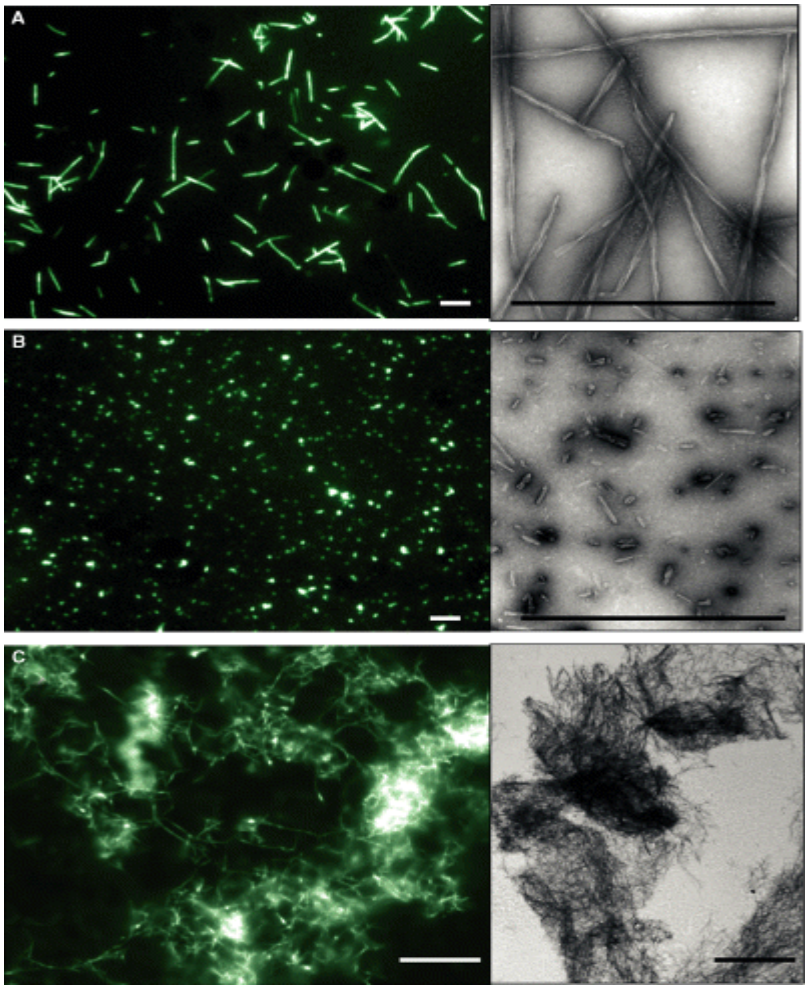

Figure 5 Variation in size distribution and ultrastructure of prion-associated amyloid fibrils formed from recombinant prion protein analysed in parallel by Thioflavin T fluorescence microscopy (left panels) and electron microscopy (right panels). (A,B) scale bars = 1 μm; (C) scale bar = 10 μm. Figure taken from Bocharova *et al.*, 2005a.

Subsequent to the elucidation of the involvement of several sequences of PrP^{c} in the conversion to the PrP^{res} structural state, certain sequences also appear to be important for amyloid formation. The loss of the N-terminal residues 23-89 results in smaller, less ordered aggregates relative to the full length protein, suggesting that the N-terminal may mediate high order aggregation (Frankenfield *et al.*, 2005).

The GPI anchor can also impact prion polymerization in several ways. The anchor can alter the specific orientation of the cellular prion protein in the plasma membrane and therefore increase effective concentration (Breydo *et al.*, 2007). The GPI anchor may also impose important steric constraints on the packing arrangement of PrP into a fibrillar structure. Whilst it is known that GPI-anchorless PrP^{res} does not reduce prion infectivity it is unclear whether a lack of GPI anchor in the cellular form of the prion protein leads to the formation of

fibrils that are arranged in a different manner and hence potentially non-infectious. The addition of a hydrophobic moiety known as N-myristoylamidomaleimidyl mimics the GPI anchor when attached to the C-terminal (Breydo *et al.*, 2007). Whilst this addition does not alter the structure of PrP it decreases fibrilisation and prohibits assembly of filaments into higher order fibrils by preventing their lateral association. This confirms that the C-terminus is involved in formation of the cross-β-structure but, in addition, may also assist in the formation of an interface between the filaments. Subsequent studies have shown that GPI-deficient PrP^{c} produces an accumulation of PK-resistant PrP^{res} deposits whereby the PrP^{res} was also anchorless. These deposits were infectious towards wild-type mice suggesting that the GPI anchor is not required to generate infectivity (Chesebro *et al.*, 2005; Lewis *et al.*, 2006a). It is however unclear whether the GPI anchor is required for generation of infectivity in cases where there is an absence of a seed-mediated conversion, for example in sCJD.

Studies into amyloidosis in prion diseases appear to also be in favour of the nucleated elongation reaction of prion propagation and the thermodynamic conversion model (Figure 4) (Baskakov *et al.*, 2004; Harris & True, 2006). Observations into the conformational changes and oligomerisation process associated with PrP^{27-30} and fragment 90-231 demonstrated a rapid (<1 min) conversion to β-sheet dimers (Post *et al.*, 1998). This was followed by the appearance of larger oligomers after 20 mins with protease resistant aggregates forming after several hours. Critically this study did not appear to require a cooperative, template assisted step. However, polymerization of the amyloidogenic yeast prion Sup35 demonstrates rapid polymerization through monomer addition (Collins *et al.*, 2004a). This appeared to occur in the absence of observable intermediates suggesting that prion-associated amyloid formation occurs separate to, and perhaps in competition with, the formation of oligomeric intermediates.

Interestingly, it appears that while amyloid formation appears reminiscent of other protein polymerization events, such as actin and tubulin, it does not appear to be completely described by simple polymerization models (Ross *et al.*, 2003; Thirumalai *et al.*, 2003). Further studies to observe the fibrilisation of recombinant PrP displayed several kinetic features that can not be explain by either model (Baskakov, 2007a). These include a dramatic effect of reaction volume on the length of the lag phase, a volume dependent threshold effect and highly cooperative sigmoidal kinetics of the polymerization process, all of which are consistent with the mechanisms of branched chain reactions (Baskakov, 2007a; Collins *et al.*, 2004a). Branched chain reactions progress through nucleation, monomer addition and are accompanied by multiplication of active centres. Presumably this occurs as a result of fibril

fragmentation which is considered to be an essential step in prion replication through the multiplication of active centres (Baskakov, 2007a). Several studies have indicated a reverse correlation between disease incubation period and the conformational stability of synthetic prions (Legname *et al.*, 2005; Legname *et al.*, 2006). Studies with AFM investigating the growth and divisions rates of three strains of Sup53 prions and their *in vivo* phenotypes have demonstrated that high fibrillar conformational stability correlated with the slowest aggregate growth rate (Tanaka *et al.*, 2006). However, this was shown to be compensated for by an increase in brittleness of aggregates, thereby generating new seeds. Short fibrils or their fragments generated through fibril fragmentation can be found in substantial quantities during the initial stages of prion conversion and also at the final stages of elongation (Sun *et al.*, 2008).

1.5. THE INFECTIOUS AGENT

There is now available a substantial body of evidence which supports the protein-only hypothesis (Castilla *et al.*, 2005a; Collinge, 2001; Prusiner, 1986; Prusiner *et al.*, 1993; Sailer *et al.*, 1994; Weissmann *et al.*, 1994). The pathological conformer of the prion protein can be co-purified with infectivity and the concentration of the prion protein has previously been demonstrated to be proportional to the infectivity titre (Gabizon *et al.*, 1989). Infectivity can be reduced by protein denaturants and antibodies targeted to the prion protein but is not affected by procedures that normally destroy nucleic acids (Alper *et al.*, 1967). Moreover, no virus or nucleic acids have been consistently associated with the infectious agent and all inherited cases of TSE are linked to PRNP mutations (Meyer *et al.*, 1991; Prusiner, 1998; Safar *et al.*, 2005). In addition, conversion of PrP^{c} to PrP^{res} has been achieved with infectivity generated *in vitro*, which is considered final proof of the prion hypothesis (Castilla *et al.*, 2005a; Deleault *et al.*, 2003; Kocisko *et al.*, 1994; Kocisko *et al.*, 1995; Legname *et al.*, 2005).

However, prion disease pathology and a clinical disease phenotype may exist in both animals and humans in the absence of detectable prion-associated amyloid and/or PrP^{res} (Piccardo *et al.*, 2007). Whilst several genetically distinct forms of GSS, vCJD and iCJD are regularly associated with amyloid deposition and the formation of plaques, several prion diseases demonstrate little, or often no, higher order amyloid formation (DeArmond & Prusiner, 1995; DeArmond, 2004; Will *et al.*, 1996). The majority of sCJD cases (with the exception of the newly classified PSPr) and BSE represent two such diseases where no prion-

associated amyloid deposition occurs (Capobianco *et al.*, 2007; Gambetti *et al.*, 2008; Murray *et al.*, 2008). Conversely, nearly all forms of TSE are associated with accumulation of PrP^{res} (with the exception of several cases of FFI) and PrP peptides comprising the hydrophobic domain have been demonstrated to be toxic to cultured neurons (Dupiereux *et al.*, 2006; Gambetti *et al.*, 1995). However, an apparent uncoupling of PrP^{res} and infectivity has been observed in lethal scrapie-like disease in mice over-expressing mutant transgenes, in wild-type mice inoculated with BSE or FFI and in transgenic mice homozygous for a mutation at residues 101, replacing a proline with a leucine (Barron *et al.*, 2007; Collinge *et al.*, 1995; Lasmezas *et al.*, 1997; Manuelidis *et al.*, 1997; Telling *et al.*, 1996). Barron *et al*., (2007) demonstrated prion infected mice with the P101L mutation exhibited characteristic vacuolation when inoculated with hamster 263K scrapie or human GSS. This disease was shown to be transmissible to 101L mice with an incubation time of 100-160 days. However, immunoblot analysis demonstrated low and sometimes non-existent PrP^{res}. Despite the acknowledgment that high titres of infectivity can not necessarily be expected in animals which display such short incubation periods of disease, subsequent studies demonstrated titres of 10^7 - 10^9 IU/g to be present in the brain, with low or no detectable PrP^{res}. In another study, isolated gut-loops inoculated with scrapie were transferred into the gut of 2-3 month old Suffolk lambs with the ARQ/ARQ genotype to investigate the mechanisms of intestinal transport of scrapie infection and early pathogenesis (Jeffrey *et al.*, 2006). Detection of PrP^{res} in villous lacteals and in sub-mucosal lymphatics was possible 15-210 minutes post-challenge in the gut and, up to 24 hours post-challenge, PrP^{res} was also detected in association with dendritic-like cells in draining lymph nodes. Surprisingly however, at 1 month post-infection (p.i.), *de novo* generated, inoculum-associated PrP^{res} was found in the Peyer's patches, distinct from that observed during the early phase which was not visible with immunochemistry prior to 30-days p.i. Two sheep which were allowed to develop clinical disease showed subsequent accumulation and pathogenesis of disease identical to those seen in natural scrapie.

Within the confines of the prion hypothesis, it is possible that in many of these studies infectivity associates with levels of PrP^{res} below immunohistochemical detection thresholds. No data has been presented using the highly sensitive PMCA method to amplify levels of PrP^{res} in these tissues. However, the PMCA technique has demonstrated *de novo* generation of PrP^{res} in the absence of a pre-existing prion seed. The generated material transmitted disease to wild-type hamsters producing a new disease phenotype with unique clinical, neuropathological and biochemical characteristics (Barria *et al*., 2009). The isolation of PrP^{res}

in PSPr would also suggest that infectivity can associate with a protease-sensitive isoform of PrP^{res}, which could potentially exist in other natural and laboratory strains but be removed through the aggressive immunohistochemical treatments used to degrade PrP^{c} prior to antibody detection. However, knockout of neuronal PrP^{c} during established brain infection results in complete reversal of early pathology and behavioural deficits, preventing neuronal loss and clinical disease (Mallucci *et al.*, 2003; Mallucci *et al.*, 2007). This occurs despite continuous production and replication of PrP^{res} in the brain which eventually reach similar levels to those observed at end-stage disease in wild-type mice.

The fact that infectious disease and PrP^{res} can exist separate from one another suggests that, whilst PrP^{res} is likely to be a major component of the infectious agent, it may not be responsible for CNS pathology. As a result, the most neurotoxic entity may not be PrP^{res} but another form of the prion protein. The fact that chronic deposition of PrP^{res} is not toxic in PRNP knockout mice is consistent with the hypothesis that an oligomeric product formed during PrP^{res} production and higher order growth may represent the toxic agent (Brandner *et al.*, 1996; Bueler *et al.*, 1993; Merlini & Bellotti, 2003).

There is growing evidence to suggest that pre-fibrillar, soluble oligomeric intermediates represent the infectious agent in GSS and several other amyloidoses such as Alzheimer's disease (Cleary *et al.*, 2005; Kayed *et al.*, 2003; Kirkitadze *et al.*, 2002). *In vivo*, 56-kDa dodecameric assemblies of Aβ 1-42 have demonstrated an association with memory deficiencies in a murine model of Aβ, resulting in transient memory impairment following inoculation into rat brain (Lesne *et al.*, 2006). This was proposed to occur independently of plaque formation or neuronal loss. In a zebra-fish embryo model, the expression of polyQ-expanded fragments of Huntington (Htt) results in their accumulation as large, SDS-insoluble cell inclusions whilst apoptotic cells are devoid of visible aggregates (Schiffer *et al.*, 2007). Interestingly, anti-prion compounds were able to prevent the formation of insoluble aggregates but did not suppress abnormal embryo morphology or cell death suggesting upstream soluble Htt assemblies are the toxic culprit.

In prion disease, there is contrasting evidence surrounding the relationship between infectivity and PrP particle size. Oligomeric PrP has been shown to be highly infectious both *in vitro* and *in vivo* (Redecke *et al.*, 2007; Silveira *et al.*, 2005). Infectivity and converting activity has been shown to peak at a particulate size of 17-27 nm (300-600 kDa) (Silveira *et al.*, 2005). In larger fibrils, the ability to demonstrate infection and stimulate PrP^{c} to PrP^{res} conversion was found to be lower and virtually absent in oligomers of ≤5 PrP molecules. This suggests non-fibrillar particles of 14-28 PrP molecules are more efficient initiators of prion

disease. Conversely, however, recombinant amyloid fibrils have demonstrated the potential to transmit prion disease (Legname *et al.*, 2004). Mature amyloid fibrils produced from full length recombinant PrP have been shown to be highly toxic to cultured cells, primary hippocampal and cerebella neurons in a time and dose dependent manner (Novitskaya *et al.*, 2007). However, the lethal effects were comparable with those exhibited by small, soluble β-oligomers, suggesting that, *in vitro* at least, both amyloid and oligomeric intermediates are neurotoxic.

Critically, kinetic data has suggested that the β-oligomer is not on the pathway to amyloid formation and therefore may not represent an intermediate structure but an alternative product of misfolding. This is supported by data from recombinant PrP demonstrating formation of two distinct β-sheet rich isoforms, a β-oligomer and amyloid fibrils (Baskakov *et al.*, 2004). Preferences for the formation of an oligomer or amyloid can be dictated by experimental conditions (Baskakov *et al.*, 2002b). An acidic pH, similar to that found in endocytic vesicles, favours an oligomeric form of PrP, with neutral pH forming amyloid. The kinetics of fibril formation at different pH values suggest that the formation of the oligomeric isoform is not on the kinetic pathway to fibrillar formation. Therefore it is likely that there are multiple routes of conversion and misfolding occurring in distinct, competitive reactions. Strain variation or altered misfolding environments presumably dictate which conversion pathway is favoured. This may be a consequence of the intrinsic ability of PrP to adopt different abnormal conformations under pathological conditions (Baskakov *et al.*, 2004).

1.6. PRION DISEASE PATHOGENESIS

The clinical presentation of prion diseases can vary significantly between the prionopathies. For example, the consequent insomnia observed in FFI is a result of bilateral degeneration of the thalamus (Belay, 1999). In contrast, the pathophysiology of kuru is targeted to the cerebellum resulting in the involuntary movements and ataxia coupled with a fine tremor of the head, trunk and limbs (Brown, 1990; Liberski & Brown, 2004). Broadly however the prion diseases are characterised clinically by rapidly progressive and devastating dementia, which may result in akinetic mutism within weeks. In addition, pyramidal and extrapyramidal signs are observed, in addition to involuntary movements such as myoclonus, dystonia and chorea (Kubler *et al.*, 2003; Poser, 2002).

Prion pathogenesis can be separated into three distinct phases: infection and peripheral replication, peripheral migration accompanied by neuroinvasion and, finally, progressive neurodegeneration producing clinical symptoms.

1.6.1. Infection and Peripheral Replication

The oral route of infection is believed to be important in the natural pathogenesis of scrapie, variant CJD and other prion diseases (Jeffrey *et al.*, 2006). However, the transmission of the infectious agent from the gut to the CNS is not fully understood. It is believed that PrP^{res} transverses the gut wall by way of the M cells of the follicle-associated epithelium (FAE) through transepithelial transport, and into the Peyer's patches through the dome (Heppner *et al.*, 2001; Neutra *et al.*, 1996). Infectivity is then detected in the gut-associated lymphoid tissue (GALT) in the very early stages of disease, as well as the tonsils, spleen and draining lymph nodes suggesting that initial replication of infectivity occurs in these tissues (Andreoletti *et al.*, 2000; Sigurdson *et al.*, 1999). Infectivity titres in the lymphorecticular system (LRS) increase towards a plateau during the early stages of incubation, a considerable amount of time prior to neuroinvasion. However, the time frame for this accumulation of infectivity and the overall prerequisite of the LRS for pathogenesis is highly dependent on the strain of the prion and/or polymorphisms of the PRNP gene (Jeffrey *et al.*, 2006). Importantly, studies have demonstrated that mice are resistant to scrapie prion infection through extraneural routes following loss of functional germinal centres of lymphoid follicles (Klein *et al.*, 1997; Mabbott *et al.*, 2000a; Mabbott *et al.*, 2000b). However, sheep homozygous for the VRQ allele demonstrate an earlier accumulation of PrP^{res} in lymphoid follicles of Peyer's patches relative to ARQ homozygotes (Andreoletti *et al.*, 2000; Jeffrey *et al.*, 2001a; Jeffrey *et al.*, 2001b; van Keulen *et al.*, 2002). In natural cases of BSE, infectivity is not detected at all in lymph nodes or the spleen following oral exposure or in the lymph nodes of Nor98 sheep (Benestad *et al.*, 2003; Somerville *et al.*, 1997; Terry *et al.*, 2003; Wells *et al.*, 2005). In the hyper (HY) strain of TME, both splenic and nodal prion replication is observed following both intra-peritoneal (i.p.) and oral inoculation (Bartz *et al.*, 2005). In contrast, PrP^{res} is not detected in the spleen or lymph nodes following i.p or oral challenge of the drowsy (DY) strain of TME. No clinical disease is observed at all with i.p inoculation. These data suggest highly variable, strain dependent modes of peripheral replication.

1.6.2. Peripheral Migration and Neuroinvasion

Accumulation of infectivity is known to occur within the follicular dendritic cells (FDC) of the LRS (Kitamoto *et al.*, 1991). Prion replication within the spleen has been demonstrated to be highly dependent on PrP^{c}-expressing FDCs (Brown *et al.*, 1999). Consequently, FDC-deficient mouse models exhibit diminished prion replications relative to wild-type mice following peripheral exposure (Prinz *et al.*, 2002). Follicular dendritic cells support formation and preservation of lymphoid microarchitecture and, in addition, play a pivotal role in the initiation and maintenance of the secondary antigen response through presentation of antigens to receptors of the complement system (Aguzzi, 2006). Transgenic mice lacking complement factors such as the C3 component display an increased resistance to peripheral scrapie inoculation (Klein *et al.*, 2001; Mabbott *et al.*, 2001).

Initial deposition of PrP^{res} in the CNS can be observed in the dorsal motor nucleus of the vagus nerve and in the intermedio-lateral column of the spinal cord indicating that neither the blood nor lymph fluid is responsible for the transportation of infection to the CNS (Jeffrey *et al.*, 2006). Data has suggested that the autonomic nervous system is responsible for transport of prion infectivity from lymphoid organs to the CNS (McBride & Beekes, 1999). Importantly, the innervation pattern of lymphoid organs is primarily sympathetic and sympathectomy has been demonstrated to delay the onset of clinical scrapie following i.p inoculation (Felten *et al.*, 1988; Glatzel *et al.*, 2001). Conversely, sympathetic hyperinnervation enhances splenic prion replication and consequent neuroinvasion. There is strong evidence to suggest that accumulation of prions within the FDCs is followed by movement of the infectious agent to neighbouring nerve endings followed by progression through a neuroretrograde mechanism to the CNS. However, there is no direct physical synapse between FDCs and sympathetic nerve endings (Heinen *et al.*, 1995). The distance between FDCs and splenic nerves has been demonstrated to reduce the velocity of neuroinvasion (Prinz *et al.*, 2003). The mechanism of the movement between FDCs and nerve endings is unclear, whether by passive diffusion or the active process of transport by mobile cells such as B cells. Importantly, blood-borne infectivity implies that mobile cells are likely to be important in the peripheral spread of prions (Llewelyn *et al.*, 2004; Peden *et al.*, 2004). The nature of the cells is likely to be haematopoietic as wild-type bone marrow has been demonstrated to restore prion replication in $PRNP^{0/0}$ spleens (Blattler *et al.*, 1997). Moreover, data suggests that in the presymptomatic stages of disease, PrP^{res} may be largely associated with white blood cells, whilst at later disease stages it is largely present, unattached to cells,

within the plasma due to brain leakage (Saa *et al.*, 2006a). As FDCs are immobile and thought to derive from non-haematopoietic stem cells, they are not directly responsible for prion transportation. However, interaction with B cells of the immune system has been shown to be highly important for peripheral migration of prions, with expression of PrP^{c} not a prerequisite for neuroinvasion (Klein *et al.*, 1997; Klein *et al.*, 1998). As a result, B cells are unlikely to represent a major replicative compartment. However, B cells are mainly localised to areas of lymphoid follicles such as the spleen, lymph nodes, tonsils and Peyer's patches and express lymphotoxin α/lymphotoxin β trimers on their surface. Interaction with this structure is required by FDCs for maturation (Aguzzi, 2006). Blockage of lymphotoxin β signalling has been shown to impair neuroinvasion, accumulation of peripheral PrP^{res} and infectivity (Montrasio *et al.*, 2000). Whilst physiologically localised to areas of lymphoreticular organs, following chronic inflammation B cells migrate to and colonise the site of inflammation. Interestingly, superimposing chronic inflammation of the liver, pancreas or kidney with prion infection has been demonstrated to result in progressive accumulation of PrP^{res} at the site of inflammation to a degree that can be expected in tissues of the LRS (Heikenwalder *et al.*, 2005).

1.6.3. Neurodegeneration

Premature cell death due to apoptosis, as identified by caspase activation, is a characteristic feature of prion disease (Ferrer, 2002). However, this is preceded by several early changes in normal cellular function. These include primary neuronal dysfunction associated with early behavioural impairments and a loss of synapses (Cunningham *et al.*, 2003; Mallucci *et al.*, 2003; Mallucci *et al.*, 2007). In ME7 scrapie-infected mice, a significant reduction in synaptophysin was observed in CA1 pyramidal cells, 13 weeks after hippocampal inoculation suggesting a loss of pre-synaptic terminals (Cunningham *et al.*, 2003). This also manifests physically as a reduction in burrowing, nesting and glucose consumption; several highly conserved behavioural changes observed in mice during the early stages of scrapie disease. Dendritic atrophy is also a prominent feature of prion disease (Jamieson *et al.*, 2001). Levels of Notch-1, which is involved in dendrite growth and maturation, and the intracellular fragment of Notch-1, increase in parallel with PrP^{res} expression in the neocortex of mice (Ishikura *et al.*, 2005).

The mechanisms of neurodegeneration leading to neuronal death and the consequent clinical symptoms remain unclear. The most widely discussed hypothesis behind the

conversion of the prion protein to a pathological conformer is attributed to a toxic gain of function whereby PrP^{res} possesses deleterious effects that are not related to the normal physiological function of PrP^{c}. Current data however suggests that the normal physiological function of PrP^{c} is crucial for the induction of prion-induced neuropathology. Expression of the cellular protein is required to render neurons in the brain susceptible to toxic affects of PrP^{res} in grafted brain tissue and neighbouring astrocytes (Brandner *et al.*, 1996; Mallucci *et al.*, 2003). Consequently, a potential loss of function could possibly be used to explain the onset of prion neuropathology whereby the normal physiological activity of PrP^{c} is lost or reduced leading to neurodegeneration upon contact with PrP^{res}. This, however, remains unlikely for several reasons. Firstly, a loss of function model for the acquisition of prion disease is contrary to the dominant mode of inheritance of familial prion diseases such as fCJD. Secondly, pre-natal and post-natal knockouts of PrP expression do not lead to pathological features associated with prion disease, although normal functioning of PrP^{c} may be adopted by another protein in its absence (Bueler *et al.*, 1992; Mallucci *et al.*, 2002). Interestingly, a loss of function has been implicated in other amyloidoses. Huntington (Htt) promotes neuronal survival under normal physiological conditions and, as such, loss of function may lead to disease pathogenesis (Cattaneo *et al.*, 2001). Mice lacking Htt demonstrate extensive cell death and lethality in the embryonic ectoderm and over-expression of this protein has been shown to lead to a decrease in cellular toxicity in Htt mutants (Rubinsztein, 2002; Zeitlin *et al.*, 1995). In Parkinson's disease, α-synuclein which can be found throughout the Lewy bodies in pathological brain tissue may possess anti-apoptotic activity. Expression of wild-type α-synuclein in primary neurons has been shown to protect against cell death in several induced stresses (da Costa *et al.*, 2000).

The theory of a subversion of function would account for the problems associated with the loss and gain of function mechanisms but is yet to be conclusively proven. This suggests that interaction with PrP^{res} leads to the cell receiving neurotoxic signals from PrP^{c} thereby subverting the normal neuroprotective role. This may be a result of aggregation of PrP^{res} at the cell surface or blocking of critical residues of PrP^{c} important for normal physiological activity. This mechanism has been supported by crucial data suggesting that the *in vivo* cross-linking of PrP^{c} with primary antibodies induces neuronal apoptosis in the hippocampus and cerebellum (Solforosi *et al.*, 2004).

1.7. FACTORS INFLUENCING PRION DISEASE TRANSMISSION

1.7.1. Prion Strains

One of the greatest challenges to the validity of the prion hypothesis has been describing the existence of multiple strains of the infectious agent, in the absence of a prion-associated nucleic acid or virus. Besides natural prion strains, there are a wide variety of experimental strains, isolated from diverse sources, that are available as laboratory models of prion disease (Table 3).

Table 3 Experimental prion strains and their origin. Adapted from Beringue *et al*., 2008b.

Name	Origin	Host
ME7	Sheep scrapie[a]	Mouse
87A	Sheep scrapie[a]	Mouse
221C	Sheep scrapie[a]	Mouse
87V	Sheep scrapie[a], SSBP/1[c]	Mouse
79A	SSBP/1[bc]	Mouse
79V	SSBP/1[bc]	Mouse
139A or RML	SSBP/1[bc]	Mouse
22C	SSBP/1[b]	Mouse
22H	Uncloned 22C	Mouse
22L	SSBP/1[b]	Mouse
22A	SSBP/1[b]	Mouse
22F	Cloned 22A	Mouse
301C	BSE	Mouse
301V	BSE	Mouse
6PB1	BSE	Mouse
139H	Cloned 139A	Syrian Hamster
263K	SSBP/1[bc]	Syrian Hamster
SC237	Subclone of 263K	Syrian Hamster
ME7-H	Cloned ME7	Syrian Hamster
HY[d]	TME	Syrian Hamster
DY	TME	Syrian Hamster

[a]Field isolate, [b]SSBP/1: sheep scrapie brain pool 1, [c]Passage of SSBP/1 through goats, [d]TME: Transmissible spongiform encephalopathy – Stetsonville isolate.

Divergent strains are defined by their altered incubation times, in addition to the biochemical properties and/or immunological properties of PrP^{res}, including glycosylation pattern and degree of PK resistance which is reflected by altered access to the N-terminal of

the prion protein (Beringue *et al.*, 2008b; Scott *et al.*, 1997). In addition, different strains also demonstrate clearly distinct patterns of PrP^{res} deposition and patterns of vacuolation, which can be expressed as pathological lesion profiles (Figure 6) (Peretz *et al.*, 2002; Safar *et al.*, 1998). These properties are stable following serial passaging in the same host.

For example, the incubation times of the two experimental prion scrapie strains ME7 and 263K are 168 and 90 days, respectively (Fichet *et al*., 2004; Guenther *et al*., 2001). Sporadic CJD and variant CJD can also be separated from one another based on their incubation times; 4 months and 13 months, respectively (Murray *et al*., 2008). The newly classified form of CJD, PsPr, has also shown an increased sensitivity to PK resistance and, therefore, biochemical stability, compared to other CJD isolates (Gambetti *et al*., 2008). In terms of the glycosylation pattern, BASE and BSE-H can be separated from each other based on their electrophoretic profile (Biacabe *et al*., 2004; Casalone *et al*., 2004). Moreover, in terms of the lesion profile and deposition of PrP^{res}, variant CJD is markedly different from kuru, demonstrating significantly increased concentrations of PrP^{res} across all areas of the CNS (McLean, 2008).

Different organ tropisms are also recognisable between strains. Some strains directly target the CNS and demonstrate a low abundance or complete absence in secondary lymphoid tissues. In contrast, other strains also exhibit deposition of PrP^{res} and infectivity in the CNS in addition to widespread distribution throughout lymphoid organs. For example, the pathogenesis of vCJD differs substantially from other forms of CJD due to the extensive and uniform colonisation of PrP^{res} throughout the lymphoreticular system (Head *et al.*, 2004; Wadsworth *et al.*, 2001). As a result, clinical diagnosis of vCJD can often be made by tonsil biopsy with comparative levels of PrP^{res} reaching 10 % of those in the CNS (Hill *et al.*, 1999; Wadsworth *et al.*, 2001). Conversely, infectivity in kuru is present in the CNS but very rarely in muscle, which would explain the distribution of disease mainly in the women and children of the Forè tribe described in section 1.2 (Brandner *et al.*, 2008).

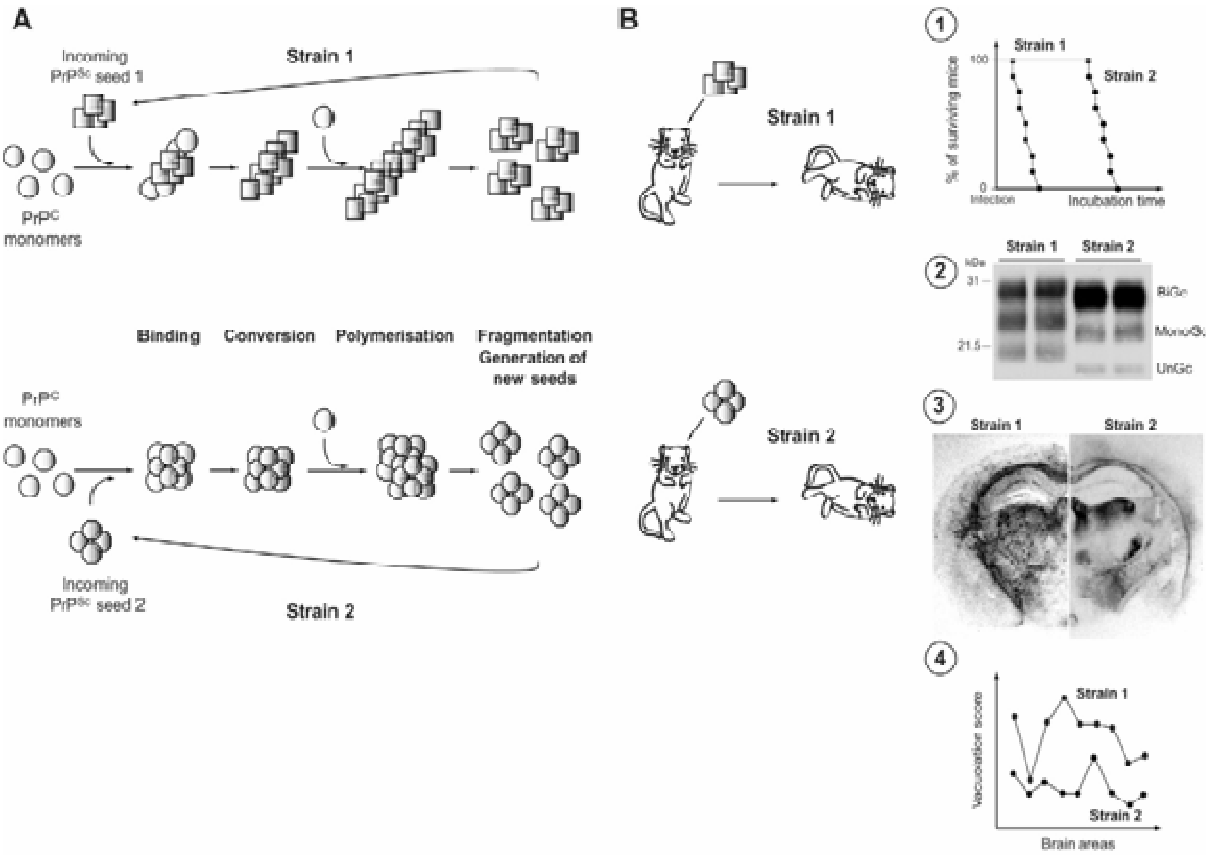

Figure 6 Strain-specified propagation of prions. A) Generation of new infectious seeds under the nucleated polymerisation model of prion replication. B) Experimental inoculation of infectious seeds from two different prions strains into rodent model results in death. Strain 1 and strain 2 demonstrated clearly distinct 1) attack rate and incubation periods preceding onset of symptoms and death; 2) Electrophoretic profiles of PrP^{res} upon detection using Western blot with three separate banding patterns corresponding to the size and relative ration of biglycosylated (BiGc), monoglycosylated (MonoGc) and unglycosylated (UnGc) glycoforms; 3) Distribution of PrP^{res} deposition throughout the CNS as demonstrated by histoblots of coronal sections; 4) Distribution and intensity of vacuolation in standardised brain areas as shown in a "lesion profile". Taken from Beringue *et al.*, 2008b.

1.7.2. The Species Barrier

It is suggested that the properties of strains are encoded within their conformation and not by the host protein, with glycosylation patterns and specific polymorphisms capable of enhancing diversity (Caughey *et al.*, 1998; Manuelidis *et al.*, 2009; Peretz *et al.*, 2002; Safar *et al.*, 1998). In addition, the role of varied aggregate fragmentation rates between strains has also been suggested (Tanaka *et al.*, 2006). However, the so-called "species barrier" is also an

important modulator of cross-species transmission which can be highly variable either resulting in a failure to generate disease, increased incubation times or a normal clinical course. The species barrier is thought to be controlled by the interplay of several host factors important for strain diversity which can impact on the structural homology of the cellular and pathogenic prion protein isoforms between donor and host (Johnson *et al.*, 2006; Moore *et al.*, 2005). The resistance of mice to hamster scrapie can be subverted by expression of hamster PrP^{c} in transgenic mice suggesting a primary role for structural differences/similarities between recipient PrP^{c} and donor PrP^{res} in regulation of the species barrier, potentially influenced by protein X (Scott *et al.*, 1989). Interestingly, resistance can be abrogated upon repeated subpassages of a strain within a resistant host reflecting a host-donor adaptation. The route of infection can also greatly modify the magnitude of the species barrier. Classically, peripheral or oral routes are less effective that i.c. inoculation, with infectivity of mouse scrapie 5-log lower upon intragastric compared with i.c. inoculation (Kimberlin & Walker, 1988). Importantly, the aspects of strain diversity and the species barrier have been brought together in several studies to assess the transmission properties of BASE and BSE-H forms of BSE. Mice are completely resistant to the BSE-H subtype (Beringue *et al.*, 2008a). However, the BASE variant has been shown to propagate in transgenic mice expressing human PrP with no significant transmission barrier. This is supported by a complete attack rate, lack of a reduction in incubation time and conservation of PrP^{res} electrophoretic profile. However, transmission of BSE to some mice demonstrates a substantial species barrier suggesting BASE may represent a higher zoonotic risk than classical BSE (Kong *et al.*, 2008). This has also been confirmed in transmission studies using primates whereby the phenotypic and biochemical properties of BASE demonstrated similarities to a subtype of sCJD patients raising the possibility that this form of sCJD may be acquired as a result of the consumption of BASE-infected meat products (Brown *et al.*, 2006; Casalone *et al.*, 2004; Comoy *et al.*, 2008).

1.7.3. Genetic Susceptibility

The influence of the PRNP gene in cross-species transmission can be observed by the difference in genetic susceptibility in several species. Sheep exhibit variable susceptibility to both experimental and natural scrapie which is highly influenced by polymorphisms at codons 136, 154 and 171 (Goldmann *et al.*, 1990; Goldmann, 2008). Amino acids alanine/valine/threonine (A/V/T), arginine/histidine/leucine (R/H/L) and arginine/histidine/ glutamine/lysine (R/H/Q/K) can be encoded as these positions, respectively. Sheep

homozygous for the VRQ alleles at these three positions are highly susceptible to classical scrapie, whereas ARR homozygote genotypes display a marked resistance to infection (Belt *et al.*, 1995; Elsen *et al.*, 1999). Interestingly, atypical scrapie cases occur, not only in classical scrapie-susceptible genotypes such as VRQ or ARQ, but also in highly resistant genotypes of classical scrapie such as ARR and AHQ (Buschmann *et al.*, 2004; Everest *et al.*, 2006). Moreover, sheep homozygous for the ARQ allele are also more susceptible to BSE infection than ARQ heterozygotes (Houston *et al.*, 2003).

In humans, several polymorphisms are thought to play a role in susceptibility. A lysine rather than a glutamine at codon 219 of PRNP may be protective against sporadic CJD (Aguzzi, 2006). Recently, Mead *et al*., (2009) identified an association between vCJD and kuru susceptibility and incubation times in a region upstream of STMN2, a gene encoding the neural growth associated protein SCG10. However, the description of CJD in two siblings unexplained by PRNP mutation suggests other susceptibility factors unassociated with the prion protein gene (Webb *et al.*, 2008).

That prion transmission proceeds more efficiently when host PrP^{c} and donor PrP^{res} are identical in structure is supported by the fact that the majority of sporadic and acquired cases of CJD occur in individuals homozygous at codon 129. The single nucleotide polymorphism at codon 129 is the greatest identified modulator of genetic susceptibility in humans, with either a methionine (M) or valine (V) encoded (Mead *et al*., 2009). Polymorphisms at this locus have been suggested to influence the exposure of the helix 1 region of PrP, potentially influencing the kinetics of amyloid formation (Lewis *et al.*, 2006b; Pham *et al.*, 2008).

It is estimated that around 39 % of the Caucasian population of the UK are homozygous for the more common allele methionine at codon 129. Approximately 50 % are known to be heterozygotes and the remainder (around 11 %) homozygous for valine (Gacia *et al.*, 2006; Will, 2003). Importantly around 85 % of all cases of sCJD occur in patients homozygous at codon 129, where around 70-75 % are MM rather than VV (Collinge *et al.*, 2006; Ena, 2005). Additionally, 50 % of patients with iatrogenic CJD and all known cases of the new prionopathy PSPr have been VV homozygotes (Ena, 2005; Gambetti *et al.*, 2008). It is therefore apparent that subjects who are heterozygotes (MV) appear to have an increased resistance to disease.

This is of critical importance in light of the BSE outbreak and subsequent risk of variant CJD in humans. All vCJD patients to date have been methionine homozygous at codon 129 (Aguzzi, 2006; Asante *et al.*, 2006). However, both valine homozygotes and heterozygotes are known to be susceptible to disease. Successful transmission of variant CJD

to "humanised" transgenic mice has been achieved for each codon 129 genotype and suggests that MV and VV individuals are likely to remain in an infectious, asymptomatic state for a significantly longer period of time before disease onset, with incubation periods occasionally exceeding the average life span (Bishop *et al.*, 2006). Moreover, in humans, transmission of vCJD through blood transfusion to an MV heterozygote has previously been described and an anonymous screening study of archived appendix tissues identified two valine homozygotes that were positive for vCJD associated PrP^{res} (Ironside *et al.*, 2006; Peden *et al.*, 2004). Therefore, if the influence of this locus is ultimately on incubation time rather than susceptibility, a second wave of vCJD cases with an increased latent period may be forthcoming.

1.7.3.1. Asymptomatic carriers

Importantly, long incubation periods exceeding 50 years have been observed in cases of kuru, relative to the standard 3-6 months usually observed (Collinge *et al.*, 2006). Eleven kuru patients with the MV genotype at codon 129 demonstrated an incubation period of between 39 – 56 years until disease onset, suggesting that this genotype is indeed associated with an increase in incubation time. A consequence of long incubation periods is the potential for asymptomatic carriers of disease. A so-called "carrier state" can be established following prion inoculation into a second species (Race *et al.*, 2001). Wild-type mice inoculated with Sc237 hamster prions have been shown to propagate mouse-adapted PrP^{res} but progress through a normal life span in the absence of disease symptoms (Hill *et al.*, 2000). Prions were shown to replicate slowly in these mice but ultimately reach titres normally associated with end-stage clinical disease. In addition, PrP^{res} is detectable in the blood of asymptomatic sheep and cattle, in the absence of either *in vitro* or *in vivo* amplification (Terry *et al*., 2009). Moreover, the saliva and blood of pre-symptomatic CWD deer have also been shown to contain detectable PrP^{res} and infectivity capable of transmitting to naïve deer (Mathiason *et al*., 2009).

In humans, an elderly patient was shown to have contracted vCJD through a blood transfusion of non-leucodepleted red cells from a patient who later developed the disease 18 months after donation (Peden *et al.*, 2004). The same report also identified seventeen other individuals who received labile blood components from donors who were later diagnosed with vCJD. A model of the future course of the vCJD epidemic, accounting for subclinical infection and a wider genetic susceptibility, optimistically estimated the number of cases between 2004

and 2080 as fifty four (Clarke & Ghani, 2005). However, a pessimistic approach suggests that 363 cases of vCJD may arise in the same time period. Screening of archived surgical specimens has suggested that 237 per million of the population may be incubating the disease (Hilton *et al.*, 2004).

1.8. IATROGENIC CREUTZFELDT-JAKOB DISEASE

The first case of iatrogenic CJD (iCJD) was reported in 1974 following a corneal transplant (Duffy *et al.*, 1974; Martinez-Lage *et al.*, 2005). Since that time cases of iCJD have been documented following dural grafts, cadaveric derived human growth hormone (hGH) and gonadotropin transfer, in addition to blood transfusions (Centers for Disease Control, 1985; Centers for Disease Control, 1987; Cochius *et al.*, 1990; Cochius *et al.*, 1992; Hammersmith *et al.*, 2004; Martinez-Lage *et al.*, 2005; Peden *et al.*, 2004; Preusser *et al.*, 2006; Sato, 2003; Thadani *et al.*, 1988; Wallis *et al.*, 2004). Approximately 400 cases of iCJD have been confirmed worldwide; with half of all cases as a result of dura mater grafts (Hamaguchi *et al*., 2009; Yamada *et al*., 2009). All iCJD cases have involved transmission of infection by material in, or adjacent to, the CNS with inoculation by the parenteral route through surgery or intramuscular injection (Will, 2003).

Consequently, there is significant concern that iatrogenic transmission of prions may occur through neurosurgery and contaminated neurosurgical instruments such as EEG depth electrodes. The infectious agent has been shown to associate avidly with surgical grade stainless steel, with particular affinity for nickel and molybdenum (Flechsig *et al.*, 2001; Luhr *et al*., 2009; Zobeley *et al.*, 1999). Moreover, the physiochemical nature of PrP^{res} creates a significant challenge for decontamination practices. Standard methods for the disinfection of bacteria and viruses, such as germicidal light, glutaraldehyde, formaldehyde and alcohol possess a negligible effect on the inactivation of TSE agents (McDonnell & Burke, 2003; Moore *et al.*, 2005). Furthermore, prion extracts from crude brain tissue of scrapie infected hamsters have been shown to withstand temperatures of up to 600 ºC and remain infective (Brown *et al.*, 2000). Whilst some antimicrobial agents, such as steam sterilisation, have shown limited ability to reduce the risks associated with surface contamination, in most cases TSE agents are clearly more resistant than traditionally used bacterial spores to validate such processes (Fichet *et al.*, 2004).

The iatrogenic spread of prions by surgical instruments has been proven as an effective route of disease transmission. Bernoulli *et al*., (1997) demonstrated cases of two patients who contracted and rapidly developed CJD through a neurosurgical electrode which had previously been inserted into the cerebral cortex of a patient with prion disease. Subsequent decontamination involved treatment with benzene, 70 % ethanol and formaldehyde vapour. Infectivity upon implantation of the same electrode tip into the brain of a chimpanzee was demonstrated several years later (Gibbs, Jr. *et al.*, 1994).

Currently, patients are routinely assessed prior to undergoing "high risk" surgical or neuro-endoscopy procedures to determine whether they have an increased risk of CJD. High risk surgery is classed as those involving either the brain, spinal cord, dura mater, cranial nerve (specifically the optic nerve and intracranial components of other cranial nerves), cranial nerve ganglia, posterior eye and the pituitary gland (guidance from the Health Protection Agency). In addition, those patients identified as receiving blood transfusions from eighty or more donors since 1980 are determined to have an increased risk of vCJD and special infection control procedures are implemented. An average of fifty such cases are identified per year (Department of Health, 2003). However, whilst the highest infectivity titres are associated with the CNS, studies into the pathophysiology of prion diseases have identified extraneural deposition of PrP^{res} in a wide range of tissues in both the variant, iatrogenic and sporadic forms of CJD. Among these, PrP^{res} is readily detected in lymphoid tissues including the spleen, tonsil, rectal tissue, skeletal muscle and blood suggesting a significant risk of transmission through extraneural surgery, in addition to neurosurgical procedures (Bruce *et al.*, 2001; Glatzel *et al.*, 2003; Peden *et al.*, 2006; Wadsworth *et al.*, 2007). Interestingly, an asymptomatic carrier state has been shown to be induced by low-dose inocula, such as may be encountered in extra-neural tissues (Thackray *et al.*, 2002). This indicates that transmission by surgical practice may be able to establish a chronic subclinical state in patients resulting in further transmission assuming ineffective instrument decontamination. Indeed, studies have implicated surgery, other than neurological procedures and corneal transplantation, as a risk factor for sporadic CJD, although with inconsistent results (Davanipour *et al.*, 1985; Harries-Jones *et al.*, 1988; Kondo & Kuroiwa, 1982; Ward *et al.*, 2002; Ward & Knight, 2008; Wientjens *et al.*, 1996; Zerr *et al.*, 2000). Endodontic and ocular surgery have been highlighted as particular risk factors (Armitage *et al.*, 2009; Bourvis *et al.*, 2007). A history of major surgery conducted over 20 years before the onset of sCJD symptoms has also been shown to be a significant risk factor (Mahillo-Fernandez *et al.*, 2008). Specifically, surgery of the digestive system, spleen, female genitalia, peripheral nerves and lymphatic system was

associated with an increased risk of sCJD. Hamster oral tissue preparations have also demonstrated transmissible scrapie with significant levels of infectivity in the trigeminal ganglia, gingival and pulpal tissues of 263K scrapie inoculated mice (Adams & Edgar, 1978; Carp, 1982; Ingrosso *et al.*, 1999). Importantly, small clusters of CJD cases with a link to previous dental procedures have been reported (Arakawa *et al.*, 1991).

1.9. DECONTAMINATION OF SURGICAL INSTRUMENTS

A risk assessment carried out by the Department of Health (DOH) and endorsed by the Spongiform Encephalopathy Advisory Committee (SEAC) indicated that improving decontamination procedures would offer the largest reduction in the risk of transmission of CJD through surgical instruments. However, a survey of decontamination services within the NHS highlighted examples where the current standards of decontamination where not being met (NHS Estates, 2001; Report of a Scottish Executive Health Department Working Group, 2001). Despite a £200 million investment in SSD services and facilities in 2001, several studies have questioned the efficiency of current standards for the decontamination of re-useable surgical instruments in the health services.

Murdoch *et al.,* (2006) assessed levels of total protein contamination on a wide range of surgical instruments as an indication of the effectiveness of current decontamination procedures. A number of instruments at the point of use demonstrated levels of protein that could pose a direct cross-contamination risk. A McIvor gag, Draffin rod and Yankaur sucker showed 1.028 mg, 1.286 mg and 2.228 mg of extractable protein respectively (Murdoch *et al.*, 2006). Lipscomb *et al*., (2006) also demonstrated large concentrations of residual contamination (0.42 – 4.2 $\mu g/mm^2$) in addition to general bioburden at the ends of diathermy forceps and pencils, instruments routinely used to cauterize vessels or dissect tissues, as well as general surgical instruments (Lipscomb *et al.*, 2006b; Lipscomb *et al.*, 2006d). An assessment of 220 endodontic files collected from 22 dental practices demonstrated visible debris on 98 % of devices at the point of use (Smith *et al.*, 2005). Residual protein was detected on all files within a range of 0.5 – 63.2 μg suggesting highly variable efficiency in the methods used to decontaminate endodontic files.

A significant issue is the current standard of instrument cleanliness validation methods utilised by sterile service departments (SSDs). These are described in the Health Technical Memorandum 2030 and based on colorimetric chemical changes such as the Ninhydrin

reaction which utilises a reaction between amino acids, peptides and proteins and 1, 2, 3-indantrione monohydrate. However, serious concerns have been raised over the sensitivity of such tests and this insensitivity could lead to significantly contaminated instruments returned to use after inadequate decontamination treatment within an SSD (Lipscomb *et al.*, 2006a). Moreover, an assessment of test soils which are routinely used to help validate cleaning cycles indicated a large degree of variability in their quality, with a number easily removed by rinsing with cold water (de Bruijn & van Drongelen, 2005).

To reduce the risk surrounding transmission of the infectious agent in prion disease, the World Health Organisation recommends extended steam sterilization and/or chemical treatment involving 1 M sodium hydroxide or 20,000 ppm sodium hypochlorite for the treatment of high-risk re-useable instruments (Sehulster, 2004; Taylor, 2004). However, due to their harsh chemical nature, these treatments are incompatible with the majority of surgical instruments, especially devices containing gum, plastic, joints or electronic components (Brown *et al.*, 2005). Moreover, whilst they have been demonstrated to be highly effective, complete inactivation of the infectious agent is not always achieved by these methods (Fichet *et al.*, 2004; Taylor, 2000). Efforts to implement single use instruments in non-emergency tonsillectomies and adenoidectomies to manage the risk of iCJD in the UK have previously been considered. Critically, their implementation resulted in an increase in postoperative haemorrhaging to 7.8 – 12 % of patients compared with 1 % observed with reusable instruments and the recommendation was withdrawn (Maheshwar *et al.*, 2003; Nix, 2003). Consequently, improved methods of decontamination have been investigated that are compatible for use on re-useable surgical instruments. Several studies have presented significant data for various enzymatic and chemical compounds which are able to remove and/or inactivate infectivity from stainless steel surfaces (Fichet *et al.*, 2004; Fichet *et al.*, 2007b; Jackson *et al.*, 2005; Peretz *et al.*, 2006). However, in the case of enzymatic compounds, it has been suggested that high concentrations, pH values >9 and high temperatures must be utilised, therefore limiting their clinical applicability (Pilon *et al*., 2009). Recently, a combined exposure of copper and hydrogen peroxide (H_2O_2) has been demonstrated to be fully effective at removal of infectious disease from surgical stainlesss steel (Lehmann *et al*., 2009). However, unlike previously published scientific studies, the decontamination of surgical instruments within a hospital SSD is typically an amalgamation of several treatments or chemistries. The potential influence of an individual chemistry on the removal of infectivity by a subsequent autoclave procedure was demonstrated whereby disease

transmission in the animal bioassay was increased using a combined enzymatic treatment followed by autoclaving compared with a single autoclave treatment alone (Yan *et al.*, 2004).

1.10. PROJECT AIMS AND RATIONALE

This body of work will detail studies which have been undertaken to address the highly relevant issue of iatrogenic transmission of CJD from surgical instruments in light of the risk of asymptomatic carriers of the disease and the prospect of further variant CJD cases in other genetically susceptible patient cohorts. The project had three general aims:

- Evaluate current methods of decontamination both within SSDs and in a laboratory setting,
- Assess prion identification techniques and,
- Improve detection techniques.

Of critical importance was that the work should address current issues and decontamination techniques for surgical instruments, rather than focus on the design or assessment of novel methods for prion inactivation so as to be relevant and applicable to SSDs. In addition, previous studies have assessed decontamination efficiency based on the presence or absence of contamination but have not included relevant guidance on how decontamination processes may be improved to yield a safer final product. This project aims to target more specific areas of the decontamination cycle, rather than the cleanliness of the end product, in order to permit more stringent working guidelines to be implicated which will improve the final outcome.

Consequently, an initial aim of the project is to assess current SSD working practices with a view to identifying areas of the cycle which could be improved to produce a cleaner end product. This work is detailed in Chapter 3.

Concurrently, another important aim of the project is to develop a laboratory method for analysing decontamination cycles, rather than single chemistries as previous studies have performed, described in Chapter 4. The objective behind using the stainless steel wires as carrier surfaces for decontamination studies is to correlate *in vitro* analysis with infectivity in the animal model, which utilises the same surface. For analysis of wire contamination, the project aims to continue the development of an *in situ*, novel, fluorescent dual stain procedure

by our group. This method utilises SYPRO Ruby to detect general protein and, more specifically, prion-associated amyloid as a biological marker of disease detected by Thioflavin T (Hervé *et al*., 2009). Whilst the development of this fluorescent staining procedure is an aspect of this project, the methodology optimisation will not be detailed herein. However, a significant objective of this body of work aims to employ this methodology for the *in situ* detection of prions under various conditions which may effect prion decontamination (Chapter 4 and 5).

During the course of this project, a significant amount of work has been performed by other groups into the relationship between prion-associated amyloid, PrP^{res} and infectivity. Consequently, I felt it was also critical to address this issue with regards to the techniques used to assess decontamination. Therefore prion-associated amyloid and PrP^{res}, as detected by Thioflavin T and Western blot, respectively, will be correlated with infecitivity.

As previously mentioned, an important aim of the project was to improve prion detection techniques. Due to the publication of a Thioflavin T analogue known as 2-(4'-Methylaminophenyl) Benzothiazole (BTA-1) for use in *in vivo* positron emission tomography (PET) imaging, the aim will be to develop an *in vitro* fluorescent detection method to enhance amyloid detection in prion disease (Klunk *et al.*, 2003; Mathis *et al.*, 2002). Consequently, through collaboration with the Department of Chemistry, University of Southampton, I aim to obtain further thiazole analogues for this project. The aim will be to assess their ability to identify, *in vitro*, prion-associated amyloid, relative to their precursors, in addition to other amyloidoses such as Alzheimer's disease. Moreover, fluorescent compounds capable of amyloid detection have demonstrated the ability to attenuate progression to end stage disease in several laboratory models of TSE. It is hoped that this work will be able to assess these novel compounds for therapeutic effects in the animal model of infectivity.

CHAPTER 2

MATERIALS AND METHODS

2.1. ANIMALS

C57BL/6J mice (Harlan-Olac Ltd) were housed in a Containment Level 2 facility within the School of Biological Sciences, University of Southampton and handled in accordance with United Kingdom Home Office Guidelines.

Syrian golden hamsters and C57BL/6J mice (Charles River, France) were held at the Institute of Emerging Disease and Innovative Therapies within the Commissariat á l'Énergie Atomique (CEA), Fontenay-aux-Roses, France. All work with the animals was carried out in a Containment Level 3 facility officially registered for prion experimental studies on rodents (agreement number A 92-032-02 for animal care facilities, agreement number 92-189 for animal experimentation).

2.2. STRAINS AND PREPARATION OF BRAIN TISSUE

2.2.1. ME7 Scrapie-Infected Brain Homogenate

ME7 scrapie-infected brains and C57BL/6J healthy brains were provided as a gift by Dr C. Cunningham and Professor V. H. Perry (School of Biological Sciences, University of Southampton). The ME7 scrapie strain was selected due to high PrP^{res} accumulation and wide-spread amyloidosis in the CNS of infected C57BL/6J mice and increased resistance to proteolytic degradation relative to other rodent strains (Cunningham *et al*., 2005; Kuczius & Groschup, 1999). Briefly, C57BL/6J mice were anesthetized through an intraperitoneal injection of 2, 2, 2-tribromoethanol (Avertin) and positioned in a sterotaxic frame. They were then injected with 1 µl of 10 % (w/v) ME7-infected C57BL/6J brain homogenate made in a solution of phosphate buffered saline (PBS) into the right dorsal hippocampal region of the brain using a 10 µl Hamilton syringe. Control animals were injected with 10% (w/v) non-infected brain homogenate (NBH), derived from a naïve C57BL/6J mouse (Cunningham *et al.*, 2005). All procedures were performed in accordance with a United Kingdom Home Office license.

Calculated by the Reed and Muench method, ME7 in this mouse strain demonstrates a median lethal dose or LD_{50} of 10^8 per gram of brain and a disease incubation period of approximately 168 days (Guenther *et al.*, 2001; Mahal *et al.*, 2007; Reed & Muench, 1938). Animals show initial clinical symptoms such as hyperactivity and motor impairments at

approximately 133 days progressing through to a further reduction in mobility, hunched posture and poor coat condition. As a result, the animals were sacrificed between 133 and 147 days post-inoculation following anesthetization with sodium pentobarbitone. The brains were removed and frozen on liquid nitrogen and stored at –80 ºC until use.

A 10 % (w/v) homogenate was then prepared in PBS. Protein concentrations of serial dilutions of the brain homogenate were determined and homogenous preparations ensured using a total protein assay (Bio-rad, Hercules, CA, USA).

2.2.2. 263K Scrapie-Infected Brain Homogenate

Hamster 263K scrapie-infected brains were provided as a gift by Dr E. Comoy at the CEA, Fontenay-aux-Roses, France. This strain was selected for the studies due to its high stability to extended PK exposure and high resistance to degradation relative to other strains (Brown *et al*., 2000; Fichet *et al*., 2007b; Kuczious & Groschup, 1999). The hamster-adapted scrapie strain 263K was stabilized and propagated in female Syrian Golden hamsters (Kimberlin & Walker, 1977). The incubation period for this strain is approximately 90 ± 2 days (Fichet *et al.*, 2004) with early clinical signs including destruction of nest and hyperactivity to noise and sudden movement (Kimberlin & Walker, 1977). As with the ME7 scrapie model, these symptoms progress through to uncoordinated movement and motor impairment, including head bobbing, ataxia of gait and generalised tremor (Seidel *et al.*, 2007). Brains of hamsters at the terminal stage of disease, typically displaying between 10^{10} and 10^{11} LD_{50} per gram were removed and frozen at –80 ºC before transport on dry ice by courier to The University of Southampton. Upon receipt, the brains were thawed and a 10 % (w/v) homogenate made in PBS with total protein assays carried out to determine protein content. Non-infected brain homogenate (NBH) was also prepared from naïve hamster brains.

2.2.3. Preparation of Brain Sections

Whole brain tissue was removed from storage at -80 ºC. The brains were embedded in the inert mounting medium Tissue Tek (OCT Embedding Compound, Sakura, Bayer, UK). Following embedding, the tissue was transferred to a Leica CM3050 Cryostat and 10 μm sections were cut from the hippocampus and placed onto aminopropylsilane (APS) coated glass slides. The sections were covered and allowed to dry overnight to prevent the formation of ice crystals within the tissue section upon freezing at -80 ºC.

2.3. CONTAMINATION OF TEST SURFACES

2.3.1. Standard Stainless Steel Wires

Surgical grade 316L stainless steel wires (Ormiston Wire Ltd; length: 5.0 mm x diameter: 0.16 mm) were cleaned using ultrasonication in a 2 % (v/v) Triton X-100 solution in deionised water for 15 min. This was followed by three separate 3 min sonications in deionised water to rinse. The wires were then dried for 1 h at room temperature before contamination.

For surfaces undergoing microscopic evaluation only, an additional step in the process was added. Subsequent to sonication, the wires were immersed in deionised water filtered through a 0.2 μm filter, autoclaved for 20 min at 121 ºC and then dried for 1 h at room temperature. This ensured a pristine surface suitable for fluorescence microscopy.

Contamination was performed through immersion of the wires in 200 μl of 10 % (w/v) prion-infected brain homogenate or NBH for 1 h at room temperature. The wires were then dried for 16 h at room temperature.

2.3.2. Artificially Degraded Stainless Steel Wires

Artificial degradation of the wires was performed by collaborators at the CEA, Fontenay-aux-Roses, France as part of a blind study. Surgical grade 316L stainless steel wires were cut to 5 mm in length and autoclaved for 18 min at 134 ºC in 1M sodium hydroxide (NaOH) to degrade the wire surface. Following autoclaving, the wires were subjected to rinsing in deionised water and were prepared as described in section 2.3.1 prior to inoculation with 10 % (w/v) 263K scrapie-infected brain homogenate or hamster NBH.

2.3.2.1. Conformation of wire surface topography

Surface tomography was assessed by microscopy comparing normal and degraded surfaces following their staining and evaluation. However, in order to quantify the degree of surface degradation and maintain the blind nature of the study, wires (n = 7) were sent to Dr I. Lipscomb, School of Engineering, University of Southampton. The degree of surface roughness was determined using a laser confocal scanning system (Xyris 4000 CL; Taicaan). The system utilises a 670 nm visible red laser with a spot size of 2 μm. Applying a sampling

rate of 1.4 kHz with a resolution of 0.1 μm, the system scanned the length of the wires. The scans were then analysed (BODDIES software, Taicaan) and mean surface roughness (R_a) calculated across 10 wires.

2.3.3. Stainless Steel Tokens

For surface Western blot studies, surgical grade 316L stainless steel tokens (length: 76 mm x width: 26 mm width x diameter 1 mm) were prepared as detailed in section 2.3.1. A volume of 20 μl of 10 % (w/v) brain homogenate was aliquoted onto each token followed by drying at room temperature for 16 h.

2.3.3.1. Contamination of stainless steel tokens by handling

The degree of proteinaceous contamination applied by a single thumb print was investigated on stainless steel tokens (n = 6) previously prepared as described in section 2.3.1. Contamination by a single thumb print from a hand wearing standard nitrile laboratory gloves was also assessed (n = 6). To compare the deposition of protein by a thumb print with that of normal handling and manipulation by bare and gloved hands, each token (n = 6 for each handling condition) was contaminated with ten thumb prints. Twelve tokens were used as untouched controls. Following staining, twenty random fields of view were imaged from each token and analysed for fluorescently labelled total protein.

2.4. SURFACE DECONTAMINATION TECHNIQUES

2.4.1. Decontamination of Wires Using a High Temperature and Pressure Autoclave Treatment

Stainless steel wires were inoculated in 10 % (w/v) hamster NBH. Immediately following inoculation, wires (n = 7) were rinsed in deionised water for 5 min and dried overnight at room temperature. Inoculated wires (n = 7) were also subjected to autoclaving at 121 ºC for 15 min after inoculation followed by a 5 min rinse in deionised water and overnight drying.

2.4.2. Decontamination Using Simulated Washer-Disinfector Cycles

Stainless steel wires were inoculated in either 10 % (w/v) ME7 scrapie-infected brain homogenate, 10 % (w/v) NBH or nanopure water (18.2 MΩ, pH 6.5) as experimental controls and either dried at room temperature overnight or processed immediately.

All wires were subject to simulated decontamination steps under laboratory conditions as described in Table 4. Each cleaner was heated to operating temperature prior to wire exposure and treatment was performed as per the manufacturer's guidelines. Each cycle commenced with a pre-treatment stage. This involved the use of an enzymatic cleaner (Klenzyme® Enzymatic Presoak and Cleaner; STERIS Ltd, 0.8 % (v/v) in water for 5 min at room temperature) or a pre-soak wetting agent designed to prevent the soil drying (PRE-Klenz™; STERIS Ltd, neat, 5 min at room temperature). As a comparison, a cycle was incorporated which did not involve a pre-treatment. Following immediate transfer into a rinse in deionised water at room temperature for 1 min, wires (n = 7) were removed and left to dry at room temperature over night.

The remaining wires were immediately immersed in the main wash alkaline chemistry (HAMO™ 100; STERIS Ltd, 0.4 or 0.8 % (v/v), 15 or 7 min at 45 ºC). Wires were then rinsed in deionised water at between 45 – 50 ºC (n = 7), removed and left to dry overnight, with the remaining wires subjected to disinfection at 90 ºC in deionised water for 1 min. Each cycle was performed in autoclaved glass tooled-neck vials (Fisher Sciences, USA) in a Reactor Station Heat Block (Fisher, UK) with magnetic stirrers to allow for gentle mixing.

Table 4 Laboratory simulated decontamination cycles describing the varying pre-treatments, concentrations and exposure times for each phase tested; 20 ºC was the approximate room temperature at the time of exposure.

Cycle phases	Exposures	Time (min)	Temp (ºC)	Concentration
Pre-treatment	Enzymatic cleaner/Pre-soak/ No pre-treatment	5	20	0.8 % / neat / -
Rinse	Deionised water	1	20	-
WIRES REMOVED				
Wash 1	Alkaline cleaner	15 / 7	45	0.4 % + 0.8 %
Rinse	Deionised water	1	45 - 50	-
WIRES REMOVED				
Disinfection	Deionised water	1	90	-
WIRES REMOVED				

2.4.3. Decontamination of Artificially Degraded Wires

Standard stainless steel wires and artificially degraded stainless steel wires were inoculated with 10 % (w/v) 263K scrapie-infected homogenate. Uninoculated wires were used as negative controls to confirm cleanliness of the wires following degradation process. Exposures, as detailed in Table 5, were carried out at the CEA, Paris as part of a blind study. For confidentiality reasons, the product names have been omitted at the request of the provider. Working solutions were prepared in deionised water.

In addition, wires were also treated with exposure to vaporised hydrogen peroxide (VHP) coupled to a VHP1000 Biodecontamination System (STERIS Ltd). Contaminated stainless steel wires were placed on plastic plates and exposed to the vacuum process at 30 ºC for 3 h maintaining a dry (non-condensing) hydrogen peroxide gas at a concentration of 1.0 to 1.5 mg/L. Following treatment, the wires were rinsed in deionised water, frozen at –80 ºC and posted on dry ice by courier to The University of Southampton.

Table 5 Chemical, enzymatic and physical treatments including corresponding exposure parameters for the treatment of surgical grade stainless steel wires inoculated with 263K scrapie or hamster NBH. Contact times of 10 + 5 min denote double treatments of the same chemistry separated by 1 h drying at room temperature; 20 ºC was the approximate room temperature at the time of exposure. NaOH: “sodium hydroxide”, NaOCl: “sodium hypochlorite”, ppm: “parts per million”, M: “molar”, mg/L: “milligram/litre”.

	Treatment	Contact time (min)	Temperature (ºC)	Concentration (% or as stated)
T1	Enzymatic A	15	50	0.5
T2	Enzymatic A	10 + 5	20	0.5
T3	Enzymatic B	10 + 5	20	0.4
T4	Enzymatic C	10 + 5	20	0.5
T5	Alkaline 1	15	43	1.6
T6	Alkaline 1	10 + 5	20	1.6
T7	Dry Autoclave	18	134	-
T8	Immersion (H_2O) autoclave	18	134	-
T9	NaOH	60	20	1M
T10	NaOCl	60	20	20,000 ppm
T11	Bleach 1	60	20	20,000 ppm
T12	Bleach 2	60	20	20,000 ppm
T13	VHP	180	30	1 - 1.5 mg/L

2.4.4. Decontamination of Wires: Methodology correlation study

Stainless steel wires were inoculated with 10 % (w/v) 263K scrapie-infected homogenate or corresponding hamster NBH. The wires (n = 7) were then placed in autoclaved glass tooled-neck vials and subjected to various chemical and enzymatic exposures from individual cleaners under the parameters described in Table 6. Treatments included five enzymatic cleaners: Enzymatic 1 (Yan *et al.*, 2004), Enzymatic 2 (a newly developed enzymatic cleaner; STERIS Ltd), Enzymatic 3 (Klenzyme®; STERIS Ltd), Enzymatic 4 (Enzycare® II; STERIS Ltd) and Enzymatic 5 (Adi-Zyme®; STERIS Ltd), in addition to an alkaline detergent; Alkaline 1 (HAMO 100™, STERIS Ltd). Working concentrations of all cleaners were constructed in deionised water (pH: ~ 7.2) as per manufacturers guidelines.

Exposures were carried out in a Reactor Station Heat Block with magnetic stirrers for gentle mixing. Following treatment, the wires were immersed in deionised water and rinsed for 3 min followed by 16 h drying overnight at room temperature.

Table 6 Chemical, enzymatic and physical treatments including corresponding exposure parameters for the treatment of surgical grade stainless steel wires inoculated with 263K scrapie-infected brain homogenate or hamster NBH; 20 ºC was the approximate room temperature at the time of exposure.

Treatments	Contact time (min)	Temperature (ºC)	Concentration (%)
Enzymatic 1	10	20	2
Enzymatic 2	15	50	0.8
Enzymatic 3	5	20	0.8
Enzymatic 4	5	60	0.5
Enzymatic 5	5	43	1
Alkaline 1	7	43	0.8

2.5. STAINING TECHNIQUES

To prevent fluorescent signal loss, all staining using fluorescent compounds was performed in the dark.

2.5.1. General Protein Stain

General protein staining was performed using SYPRO Ruby (Invitrogen). Static surfaces were immersed in 100 % (v/v) SYPRO Ruby for 15 min. To remove excess and non-specifically bound stain, the surface was subjected to two 3 min PBS rinses followed by one 1 min deionised water rinse to prevent the formation PBS crystals and therefore remove the possibility of light scatter.

Seperately, a known concentration of protein, as analysed by a total protein assay, was stained with SYPRO Ruby, permitting quantification of proteinaceous contamination in ng/mm^2.

2.5.2. Prion Amyloid Stain

Fluorescent labelling of prion-associated amyloid was performed using Thioflavin T (Sigma Aldrich). For tissue section staining, pre-cut slides were removed from storage at –80 ºC and incubated for 30 min at 37 ºC. The tissue was then statically immersed in a working solution of 1 mg/ml Thioflavin T (Sigma-Aldrich) made in 0.1 % (v/v) hydrochloric acid (HCl) for 10 min followed by one 1 min rinse in PBS. To remove excess and non-specifically bound Thioflavin T, the sections were rinsed in 0.1 % (v/v) acetic acid for 10 min followed by a further PBS rinse for 3 min and a final rinse for 1 min in deionised water. Brain sections stained with Thioflavin T were cover-slipped using SHUR mount (Electron Microscopy Sciences), a toluene-based acrylic resin mounting medium.

2.5.3. Thioflavin T/SYPRO Ruby Dual Staining Technique

To differentiate between general tissue protein and prion-associated amyloid, a dual staining protocol has been developed. This procedure allows for the fluorescent detection of prion-associated amyloid using Thioflavin T. This is counterstained with SYPRO Ruby to indiscriminately identify total protein.

A working solution of 1 mg/ml Thioflavin T was made in 0.1 % (v/v) hydrochloric acid (HCl) and applied onto static samples for 10 min followed by a 1 min rinse in PBS. This was followed by a 10 min rinse in 0.1 % (v/v) acetic acid and a further 1 min rinse in PBS. The samples were counter-stained with a 100 % (v/v) solution of SYPRO Ruby for 15 min followed by two 3 min rinses in PBS and a final deionised water rinse. Using a known

concentration of brain homogenate fluorescently labelled with SYPRO Ruby, quantification of proteinaceous contamination in ng/mm^2 was achieved. As previously described, amyloid concentration was estimated as a function of the total protein (Hervè *et al*., 2009). Following this, Thioflavin T positive signal on ME7 scrapie wires was normalised against non-specific fluorescence on corresponding NBH wires.

2.5.4. 2-(4'-Methylaminophenyl) Benzothiazole (BTA-1) Stain for Prion Amyloid

To further enhance the sensitivity of amyloid detection, optimisation of a fluorescent staining method of the Thioflavin T derivative BTA-1 (Sigma Aldrich) was performed. Through personal correspondence with Professor W. Klunk, University of Pittsburgh, an initial 500 μM stock solution was prepared in dimethyl sulfoxide (DMSO). To optimise the working concentration, various nanomolar (nM) dilutions of the stock solution in PBS were constructed. Prion infected 263K scrapie and naïve brain sections were removed from storage at –80 ºC and incubated for 30 min at 37 ºC. The working solutions were applied to sections for 15, 30, 45 min or 1 h time frames. Following incubation in BTA-1, the slides were immersed in PBS for 10 seconds to rinse and the sections cover-slipped using Fluorescent Mounting Medium (DAKO). A final working concentration of 50 nM and a 45 min contact time was concluded.

2.6. ANALYSIS OF THIAZOLE ANALOGUES

Synthesis of fourteen Thioflavin T analogues and twenty-one BTA-1 analogues was carried out by Mr. Christopher Ryan and Dr. H. Franks under the supervision of Dr. A. Ganesan within the Department of Chemistry, University of Southampton. A brief overview of the routes of analogues synthesis, including the chemical structures of the thirty-five compounds is contained in the Appendix A.

Methods detailing the subsequent initial testing of the analogues and isolation of a compound of interest for further evaluation are described herein. Due to low product yields, the extent to which further evaluation could be conducted was limited.

2.6.1. Assessment of Analogue Staining Efficiency

Initial evaluation of the analogues was carried out based on their ability to identify amyloid plaques in ME7 scrapie-infected brain sections relative to naïve brain sections from healthy mice.

Prion infected ME7 scrapie-infected and naïve brain sections were removed from storage at –80 ºC and incubated for 30 min at 30 ºC. Due to the constraints imposed by the total volume of each analogue synthesised a simple staining procedure was carried out. The analogues were separated based on the structural similarity to their precursor, either Thioflavin T or BTA-1, and fluorescent staining was carried out using the precursor's respective previously optimised protocols (sections 2.5.2 and 2.5.4). In the case of BTA-1 analogues, working concentrations of 100 nM and 50 nM were evaluated. Each analogue was applied to ME7 and naïve sections in triplicate, in parallel with its precursor for comparison. Blank section controls, where no staining was performed, were also evaluated for potential sample autofluorescence. Photomicrographs were imaged and assessed by four volunteers using an arbitrary scale of X → ✓✓✓✓✓. Assessment was carried out based on the presence of positive/potential positive signal in comparison to precursor staining, where X indicated no positive signal. This increased to ✓✓✓✓✓ where analogue and precursor staining were indistinguishable from one another in respect of their ability to identify prion amyloid deposits. Average scores were attributed to each analogue based on a majority opinion where X = 0 and ✓✓✓✓✓ = 5. The scores of each volunteer were recorded blind.

2.6.2. Analysis of 2-(4'-Dimethylaminophenyl)-6-Methyloxybenzothiazole (28d) Binding Specificity

Initial evaluation identified the compound 2-(4'-Dimethylaminophenyl)-6-Methyloxybenzothiazole (28d), a BTA-1 analogue, for further appraisal.

263K scrapie-infected and naïve sections were removed from storage at –80 ºC and incubated for 30 min at 37 ºC. Sections were fluorescently labelled using 28d and BTA-1 at a working concentration of 50 nM as described in section 2.5.4. At a constant exposure, amyloid plaques (n = 10) of similar dimensions were imaged using each compound and analysed for amyloid-bound pixel intensity versus background pixel intensity in naïve brain tissue.

Using the Image Pro Plus software package, a mean pixel intensity value for every 10 pixels was obtained, followed by the mean pixel value for the entire amyloid plaque. This was

compared against the average surrounding pixel intensity produced through binding of the respective thiazole to naïve tissue. This allowed a measure of binding specificity to be calculated as a function of the ratio between amyloid specific and non-specific labelling by both 28d and BTA-1.

2.6.3. Analysis of the Rate of Photobleaching of 2-(4'-Dimethylaminophenyl)-6-Methyloxybenzothiazole (28d) Relative to BTA-1.

Strain 263K scrapie-infected and naïve sections, as negative controls, were removed from storage at –80 ºC and incubated for 30 min at 37 ºC. The sections were fluorescently labelled with either 28d or BTA-1 using the optimised protocol detailed in section 2.5.4. Amyloid plaques of similar dimensions (n = 3 per compound) were visualised over a 10 min time-course at a constant exposure. Photomicrographs were imaged every 10 seconds.

Using the Image Pro Plus software package, pixel intensity was measured for each 10 second photomicrograph taken across ten separate points within the centre of the amyloid plaque. Mean signal intensity was calculated and plotted against time to assess fluorescent signal loss for each compound.

2.6.4. Correlation of 2-(4'-Dimethylaminophenyl)-6-Methyloxybenzothiazole (28d) and BTA-1 Fluorescence with the Monoclonal Anti-PrP Antibody 6H4.

Brain sections of 263K scrapie infected and naïve hamsters were removed from storage at –80 ºC and incubated for 30 min at 37 ºC. The sections were then fluorescently labelled with BTA-1 as described in section 2.5.4 and visualised using EDIC/EF. Prion-associated amyloid deposits labelled with BTA-1 were imaged. Following an overnight rinse in 50 % ethanol, the removal of BTA-1 fluorescence was confirmed and the protocol described in section 2.5.4 was repeated utilising 28d. Visualisation and imaging of the same prion-amyloid deposits was once again carried out using EDIC/EF. Following this, further fixation was carried out using 100 % ethanol for 10 min at 4 ºC. Following a 1 min rinse in PBS, the sections were immersed in deionised water and autoclaved for 15 min at 121 ºC. The slides were left *in situ* for 5 min and then removed and left to cool. To further denature PrP^c, the slides were immersed in 95 % (v/v) formic acid for 5 min, followed by 1 % (v/v) H_2O_2 in PBS for 10 min to remove endogenous peroxidases.

Using a Vectastain ABC Kit (Mouse IgG; Vector Laboratories), slides were incubated with mouse-on-mouse (MOM) Ig blocking reagent for 1 h. An overnight incubation was then performed at 4 ºC using the primary antibody 6H4 (Prionics; 1/4000 dilution). This primary antibody recognises the highly conserved sequence DYEDRYYRE of the prion protein, corresponding to amino acids 144 – 152 in humans (Zanusso *et al.*, 2004). In both murine and hamster species, the tyrosine at position 145 is substituted by a tryptophan although this does not affect binding.

Subsequently, the slides were incubated with a horseradish-peroxidase-conjugated secondary antibody for 10 min followed by application of the ABC reagent for 30 min. The reaction was developed with a 3, 3'-diaminobenzidine tetrahydrochloride solution and counterstained with haematoxylin. The sections were dehydrated through ethanol to xylene and mounted with DPX neutral mounting medium (Lamb).

2.7. EPISCOPIC DIFFERENTIAL INTERFERANCE CONTRAST MICROSCOPY COUPLED WITH EPI-FLUORESCENCE (EDIC/EF)

Standard Differential Interference Contrast (DIC) microscopy implements the destructive/constructive nature of light waves. In standard DIC, light passes through a polarizer beneath the substage condenser which produces the necessary plane-polarised light for interference imaging (Figure 7). The polarised light then passes through a Nomarski-modified Wollaston prism located below the condenser. This prism, also known as a condenser prism, is composed of two precisely ground and highly polished quartz wedges which are cemented together at the hypotenuse. The original polarised light beam is split into two separate rays, vibrating perpendicular to one another. These rays intersect at the front focal plane of the condenser and pass through, travelling parallel to one another until contact with the specimen. The wave paths of both beams are altered based on the properties (thickness, slope and refractive index) of the sample. Subsequent to traversing the specimen, the optical path difference of the parallel beams is altered for varying areas of the sample.

Upon passing through the objective, the beams are focused. The distance between the rays, known as the shear, and the original path difference between the beams is then removed by a second Nomarski prism or objective prism. A second polariser, known as the analyser, is positioned above the objective prism in order to generate interference. This is accomplished by bringing the beams, which up until this point have had a different path length, into the same

plane and axis. The light then passes on through the eye piece where it is viewed as differences in intensity and colour, leading to a pseudo-three dimensional appearance.

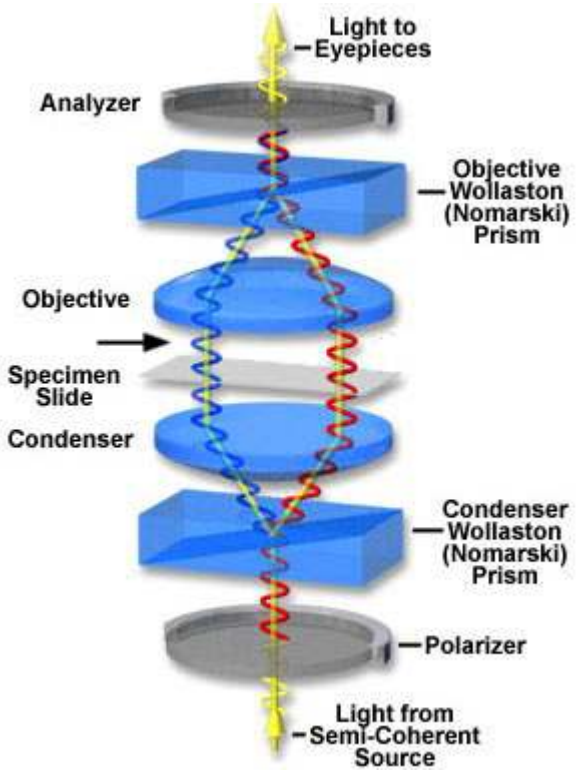

Figure 7 An illustration of the passage of light in Differential Interference Contrast (DIC) microscopy from the light source through to the eye pieces where a pseudo-three dimensional image is viewed. Image taken from the Olympus Microscopy Resource Center.

A disadvantage of the standard DIC set-up is the requirement of cover-slips and oil immersion lenses which is inadequate for visualisation of opaque or curved surfaces such as surgical instruments. An improvement of the DIC set-up, Episcopic Differential Interference Contrast microscopy, coupled with epi-fluorescence (EDIC/EF) rearranges the polarizer and Nomarski prisms into the headpiece above the stage, rather than below (Keevil, 2003). An adjustable analyser is fitted to the main body between the DIC block and eye piece which can be withdrawn for epi-fluorescence with a filter block, incorporating the excitation filter, dichroic mirror and barrier filter, moved into the light path. This gives the microscope the ability to switch between EDIC and epi-fluorescence without the need for lens changing and the stage/lighting to be altered. Incorporation of a slider housing for the DIC and fluorescent

filter blocks into the microscope allows dual staining and image superimposition to be performed, with realisation of a particulates position in or on a detailed surface using DIC.

The EDIC/EF system is coupled with the implementation of non-contact, long distance working objective lenses. Substrata are illuminated with a metal halide lamp (120 W). The lamp posses a spectrum range of 300-750 nm and a life span of 1500 hours. In addition, an adjustable disphragm allows control of the light intensity output from 100, 50, 25, 12 and 0 %. Moreover, a fully automated stage is utilised to allow x, y and z specimen scanning. Image capture is performed using a CCD camera (Roper Industries, UK). Data quantification is performed using the image analysis software Image Pro Plus software, purchased separate to the microscope from MediaCybernetics (Bethesda, MD, USA). This software allows 2D and 3D image processing and analysis and incorporates extensive measurement and customisation features. Importantly for this work it permits image tiling and alignment to allow large areas of a surface, such as a surgical instrument, to be scanned along the x and y plane and the production of a composite image. Features such as background correction and subtraction, in addition to co-localisation of fluorescence through two different channels enhance image quality. Through the construction of an automated set of macros, specific for the emitted light following SYPRO Ruby, Thioflavin T and BTA-1 staining, image analysis is both sensitive and rapid.

2.7.1. Epi-fluorescence Filter Blocks

Routinely used throughout the work in the following chapters were the fluorophores SYPRO Ruby, Thioflavin T and BTA-1. Filter blocks were custom designed for each of these fluorescent compounds and the spectral data for each of these is shown in Table 7. The dichroic mirror or transition wavelength value separates the excitation and emission light paths. The mirror is incorporated into the filter block to reflect the light below the transition wavelength value and transmit wavelengths above this value.

Table 7 Filter block spectral data for three fluorophores: SYPRO Ruby, Thioflavin T and BTA-1 showing excitation filter, dichroic mirror and barrier filter ranges.

Fluorophore	Excitation filter (nm)	Dichroic mirror	Emision filter (nm)
SYPRO Ruby	465 – 495	505	605 – 655
Thioflavin T	405 – 445	460	475
BTA-1	340 – 380	400	420

2.7.2. Statistical Analysis

The aim of statistical analysis in this body of work was to determine significance between data means. Consequently, analysis was carried out using T-tests, in the majority of cases, and Analysis of Variance (ANOVA) methods where stated in the text, with the null hypothesis that there was no significance between data sets. At a 95 % confidence interval, a P value of less than 0.05 resulted in rejection of the null hypothesis in favour of the alternative (ie. a statistically significant difference between the data sets). Conversely, a P value greater than 0.05 at the 95 % confidence interval resulted in an acception of the null hypothesis.

2.8. WESTERN BLOT

2.8.1. Preparation of Samples – Suspension Studies

Working solutions of each chemistry were prepared and pre-warmed. Twenty microliters of either 10 % (w/v) ME7 scrapie-infected or 263K scrapie-infected homogenate were aliquoted into sterile eppendorfs in a ratio of 1:4 (v/v) with 80 µl of cleaner. Exposure was carried out in the presence of regular, gentle agitation to mix. The samples were then centrifuged for 5 min at 13,000 g to pellet. The eluate was removed without disturbing the pellet and replaced with 80 µl of deionised water (pH: ~ 7.2). Following re-suspension of the pellet, the sample was kept on ice prior to use.

2.8.1.1. Exposure parameters intended for the preparation of homogenate samples for antibody mapping of PrP^{res}

Exposure of 10 % (w/v) 263K-infected brain homogenate was performed as described in section 2.8.1. Parameters for the treatment of prion-infected brain homogenate samples are described in Table 8. These treatments included three enzymatic cleaners: Enzymatic 1 (Yan *et al.*, 2004), Enzymatic 2 (a newly developed enzymatic cleaner; STERIS Ltd) and Enzymatic 3 (Klenzyme®; STERIS Ltd), in addition to an alkaline detergent: Alkaline 1 (HAMO 100™; STERIS Ltd) and two phenolic chemistries: Phenolic 1 (LpH; STERIS Ltd) and Phenolic 2 (LpHse; STERIS Ltd). Exposure to a 1M solution of sodium hydroxide (NaOH) was also performed.

Table 8 Chemical and enzymatic treatments including corresponding contact parameters for the exposure of 263K scrapie-infected brain homogenate for subsequent analysis of PrP^{res} structure by Western blot; 20 ºC was the approximate room temperature at the time of exposure. M: "molar".

Treatments	Contact time (min)	Temperature (ºC)	Concentration (% or as stated)
Enzymatic 1	10	20	2
Enzymatic 2	15	50	0.8
Enzymatic 3	5	20	0.8
Alkaline 1	7	43	0.8
Phenolic 1	5	20	5
Phenolic 2	5	20	5
NaOH	0.5	90	1 M

2.8.2. Preparation of Samples – Surface Studies

Immunoblots, incorporating elution of samples from stainless steel tokens, were carried out as part of a blind study and performed by Dr G. Fichet at the CEA, Fontenay-aux-Roses, France.

Stainless steel tokens were prepared and inoculated as detailed in section 2.3.3 and exposure was carried out under the parameters described in Table 6, in autoclaved glass vials with gentle mixing. Following treatment, the dried inoculum was manually removed along with the upper layer of the token and the sample was re-suspended in 120 µl deionised water and kept on ice until use.

2.8.3. Western Blot Protocol

The samples were first treated with increasing concentrations of proteinase K (PK; Sigma Aldrich) for 1 h at 37 ºC to degrade PrP^{c}. Following transfer onto ice to slow enzymatic digestion, Pefabloc (Sigma Aldrich), added at half the concentration of PK, was used to completely inactivate PK. Samples were then boiled for 5 min in Laemmli's buffer containing 2 % (w/v) sodium dodecyl sulphate (SDS), 10 % (v/v) glycerol, 2 % (v/v) β-mercaptoethanol and 0.001 % (v/v) of the dye bromophenol blue in 50 mM Tris/HCL, pH 6.8. The SDS content of the buffer surrounds the protein with a negative charge, the β-mercaptoethanol prevents reformation of disulphide bonds and the glycerol increases the sample density against the running buffer aiding sample loading. Following boiling, the samples were cooled on ice and then loaded onto a 12 % (w/v) polyacrylaminde gel (Bio-rad; brain homogenate equivalent to

50 µg per well) and separated using electrophoresis at 70 V/h. Transference to a polyvinylidene fluoride (PVDF) membrane (Biorad) was performed overnight at 30 V/h.

Subsequent blocking of the membrane was accomplished using a 5 % (w/v) non-fat dry milk solution in PBS containing 0.1 % (v/v) Tween 20 (PBS-T; Sigma Aldrich) for 1 h at room temperature. Following two 3 min rinses in PBS-T, PrP was detected using one of six mouse monoclonal antibodies shown in Figure 8. These antibodies were a gift from Dr E. Comoy at the CEA, Fontenay-aux-Roses, France. The primary antibody was added at the concentration detailed in Figure 8 in PBS-T for 1 h. This was followed by three 3 min rinses in PBS-T and application of a horseradish peroxidase-conjugated anti-mouse IgG secondary antibody (1/5000 in PBS-T; GE Healthcare) for 1 h. Following a further four 3 min rinses in PBS-T, immunoreactive bands were visualised using enhanced chemiluminescence utilizing the ECL Plus Western blotting detection reagent (ECL, Amersham Biosciences; 5 ml reagent A, 125 µl reagent B) added for 3 min. Development was carried out in an automatic xograph film processor using ECL Hyperfilm (ECL, Amersham Biosciences).

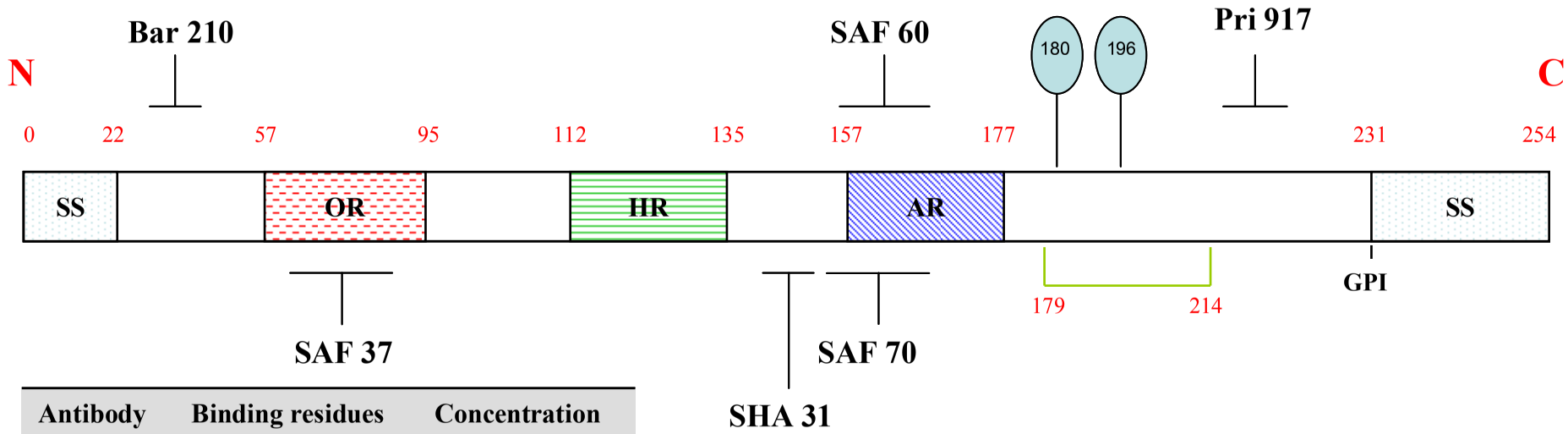

Antibody	Binding residues	Concentration
Bar 210	26 – 34	1/5,000
SAF 37	59 – 89	1/10,000
SHA 31	145 – 152	1/5,000
SAF 60	157 – 161	1/5,000
SAF 70	156 – 162	1/5,000
Pri 917	216 – 221	1/2,000

Figure 8 Binding sites along the prion protein of six primary antibodies (Bar 210, SAF 37, SHA 31, SAF 60, SAF 70 and Pri 917) utilized for immunoblotting. Green linker between residues 179 – 214 indicates disulphide bond with two N-linked glycosylation sites at residues 180 and 196 (blue lollipops). SS: Signal sequences; OR: Octapeptide repeat region; HR: Hydrophobic region; AR: Amphipathic region; GPI: Glycosyl-phosphatidylinositol anchor region. Table (inset) displays the binding sites and working concentration of each of the six primary antibodies.

2.9. ANIMAL BIOASSAY STUDIES

Animal bioassays were carried out by our collaborators at the CEA, Fontenay-aux-Roses, France under the supervision of Dr E. Comoy using previously published methodology (Fichet *et al.*, 2004; Fichet *et al.*, 2007c).

Normal and artificially degraded surgical grade 316L stainless steel wires were prepared and contaminated as detailed in section 2.3.1 and 2.3.2 respectively and inoculated with 10 % (w/v) 263K scrapie-infected brain homogenate. Decontamination of the wires was carried out as described in section 2.4.2.

Following exposure, the wires were individually implanted into the prefrontal subcortical region of anesthetized 6 week-old Syrian golden hamsters. The animals were regularly monitored for clinical signs of TSE and sacrificed at the terminal stage of disease. Diagnosis of prion disease was confirmed by the immunohistochemical detection of PrP^{res} in the brains according to a previously described protocol (Barret *et al.*, 2003).

2.10. HOSPITAL STERILE SERVICE DEPARTMENT (SSD) STUDIES

This work was carried out with the assistance of The Basingstoke and North Hampshire Hospital Sterile Service Department.

2.10.1. An Assessment of the Effectiveness of a Validated Washer-Disinfector Cleaning Cycle

A set of new instruments was allowed to progress through an initial cleaning cycle upon removal from the manufacturers packaging. The instruments were then sent to the operating theatre and, upon return to the SSD, were cleaned according to an automated washer-disinfector cycle similar to those detailed in section 2.4.1. This cycle of cleaning incorporated a PRE-Klenz™ pre-soak and wetting agent (STERIS Ltd) immediately after use in the operating theatre. The instruments were kept immersed in this wetting agent until loading into the washer-disinfector. They were then decontaminated using an automated HAMO T-21 washer disinfector cycle incorporating HAMO™ 100 (STERIS Ltd; 0.4 % (v/v), 4 min). In addition, a set of instruments was removed from circulation following failure of

visual inspection. The instruments were packaged for transport and taken for microscopic analysis following fluorescent labelling for general protein using SYPRO Ruby.

2.10.2. An Assessment of the Acquisition of Proteinaceous Contamination Through Handling by SSD Staff in the Clean Room

Two new sets of surgical instruments were recovered after ten surgical procedures and confirmed to possess similarly low levels of proteinaceous contamination. Each set included plain dissecting forceps, scissors angled on flat, Hagar dilator, straight mosquito forceps, curved mosquito forceps, and curved Dunhill artery forceps. Following a subsequent cleaning cycle in the SSD washer-disinfector unit, staff in the clean room were instructed to handle one instrument set with bare hands as per normal SSD operating procedures carrying out a visual inspection of each instrument. The other instrument set was handled in an identical way by staff wearing standard latex gloves. Each instrument set was then sterilised through a high temperature and pressure autoclave treatment and taken for staining using SYPRO Ruby.

Analysis was performed using a previously published contamination index (Lipscomb *et al.*, 2006b; Lipscomb *et al.*, 2007c). This index utilises an increasing scale from 0 – 4 taking into account surface coverage as well as particulate height and width to rapidly assess proteinaceous contamination of a surface. For example, Index 0 refers to no visible contamination. This increases to Index 4 where surface coverage is <50 % and contaminant height and width exceed 20 – 100 μm and 50 μm respectively. Representative photomicrographs of contamination index scores are shown in Figure 9.

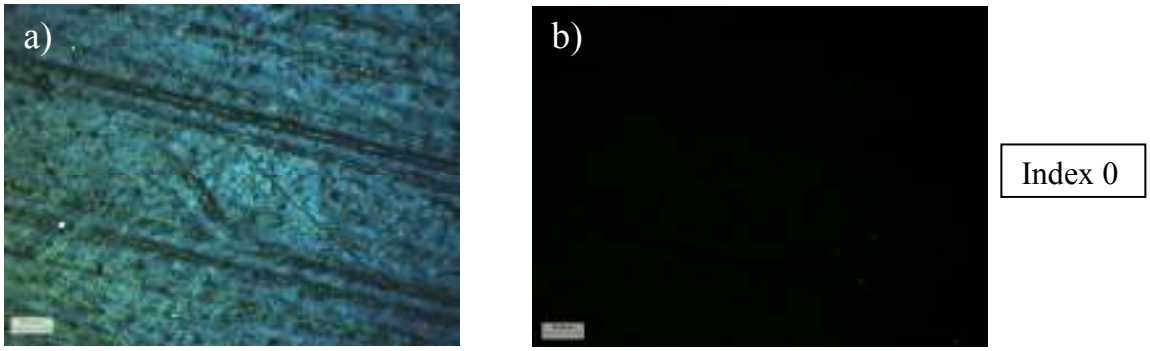

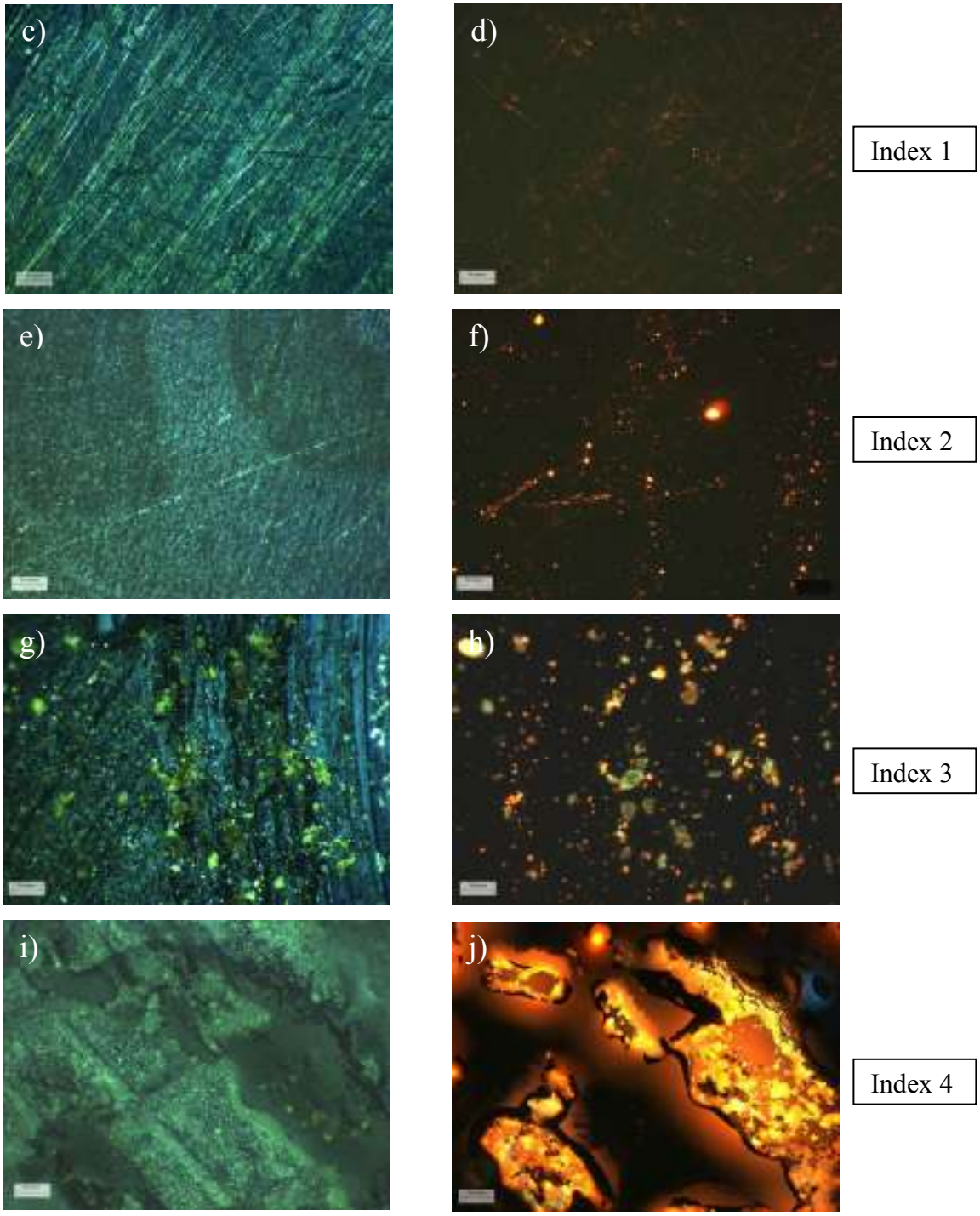

Figure 9 Representative photomicrographs showing increasing contamination of surgical instrument relative to the increasing contamination index; (a),(c),(e),(g),(i) display white light images taken of the instrument surface, (b), (d), (f), (h), (j) show the corresponding SYPRO Ruby images of the identical instrument region. Taken from Lipscomb *et al*., 2006c.

Twenty areas displaying representative instrument contamination were photographed from four separate areas of the instrument surface; the handle, arm, joint and tip/blade. In a blind study, using comparative photomicrographs of the contamination index, five volunteers

allocated scores accordingly for each of the images. Each of the four areas of each instrument was then given a mean contamination index value.

CHAPTER 3

ASPECTS OF THE DECONTAMINATION OF SURGICAL INSTRUMENTS IN HOSPITAL STERILE SERVICE DEPARTMENTS

3.1. INTRODUCTION

The effective implementation of decontamination procedures within SSDs is crucial in order to render re-useable surgical instruments safe for both patients and hospital staff. The build up of organic material such as tissue and bodily fluids through inefficient instrument reprocessing can decrease the effectiveness of subsequent disinfection and sterilisation procedures (Ransjo *et al.*, 2001). Other solutions such as iodine and saline can also discolour and corrode stainless steel if allowed to dry for any length of time (Khammo & McDonnell, 2006).

The inherent risks to a patient's health during surgical procedures increase when preceded by poor ineffective decontamination processes. Blood borne pathogens such as the Hepatitis B virus (HBV) represent a particular concern for both medical and dental practices (Lowe *et al.*, 2002). The risk of iatrogenic transmission of vCJD through neurosurgical procedures creates further problems for SSDs due to the resistance of the causative prion protein to standard sterilisation methods (Gibbs, Jr. *et al.*, 1994).

Using EDIC/EF microscopy it is possible to visualise both proteinaceous and non-proteinaceous contaminants *in situ* without the need for elution of soiling from the instrument surface which can decrease the sensitivity of detection (Keevil, 2003; Lipscomb *et al.*, 2006b). Rather, the sensitivity of EDIC/EF microscopy is in fact influenced by the choice of fluorescent stain. SYPRO Ruby is a luminescent metal chelate stain incorporating ruthenium into an organic complex with the capacity to fluorescently label proteins. A previous study has demonstrated a detection sensitivity of 0.25-1 ng protein/mm^2 on PVDF membranes (Berggren *et al.*, 1999). However, coupled with EDIC/EF microscopy, SYPRO Ruby has been shown to be able to fluorescently label protein concentration of <400 pg/mm^2 on surgical grade stainless steel (Lipscomb *et al.*, 2006b). This technique has lead to the proposal and subsequent application of a contamination index able to sensitively and rapidly assess instrument contamination levels as a function of particulate size and area coverage (Lipscomb *et al.*, 2006b; Lipscomb *et al.*, 2007c).

In this chapter EDIC/EF microscopy, coupled with SYPRO Ruby, has been utilised to evaluate the effectiveness of SSD decontamination procedures. An initial assessment was performed to evaluate the efficacy of a decontamination cycle within a sterile service department. A set of new instruments was recovered after a single surgical procedure and subsequent decontamination. *In situ* levels of protein contamination were compared against a significantly older set of instruments where one device had failed a visual inspection.

In addition, concerns regarding the potential for reapplication of contamination onto instruments following cleaning were addressed, specifically the risk of unnecessary transference of proteinaceous contamination following cleaning through instrument handling by department staff. The transference of protein by a single fingerprint onto a PVDF membrane as detected by SYPRO Ruby has been shown previously although this has not subsequently been demonstrated on stainless steel (Berggren *et al.*, 1999). Importantly, handling of the instruments following a washer-disinfector cycle is performed in a clean room prior to sterilisation, typically in high temperature and pressure autoclaves. As a result, contamination applied within the clean room is likely to be encrusted onto the instrument due to the sterilisation process, therefore decreasing the effectiveness of further decontamination procedures.

3.2. MATERIALS AND METHODS

The methodology for this section of work is described in Chapter 2. An initial assessment of a washer-disinfector cycle in use at The Basingstoke and North Hampshire Hospital sterile service department was undertaken as described in section 2.10.1. In addition, the risk of transmission of proteinaceous contamination onto surgical instruments following cleaning by means of handling by the SSD staff in the clean room was addressed. Laboratory studies to determine the potential for protein transference by hand onto stainless steel tokens are described in section 2.3.3.1. In addition, stainless steel wires were prepared as described in section 2.3.1 and inoculated with hamster NBH. To evaluate the effect of high temperature and pressure sterilisation on the tenacity of proteinaceous wire contamination to subsequent removal the wires were treated as detailed in section 2.4.1. Subsequent to this, the impact of protein deposition by handling, and its alleviation by implementation of gloves, on the total protein levels on surgical instruments was determined (section 2.10.2). Fluorescent labelling of proteinaceous contamination on all stainless steel instruments and tokens was performed using the luminescent compound SYPRO Ruby, as detailed in section 2.5.1, and analysis was completed using EDIC/EF (section 2.7 and 2.7.1).

3.3. RESULTS

3.3.1. Evaluation of a Washer-Disinfector Cycle

The effectiveness of a single washer-disinfector cycle was evaluated on a set of new instruments which had undergone a single surgical procedure and fully decontaminated according to the department's SSD protocols for instrument reprocessing. Visual inspection of the instruments identified low levels of proteinaceous contamination across several locations of the device; including the tip/blade, outer surface and the hinges or box joints (Figure 10). However, protein deposition was visualised at relatively low concentrations, often associating with areas of scarring or abrasion (Figure 10e) and insignia branding sites (Figure 10f).

A significantly larger concentration of proteinaceous contamination was observed on devices within a set which had previously failed a visual inspection (Figure 11) relative to the new instruments. As noted upon inspection of the new set of instruments, protein deposition was often situated around and within damaged or heavily scarred regions of the devices (Figure 11a and 11d). The damage observed on the instruments was increasingly more severe than that observed on the new instruments. However, there was also a marked increase in *in situ* protein observed within box joints (Figure 11c and 11d), teeth (Figure 11e and 11f) and on the outer surface (Figure 11a and 11b).

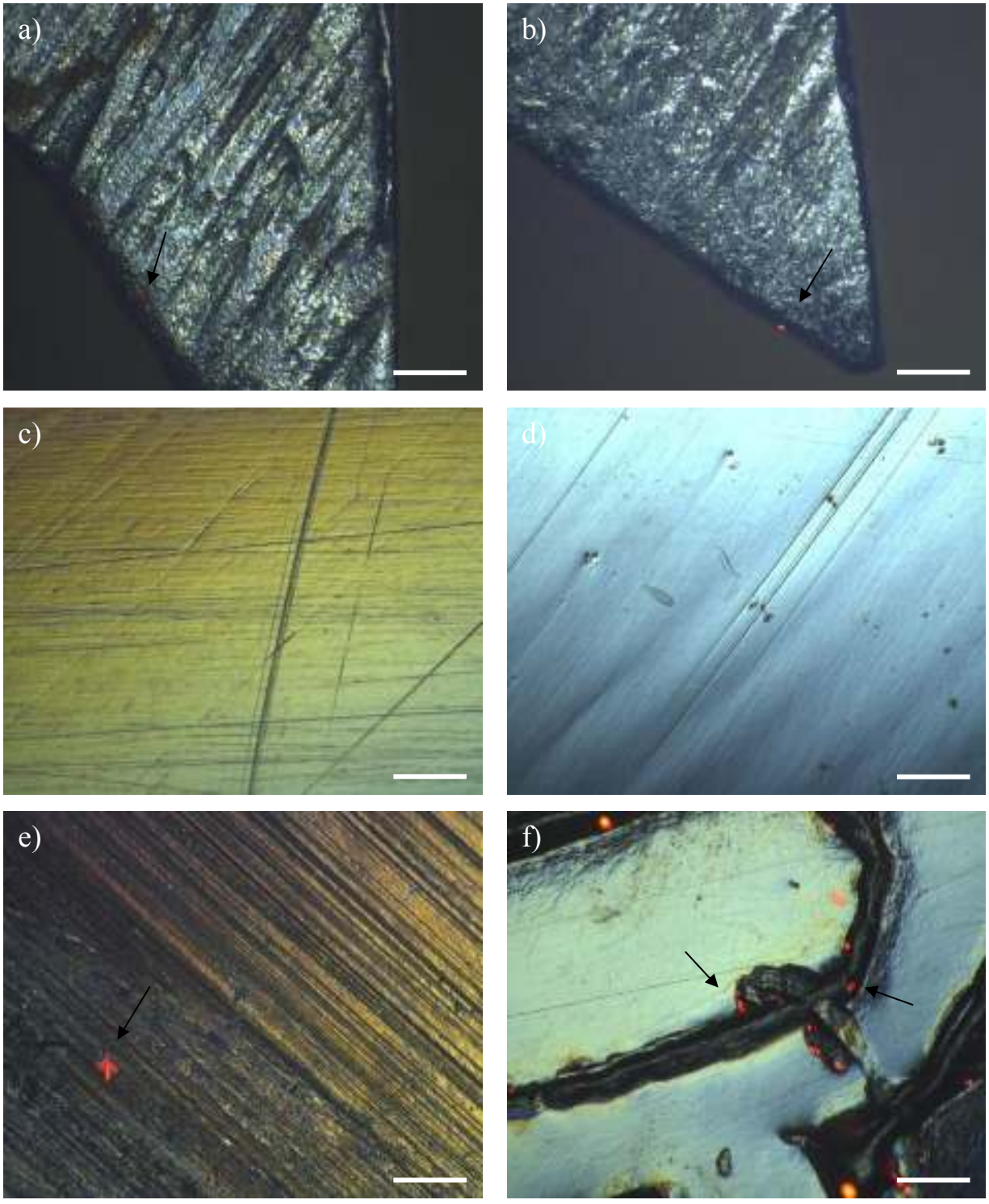

Figure 10 Representative photomicrographs taken using EDIC/EF after staining of proteinaceous contamination on surgical instruments using SYPRO Ruby and following a single surgical procedure and decontamination cycle. a) & b): instrument blade tip, c) & d): outer surface of instrument, e): box joint, f): manufacturer insignia branded onto instrument surface. Arrows indicate areas of protein deposition. Scale bars: 100 µm

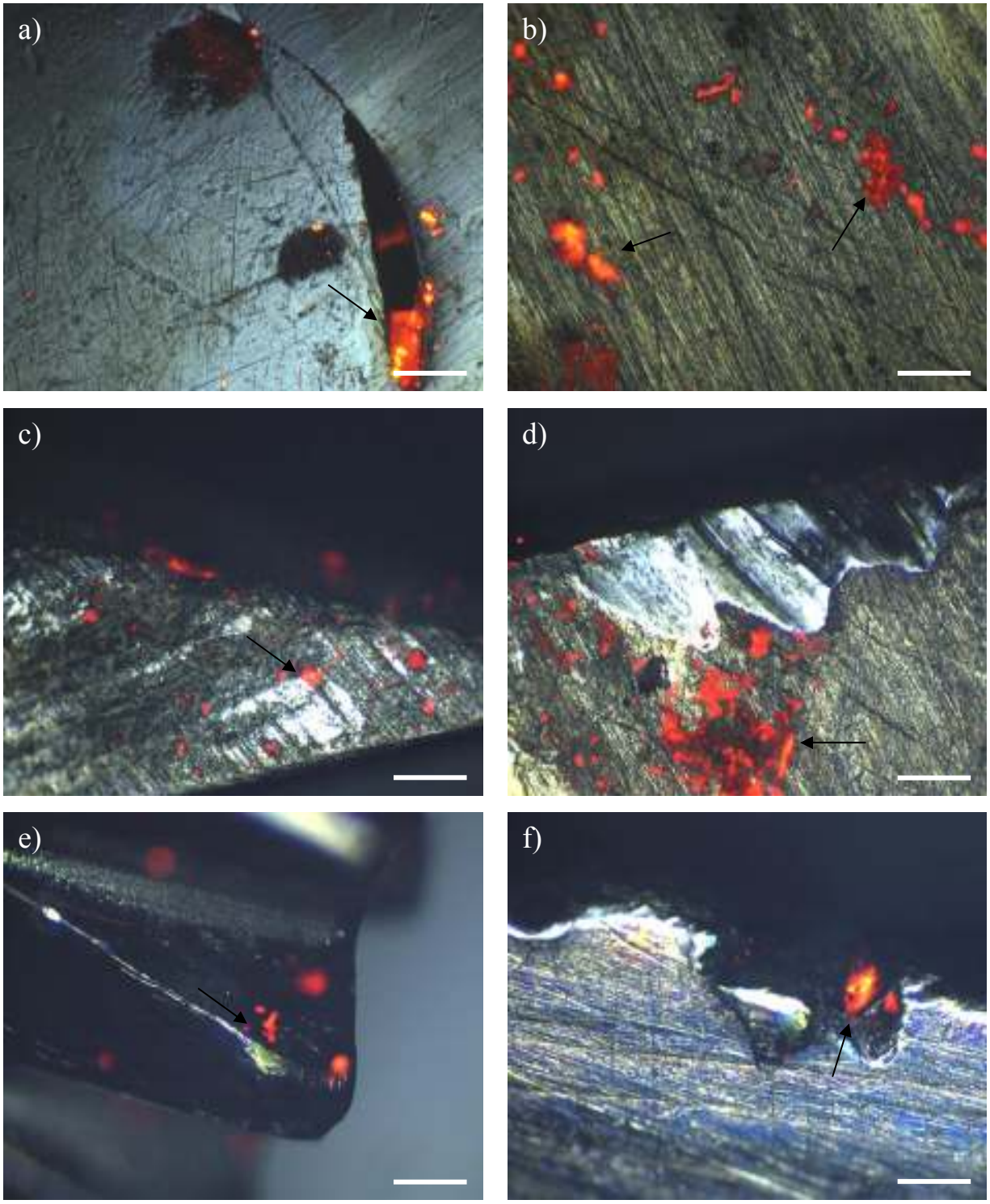

Figure 11 Representative photomicrographs taken using EDIC/EF after staining of proteinaceous contamination using SYPRO Ruby on surgical instruments removed from circulation due to a failure of a device during visual inspection. a) & b): outer surface of instruments, c) & d): box joints, e) & f) blade/tip. Arrows indicate areas of protein deposition. Scale bars: 100 µm

3.3.2. Protein Contamination of Stainless Steel by Hand

Using a known concentration of brain homogenate extract stained with SYPRO Ruby as a standard reference, the quantity of protein transferred onto stainless steel through handling was calculated (Figure 12 and 13). One thumb print was able to transfer 0.51 ng/mm^2 of protein. Handling, as mimicked by ten thumb prints to the surface of the token, corresponded to a mean level of proteinaceous contamination of 0.67 ng/mm^2. Statistical analysis showed that there was no significant difference between the mean concentration of protein observed following a single thumb print and handling of the tokens with bare hands (P = 0.24). Importantly, <0.06 pg/mm^2 was detected on the surface of the token following a thumb print by a gloved hand. This concentration was not statistically different from the quantity of protein observed on clean, untouched control tokens (P = 0.195).

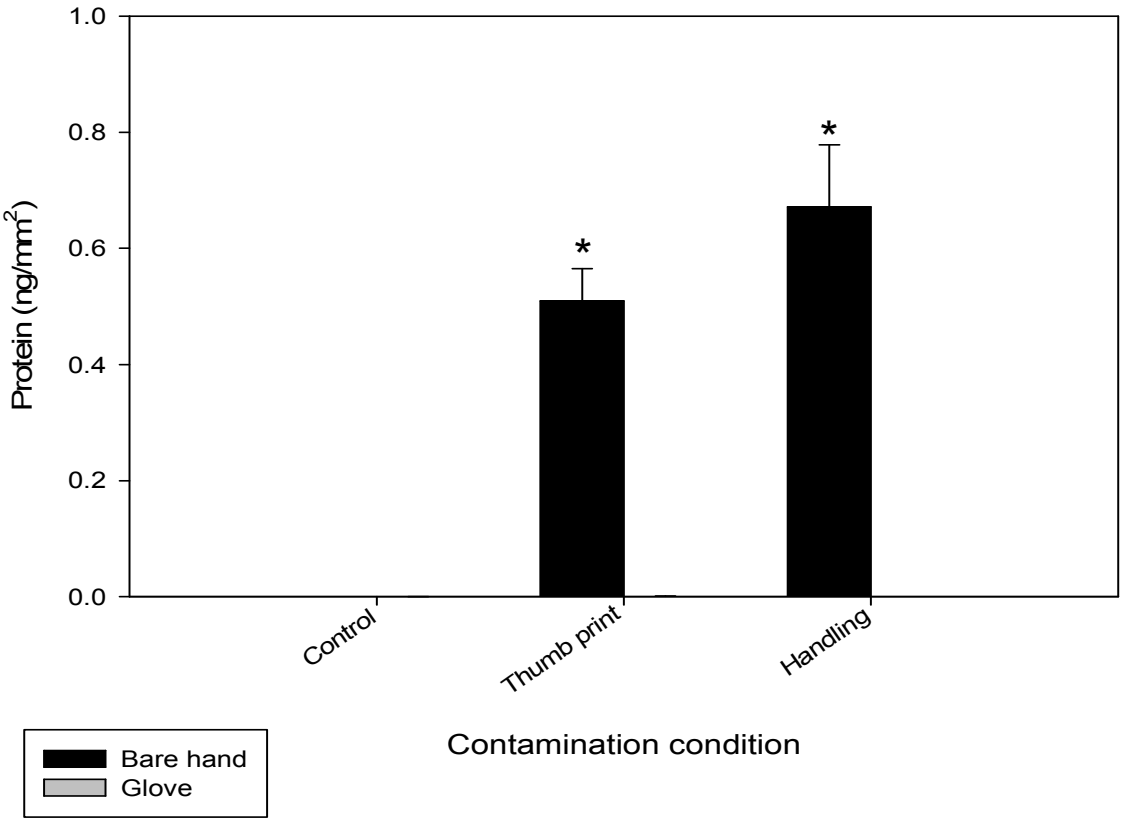

Figure 12 Mean levels of proteinaceous contamination observed on stainless steel tokens (n=6/treatment condition) following either a thumb print or handling using bare and gloved hands. * denotes two sets of data with no statistically significant difference as calculated by a T-test to compare data means.

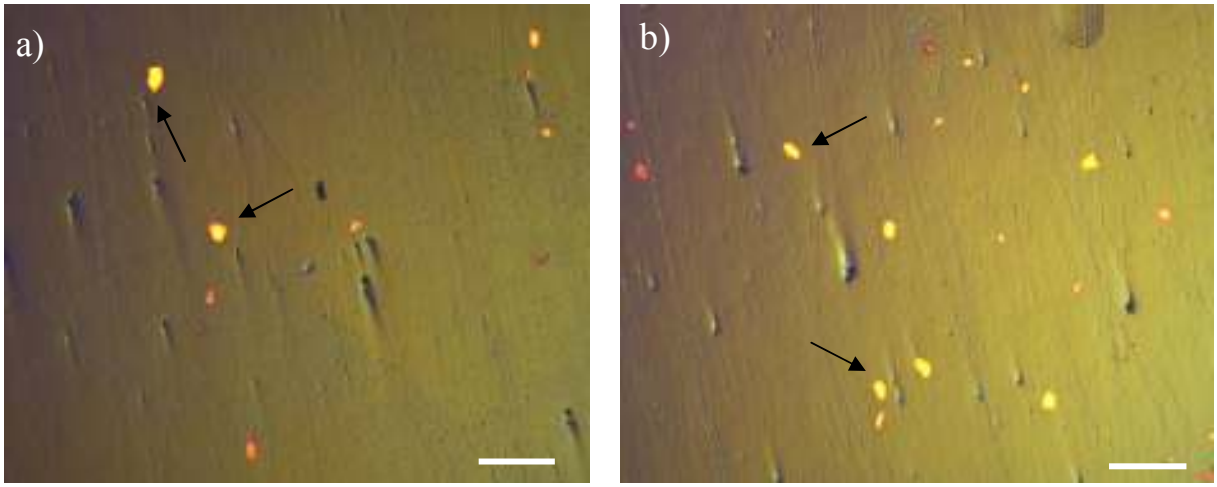

Figure 13 Representative photomicrographs of the surface of stainless steel tokens (n=6/ treatment condition) following contamination with bare hands from a) a single thumb print and b) handling. Arrows indicate several proteinaceous deposits. Scale bars: 100 μm.

3.3.3. Protein Contamination of Surgical Instruments by Hand

Assessment of proteinaceous contamination using the contamination index is displayed for each individual instrument as well as instrument sample regions in Figure 14. Each instrument handled by staff wearing gloves displayed a statistically significant decrease in the mean contamination index score ($P = 0.0$ for five of the six instruments, $P = 0.012$ for straight mosquito forceps). For five of the instruments analysed, this difference corresponded to an approximate one index score less than corresponding instruments handled with bare hands. Representative photomicrographs of protein deposits taken *in situ* on the surface demonstrated the increased level of contamination of instruments handled by bare hands (Figure 15). Instruments handled with gloved hands demonstrated much lower concentrations of protein contamination, despite the surfaces appearing heavily scarred and pitted due to repeated cleaning cycles. Interestingly, many of the protein deposits visualised on the instruments showed similarities in size and estimated protein concentration with those observed on the stainless steel tokens (~15 μm diameter, 9.71 pg ± 0.8).

Isolation of the contamination index scores by sample region also demonstrated a statistically significant difference between the two handling conditions (inside hinge and arm: $P = 0.0$, blade/tip and outside hinge: $P = <4 \times 10^{-7}$). An increase in index score by a factor of one was observed on the outside hinge joint and arm sampling regions of instrument handled by bare hands. The difference in score was less pronounced from inside the hinge joint and the

blade/tip sampling regions, although significant proteinaceous contamination was observed in these sampling regions relative to instruments handled with gloves.

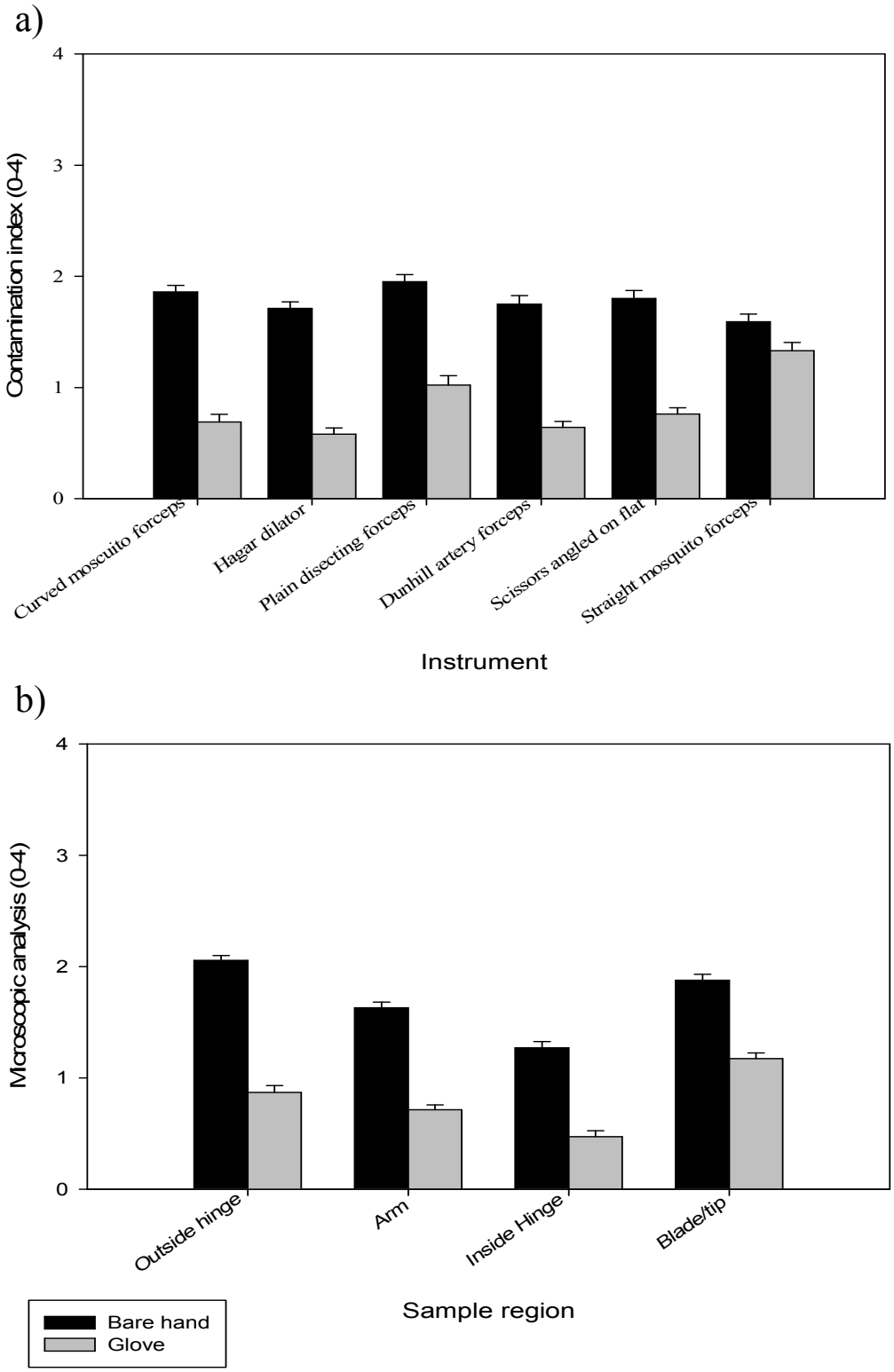

Figure 14 Mean contamination index scores obtained attributed to surgical instruments (n=6/set) under two separate handling conditions within the clean room prior to sterilisation. a) contamination index expressed as variations between instruments within a single set; b) regional variation of mean contamination index scores for all six instruments.

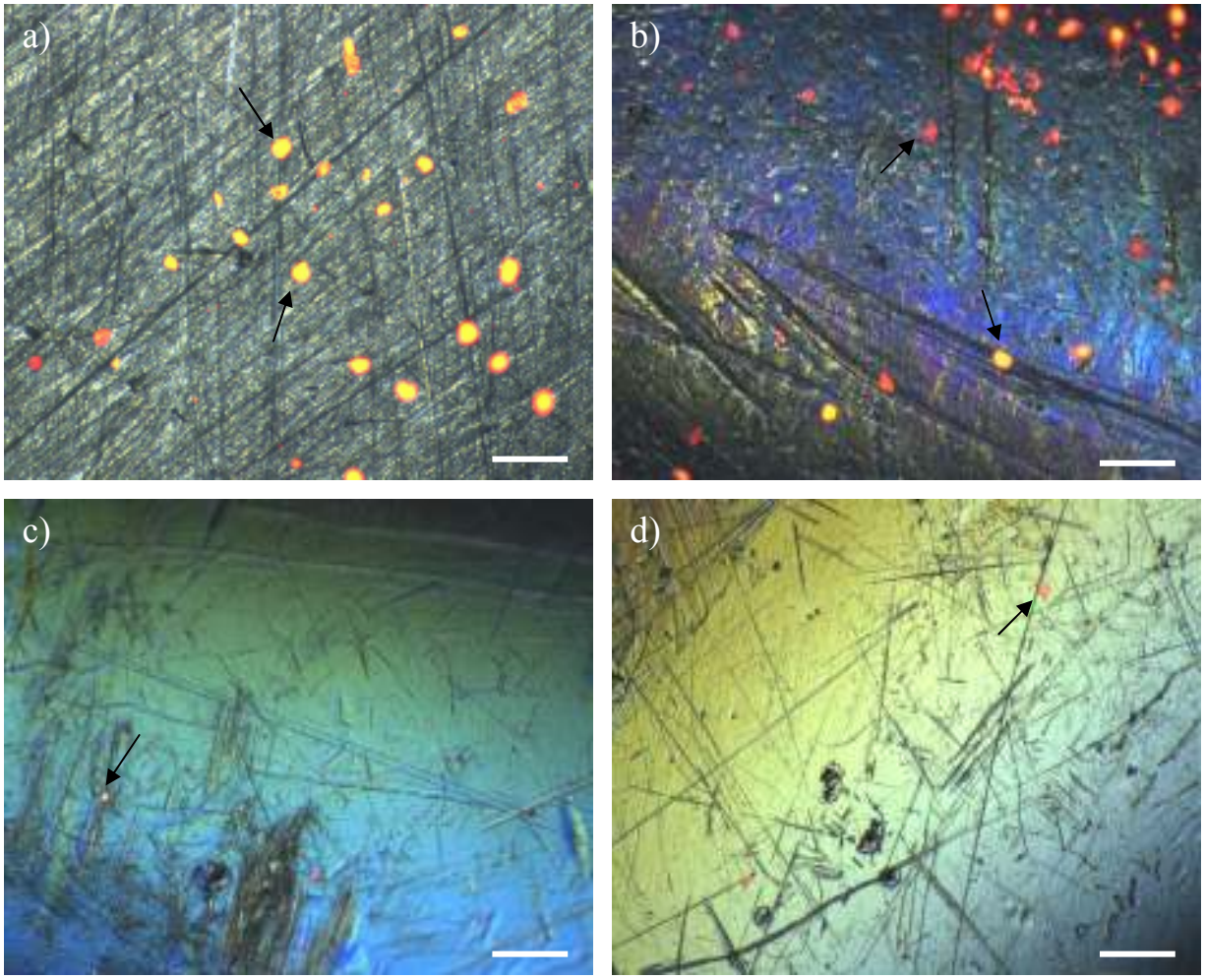

Figure 15 Representative photomicrographs taken using EDIC/EF microscopy of surgical instruments (n=6/set) following handling with bare hands; a) & b) and gloved hands; c & d) within the clean room prior to sterilisation. Arrows indicate several proteinaceous deposits. Scale bars: 100 µm.

3.3.4. Effect of Autoclave Treatment on Protein Attachment to Stainless Steel

Hamster NBH control wires demonstrated a protein surface coverage of 7.1 ng/mm^2, as identified by SYPRO Ruby (Figure 16). Following a 5 min rinse of control wires with deionised water subsequent to inoculation, total protein levels were markedly decreased, with a residual coverage of 0.17 ng protein/mm^2. In contrast, 11.7 ng/mm^2 of protein was detected on inoculated wires subjected to an autoclave treatment followed by a 5 min rinse in deionised water. There was no statistically significant difference in protein concentrations between control wires and autoclaved wires (Figure; P = 0.084).

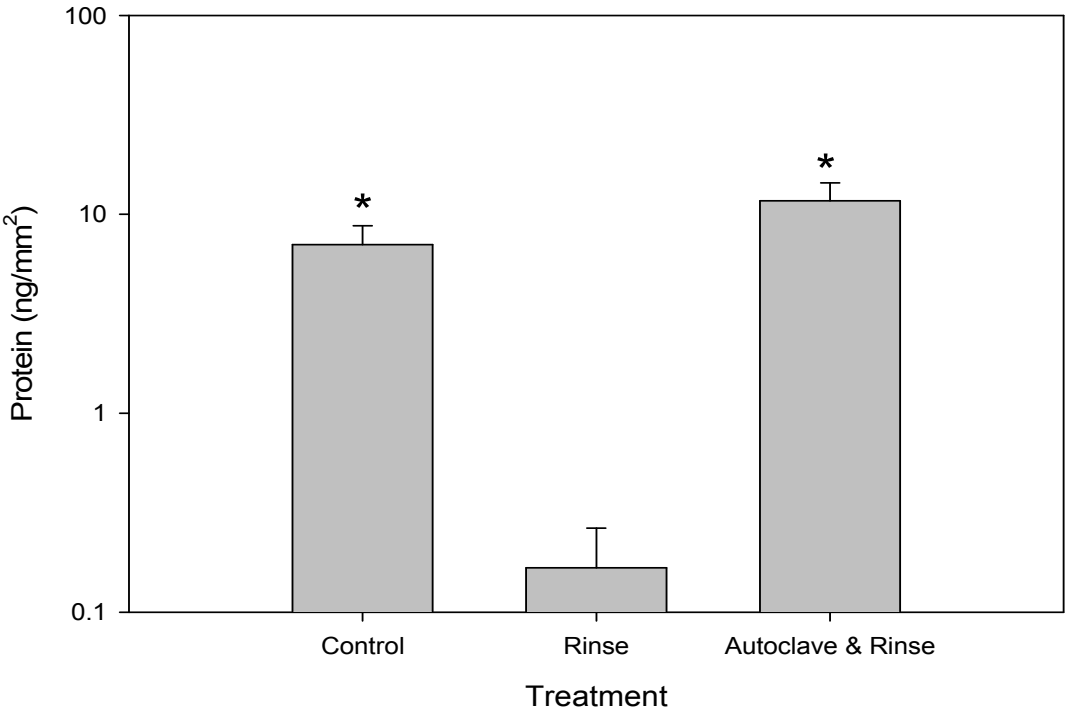

Figure 16 The effect of a high temperature and pressure autoclave treatment on the tenacity of bound protein to stainless steel wires (n=7/treatment group).* denotes two sets of data with no statistically significant difference as calculated by a T-test to compare data means.

3.4. DISCUSSION

Decontamination is an amalgamation of practices used to render a re-useable item safe for further use for both patients and staff (NHS Estates, 2003). The life cycle of a surgical instrument begins upon purchase, through both cleaning and disinfection to sterilisation and use. For efficient decontamination, high standards must be set and implemented at all stages of the life-cycle in order to minimise the risk of transmitting infection to a patient during surgical procedures. These high standards must involve the application of effective pre-cleaning procedures, such as the prevention of drying of soil onto instruments which has been shown to decrease the effectiveness of subsequent cleaning as well as damage and discolour stainless steel devices (Khammo & McDonnell, 2006; Lipscomb *et al.*, 2007b). Upon reaching the cleaning stage, it is crucial that an effective washer-disinfector cycle is employed. Failure of a validated washer-disinfector cycle to efficiently remove soiling from the device is likely to be amplified as an instrument ages. Damage and scarring through everyday use creates a surface

with a greater resistance to decontamination and the subsequent build-up of soiling over time is likely to lead to ineffectual sterilisation with a consequent increase in risk to the patient.

In this chapter, visualisation of proteinaceous contamination on both new and significantly older surgical instrument sets was performed. Each set had been decontaminated and sterilised using identical procedures for the duration of their use. This protocol included the use of a wetting agent to prevent the drying of surgical soil onto the instrument, followed by treatment with an alkaline cleaner within a validated washer-disinfector cycle. The instruments are then visually inspected and sterilised in high temperature and pressure autoclaves. The new set of instruments displayed low levels of *in situ* protein following fluorescent labelling with SYPRO Ruby suggesting an extremely efficient decontamination protocol for instrument reprocessing within this particular SSD. Detectable residual protein was located within areas of scarring and damage, as a likely result of the manufacturing process or preceding surgical procedure, or within the heavily blemished area of the producer's insignia. In contrast, the older instruments demonstrated markedly increased degrees of scarring and damage to the surface. As a consequence, the effectiveness of the decontamination process has been reduced with the accumulation of large concentrations of residual protein associating with these areas of damage. However, large concentrations of proteinaceous contamination were also visualised on areas of the instruments such as the box joints, teeth and outer surface. Given the absence of protein in these areas on the new instruments and the efficiency of the instrument reprocessing protocol this suggests that residual protein in these areas is a likely result of inaccessibility of the areas to the actions of the decontamination process. This may be a result of the complexity of the instruments (in the case of the teeth or box joints) or due to poor loading practice of the instruments into the washer-disinfector. The latter may also explain the presence of large concentrations of proteinaceous deposition on the outer surface of the instrument in the absence of any association with areas of damage or scarring. However, protein deposition onto the instrument surface is also feasible following cleaning within the washer-disinfector.

The majority of focus into the effectiveness of SSD practices centres on two main stages of an instrument life cycle: instrument treatment immediately after use in surgical theatre and the effectiveness of various cleaning chemistries at the removal of general bioburden and pathogens. However the process of handling and cleanliness evaluation within the clean room has the potential to reinstate contamination onto instruments following cleaning if not properly controlled.

This chapter has addressed the influence of current clean room practices in the handling of devices and the possibility for the transference of protein from hands to stainless steel instruments. Laboratory studies using stainless steel tokens were able to determine that a single finger print could apply an estimated 0.51 ng/mm^2 of protein. This figure did not increase significantly following mimicked handling of the token, whereby 0.67 ng/mm^2 was observed, demonstrating that one finger print can introduce a substantial quantity of protein onto stainless steel. Importantly, the use of standard laboratory nitrile gloves resulted in a significant reduction in the concentration of protein applied to the token following a thumb print and none following mimicked handling. The former displayed an observed protein concentration of <0.06 pg/mm^2 which was not statistically significant when compared to untouched controls. This level of protein detection on stainless steel is in agreement with previous studies demonstrating an increased sensitivity of fluorescent protein detection using the SYPRO Ruby protein stain when compared with the sensitivity of currently recommended Ninhydrin and Biuret tests for instrument cleanliness (9.25 μg and 6.7 μg protein, respectively) (Lipscomb *et al.*, 2006a).

Using a previously proposed contamination index, studies were conducted into whether handling in the clean room may contribute to observed levels of protein on surgical instruments within current SSD working procedures. Using the contamination index, an increase in index by a factor of one was observed on the majority of instruments relative to those handled by staff wearing gloves. This corresponds to an increase in field of view coverage from 1 – 2 % to 5 – 10 % following handling with bare hands, representing a five to ten-fold increase in proteinaceous contamination.

Data obtained from laboratory studies into the tenacity of stainless steel bound protein indicates that removal is more difficult when preceded by a high temperature and pressure autoclave treatment. There was no statistically significant difference between *in situ* protein detected on untreated control wires and those exposed to autoclaving at 121 ºC for 15 min followed by a rinse. The increase in mean protein on autoclave exposure wires relative to controls (11.7 ng/mm^2 and 7.1 ng/mm^2, respectively) is a likely result of structural alterations in protein as a consequence of high temperatures resulting in an increase in SYPRO Ruby fluorescence.

Assuming that subsequent sterilisation of instruments following handling in the clean room results in the fixation of 100 % or 75 % of the total protein estimated to be transferred by a single finger print, following 50 decontamination cycles, 25.5 – 19 ng/mm^2 of protein, respectively, will be present on an instrument as a result of current clean room handling

guidelines. Moreover, poor decontamination protocols will be amplified over any given time period as residual bioburden following each cycle of instrument reprocessing is heat fixed to the surface of the device. While unlikely to pose a direct risk to patient health, protein acquired by handling will add to the bioburden of an instrument and decrease the effectiveness of successive cleaning and sterilisation cycles. This will subsequently increase the risk to patient health over an instrument life-cycle as levels of fixed contamination rise. This study suggests that the implementation of gloves for use by SSD staff working within the clean room will ensure that the acquisition of soiling following cleaning is significantly reduced.

CHAPTER 4

DECONTAMINATION OF TISSUE PROTEIN AND PRION AMYLOID FROM SURGICAL STAINLESS STEEL DURING SIMULATED WASHER-DISINFECTOR CYCLES

4.1. INTRODUCTION

The prospect of asymptomatic carriers and long incubation periods in prion disease means that efforts to guarantee the prevention of iatrogenic transmission of prions must be actively sought (Collinge *et al.*, 2006; Peden *et al.*, 2004; Race *et al.*, 2001). This is coupled with the pathophysiology of the infectious agent in both variant and sporadic CJD which is known to result in colonisation of extra-neural tissues suggesting a significant risk to patients undergoing a range of different surgical procedures (Bruce *et al.*, 2001; Glatzel *et al.*, 2003). Consequently, a variety of new decontamination measures have been proposed (Fichet *et al.*, 2004; Fichet *et al.*, 2007b; Jackson *et al.*, 2005). However, even without the implementation of these new procedures, the incidence of proven iCJD through surgery remains low. There have been only 7 cases of iCJD through contaminated neurosurgical instruments or intracerebral electrodes to date (NHS, 2006).

The negative influence of a single product on the efficiency of prion decontamination has previously been demonstrated (Yan *et al.*, 2004). As such, for the assessment of chemistries to be relevant to decontamination practices, they must be analysed within the context of the various pre-cleaning and validated cleaning steps to assure the safety of such practices. In this study, current decontamination processes in sterile service departments have been evaluated using simulated washer-disinfector cycles for the first time. Surgical grade stainless steel suture wires inoculated with scrapie brain homogenate were passed through an entire cycle incorporating no pre-treatment or a pre-treatment (with a transport gel, or an active enzymatic formulation). This was followed by an alkaline detergent based main wash and disinfection, with removal of wires after each stage. The effect of the concentration and contact time of the main-wash alkali detergent and the initial drying time of inoculum onto the wires were determined. *In situ* visualisation of the wires was carried out using EDIC/EF and a previously described dual staining technique (Hervé *et al.*, 2009). This method utilises a sensitive amyloid fluorophore, Thioflavin T, for *in situ* detection of prion-associated amyloid (Hervé *et al.*, 2009; Lipscomb *et al.*, 2007a). The surface was then counter-stained with SYPRO Ruby to fluorescently label total protein. As such, tracking of both general protein soiling and prion-associated amyloid, as a marker of disease, was performed throughout each stage of the decontamination process.

4.2. MATERIALS AND METHODS

The methodology for this section of work is described in Chapter 2. Standard stainless steel wires were prepared and inoculated with ME7 scrapie homogenate as described in section 2.3.1. Decontamination using laboratory simulated SSD decontamination practices was carried out as detailed in section 2.4.2. Following treatment, the wires were fluorescently labelled for both total protein and prion-associated amyloid (section 2.5.3) and analysed using EDIC/EF (section 2.7 and 2.7.1). Western blot analysis of the effectiveness of the enzymatic and alkaline treatments used in this study was carried out in suspension as described in section 2.8.1 and 2.8.3 using the mouse monoclonal antibody SAF 60 raised against hamster PrP codon 142–160. For Western blotting, exposure of the enzymatic (Klenzyme® Enzymatic Pre-soak and Cleaner; STERIS Ltd) was carried out at a concentration of 0.8 % (v/v) at room temperature for 5 min, identical to the wires. The alkaline detergent (HAMO™ 100; STERIS Ltd) was added at 0.4 % (v/v) and 0.8 % (v/v) at 45 ºC for 15 min.

4.3. RESULTS

The effect of the enzymatic pre-treatment and alkali detergent on PrP^{c}, PrP^{res} and its associated protease resistance was determined by Western blot using the primary antibody SAF 60 targeted to the central core of the prion protein (Figure 17). The enzymatic pre-treatment (which contains proteases) reduced the total detectable protein at room temperature; however PrP^{res} (indicated by resistance to 200 µg/ml of proteinase K) had only a slight reduction in the overall signal relative to controls. Treatment with the alkaline detergent (ingredients including potassium hydroxide) resulted in degradation of PrP^{res} and sensitisation to proteinase K, which was evident under exposure at the lowest test concentration (0.4 % v/v).

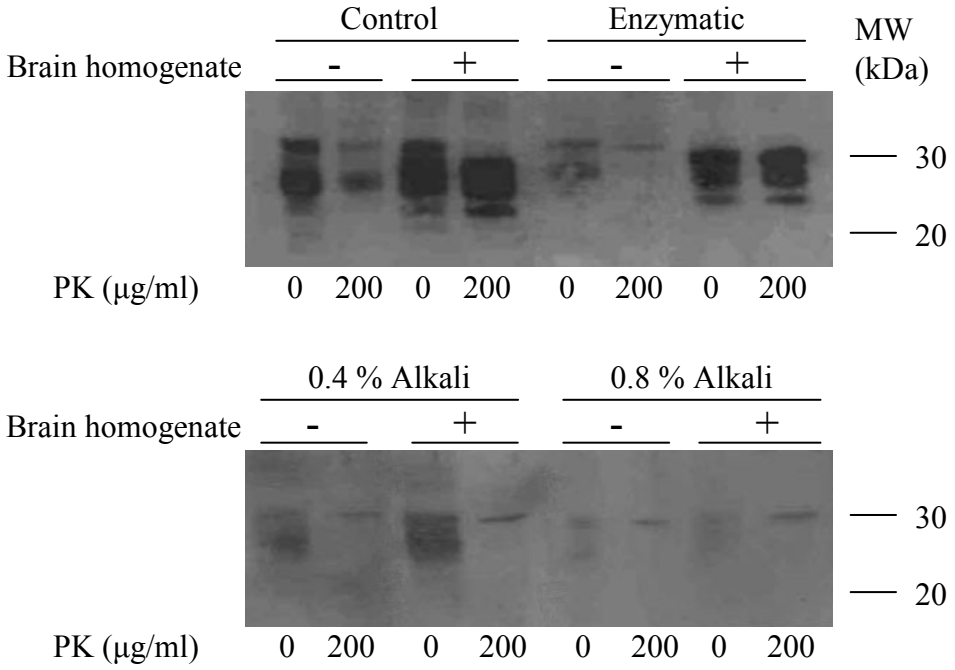

Figure 17 Western blot analysis demonstrating the effectiveness of PrP and PrP^{res} degradation in NBH (- brain homogenate) or ME7 (+ brain homogenate) upon treatment with an enzymatic pre-treatment or alkaline detergent. All lanes correspond to the analysis of 50 µg of brain equivalent.

A dual staining procedure to distinguish general protein contamination and prion-associated amyloid on surfaces was applied to wires subjected to various decontamination steps. Using a known protein concentration of brain homogenate as a standard, quantification of wire-bound protein was determined. From this, amyloid content was estimated as a function of the total protein. Thioflavin T positive signal observed on ME7-scrapie inoculated wires was normalised against non-specific fluorescent signal present on corresponding wires contaminated with NBH. Dual stain analysis of uninoculated wires confirmed the cleanliness of the wire surface prior to inoculation (data not shown). However, analysis of experimental control wires inoculated with nanopure water throughout each cycle phase allowed an overall cut-off value or limit of detection of 0.001 ng/mm^2 to be established. Consequently, wire bound contamination below this cut-off was not considered significant and the wires were assessed as clean.

Tracking of total protein and prion-amyloid removal was initially performed on a decontamination cycle integrating the pre-soak, an alkaline wash at 0.8 % (v/v) for 15 mins and disinfection (Figure 18a). It is important to note the brain inoculum had been allowed to dry for 16 h prior to testing. As a result, wires inoculated with normal or scapie brain

homogenates displayed less than a 1-log reduction in total protein following the pre-soak treatment and subsequent water rinse relative to controls. Similarly, levels of bound amyloid were not statistically different from those observed on control wires (T-test to compare data means; P = 0.519). Wires subjected to subsequent alkaline cleaning demonstrated a significant decrease in both total protein and amyloid.

Wires allowed to continue into the disinfection stage of the cycle demonstrated an increase in non-specific background signal in several cycles (Figure 19a and 19b). Consequently, whilst disinfection was included in subsequent cycles, analysis of residual amyloid levels was performed following alkaline washing. Importantly, an estimated 0.09 ng/mm^2 of prion-associated amyloid was found to remain on the wires following alkaline treatment in this cycle. Furthermore, at both pre-soak and alkaline treatment stages, decontamination of total protein as identified by SYPRO Ruby from wires initially inoculated with NBH was more efficient than the corresponding scrapie-infected brain inoculated wires (P = 0.00414 at the pre-treatment stage; P = 0.0179 following alkali treatment). However, subsequent cycle analysis showed that this apparent resistance of ME7-scrapie homogenate to decontamination over NBH was mainly prevalent during the pre-treatment stages (Figure 19)

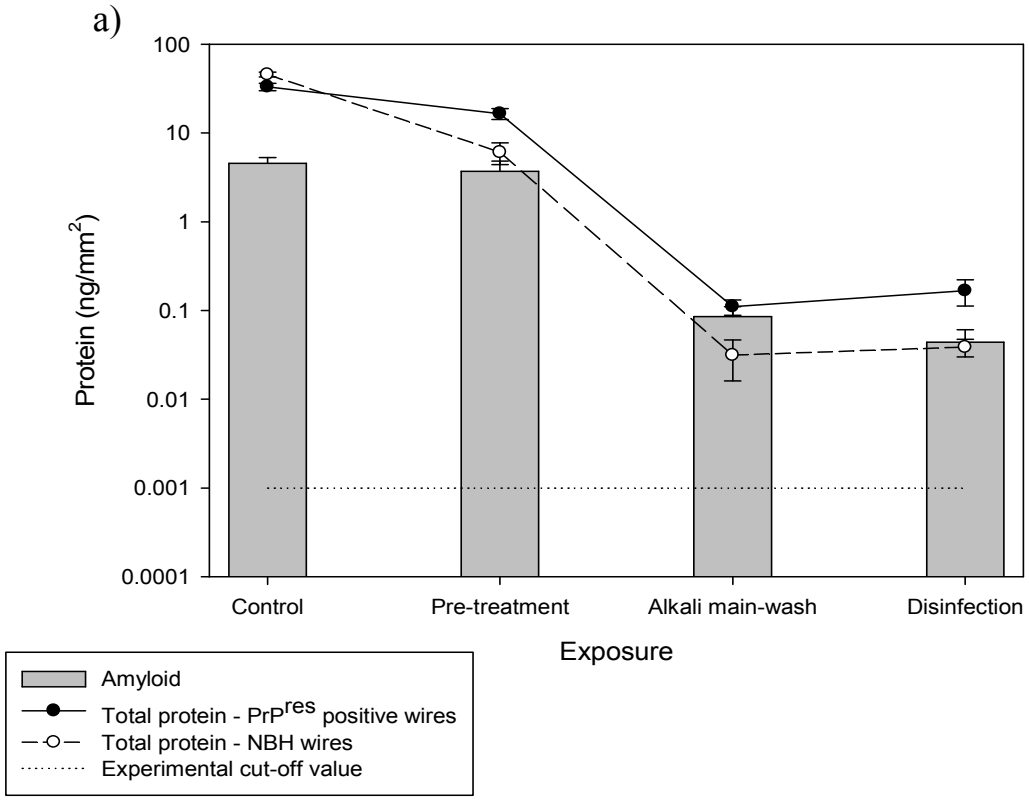

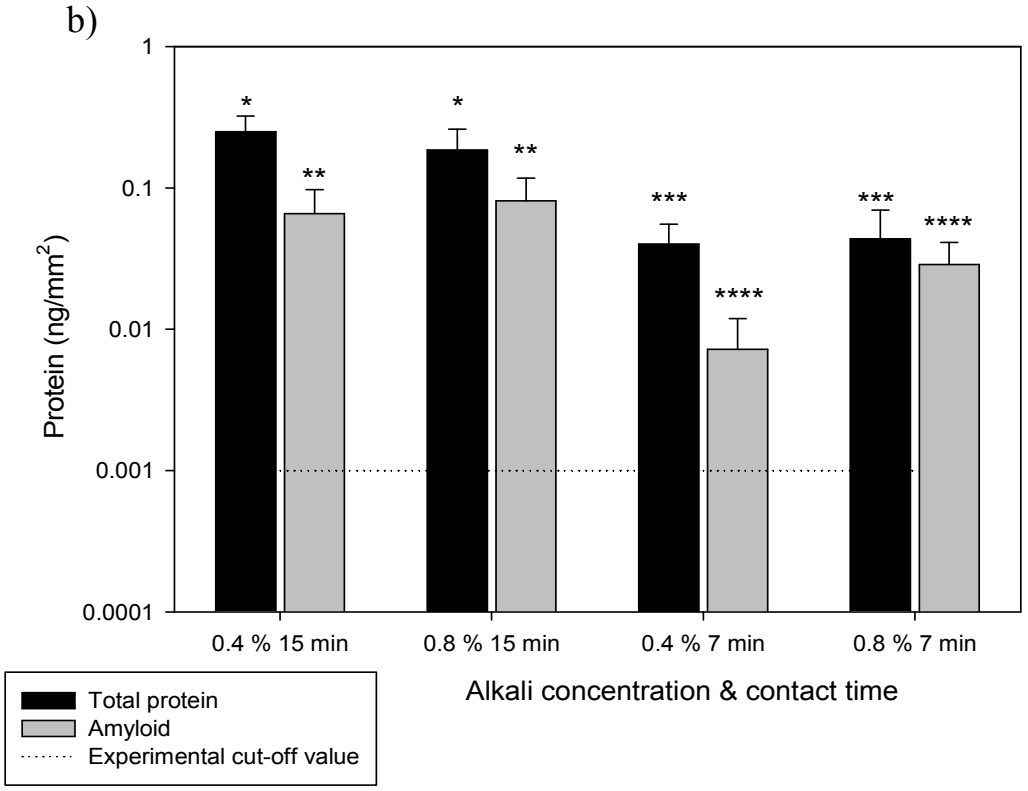

Figure 18 (a) Application of a dual stain method for the identification of total protein and prion-associated amyloid on surgical grade stainless steel wires (n=7/treatment group) subjected to a simulated washer-disinfector cycle. (b) Total protein and prion-associated amyloid on wires inoculated with ME7-scrapie homogenate and subjected to variations in alkaline cleaning contact time and concentration. *denotes two sets of data demonstrating no statistically significant difference as calculated by a T-test to compare data means.

Further analysis of decontamination cycles incorporated variations in pre-treatment and inoculum drying time. This analysis also involved the application of a reduced concentration of alkaline detergent from 0.8 % to 0.4 % and, in addition, a reduction in contact time from 15 min to 7 min. Results demonstrated that a reduction in concentration had no significant effect on either protein or amyloid removal within the 15 min and 7 min time cohorts, as denoted by pairs of corresponding asterixes in Figure 18b. Conversely, a reduced mean protein and prion-associated amyloid concentration was observed on wires under identical cycle conditions where the only parameter altered was a shorter contact time of the alkaline detergent. However, in all but one group (total protein between 0.4 %, 15 min and 0.4 %, 7 min; $P = 0.037$) this difference was not statistically significant (0.4 %, 15 min and 7 min amyloid: $P = 0.109$; 0.8 %, 15 min and 7 min protein: $P = 0.19$; 0.8 %, 15 min and 7 min amyloid: $P = 0.053$).

Comparison of variations in pre-treatment and inoculum drying time were assessed under alkali exposure conditions of 7 min at 0.8 % (v/v) concentration (Figure 19). The enzymatic pre-treatment was the most effective in terms of both total protein (Figure 19 a & b) and amyloid (Figure 19c) removal with a reduction of approximately 2-log in comparison to the pre-soak (which does not include any physical removal) under conditions where inoculum had been allowed to dry (Figure 19a). Following immediate processing after inoculation, the enzymatic pre-treatment was a further 1-log more efficient at removal of amyloid. In cycles where the pre-soak was utilised, immediate processing of the wires following inoculation resulted in a 2-log and 1-log reduction in total protein and amyloid respectively compared to dried soil wires.

a)

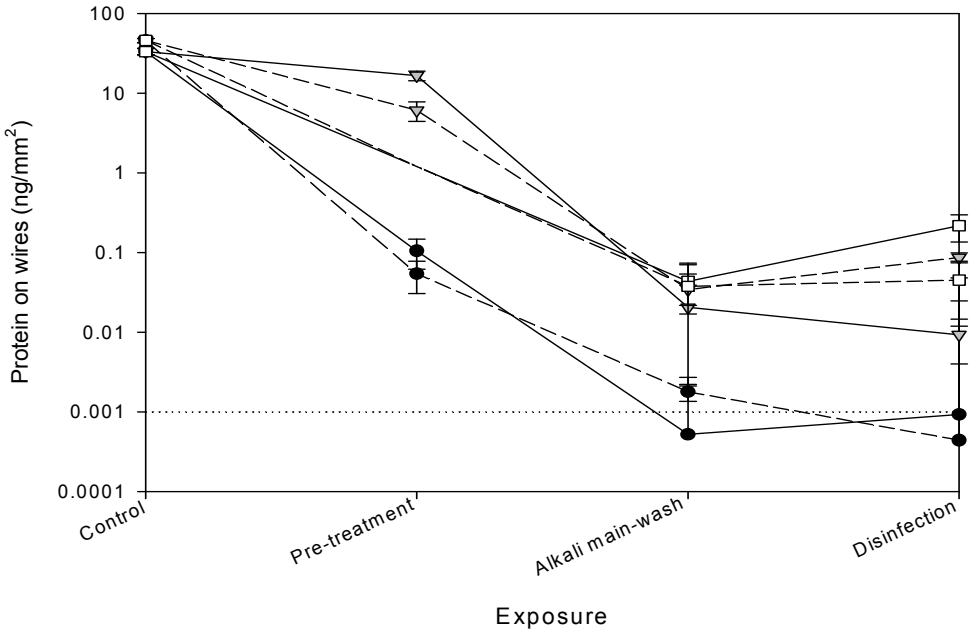

b)

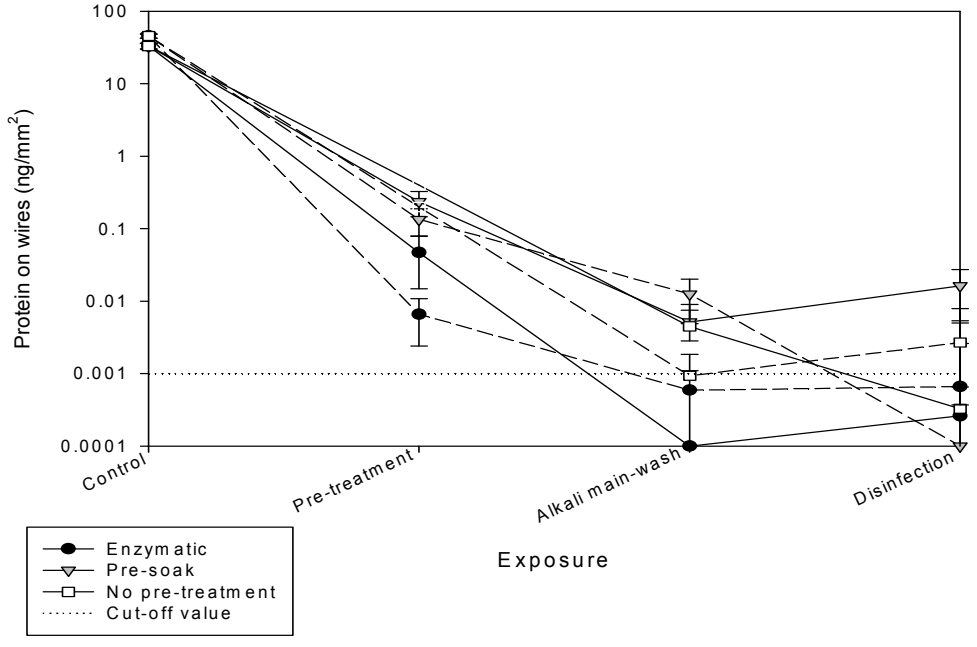

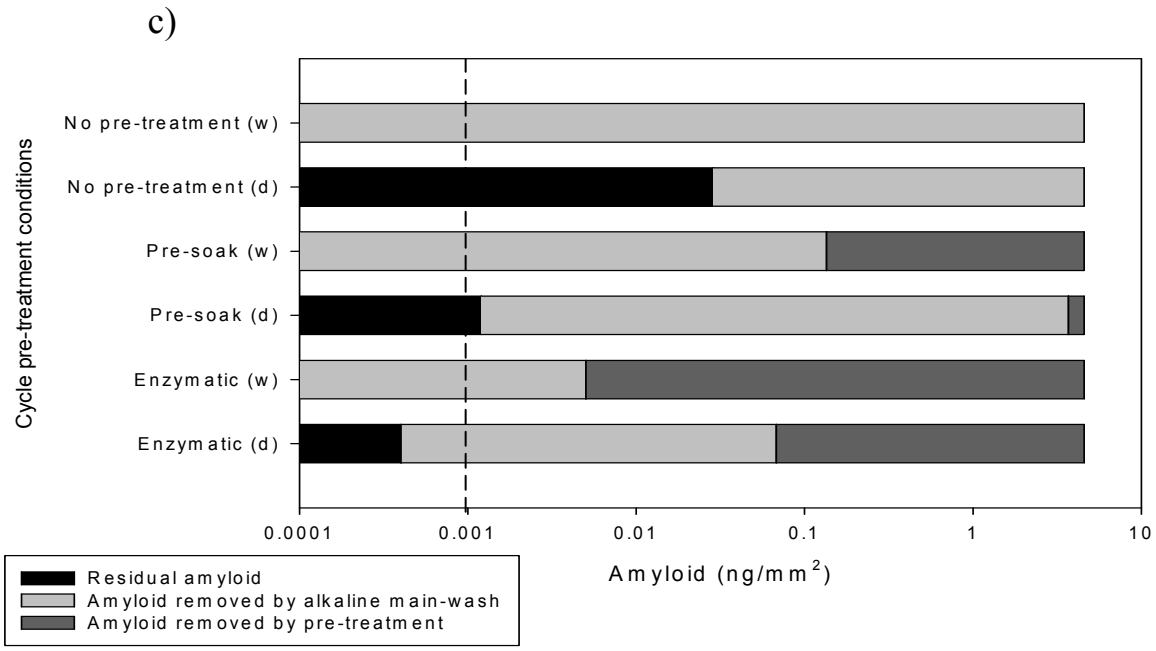

Figure 19 Tracking of total protein and prion-associated amyloid removal from stainless steel wires (n=7/treatment group) during typical decontamination cycles with variations in pre-treatment involving either an enzymatic cleaner, a pre-soak or in the absence of any pre-treatment. Exposure of the alkaline detergent was carried out for 7 min at 0.8 % in all cycles. a) Removal of total protein from wires where the inoculum was allowed to dry for 16 h before decontamination. b) Removal of total protein from wires where decontamination was initiated immediately following inoculation. Solid lines represent ME7-scrapie inoculated wires; dashed lines represent NBH inoculated wires. c) Mean residual amyloid on wires following different stages of a washer-disinfector cycle where decontamination was carried out following drying of inoculum for 16 h (d) or immediately post inoculation (w); line represents experimental cut-off value at 0.001 ng/mm^2.

Following alkaline treatment in a cycle beginning with the active enzymatic pre-treatment, total protein and prion-associated amyloid concentrations were reduced below the experimental cut-off value of 0.001 ng/mm^2. This occurred irrespective of whether the inoculm had been allowed to dry or not. Conversely, under either drying condition, residual total protein, as identified by SYPRO Ruby, was detected following alkaline treatment in cycles initiated with either the pre-soak or no pre-treatment with the exception of one cycle (Figure 19b; NBH inoculated, no pre-treatment wire cohort). However, there was no statistically significant difference in either ME7 or NBH total protein levels following alkaline cleaning between wires processed immediately or those dried for 16 h prior to

decontamination (pre-soak: ME7 P = 0.427, NBH P = 0.268; no pre-treatment:ME7 P = 0.179, NBH P = 0.061 using a T-test to compare data means).

With respect of prion-associated amyloid, alkaline cleaning subsequent to a pre-soak pre-treatment was able to completely remove detectable amyloid from the wires which were immediately processed (Figure 19c). Residual prion-associated amyloid following alkaline treatment on wires initially dried for 16 h was not significantly different from the experimental cut-off (P = 0.97). Critically, cycles which did not incorporate a pre-treatment step displayed an estimated 0.03 ng/mm^2 of residual prion amyloid on wires following drying of soil and treatment with the alkaline detergent. Similar to the two other pre-treatment conditions, immediate processing of the wires following contamination resulted in complete removal of detectable prion-associated amyloid through treatment with the alkaline detergent alone.

Importantly, correlation of EDIC/EF detection of prion-associated amyloid (Figure 19c) with the Western blot method (Figure 17) suggests a relative increase in sensitivity of the staining procedure. Both the Western blot and EDIC/EF detection method were capable of identifying residual PrP^{res} following treatment with the enzymatic pre-treatment. However, PrP^{res} signal by Western blot is almost completely removed following alkaline treatment, in contrast to EDIC/EF detection of prion-associated amyloid (Figure 19c; no pre-treatment).

4.4. DISCUSSION

The emerging pathophysiology of the infectious agent in prion disease suggests that iatrogenic transmission of CJD from surgical instruments should pose a greater risk to patient health than has currently been documented. Nevertheless, concerns remain over the lack of world-wide accepted methods for prion inactivation and reports persist over possible iatrogenic cases of CJD after neurosurgical procedures (Keeler *et al.*, 2006). In the UK for example, there have been 317 documented incidents of potential iatrogenic exposure to CJD from surgery between 1 January 2000 and 30 June 2007 where instruments potentially contaminated with the infectious agent have been subsequently re-used on further patients (Health Protection Agency, 2007). However, of these, only 17 incidents were considered to be in serious danger of exposure to CJD, with a further 72 considered “at risk” of CJD.

New decontamination procedures have been proposed to ensure the safety of surgical and medical devices as a result of the incompatibility of current WHO guidelines. To date, assessment techniques involve immunoblotting and animal bioassays. The lack of sensitivity

of the immunoblot technique has been well documented (Lipscomb *et al.*, 2007a; Solassol *et al.*, 2004). However, *in vivo* animal models have been developed which utilise an assay based on the insertion of stainless steel suture wires into the rodent CNS to simulate the contact of surgical instruments in living organisms (Zobeley *et al.*, 1999). The technique has been shown to detect infectivity down to a 1 x 10^{-6} dilution of positive scrapie brain into negative brain homogenate and is currently considered the best standardised *in vivo* model for evaluating prion inactivation ability (Fichet *et al.*, 2004; Fichet *et al.*, 2007c; Peretz *et al.*, 2006). However, experimental time-course, in addition to cost and ethical issues, limit the application of this method. Alternative cell culture methods are currently being developed but require further optimization although a recent assay for the detection of prions on stainless steel has been described which may provide an effective method to assess methods of decontamination (Edgeworth *et al*. 2009).

In this study, a fluorescent staining method has been applied to evaluate established decontamination procedures within the context of conditions for the reprocessing of surgical instruments currently used in the hospital environment. Thioflavin T, routinely used for amyloid detection and fibril formation studies, has demonstrated *in situ* levels of prion detection on stainless steel 2-log higher than that of standard Western blot and a maximal detection level in the picogram range (Colby *et al.*, 2007; Hervé *et al.*, 2009; Leffers *et al.*, 2005; Lipscomb *et al.*, 2007a; Roostaee *et al*., 2009; Stohr *et al.*, 2008). Several other studies have demonstrated Thioflavin T detection of oligomeric sub-species of murine tandem PrP and Aβ oligomers by analogues of Thioflavin T in fluorescence intensity studies (Maezawa *et al.*, 2008; Simoneau *et al.*, 2007). This suggests a sensitivity of Thioflavin T greater than the detection of aggregated amyloid deposits and is likely to include PrP^{res} molecules under certain experimental conditions. As such, this method represents a rapid and highly sensitive means for *in situ* detection of prion amyloid and analysis of prion decontamination techniques.

Utilisation of existing cleaning chemistries used for manual or automated cleaning cycles has confirmed previous reports on the reduced sensitivity of the Western blot technique relative to other detection assays (including EDIC/EF combined with Thioflavin T), to assess the effectiveness of PrP^{res} degradation. The removal or disruption of antibody binding epitopes, in addition to altered solubility of PrP^{res} following treatment, is likely to account significantly for this loss of sensitivity which procedures such as the EDIC/EF dual stain technique are not affected by. This study respresents the first application and critical assessment of the EDIC/EF dual stain method for the evaluation of decontamination procedures for which this assay was designed. Importantly, under conditions used to assess

decontamination, this study established an experimental cut-off of 0.001 ng/mm^2, 1-log lower than the picogram maximal level of detection previously described (Hervé *et al.*, 2009; Lipscomb *et al.*, 2007a). Moreover, following heat-treatment, an increase in background fluorescence of negative control/NBH wires was observed suggesting limitations of the dual stain under high temperature conditions where protein structural modification can occur.

Both EDIC/EF and Western blot methods were able to confirm residual PrP^{res} following enzymatic exposure. Immunoblotting suggests that the enzymatic treatment had no obvious effect on the structure of PrP^{res}, with the reduction in amyloid observed using Thioflavin T a result of removal from the wires rather than degradation. Previously published *in vivo* data, under identical wire preparation and disinfection conditions on the 263K scrapie strain, demonstrated transmission of disease in all rodent test subjects following treatment with the same enzymatic chemistry (Fichet *et al.*, 2004). Both the dual stain and Western blot procedures confirmed the presence of PrP^{res} in solution and bound to stainless steel following treatment with the main-wash alkali; although at varying sensitivities. However, the immunoblot assay suggests a sensitisation of residual PrP^{res} to protease degradation following treatment. No transmissible disease in the 283K animal model under 7 min exposure at 0.8 % (v/v) was observed in another study (Fichet *et al.*, 2007c).

Analysis of the effect of a reduction in the concentration of the alkali detergent on total protein and amyloid removed from stainless steel there was no statistically significant effect. A reduction in contact time of the alkali detergent led to a drop in mean residual protein and amyloid, although this was not significant in all but one case. It is unclear why reducing the contact time provided more efficient removal. The close correlation of data between the groups of wires where concentration was the only altered parameter would argue against variability within the test method suggesting it may be an effect driven by the formulation of the alkaline detergent.

Analysis of simulated decontamination cycles using the EDIC/EF dual stain method suggested that, predictably, the enzymatic chemistry used in this study was the most effective pre-treatment. Importantly, the data indicate that it is during the pre-treatment stage where the effects of soil drying time are most prevalent. The enzymatic pre-treatment was 1-log more effective at removal of prion-associated amyloid following immediate processing relative to dried inoculum. Moreover, following drying of the inoculum, addition of the pre-soak transport gel had little effect on protein removal and no significant effect on *in situ* amyloid. This is not surprising as the recommended use of this product is following immediate contamination in order to prevent soil drying. As such, immediate immersion in the pre-soak

gel following inoculation of the wires resulted in a 1-log reduction in amyloid and a 2-log reduction in total protein through a water rinse alone.

However, when taken in context of the end product of the entire cycle, soil drying time had no effect on the efficacy of cycles which incorporated pre-treatments. Concentrations of total protein demonstrated no statistically significant difference between drying conditions. Moreover, prion-associated amyloid levels were removed to levels below, or not significantly different from the experimental cut-off. Even in cycles without a pre-treatment, total protein levels were not significantly different between drying conditions. This implies that the subsequent alkaline wash used in this cycle was sufficiently effective to account for an unsuccessful, or lack of a pre-treatment in terms of protein removal in all cycles and, with respect to prion-associated amyloid in those cycles with pre-treatments. This data clearly highlights the need to assess decontamination in the context of an entire cycle rather than individual treatments.

Critically, it is important to note that cycles with no pre-treatment following drying of the inoculum were the least effective in terms of amyloid removal. A concentration of 0.03 ng/mm^2 of prion-associated amyloid was detected *in situ* on the wires. However, even in the absence of a pre-treatment, immediate processing of the wires following inoculation resulted in complete removal of detectable prion-associated amyloid.

This study has, for the first time in the field, assessed prion decontamination techniques within the context of typical reprocessing conditions in an SSD. It has demonstrated that not only the chemistry type but also the various decontaminations steps involved can have a profound effect on the overall outcome of instrument decontamination. Moreover, the data also demonstrate that whilst immediate processing was clearly beneficial in all cycles, even with soil drying, particular cycles were capable of significant, and in some cases complete reduction of detectable total protein and prion-associated amyloid. As a result, current decontamination processes, with validated chemical formulations, combined with the prevention of contaminant drying and/or immediate processing, are likely to provide a highly effective safe-guard against iatrogenic transmission of prions. This is in agreement with previous reports (Fichet et al., 2007a). Assuming these practises are carried out, it may also account for the low incidence of iCJD from surgical instruments.

CHAPTER 5

THE EFFECT OF SURFACE DEGRADATION ON THE EFFICIENCY OF PRION DECONTAMINATION

5.1. INTRODUCTION

Chapter 3 demonstrated that even with an effective decontamination cycle, a significant accumulation of surface proteinaceous material still occurs during the life cycle of a surgical instrument. Instrument bioburden is likely to increase in parallel with scarring and damage, thereby creating a surface which is less amenable to decontamination techniques.

The impact a heavily scarred surface may have on the efficiency of prion decontamination has not previously been assessed. The removal of PrP^{res} and infectivity is often assessed on prion-infected brain homogenate in suspension or using the stainless steel wire implant model, which do not represent a worst-case scenario in terms of a typical instrument surface which is likely to be encountered within an SSD.

Consequently, this chapter aims to assess the effect of surface degradation on prion removal. Stainless steel wires were artificially degraded using an immersion autoclave treatment in 1M sodium hydroxide. Following inoculation with 263K scrapie-infected homogenate, the effect of surface degradation on transmission and incubation period was assessed in untreated controls. *In situ* detection of total protein and prion-associated amyloid following various physical, chemical and enzymatic decontamination techniques was achieved using the fluorescent labelling technique described in Chapter 4. Correlation of this method with infectivity was also performed for the first time.

5.2. MATERIALS AND METHODS

The methodology for this section of work is described in Chapter 2. Standard stainless steel wires were prepared and inoculated with 263K scrapie-infected homogenate as described in section 2.3.1. To compare the effects of surface degradation on the efficiency of prion decontamination, wires were artificially degraded and inoculated as detailed in section 2.3.2. An assessment of the extent of wire surface degradation was performed (section 2.3.2.1) and decontamination was carried out under the conditions described in section 2.4.3. The treated wires were then fluorescently labelled using a dual staining technique to identify total protein and prion-associated amyloid (section 2.5.3) and analysed using EDIC/EF (section 2.7 and 2.7.1). Removal of infectious disease from the wires was determined using the animal bioassay as described in section 2.9.

5.3. RESULTS

5.3.1. Degradation of Stainless Steel Wire Surface

Evaluation of artificially degraded stainless steel wire topography was performed by visual analysis with EDIC (Figure 20) and using a laser confocal scanning system to determine average surface roughness (Figure 21).

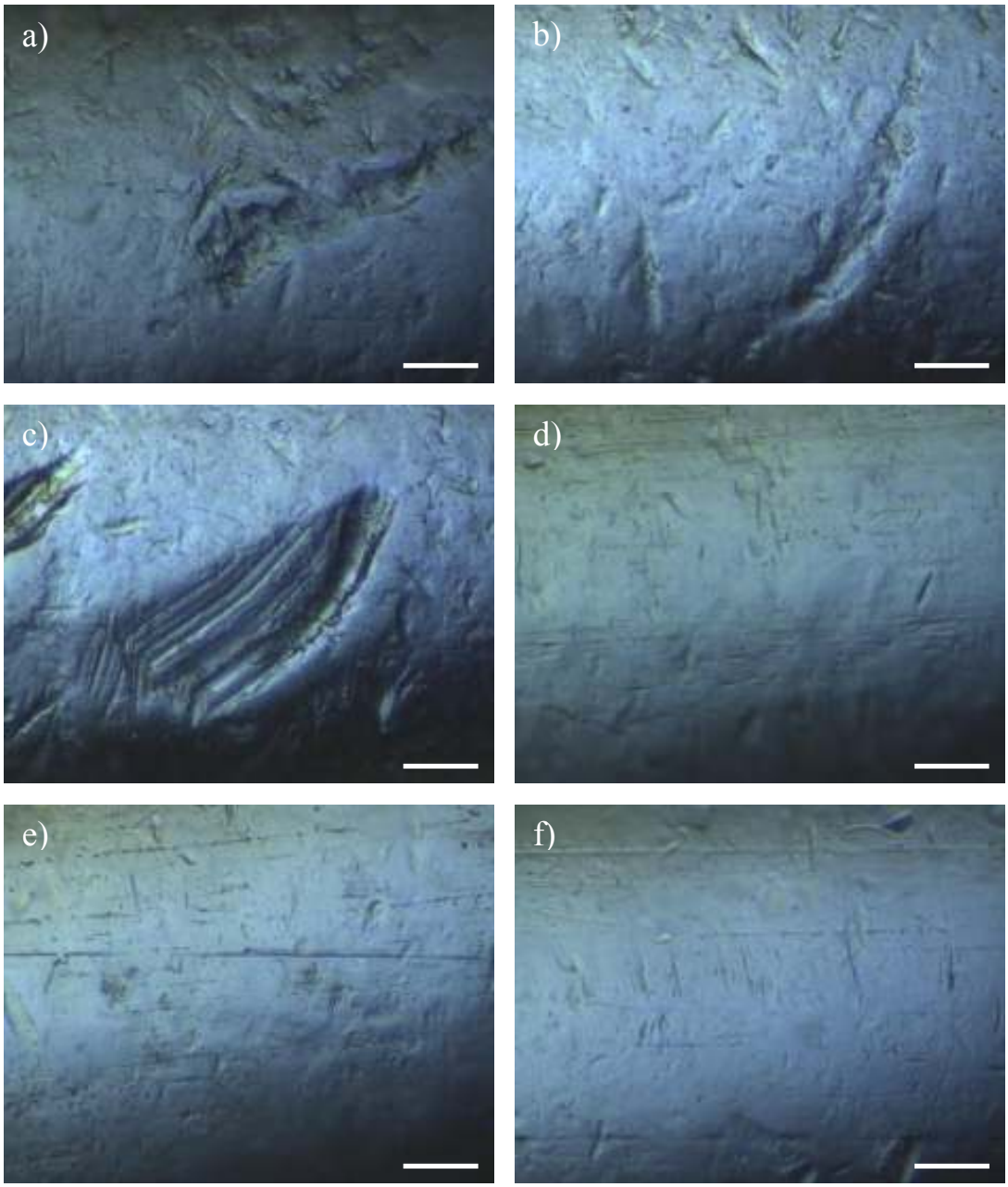

Figure 20 Representative photomicrographs taken using EDIC/EF of the surface of artificially degraded (a, b & c) and normal (d, e & f) stainless steel wires (n=7/treatment group). Scale bar: 10µm.

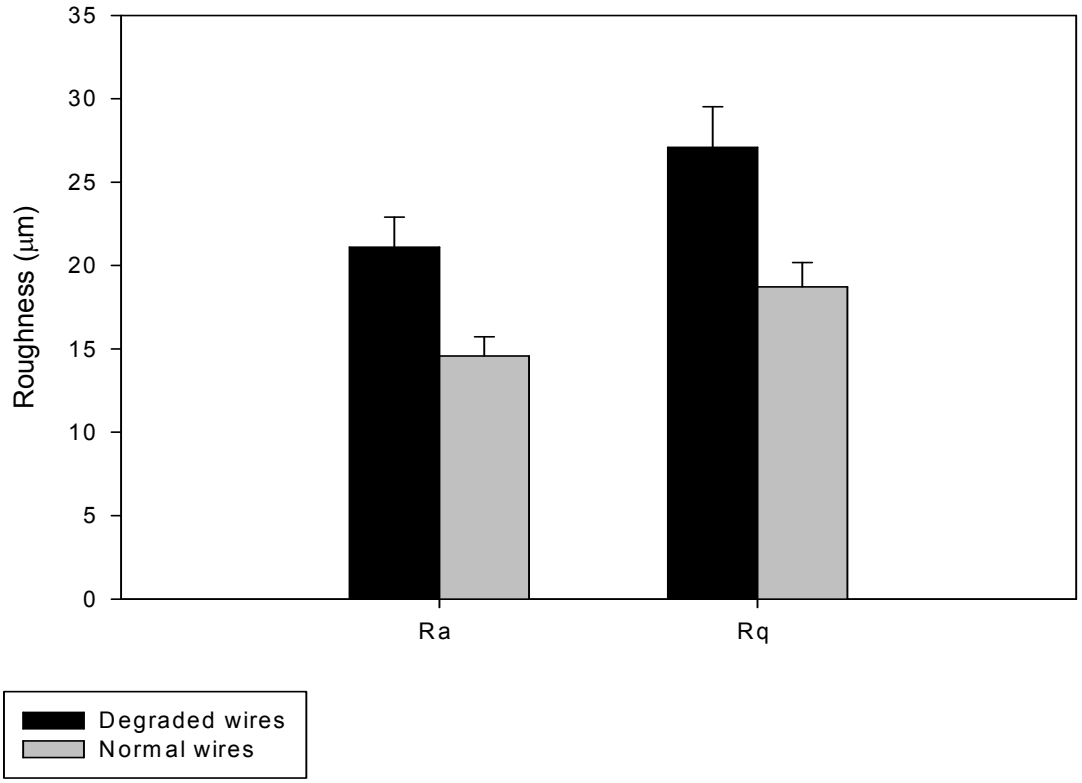

Figure 21 Analysis of the mean surface roughness (Ra) of degraded and normal stainless steel wires (n=7/treatment group) using a laser confocal scanning system to quantify surface degradation. Rq indicates the varying quadratic mean.

Assessment of the surface degradation method by visual analysis using EDIC indicates an overall increase in surface roughness relative to unaltered wires. While small degrees of scarring were present on unaltered stainless steel wires this was rarely observed and a likely product of the drawing process used in their manufacture (Figure 20). Stainless steel wires subjected to the degradation process demonstrated pitting and an increase in the size and degree of scarring of the surface. To exclude the possibility of viewer bias, these findings were confirmed in a blind study to observe the average surface roughness using a laser confocal scanning system. This permitted quantification of the degree of surface degradation and assessment to be performed by a t-test to compare data means. A statistically significant difference was observed in both the average surface roughness ($P = 0.0079$) and the root mean squared, otherwise described as the quadratic mean to assess the statistical measure of a varying quantity ($P = 0.0093$).

5.3.2. Removal of Total Protein and Prion-Associated Amyloid from Normal and Degraded Stainless Steel Wires

Fluorescence analysis of bound total protein and prion-associated amyloid from untreated normal and degraded control wires is shown in Figure 22, with representative photomicrographs displayed in Figure 23. Quantification of *in situ* prion-associated amyloid suggests statistically similar concentrations attached to each wire (P = 0.222), although the mean of the degraded wire cohort was increased relative to normal wires (11.5 ng/mm^2 compared to 7.5 ng/mm^2). However, a statistically significant (P = 0.049) increase was observed in concentrations of *in situ* total protein on degraded wires in comparison to normal wires. Visual analysis with EDIC confirmed that, rather than an increase in surface coverage, this statistically significant increase of *in situ* total protein was a likely consequence of larger aggregates of protein able to attach and remain bound to the degraded surface.

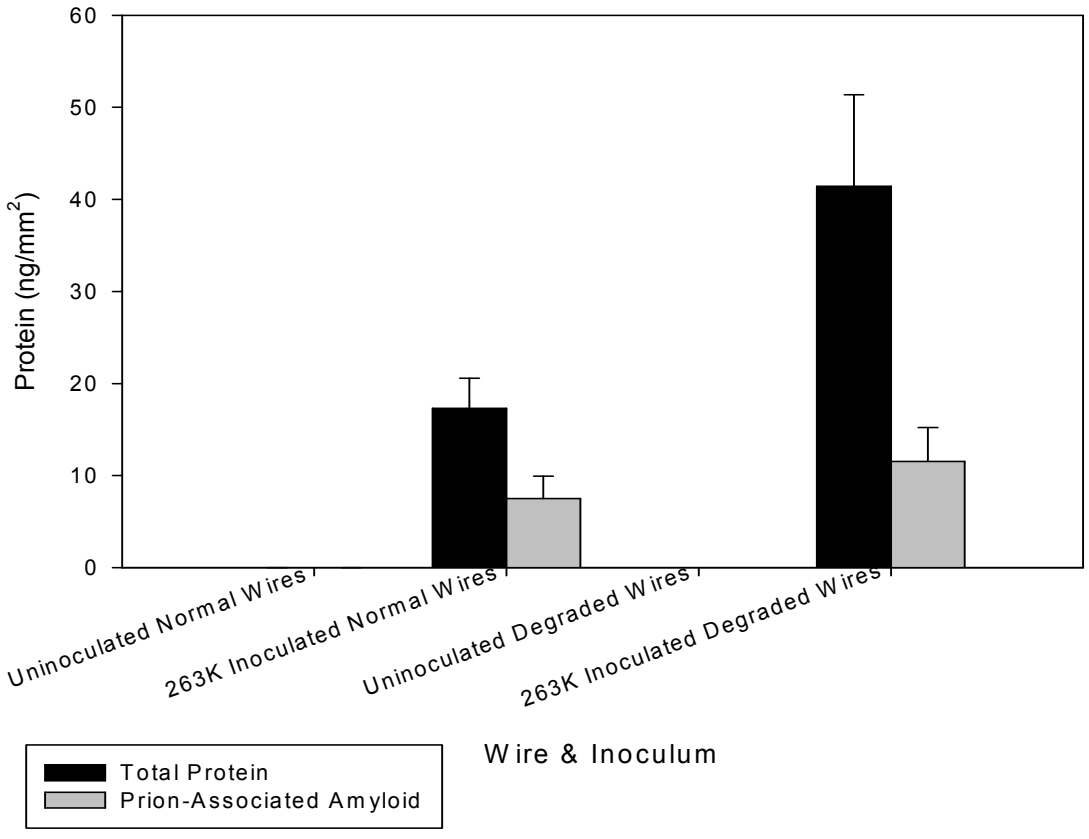

Figure 22 Variation in binding of total protein and prion-associated amyloid, as identified by SYPRO Ruby and Thioflavin T, respectively, to normal and degraded stainless steel wires (n=5/treatment group) inoculated with 263K scrapie-infected homogenate.

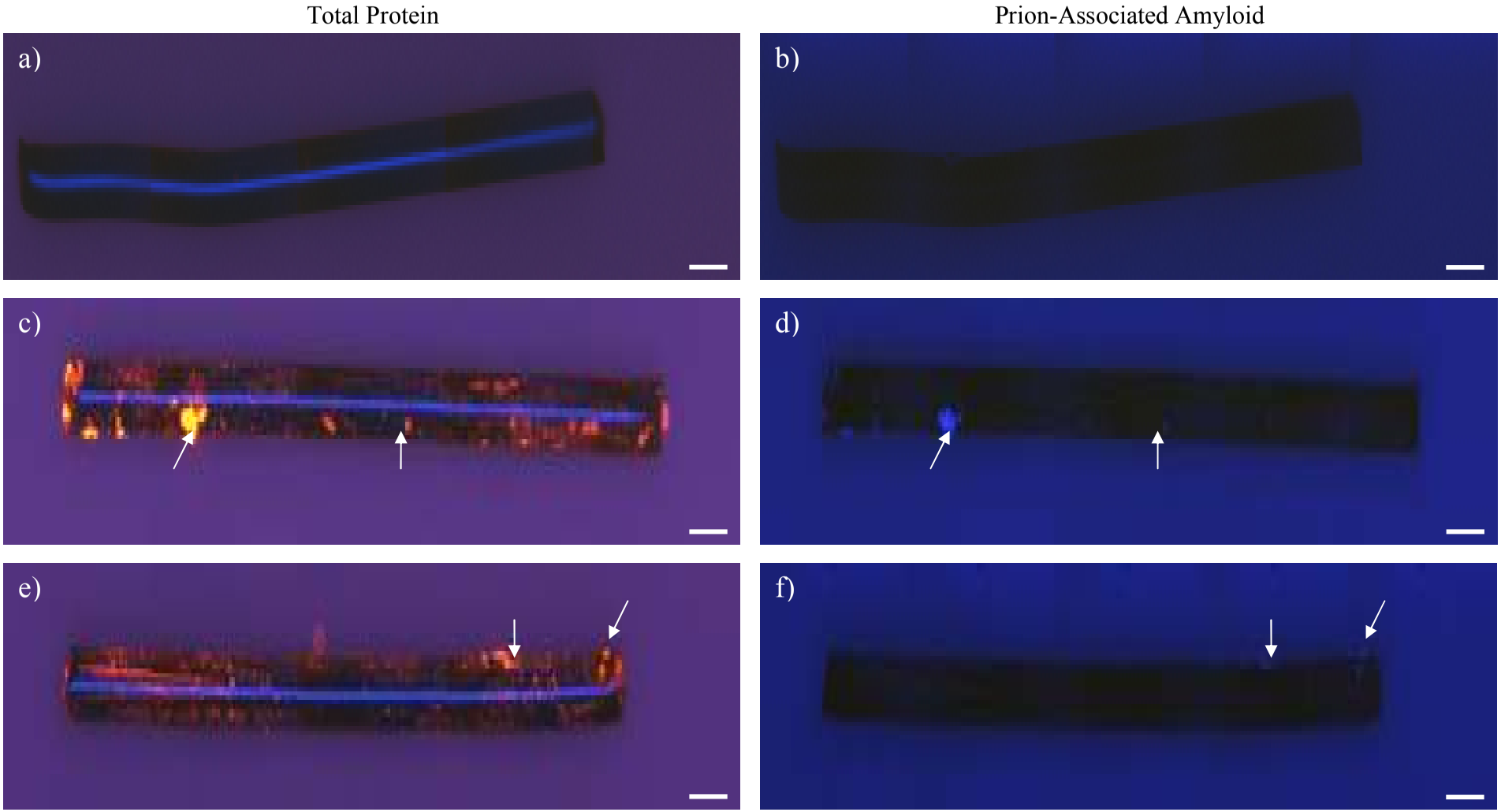

Figure 23 Representative photomicrographs taken using EDIC/EF analysing total protein (a, c & e) and prion-associated amyloid (b, d & f), as identified by SYPRO Ruby and Thioflavin T, respectively, bound to uninoculated stainless steel wires (a & b) and degraded stainless steel wires (c & d) and normal wires (e & f) inoculated with 263K scrapie-infected homogenate. Arrows indicate amyloid deposits. Scale bar: 100µm.

Incorporating the previously established cut-off of 0.01 ng/mm^2 under decontamination conditions, Figure 24 illustrates the residual *in situ* total protein and prion-associated amyloid concentrations on wires following various decontamination techniques. None of the enzymatics (both T1 and its double treatment T2, in addition to T3 and T4) were capable of removing protein to levels below 1 ng/mm^2 on either the normal or degraded wires. With the exception of T4 (P = 0.04), there was no statistically significant difference between protein removal from normal or degraded wires treated with either T1, T2 or T3. In the case of T4, removal of protein was significantly more difficult from degraded wires (mean residual protein: 1.83 ng/mm^2 on normal wires; 4.89 ng/mm^2 on degraded wires). However, less than 0.1 ng/mm^2 of prion-associated amyloid was visualised *in situ* following treatment on all wires, with the exception of T2 treated degraded wires (D-T2, mean: 0.11 ng/mm^2). Complete removal of detectable amyloid was observed on both normal and degraded T4 treated wires and there was no statistically significant difference observed between the experimental cut-off of 0.01 ng/mm^2 and residual prion-associated amyloid observed on degraded wires treated with T1 (P = 0.182). Importantly, no significant difference was observed between amyloid removal from either normal or degraded wires in all enzymatic treatment cases. Statistical analysis using the analysis of variance (ANOVA) method also suggests that there was no statistically significant difference between T1 and T2 treatment on normal and degraded wires (P value of F-test: protein: 0.062, amyloid P = 0.11).

Complete removal of detectable amyloid was also noted following treatment with T5 on normal and degraded wires. Interestingly, treatment with T6 (a double treatment of the same alkali chemistry as T5) was less effective at removing prion-associated amyloid from both normal and degraded wires and statistical analysis suggests residual amyloid on N-T6 and D-T6 wires was significantly different from the experimental cut-off. In addition, there was no statistically significant difference between protein removal following T5 and T6 treatment between normal and degraded wires.

Critically, analysis of T7 treatment wires, involving an autoclave treatment at 134 ºC for 18 min, suggests an increase in non-specific fluorescence which can also be observed in Figure 25. Whilst a statistically significant difference was detected between *in situ* protein on untreated control wires and T7 treated normal (P = 0.001) and degraded wires (P = 0.0004), indicating a decrease in total protein, no removal of amyloid was observed. Mean concentrations of *in situ* prion-associated amyloid were determined to be 8.29 ng/mm^2 following T7 treatment, relative to 7.51 ng/mm^2 of amyloid detected on untreated normal control wires. Whilst this difference was not statistically significant in the case of the normal

wires (P = 0.79), analysis of degraded wires demonstrated a significant increase (P = 0.02) in amyloid, with mean concentrations of 30.93 ng/mm^2 detected relative to 11.54 ng/mm^2 on untreated degraded control wires.

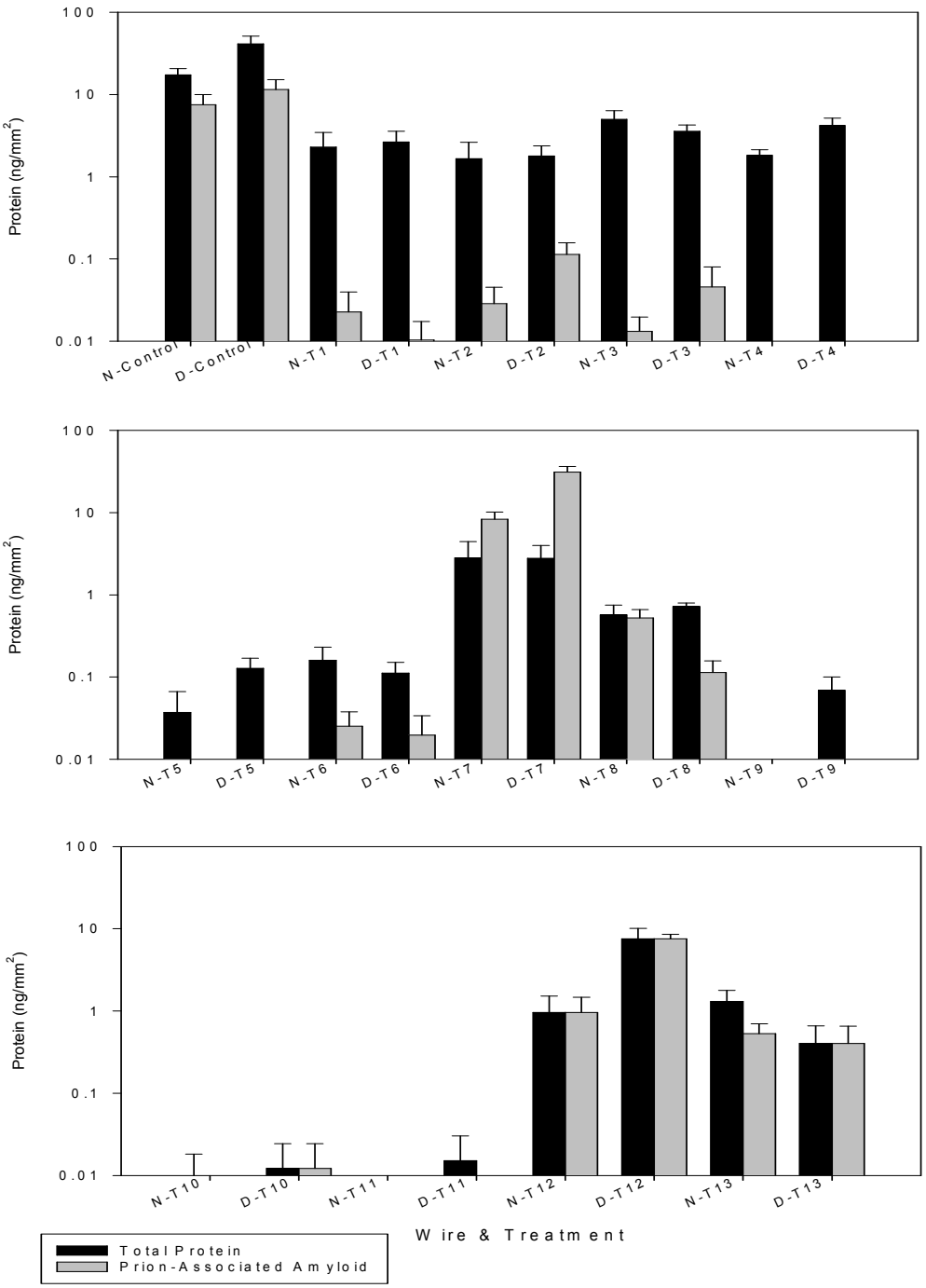

Figure 24 Analysis of total protein and prion-associated amyloid, as identified by SYPRO Ruby and Thioflavin T, respectively, bound to normal (N) and degraded (D) stainless steel wires (n=5/treatment group) inoculated with 263K scrapie-infected homogenate following decontamination with a variety of enzymatic, chemical and physical processes. Control wires represent untreated wire cohorts.

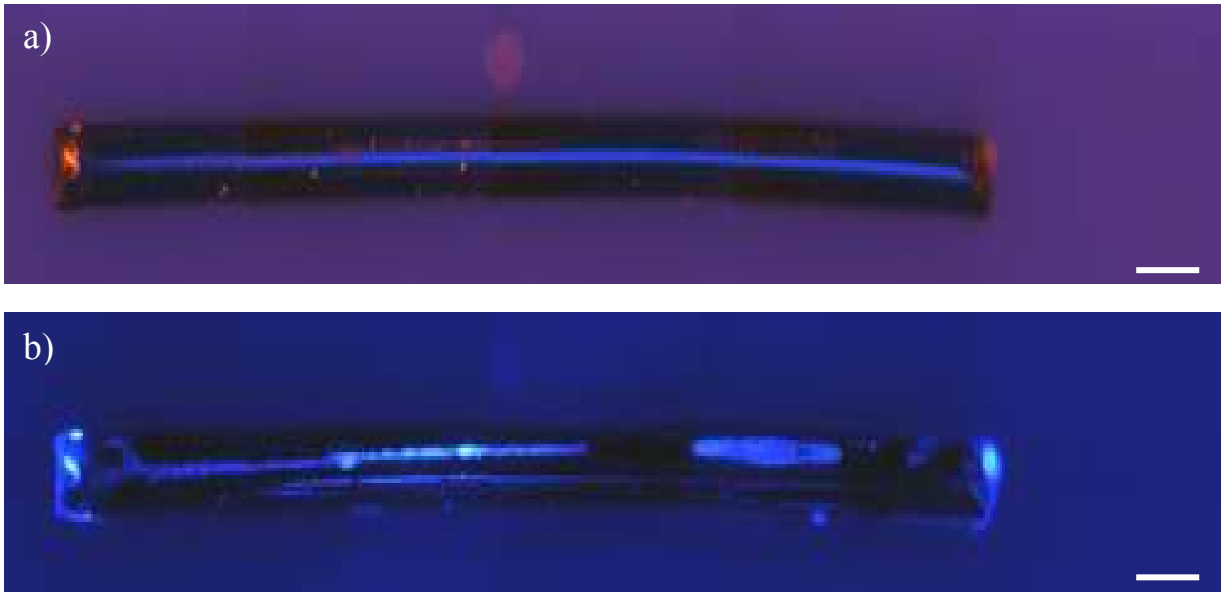

Figure 25 Representative photomicrographs taken using EDIC/EF of wires (n=5) inoculated with 263K scrapie-infected homogenate and decontaminated using a high temperature and pressure autoclave treatment (T7). a) Protein as detected by SYPRO Ruby; b) Amyloid as detected by Thioflavin T. Scale bars: 100 µm

An increase in protein removal was observed following immersion autoclaving (T8) relative to T7. Non-specific amyloid fluorescence also appeared to be reduced upon analysis of T8 treated wires. However, prion-associated amyloid removal was significantly improved on T8 treated degraded wires, relative to normal wires ($P = 0.014$). Conversely, protein removal was more efficient upon treatment of normal wires compared with degraded wires following exposure to 1M NaOH (T9). Treatment with T9 also removed all detectable prion-associated amyloid from both wire groups. Complete removal of detectable prion-associated amyloid, in addition to total protein, was also observed on normal wires following treatment with T10 (sodium hypochlorite) and T11 (Bleach 1). Whilst the residual mean total protein and prion-associated amyloid were increased on degraded wires relative to normal wires, the concentrations were not significantly different from the experimental cut-off. Interestingly, T12 (Bleach 2), was less effective than NaOCl and Bleach 1 at both total protein and prion-amyloid removal, with only an approximate 1-log in total protein. Concentrations of residual total protein and prion-associated amyloid were comparable, as can be seen in Figure 24. However, more efficient removal of both total protein and amyloid was observed on normal wires compared to degraded wires (total protein: $P = 0.043$, prion-associated amyloid: $P = 0.0007$). Residual protein and prion-associated amyloid was visualised on the wires following

T13 treatment on both normal and degraded wires, with no statistically significant difference between the two wire cohorts (total protein: P = 0.13, prion-associated amyloid: P = 0.7).

High resolution EDIC/EF imaging of the wire surface is shown in Figure 26 and 27. Residual protein and prion associated amyloid was seen to associate largely, although not entirely, with areas of scarring and damage on both normal and degraded wires. Those areas of scarring and roughing were considerably more extensive on degraded wires, confirming initial assessments (Figure 20 and 21).

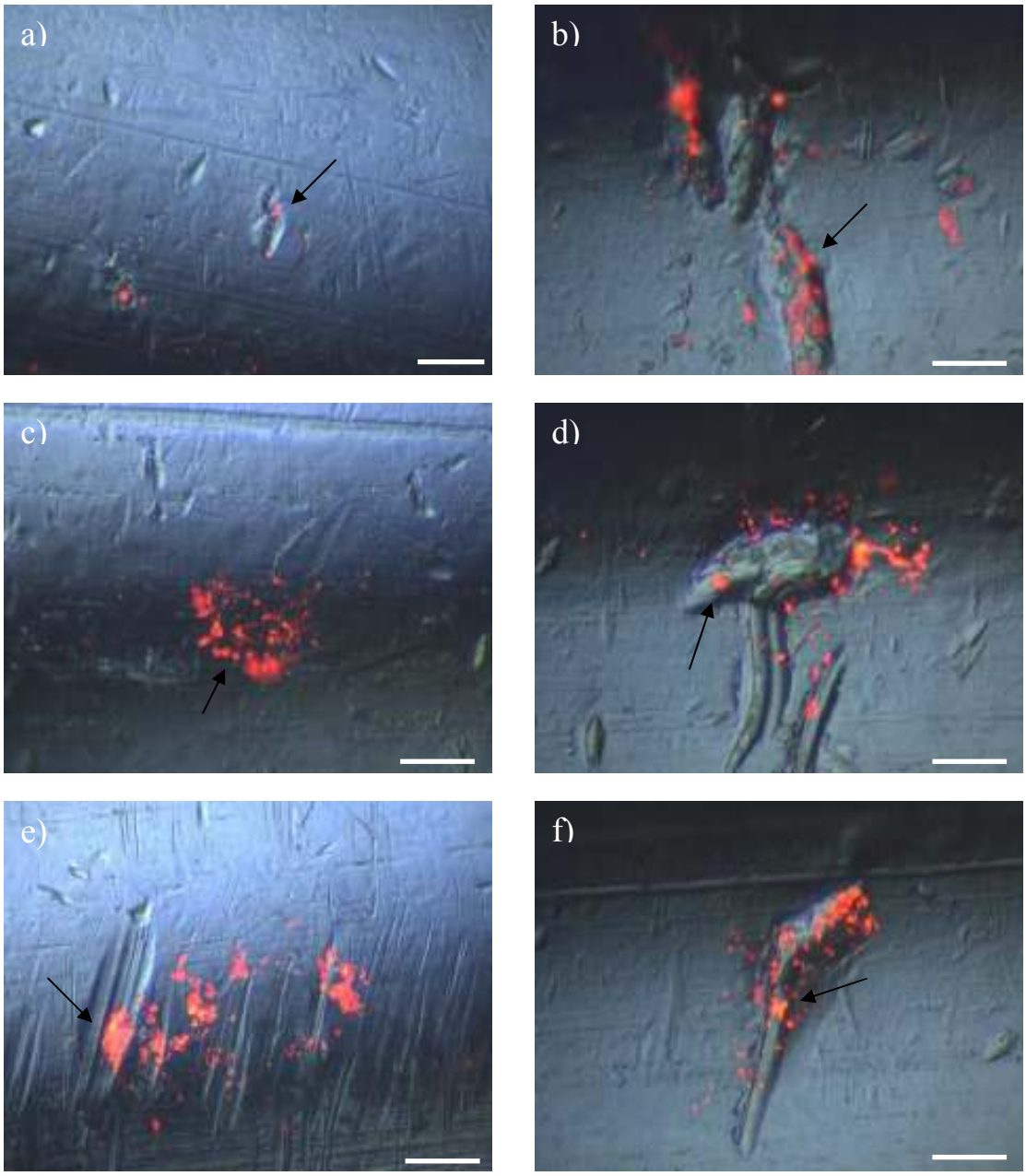

Figure 26 Representative photomicrographs taken using EDIC/EF of residual proteinaceous deposits staining with SYPRO Ruby following decontamination with a) TN1; b) TD1; c) TN2; d) TD2; e) TN3 & f) TD3. Arrows indicate protein deposits. Scale bars: 10 µm.

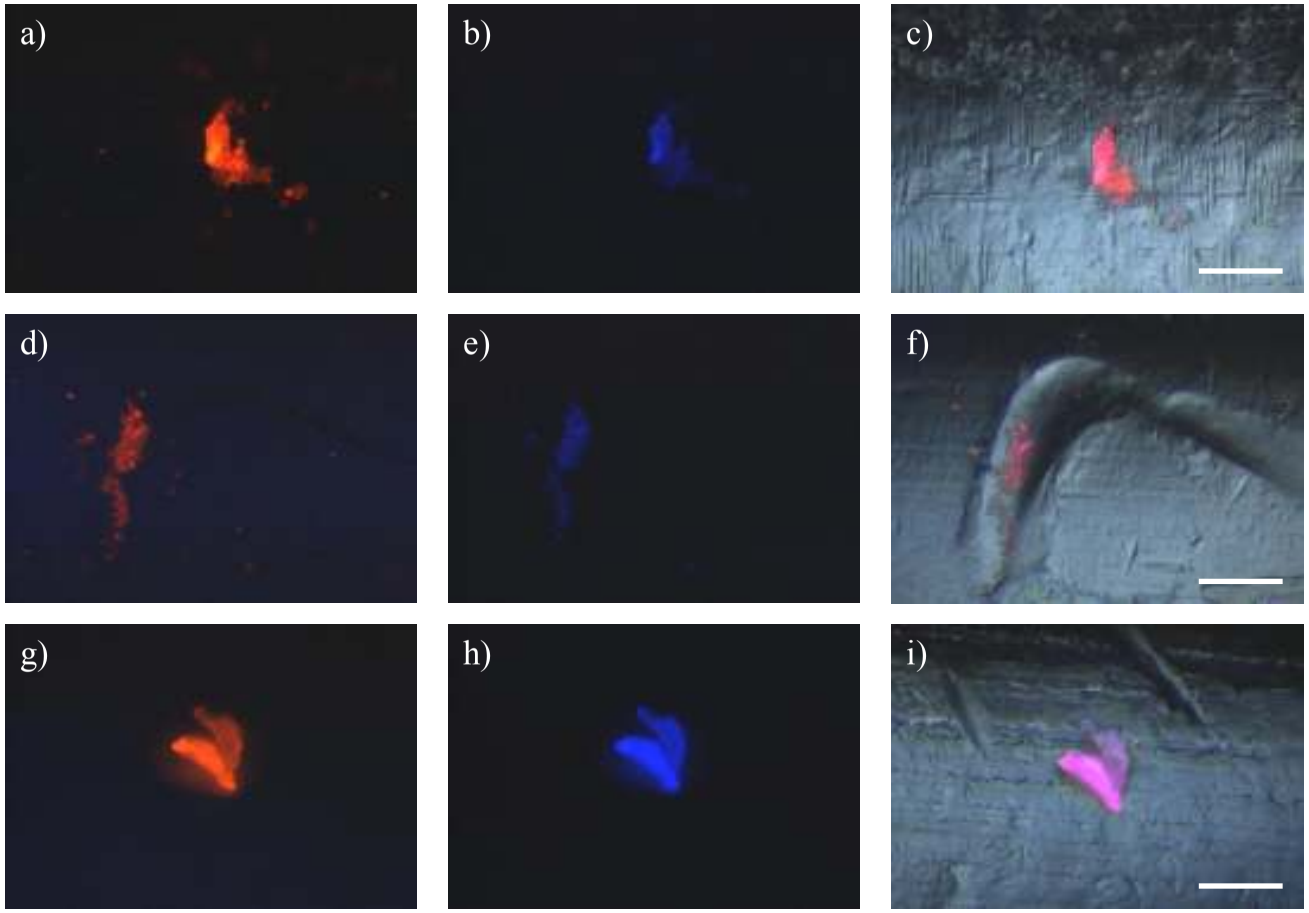

Figure 27 Representative photomicrographs of residual prion-associated amyloid on stainless steel wires (n=5/treatment) following various decontamination techniques: a), b) & c) TD9; d), e) & f) TD8: g), h) & i) TN4. Images a), d) & g) represent general protein as detected by SYPRO Ruby; Images b), e) & h) represent prion associated amyloid as detected by Thioflavin T; Images c), f) & i) represent composite image of protein and amyloid overlaid with the white light image of the wire surface. Scale bars: 10 µm.

5.3.3. Removal of Infectivity from the Surface of Normal and Degraded Stainless Steel Wires

Infectivity was assessed using the rodent bioassay model by the implantation of stainless steel wires into the CNS of hamsters. The effect of the carrier surface on wires inoculated with serial dilutions of a 10 % (w/v) 263K-infected brain homogenate into NBH are shown in Table 9. All dilutions of the wire inoculum induced disease in the rodent model on both normal and degraded carrier surfaces. Interestingly, degradation of the wire surface indicated a prolonged incubation period relative to the same dilution series inoculated onto normal wires. However, whilst the mean incubation period was increased with degradation of the wire surface in all dilutions, it was only significantly different at the 10^{-1} dilution.

Table 9 Surface infectivity of normal and degraded stainless steel wires (n=11/wire group) inoculated with serial dilutions of 10 % (w/v) 263K scrapie-infected homogenate into NBH indicating percentage transmission to hamsters and the incubation period of scrapie disease.

Dilution	Normal Wires		Degraded Wires	
	Transmission (%)	Incubation (days)	Transmission (%)	Incubation (days)
10^{-1}	100	90 ± 2	100	100 ± 5
10^{-2}	100	98 ± 5	100	111 ± 8
10^{-3}	100	117 ± 6	100	133 ± 13
10^{-4}	100	124 ± 11	100	138 ± 16

Infectivity of the wires following decontamination treatments is shown in Table 10. None of the enzymatic chemistries (T1, T2, T3 and T4) used in this study were capable of completely removing infectious disease. Neither T3 nor T4 induced any effect on transmission rate or incubation period, with no log reduction of infectious load. A single treatment with T1 resulted in a 3-log reduction in infectivity but no effect on overall transmission. A double treatment with the same enzymatic (T2) produced a 37 % reduction in transmission of disease and a further 1-log reduction in infectious load relative to T1.

Treatment with the alkali T5, 1 M NaOH (T9), NaOCl (T10) and immersion autoclaving in water (T8) completely eliminated infectivity. A dry autoclave procedure (T7) produced a 40 % reduction in transmission of disease and a 4.4-log reduction in infectivity.

Interestingly, a 0.1-log increase in reduction of infectious load was observed following treatment with T13, relative to T7. Incubation periods between the two treatments were comparable, however transmission of infectious disease was only noted in 33 % of the rodents following treatment with T13 relative to 60 % of the T7 animal group.

Table 10 Surface infectivity of normal and degraded stainless steel wires inoculated with 10 % (w/v) 263K scrapie-infected brain homogenate indicating percentage transmission to hamsters, incubation period of scrapie disease and log reduction of infectivity following various decontamination methods. --- indicates exposure not tested.

Treatment	Normal Wires			Degraded Wires		
	Transmission[a] (%)	Incubation (days)	Log.Red.[b]	Transmission[a] (%)	Incubation (days)	Log.Red.[b]
T1	---	---	---	100	179 ± 22	3
T2	---	---	---	63	316 ± 36	4
T3	---	---	---	100	102 ± 6	0
T4	---	---	---	100	99 ± 4	0
T5	0	> 365	5.5	---	---	---
T6	---	---	---	---	---	---
T7	60	197 ± 86	4.4	---	---	---
T8	0	> 365	5.5	---	---	---
T9	0	> 365	5.5	0	> 365	5.5
T10	0	> 365	5.5	---	---	---
T11	---	---	---	---	---	---
T12	---	---	---	---	---	---
T13	33	170 ± 33	4.5	---	---	---

[a]Experiment stopped at 365 days.

[b]Log reduction of infectivity was estimated from the initial infectivity of 10 % brain homogenates used to inoculate test surfaces.

5.4. DISCUSSION

The influence of surface degradation and roughing on decontamination and, more specifically prion removal from surgical stainless steel, has not been investigated previously. It is clear that surgical instruments which have been in circulation longer within SSDs are more

difficult to clean than those recently introduced. A significant cause of this is the increase in surface scarring, roughing and damage. This can be acquired through interaction with other devices or through the gradual loss of the passivation layer creating a surface upon which decontamination processes involving reverse osmosis (RO) water and high pH chemistries can impact upon (personal communication with J.Harrison).

Immersion autoclave treatment with 1 M sodium hydroxide is known to both damage and degrade stainless steel instruments (Brown *et al.*, 2005; McDonnell & Burke, 2003). This process was employed in order to provide a worst-case scenario, damaged, stainless steel wire surface which was less amenable to decontamination. Assessment of the degraded wires by visual analysis using EDIC, and in a blind study using a laser confocal scanning system, confirmed that autoclaving in 1 M NaOH significantly altered wire surface integrity relative to normal, untreated wires. Significant surface roughing was present following treatment which was not visualised on normal wires. Moreover, residual protein and prion-associated amyloid deposits were observed to largely associate with areas of induced and existing surface degradation on degraded and normal wires, respectively.

Consequently, the wires were inoculated with 263K scrapie-infected homogenate. Importantly, concerns have been raised recently over the use of experimental animal prion strains (Giles *et al.*, 2008). The applicability of conclusions due to the divergent physical and biochemical properties of these strains, relative to those such as vCJD and BSE for which the work is intended, has been brought into question. However, the use of vCJD and BSE strains is severely limited by the availability of adequate facilities to handle such material, in addition to attainable material. Moreover, experimental prion strains such as 263K scrapie have been demonstrated to be highly resistant to decontamination methods. Studies have indicated that 263K scrapie in particular is one of the most biochemically stable and resistant strains of TSE (Fernie *et al.*, 2007). This strain has been shown to be more resistant than mouse-adapted BSE and comparable to human CJD and bovine BSE strains in terms of resistance to decontamination methods (Brown *et al.*, 2000; Fichet *et al.*, 2007b; Fichet *et al.*, 2007c). As such, 263K scrapie represents an extremely pertinent prion strain to evaluate the efficiency of decontamination processes. The 263K animal bioassay model is used extensively as an assessment of residual infectivity on stainless steel wires and has been shown to be highly reproducible (Fichet *et al.*, 2007c; Lemmer *et al.*, 2008; Lemmer *et al.*, 2004; Yao *et al.*, 2005). In this study, the use of this method permitted an assessment of the effect of surface degradation on disease transmission and also correlation of infectivity with EDIC/EF and Thioflavin T detection of prion-associated amyloid.

Analysis of both normal and control wires using the fluorescent dual staining method suggested that, whilst both wire cohorts possessed similar concentrations of prion-associated amyloid, there was a significantly greater concentration of total protein bound to degraded wires relative to normal wire controls. Visual inspection of the wires and representative images displayed in Figure 23 suggests that the degradation of the surface permitted attachment of larger aggregates of protein. Implantation of both normal and degraded wires into the hamster prefrontal subcortical region induced disease in 100 % of animals at all serial dilutions of the wire inoculum. The reproducibility of the 263K animal model has previously been demonstrated and data has closely correlated despite separate homogenate inoculum preparations (Fichet *et al.*, 2007c). However, a prolonged incubation period was observed in this study at all inoculum dilutions on degraded wires (mean increase in incubation period: 10^{-1} dilution: 10 days, 10^{-2}: 13 days, 10^{-3}: 16 days and 10^{-4}: 14 days). Whilst this observed increase was only statistically significant at one out of the four inoculum dilutions, these data suggest that surface degradation can potentially influence the time-course to clinical disease, potentially resulting in a longer subclinical incubation period. Previous data up to a 10^{-4} inoculum dilution argues against the possibility that the variation in incubation period observed in this study was a result of the intrinsic variability of the testing method, although due to statistical data, this can not be discounted (Fichet *et al.*, 2007c). Importantly, it is clear that the wire implant model presented in this chapter can not reproduce the degree of surface degradation and damage that is observed on surgical instruments. Indeed, only following T4, T9 and T12 exposure was a statistically significant increase in residual total protein observed on degraded wires in relation to normal wires. This is likely to explain the lack of statistical significance in incubation periods between wire cohorts at three of the four inoculum dilutions. However, a potential implication of the wire data is that disease incubation period may increase in parallel with the extent of surface damage.

Various enzymatic, chemical and physical decontamination techniques were evaluated using EDIC/EF and the fluorescent dual stain technique to detect both total protein and prion-associated amyloid on normal and degraded wires. All of the enzymatic treatments, designated T1, T2, T3 and T4, demonstrated concentrations of residual total protein greater than 1 ng/mm^2 following exposure on either normal or degraded wires. With the exception of T2 treatment of degraded wires, prion-associated amyloid was removed to concentrations below 0.1 ng/mm^2 on all wires exposed to the enzymatic chemistries. Interestingly, T2 represents a double treatment of the same enzymatic as T1. However, on both normal and degraded wires, no statistically significant difference was observed between either protein removal or prion-

amyloid removal suggesting an increased treatment with the same chemistry had no effect on protein and amyloid removal. Conversely, complete removal of detectable prion-associated amyloid was following a single treatment of an alkali-based chemistry (T5) but a double treatment with the same chemistry proved less effective with concentrations of amyloid significantly elevated above the experimental cut-off. These data correlate with Figure 18 in Chapter 4 using the same alkali confirming that prolonged exposure to this particular chemistry can decrease the effectiveness of decontamination relative to a shorter contact time. This chapter also confirms that high heat and pressure autoclave treatment increases the background signal associated with Thioflavin T, thereby decreasing the sensitivity of the dual stain procedure. Whilst a decrease in total protein on both normal and degraded wires was observed, no significant difference was observed between prion-associated amyloid concentrations on normal wires relative to controls. On degraded wires, a statistically significant increase was observed with mean prion-associated amyloid detected by Thioflavin T increasing from 11.54 ng/mm^2 to 30.93 ng/mm^2 following treatment. This can be observed in Figure 25 as an increase in the concentration of protein which is identified as amyloid by the Thioflavin T fluorophore.

Complete removal of both detectable total protein, including prion-associated amyloid, was observed following treatment with 1 M NaOH (T9), 20,000 ppm NaOCl (T10) and bleach 1 (T11) from normal wires. Prion-associated amyloid was also removed from degraded wires although residual protein was observed *in situ* at concentrations above the experimental cut-off following treatment with T9. Residual protein on degraded wires following treatment with T10 and T11 was not significantly different from the experimental cut-off. Interestingly, a second bleach product (T12) demonstrated only a 1-log and >1-log reduction in total protein and prion-associated amyloid respectively.

Whilst infectivity data were not available for T12 or T11, the animal bioassay demonstrated removal of infectivity from the wires following treatment with T9 and T10, confirming the effectiveness of WHO approved recommendations for the treatment of reusable surgical instruments at risk of CJD contamination (Sehulster, 2004; Taylor, 2004). The absence of transmissible disease correlates with a removal of prion-associated amyloid from the wires and was also noted following T5 exposure. In addition, a correlation between *in situ* prion-associated amyloid and infectivity was also detected following treatments T2, T3 and T13. However, critically for the identification of prion-associated amyloid as a marker of disease, infectivity was observed in the absence of prion-associated amyloid following

treatments T1 and T4. Conversely, the presence of prion-associated amyloid was also observed in the absence of infectious disease following T8 exposure.

These data confirm that prion-associated amyloid and infectious disease can be disassociated from each other under certain exposure conditions. As a result, the use of prion-associated amyloid as a marker for disease is highly dependent on the decontamination techniques employed and their direct impact on prion-associated amyloid. Enzymatic chemistries such as T1 and T4, exposure to which results in removal of infectivity in the animal bioassay, appear to break down larger amyloid deposits to levels below the detection limit of Thioflavin T. Therefore, improvement of fluorescent amyloid detection techniques may elicit a better correlation with infectivity than is demonstrated by Thioflavin T in cases where infectious disease is evident in the absence of detectable amyloid.

Degradation of the wire surface in order to provide a worst-case scenario surface for the wire implant model proved effective under certain treatment conditions in terms of removal of proteinaceous contamination as identified by SYPRO Ruby. Importantly, initial observations suggest a prolonged incubation period may be induced by a prion-contaminated, degraded stainless steel surface. This may be a direct consequence of the altered surface integrity of degraded wires relative to normal, unaltered wires or due to the increase of surrounding total protein resulting in a dissemination of the infectious agent to surrounding tissues. Critically, however, these initial findings require further assessment in order to be confirmed.

CHAPTER 6

CORRELATION OF *IN VITRO* AND *IN VIVO* METHODS OF PRION DETECTION

6.1. INTRODUCTION

In prion diseases, little is known about the relationship between infectivity and particle size. Many of the studies appear in agreement with a smaller oligomeric PrP molecule as the infectious agent. Whilst oligomeric PrP has been demonstrated to be highly infectious *in vitro* and *in vivo* (Redecke *et al.*, 2007; Silveira *et al.*, 2005), other studies have disagreed with their infectivity levels relative to higher order amyloid. One such study showed mature amyloid fibrils produced from full length recombinant PrP to be highly toxic to cultured cells, primary hippocampus and cerebella neurons in a time and dose dependent manner. However, the lethal effects were comparable to those exhibited by small, soluble β-oligomers, suggesting that, *in vitro* at least, both amyloid and oligomeric intermediates are neurotoxic (Novitskaya *et al.*, 2007). Importantly, an oligomeric subspecies of PrP is yet to be classified, in addition to the role of PrP^{res} and amyloid in prion disease.

Methods to assess the effectiveness of decontamination techniques currently include conventional immunoblotting and infectivity bioassays using the rodent wire implant model (Fichet *et al.*, 2004; Fichet *et al.*, 2007b; Fichet *et al.*, 2007c; Yan *et al.*, 2004). The latter method is expensive and time consuming to undertake, in addition to the ethical implications of such work, but provides an assessment of the presence or absence of infectivity irrespective of the size or nature of the infectious unit. Immunoblotting utilises antibodies targeted to specific amino acid sequences of the prion protein and, combined with a protease such as proteinase K to degrade normal cellular PrP, identifies PrP^{res} as a marker of disease. The loss of antibody binding epitopes through enzymatic or chemical decontamination treatments has the capacity to drastically decrease the sensitivity of this method. This is combined with the uncertainty over the relationship of PrP^{res} with transmissible disease. Furthermore, immunoblotting can be carried out in suspension or surface studies whereby only the extent of degradation or denaturation of PrP^{res} is considered in suspension. Surface studies observing the physical removal of the prion protein from a test surface incorporate manual removal of a treated sample which may further reduce the sensitivity of this procedure thus overestimating the effectiveness of decontamination techniques.

The present study has aimed to correlate infectivity in the rodent wire implant model with fluorescent detection of amyloid using Thioflavin T on wires treated with enzymatic and alkali chemistries. In addition, suspension and surface immunoblotting was undertaken in parallel to observe the effect of the treatments on denaturation and physical removal of PrP^{res}. Antibody mapping of PrP^{res} using Western blot following treatment with enzymatic, alkali and

phenolic chemistries was also performed to assess the correlation between removal or degradation of epitopes and infectious disease.

6.2. MATERIALS AND METHODS

The methodology for this section of work is described in Chapter 2. Stainless steel wires were prepared and inoculated with 263K scrapie brain homogenate as described in section 2.3.1. Decontamination was performed (section 2.4.4) and the treated wires were then fluorescently labelled using a dual staining method to identify total protein and prion-associated amyloid (2.5.3). Examination of the wires was carried out using EDIC/EF (section 2.7 and 2.7.1). Standard Western blot analysis was performed in suspension and surface studies as described in section 2.8 using the mouse monoclonal antibody SAF 60 raised against hamster PrP codon 142–160. Sample exposure conditions were identical to those described for the wire treatment in section 2.4.3. Protocols for antibody mapping Western blot analysis as described in section 2.8.1.1. Western blots were performed in suspension utilising six different monoclonal antibodies (Figure 8). These identification methods were correlated with infectious disease determined using the animal bioassay as described in section 2.9.

6.3. RESULTS

6.3.1. Correlation of the EDIC/EF Dual Stain with Immunoblotting and the Animal Bioassay

In vitro analysis of the wires was performed using the fluorescent dual staining method previously described (Figure 28). Control wires demonstrated a mean concentration of bound total protein of 11.1 ng/mm^2 and bound prion-associated amyloid of 6.7 ng/mm^2. Statistical analysis suggested there was no significant difference between the two values ($P = 0.74$).

Analysis of total protein levels following treatment indicated that, in the case of Enzymatic 3 and 4 and Alkaline 1 cleaners, 263K inoculated wires were more difficult to decontaminate than corresponding negative control wires ($P = 0.019$, 0.021 and 0.034, respectively). No statistically significant difference was noted in total protein between 263K and NBH inoculated wires following exposure with Enzymatic 1, 2 and 5 cleaners.

Fluorescently labelled prion-associated amyloid was detected *in situ* following treatment with enzymatic 1, 3, 4 and 5 and Alkaline 1 cleaners (estimated residual amyloid; Enzymatic 1: 15 pg/mm^2, Enzymatic 3: 7.9 pg/mm^2, Enzymatic 4: 3.7 pg/mm^2 and Alkaline 1: 5.1 pg/mm^2). A 3 – 3.5-log reduction in amyloid relative to controls was observed with each of these treatments although no statistically significant difference in residual amyloid was observed between the treatment groups. Interestingly, complete removal of detectable prion-associated amyloid was observed on wires treated with Enzymatic 2 in the presence of a relatively poor removal capacity of total protein, as identified by SYPRO Ruby. In the case of the NBH inoculated control and Enzymatic 2 treated NBH wires, wire bound total protein levels were not statistically different ($P = 0.42$). The least effective treatment at removal of amyloid was Enzymatic 5 with a mean level of residual amyloid of 0.2 ng/mm^2.

Analysis of the degradation and removal of PrP^{res} by each treatment was performed by immunoblotting carried out in suspension and surface studies (Figure 29 & 30). In contrast to the data obtained through fluorescent amyloid detection in the Enzymatic 1, 3, 4 and 5 and Alkaline 1 treatment cohorts, all of the enzymatic treatments displayed complete removal of detectable PrP^{res} signal from the stainless steel tokens. Only treatment of test surfaces with Enzymatic 2 demonstrated a positive correlation between Thioflavin T amyloid detection and Western blot data with complete removal of detectable prion-associated amyloid and PrP^{res}. However, transmissible disease in the animal bioassay model was observed following treatment with Enzymatic 2, as well as Enzymatic 3 and 4 in this study (Table 11). Enzymatic 1 previously demonstrated a 100 % transmission rate, but also an increase in prion resistance, under the experimental conditions tested in this study on the 263K scrapie model (Yan *et al.*, 2004). Enzymatic 5 was unavailable for evaluation at the time of the study.

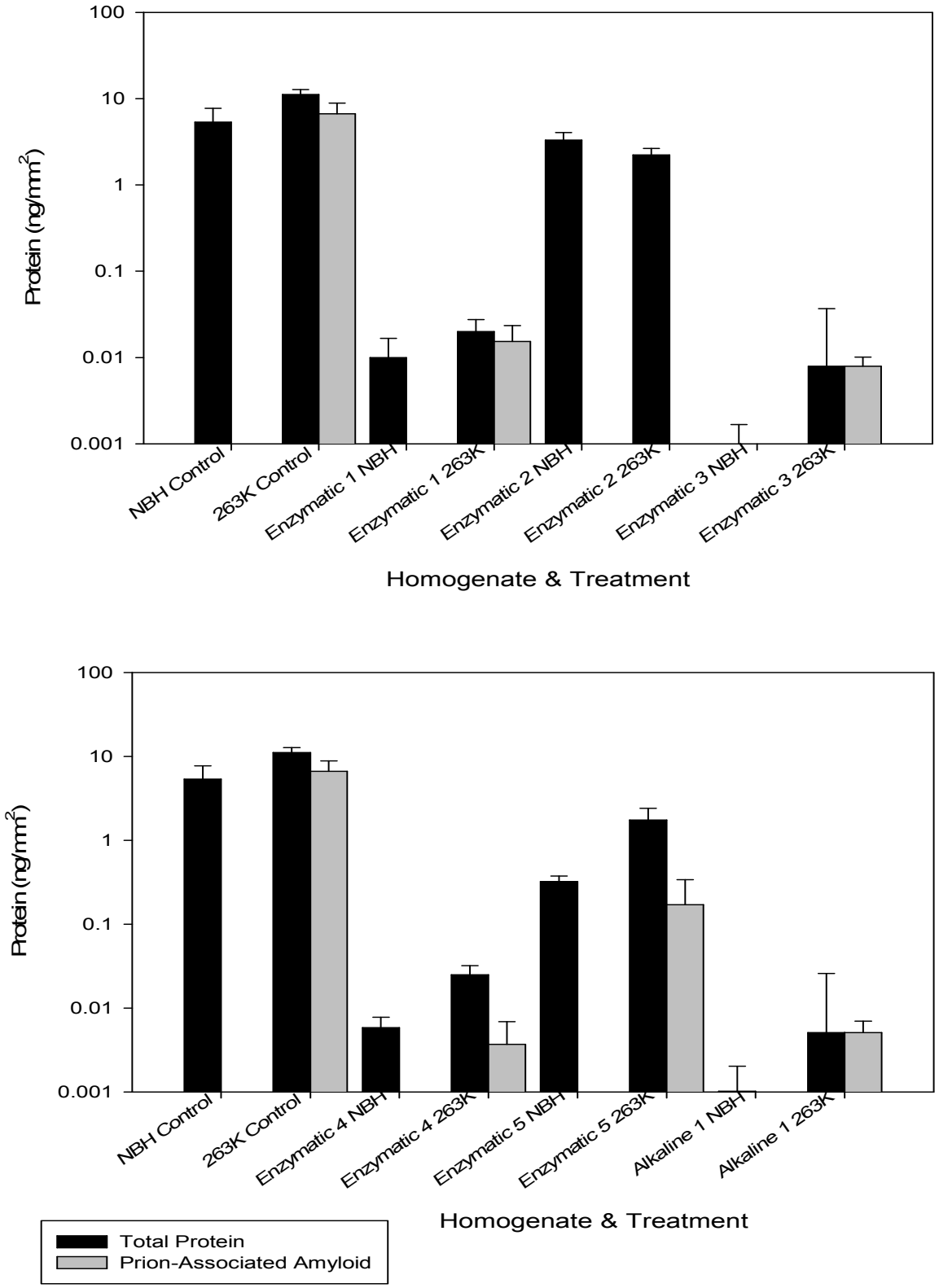

Figure 28 Analysis of bound total protein and prion-associated amyloid, fluorescently labelled with SYPRO Ruby and Thioflavin T, respectively, for wires (n=7/treatment) inoculated with either 10 % (w/v) 263K scrapie-infected brain homogenate or NBH and decontaminated with various enzymatic and alkali chemistries.

Table 11 Surface infectivity of stainless steel wires (n=11/treatment) inoculated with 10 % (w/v) 263K scrapie-infected brain homogenate indicating percentage transmission to hamsters, incubation period of scrapie disease and log reduction in infectivity following various decontamination methods.

Treatment	Transmission (%)[a]	Log. Red[b]
Enzymatic 2	10/10	1
Enzymatic 3	10/10	3.5
Enzymatic 4	7/8	~ 3
Alkali 1	0/0	5.5

[a]Experiment stopped at 365 days.

[b]Log reduction in infectivity was estimated from the initial infectivity of 10 % brain homogenates used to inoculate test surfaces.

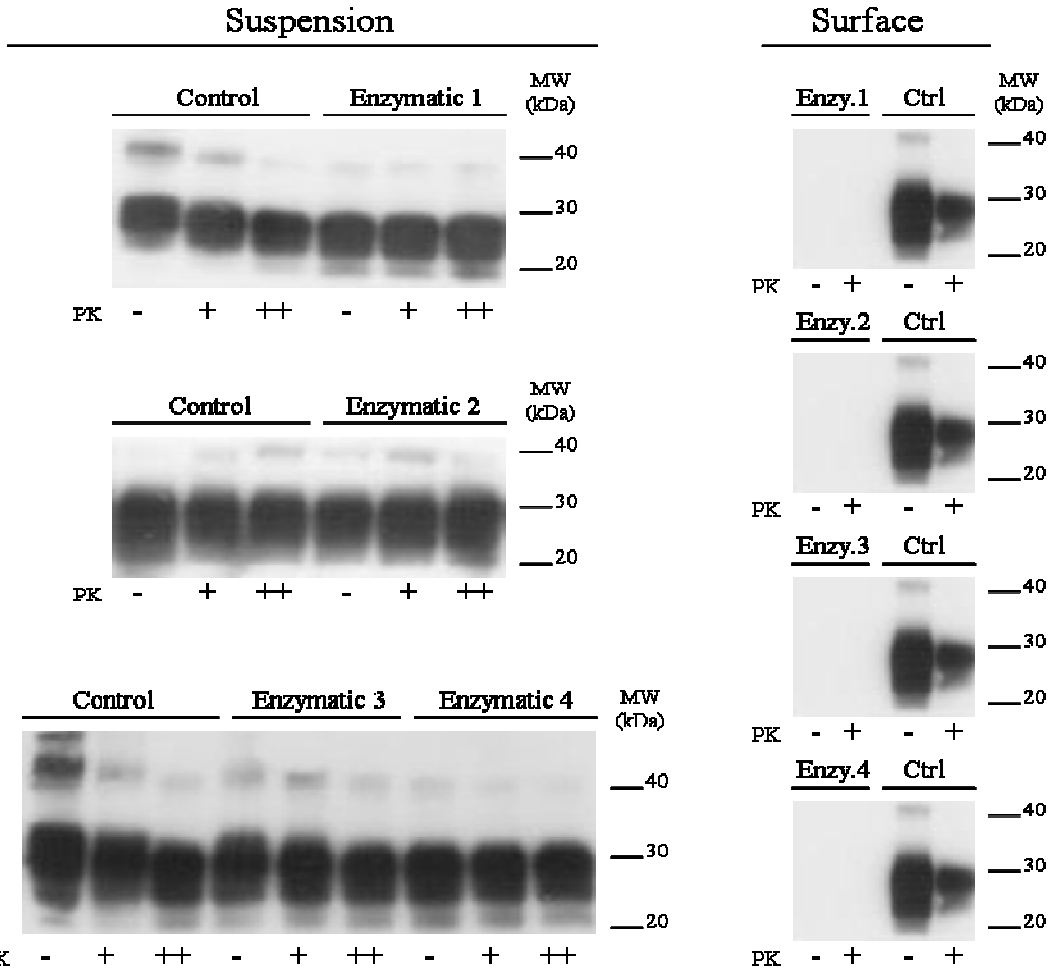

Figure 29 Western blot analysis of the effectiveness of PrP^{res} degradation and removal upon treatment with different enzymatic chemistries in suspension studies or on samples eluted from stainless steel tokens. All lanes correspond to the analysis of 50 µg of brain equivalent.

Importantly, none of the enzymatic treatments displayed any detectable capacity to degrade PrP^{res} or render it PK sensitive as observed by Western blot. Variations in concentration of enzyme chemistry, (an example of which is shown in Figure 30) demonstrate that even upon a two-fold increase, PrP^{res} remains stable in suspension. Alkaline 1 demonstrated residual PrP^{res} signal both in suspension and surface studies at a concentration of 0.1 %. Both physical removal from the token and degradation in suspension were achieved at a concentration of 0.4 %. Infectivity data obtained from the animal bioassay model indicate removal/inactivation of the infectious agent in the Alkaline 1 treatment cohort alone (total death/total #: 0/10) suggesting that any residual amyloid detected by Thioflavin T was unable to transmit disease.

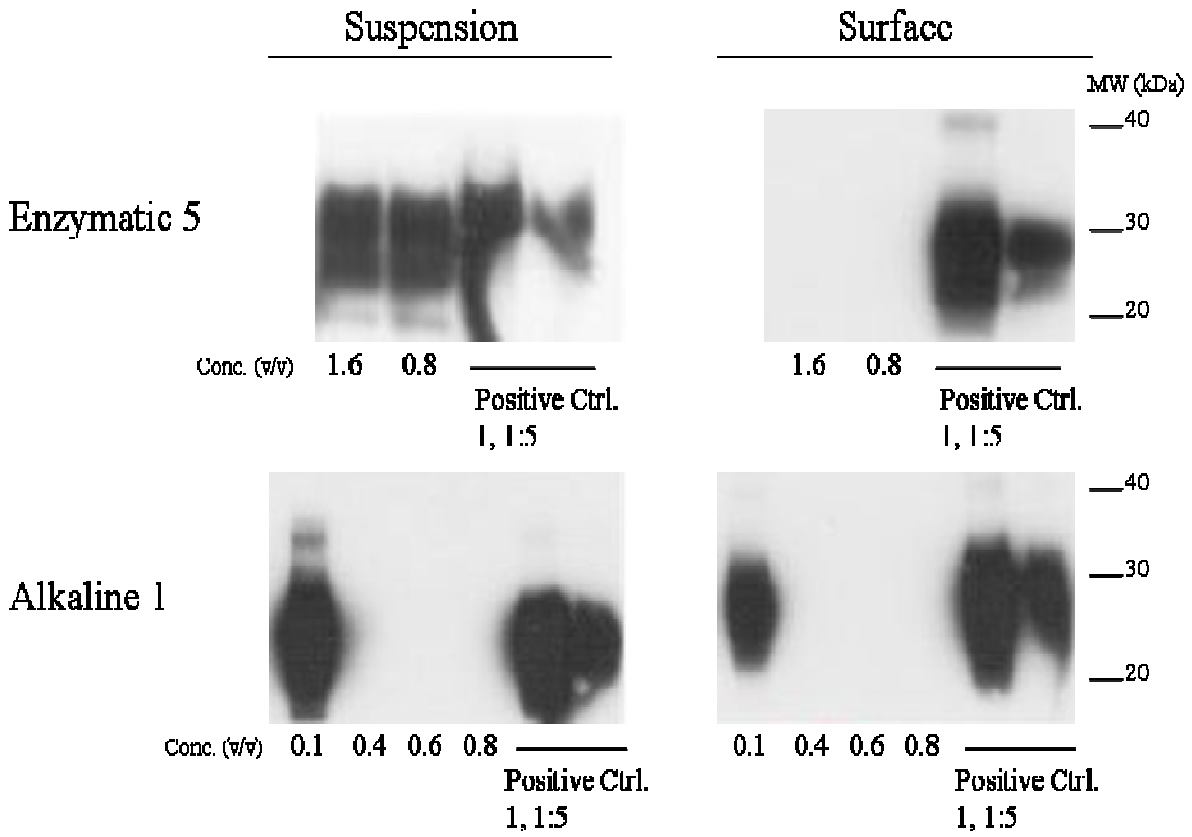

Figure 30 Western blot analysis of the effectiveness of PrP^{res} degradation and removal upon treatment with an enzymatic and alkali chemistry in suspension studies or on samples eluted from stainless steel tokens. All lanes correspond to the analysis of 50 µg of brain equivalent.

6.3.2. Correlation of Structural Alterations in PrP^{res} and Infectivity

Immunoblotting was performed using six different antibodies targeted to different regions of the prion. Homogenates of scrapie strain 263K were treated with Enzymatics 1, 2 and 3, Alkali 1 and two phenolic compounds designated Phenolic 1 and 2 (Figure 31). In addition, homogenates were also treated with a 1 M solution of NaOH (Figure 32). Exposure time for the NaOH treatment was limited to 30 sec in order to detect early structural alterations to PrP^{res}. Exposure for a time greater than 90 sec demonstrated total degradation of PrP^{res} beyond the detection levels of the conventional immunoblot.

Treatment with Enzymatic 1 and 3 resulted in almost complete removal of the Bar 210 binding epitope. Whilst SAF 37, SAF 70, SHA 31, SAF 60 and Pri 917 signal was reduced relative to untreated controls, the remaining PrP^{res} was resistant to increasing concentrations of PK.

Enzymatic 2 treatment indicated an almost complete removal of Bar 210, SAF 37 and Pri 917 binding epitopes. However, the central core of SHA 31, SAF 60 and SAF 70 labelled epitopes remained stable to increasing PK concentrations. In contrast, PrP^{res} treated with Alkaline 1 demonstrated removal of Pri 917 and Bar 210 binding epitopes with sensitisation of the central core to PK, as has been demonstrated in preceding chapters.

Phenolic 1 treatment of PrP^{res} resulted in an almost complete degradation of the Bar 210 and SAF 37 binding epitopes. However, the remaining epitopes were stable and resistant to degradation under increasing concentrations of PK, as were SHA 31 and SAF 70 epitopes. In contrast, the SAF 60 epitope was sensitive to PK degradation.

Treatment of PrP^{res} with Phenolic 2 almost completely degradeed Bar 210, SAF 37, SAF 70 and SAF 60 binding sites. However, these epitopes, in addition to Pri 917 and SHA 31 epitopes were resistant to PK.

At a 30 sec exposure time of 1 M NaOH, Pri 917 and Bar 210 epitopes were completely removed. The central core binding epitopes labelled by SAF 60, SAF 70, SHA 31 and SAF 37 were reduced in concentration and remain sensitive to PK (Figure 32). An extension of exposure time from 30 sec to 90 sec to 1 M NaOH completely degraded all binding epitopes.

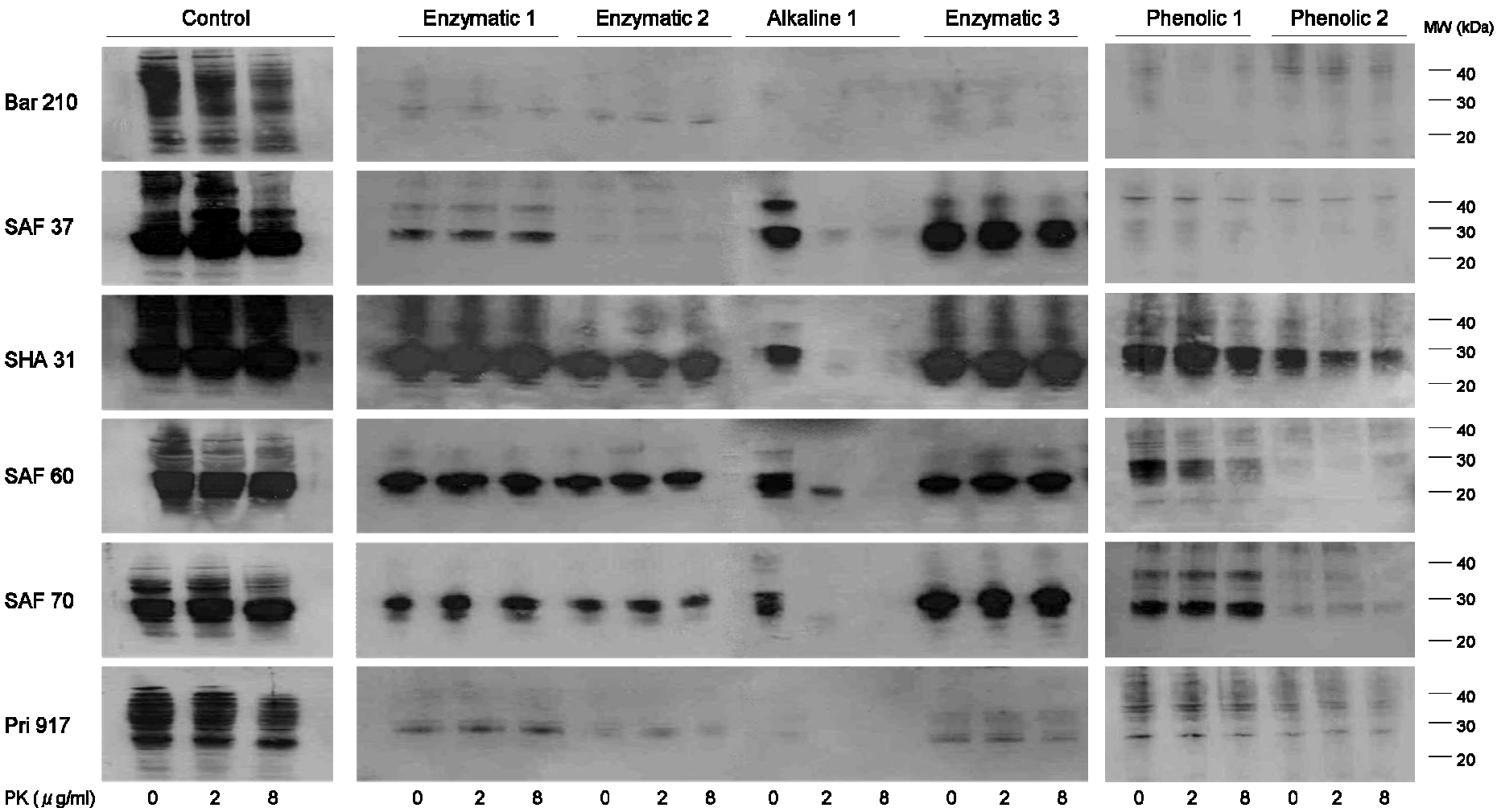

Figure 31 Western blot analysis of the effectiveness of PrP^{res} degradation upon treatment with various enzymatic, alkali or phenolic chemicals with detection performed using six different primary antibodies Bar 210, SAF 37, SHA 31, SAF 60, SAF 70 and Pri 917. All lanes correspond to the analysis of 50 µg of brain equivalent.

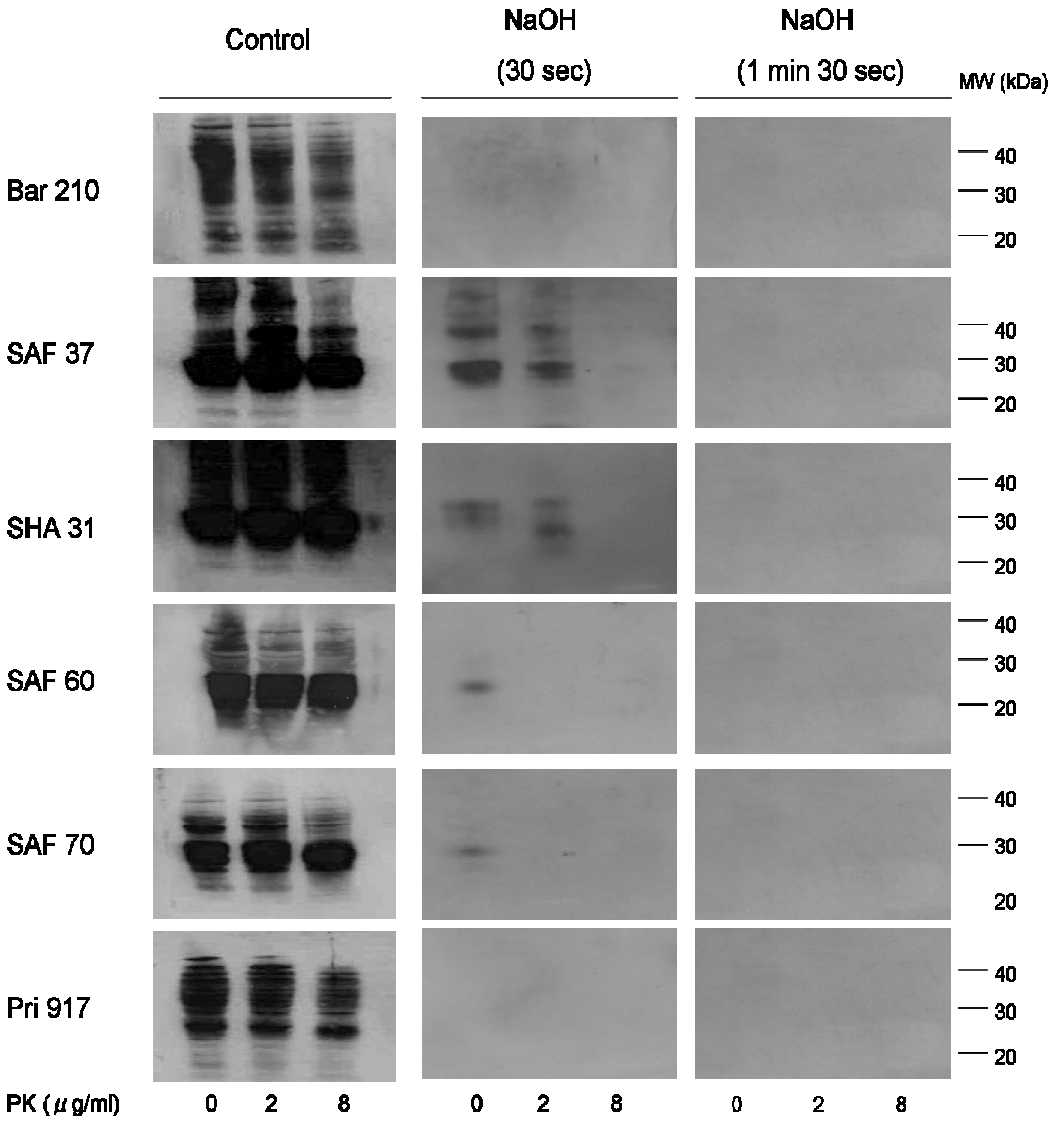

Figure 32 Western blot analysis of PrP^{res} degradation following treatment with 1M NaOH at 100 ºC for 30 sec and 1 min 30 sec. Detection was performed using six different primary antibodies. All lanes correspond to the analysis of 50 μg of brain equivalent.

6.4. DISCUSSION

Ambiguity over the infectious agent in prion disease has clinical implications, including the uncertainty over detection techniques for the validation of methods used to remove or inactivate infectivity from surfaces, such as surgical instruments. The current gold standard approach is the rodent bioassay. Aside from ethical and financial concerns, the time course for disease development is slow with studies routinely lasting a year before a complete set of results can be obtained (Fichet *et al.*, 2007c; Yan *et al.*, 2004).

Techniques such as immunoblotting and fluorescent amyloid detection are limited in their range of sensitivity and may not encompass, at least entirely, the infectious agent.

6.4.1. Correlation of the EDIC/EF Dual Stain with Immunoblotting and the Animal Bioassay

In this study, stainless steel suture wires were inoculated with 263K scrapie homogenate. Treatment was carried out using a selection of commercially available decontamination chemistries that were enzymatic, phenolic and alkaline in nature. The effect of these treatments on transmissible disease was determined using the animal bioassay which was correlated with two routinely used methods. Firstly, standard Western blots were used to assess the activity of these chemistries on PrP^{res} in suspension and its removal from surfaces using previously published methodology (Fichet *et al.*, 2004). Secondly, stainless steel wires, identical to those used in the *in vivo* rodent wire implant model, were fluorescently labelled with the EDIC/EF dual staining procedure to identify total protein and prion-associated amyloid.

Analysis of control wires demonstrated a significant concentration of amyloid present on the wires as a result of the amyloid-rich nature of the cerebral cortex in the 263K scrapie strain. A calculated mean concentration of 6.7 ng/mm^2 of prion-associated amyloid was identified on the wires' surface relative to 11.1 ng/mm^2 of total protein. As such, removal of 263K infected homogenate was significantly more difficult than NBH following treatment with Enzymatic 2, 4 and Alkaline 1. However, the increased resistance of 263K homogenate to removal relative to NBH was dependent on the treatment with Enzymatic 1, 2 and 5 showing no difference in removal capacity.

In situ residual amyloid was detected on wires following treatment with Enzymatic 1, 3, 4 and 5, as well as Alkaline 1 despite a 3 – 3.5-log reduction for each treatment. This is in contrast with surface studies by Western blot which demonstrated a complete removal of PrP^{res} signal following treatment with all of the enzymatic chemistries. This is likely a result of the difficulties and sensitivity issues surrounding elution of the treated sample from the stainless steel tokens. In addition, this study also demonstrates residual amyloid on the wires following treatment with a 0.8 % working concentration of Alkaline 1 where PrP^{res} signal detected by suspension Western blotting was lost subsequent to treatment with a 0.4 % concentration. This study is in agreement with previously published data demonstrating an increased sensitivity of fluorescent amyloid detection by Thioflavin T relative to Western blot (Hervé *et al.*, 2009; Lipscomb *et al.*, 2007a). Importantly, in the study by Lipscomb *et al*., (2007a), Western blotting was performed in suspension without

the need for elution of the sample from a surface. As such, the relative sensitivity of Thioflavin T detection is likely to be further increased relative to surface Western blotting and it must also be noted that the 20 µl homogenate aliquoted onto the tokens will be significantly greater than the concentration absorbed onto the wires during inoculation. It is important to note that a previous study utilising surface Western blot demonstrated several cases where no correlation between immunoblot data and infectivity was observed, one of which was shown to induce a complete reduction in infectivity but no effect on PrP^{res} in the Western blot (Fichet *et al.*, 2004).

Although Thioflavin T amyloid labelling clearly displayed a greater degree of sensitivity over surface Western blot studies, only Western blot data carried out in suspension correlated, in all treatment cases, with infectivity in the animal bioassay. Analysis of fluorescently labelled amyloid on the wires demonstrates correlation with infectivity in only two out of four cases (Enzymatic 3 and 4). Retrospective correlation of Enzymatic 1 analysis with previously published infectivity data for this treatment also demonstrated an association between *in situ* amyloid and infectivity (Yan *et al.*, 2004). Whilst Enzymatic 5 was not available for evaluation using the animal bioassay, it is hypothesised that, given its relatively lower removal of prion-associated amyloid in comparison with the other treatments and its lipase-based enzymatic activity, a full rate of transmission of disease would be expected. In the case of Enzymatic 2, complete removal of detectable amyloid was demonstrated in the presence of infectivity and without degradation of PrP^{res}. Interestingly, this occurred with relatively little removal of general protein from the wires when compared with untreated controls suggesting that rather than an unlikely preferential removal of amyloid, treatment disrupted amyloid fibre stability with separation into monomers or concentrations below the detection limit of Thioflavin T. In contrast, Alkaline 1 treatment resulted in an absence of transmissible disease with an estimated 5.1 pg/mm^2 of residual prion-associated amyloid on the wires. Previous studies using this alkaline detergent have also demonstrated a removal of infectivity from the wires in parallel with the presence of a proteinase K sensitive form of PrP^{res} (Fichet *et al.*, 2004). Given the correlation of suspension Western blots with infectivity, this suggests that the *in situ* methods of detection used within this study are either too insensitive (surface immunoblots) or do not label the infectious agent, in the case of Thioflavin T detection of amyloid. The latter finding is in agreement with studies indicating that mice expressing PrP lacking the GPI-anchor demonstrated dense accumulations of amyloid plaques in the brain and extraneural tissues, including the heart, accompanied by minimal clinical manifestations (Chesebro *et al.*, 2005). The blood and cardiac tissue of these GPI-anchorless transgenic mice has been shown to induce scrapie disease in wild-type mice

(Trifilo *et al.*, 2006). This is also replicated in a case of GSS whereby brain tissue demonstrated no spongiform degeneration and subsequent inoculation of the brain homogenate into transgenic mice resulted in striking amyloid deposition in the absence of disease (Piccardo *et al.*, 2007).

6.4.2. Correlation of Structural Alterations in PrP^{res} and Infectivity

Due to the correlation of suspension Western blots with infectivity, further studies attempted to detect a relationship between the presence or absence of prion epitopes and infectivity. This was performed using six different primary antibodies targeted to distinct regions of the prion protein following various decontamination treatments. The N- and C-terminals were labelled using Bar 210 and Pri 917 respectively. The octapeptide repeat region was identified using the antibody SAF 37 and three antibodies were chosen to label the central core: SHA 31 (residues 145-152) encompassing the H1 region, SAF 60 (residues 157-161) and SAF 70 (residues 156-162). Both SAF 60 and SAF 70 are targeted to similar amino acid residues of PrP^{res}. Interestingly, following treatment with Alkali 1, the SAF 60 binding region appears more sensitive to PK degradation relative to SAF 70 with the opposite observed following treatment with Phenolic 1. This suggests variable detection capabilities of the prion protein by Western blot analysis, dependent on the antibody and decontamination method.

Infectivity data from the animal bioassay, shown in Table 11, demonstrates a complete removal of infectivity following treatment with Alkali 1. Complete transmission of disease was observed in all animals following Enzymatic 2 and Enzymatic 3 treatment, with a corresponding 1 and 3.5-log reduction in infectivity, respectively. Enzymatic 1 has shown full transmission of disease and previously published infectivity data by collaborators indicates no transmissible disease following Phenolic 1 and NaOH treatment (Fichet *et al.*, 2004; Yan *et al.*, 2004). Conversely, Phenolic 2 has demonstrated full transmission of disease in the animal model and is four to five-fold less effective than Phenolic 1 (Race & Raymond, 2004).

Comparisons with infectivity and structural degradation of PrP^{res} suggest a distinct lack of correlation between the two. Western blotting following Alkali 1 treatment indicates a removal of the N-terminus residues 26-34 and the C-terminus residues 216-221, identified by Bar 210 and Pri 917 respectively. The OR region and central core residues are detectable using Western blot but are rendered PK sensitive. This is also observed in the early stages of NaOH degradation of PrP^{res}. Importantly, treatment with Phenolic 1, the only other chemical evaluated which demonstrated complete removal of infectious disease

in the animal bioassay, demonstrated an almost complete degradation of the N-terminal and OR region. However, a confounding factor in the conclusion that the N-terminus is involved in infectious disease is the removal of this epitope following treatment with both Phenolic 2 and Enzymatic 3, two chemistries which have no effect on overall transmission rate, although Enzymatic 3 demonstrates a 3.5-log reduction in infectivity. Moreover, whilst the C-terminus is also removed during Alkaline 1 and early NaOH exposure, it is detected by Pri 917 following treatment with Phenolic 1.

Interestingly, despite a 100 % transmission rate, Phenolic 2 appears extremely effective at the decontamination of PrP^{res} when analysed by Western blot. With the exception of the H1 domain and C-terminus, Phenolic 2 is capable of a significant reduction in all other epitopes relative to the untreated controls and other chemistries. The N-terminus, OR region and central core residues identified by SAF 60 and SAF 70 are almost completely degraded by this chemistry allowing for highly misleading conclusions to be drawn on the effectiveness of this cleaner if taken separately from the infectivity data.

Critically, EDIC/EF data displayed in Figure 28 suggests that both Enzyme 1 and 3 are efficient at removal of protein from a surface. Residual protein concentrations are comparable with those following treatment with Alkaline 1 implying that residual infectivity is largely a result of the direct action of the chemical on PrP^{res}, rather than removal from the surface. It remains possible that infectivity resides within other epitopes of the prion protein than are identified by the primary antibodies utilised in this study. Importantly however, the structural changes associated with the rendering of PrP^{res} highly PK sensitive by Alkaline 1 and NaOH treatment appear able to remove the capability of the prion protein to transmit disease.

Correlation of methodologies has highlighted the lack of sensitivity of Western blotting where elution of sample material from a surface is carried out and the relative improved sensitivity of Thioflavin T detection by EDIC/EF against conventional Western blotting, in suspension or surface studies. However, this study has observed infectivity in the absence of detectable amyloid and, conversely, wire bound prion-associated amyloid in the presence of transmissible disease. Interestingly, the former of these observations demonstrated a breakdown of amyloid by the enzymatic treatment but no effect on overall PrP^{res} and infectivity. This is perhaps of note to therapeutic interventions in the amyloidoses which target amyloid aggregates. As such, whilst amyloid, as detected by Thioflavin T and EDIC/EF, may be a more sensitive biomarker relative to PrP^{res} detection with Western blot, it appears less likely to correlate with infectivity than PrP^{res} and therefore can not be considered as a marker for infectious disease. Improving the

sensitivity of fluorescent amyloid detection by Thioflavin T analogues such as BTA-1 which demonstrate a fifty-fold higher affinity for amyloid may provide better correlation with infectivity (Klunk *et al.*, 2001; Klunk *et al.*, 2003). Whilst this does not suggest that amyloid is not infectious in an untreated state it is clear that under conditions designed to break down and denature amyloid and PrP^{res}, the infectious agent is smaller than the detection capacity of Thioflavin T. This study can not rule out PrP^{res} as the infectious agent, given the correlation with suspension Western blot and infectivity. However, antibody mapping of the prion protein to identify epitopes associated with infectivity was inconclusive. Epitopes such as the C- and N-terminus removed by NaOH and Alkali 1 treatment, in addition to the OR region almost entirely removed by Phenolic 1, were also absent following treatment by chemistries which displayed no effect on transmissible disease, such as Phenolic 2 or Enzymatic 3. Given the uncertainty over the infectious unit in prion disease, infectivity assessment using the animal bioassay remains the only guaranteed method of prion disease detection.

CHAPTER 7

ISOLATION AND EVALUATION OF A THIAZOLE ANALOGUE FOR THE FLUORESCENT DETECTION OF PRION-ASSOCIATED AMYLOID

7.1. INTRODUCTION

Thioflavin T (ThT) was first introduced by Vassar and Culling (1959) who demonstrated enhanced fluorescence and highly specific binding of the cationic benzothiazole dye to amyloid in the kidney. Thioflavin T binding is a universal feature of all amyloid fibrils and consequently it has been utilised in fibril formation studies, in addition to *in vitro*, *in vivo* and *in situ* imaging of the Aβ peptide and PrP among other amyloidotic, disease-associated proteins (Ban *et al.*, 2003; Colby *et al.*, 2007; Klunk *et al.*, 2001; Lipscomb *et al.*, 2007a; Mathis *et al.*, 2003).

Investigations into the association of amyloid fibres and Thioflavin T have suggested a specific and regular binding model, with studies using laser confocal microscopy detecting a consistent pattern of emission (Krebs *et al.*, 2005). Further confocal microscopy work has indicated that ThT binds to fibrils with the long axes of both fibril and dye parallel to each other, indicating that binding occurs in 'channels' formed by β-sheet side chains which stretch the length of the structure (Groenning *et al.*, 2007; Krebs *et al.*, 2005). The proximity of the β-sheet side chain structures when associated with Thioflavin T leads to steric interactions producing intense fluorescence when in a bound state. Fluorescence is associated with a large Stoke's shift, with excitation at around 353nm and emission at 482nm (Lockhart *et al.*, 2005). However, although the interaction with amyloid fibrils is specific, it occurs with varying efficiency (Krebs *et al.*, 2005). Moreover, ThT also possesses low lipophilicity. Structurally, Thioflavin T contains a hydrophobic terminal, with a dimethylamino group attached to a phenyl, linked to a benzothiazole containing the polar nitrogen and sulphur (Khurana *et al.*, 2005) (Figure 33). Consequently, the compound is charged at physiological pH and therefore does not traverse the blood brain barrier limiting its use as an *in vivo* fluorescent probe. This fact has also been attributed to the identification of ThT as a substrate for P-glycoprotein, a member of the ABC transporter family of membrane proteins (Darghal *et al.*, 2006). For this reason, ThT is generally considered as a potential pharmacophore for the development of further amyloid imaging agents (Klunk *et al.*, 2001; Voropai *et al*., 2003).

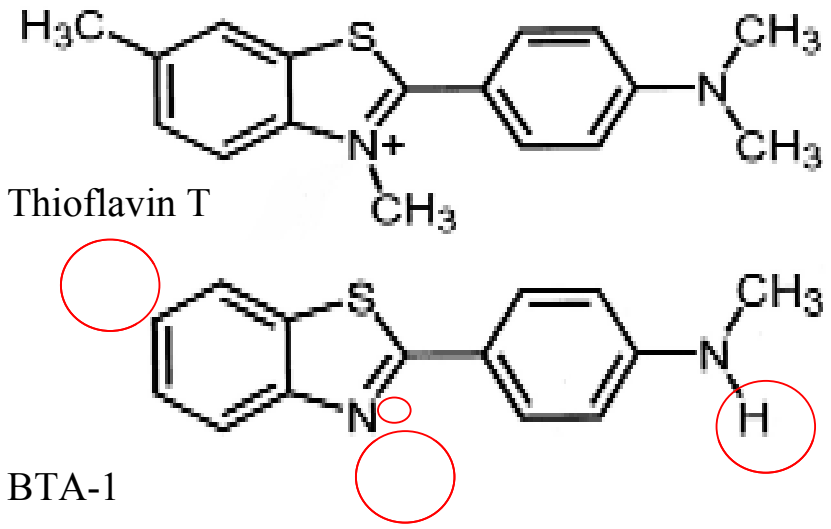

Figure 33 Chemical structure of Thioflavin T and its derivative BTA-1. Red circles indicate modified or removed chemical groups of BTA-1 relative to the precursor Thioflavin T and the loss of the positive charge on the quaternary heterocylic nitrogen.

The compound 2-(4'-Methyaminophenyl) Benzothiazole (BTA-1) is a relatively new derivative of Thioflavin T (Figure 33). It is more lipophillic than its precursor due to a loss of the positive charge of the quaternary heterocylic nitrogen of the benzothiazolium group (Klunk *et al.*, 2003). Relative to ThT, BTA-1 also demonstrates a fifty-fold higher affinity for Aβ fibrils and amyloid plaques in post-mortem AD and prion-positive brain tissue, where the K_i of BTA-1 is equal to 20.2 ± 3 nm, relative to Thioflavin with a Ki of 890 nM (Klunk *et al.*, 2001; Klunk *et al.*, 2003; Mathis *et al.*, 2002; Mathis *et al.*, 2003).

Consequently, in this chapter, BTA-1 was assessed for its ability to fluorescently label prion-associated amyloid using EDIC/EF and a staining protocol was optimised. In collaboration with the Department of Chemistry, University of Southampton, fourteen Thioflavin T analogues and twenty-one BTA-1 analogues were synthesised. Evaluation of each analogue was performed, permitting isolation of a compound of interest for which further testing was undertaken.

7.2. MATERIALS AND METHODS

The methodology for this section of work is described in Chapter 2. ME7 and 263K scrapie and naïve brain tissue sections were prepared as detailed in section 2.2.3. Optimisation of a fluorescent staining protocol for the thiazole derivative BTA-1 was performed. Subsequent to this work, analysis of a series of thiazole analogues was performed as described in 2.6.1. Following isolation of a compound known as 2-(4'-

Dimethylaminophenyl)-6-Methyloxybenzothiazole or 28d, further evaluation was undertaken as detailed in sections 2.6.2, 2.6.3 and 2.6.4. Visualisation and analysis was carried out using EDIC/EF (section 2.7 and 2.7.1).

7.3. RESULTS

7.3.1. Optimisation of a BTA-1 Protocol for the Fluorescent Labelling of Prion-Associated Amyloid

The previously optimised protocol for the fluorescent labelling of prion-associated amyloid by Thioflavin T was utilised as a starting methodology. Through personal correspondence with Professor W. Klunk, University of Pittsburgh, an initial 500 μM stock solution was prepared in dimethyl sulfoxide (DMSO). Various exposure times and working concentrations were subsequently evaluated and assessed on hippocampal sections of ME7 scrapie-infected brains (Figure 34). A final exposure time of 45 min and a working concentration of 50 nM were chosen based on the clear identification of prion-associated amyloid against surrounding tissue and relative to staining of naïve brain tissue sections (Figure 35). As a consequence of the lipophilic nature of BTA-1 the acetic acid rinse step, used to reduce non-specific background staining by Thioflavin T, was removed from the protocol and a brief rinse in PBS was incorporated to remove excess BTA-1 solution.

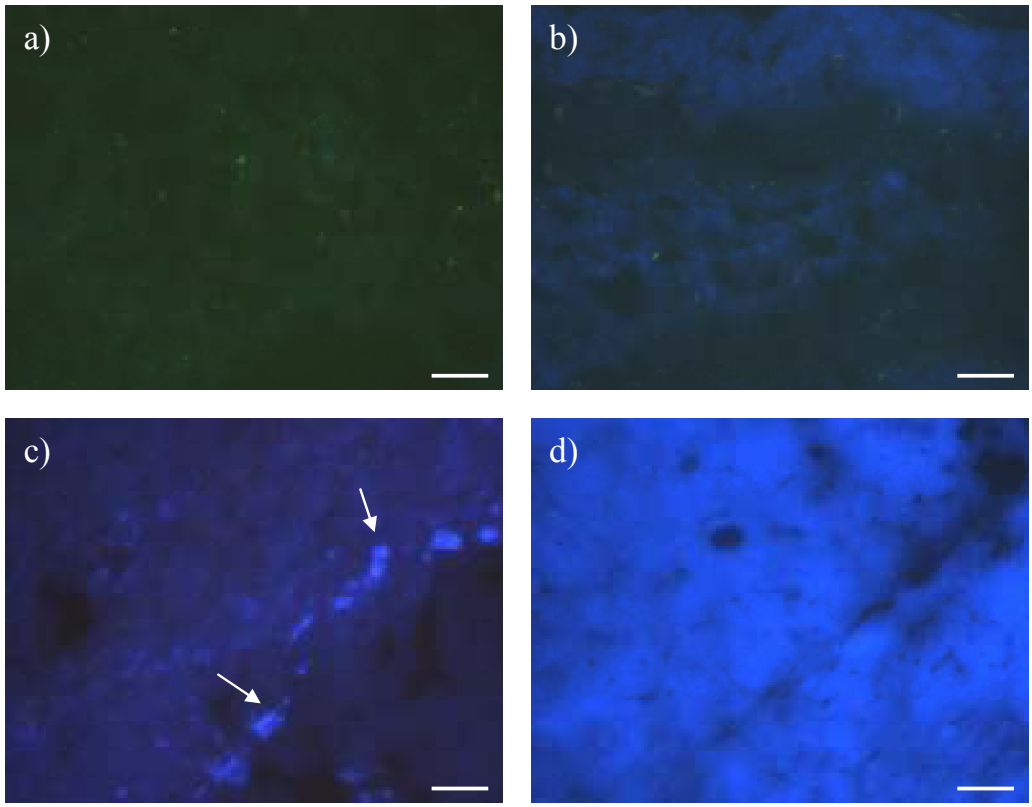

Figure 34 Photomicrographs taken using EDIC/EF of ME7 scrapie-infected tissue sections (n=6/concentration) fluorescently labelled with increasing concentrations of BTA-1: a) 500 pM, b) 1 nM, c) 50 nM & d) 500 µM. Arrows indicated prion-associated amyloid deposits. Scale bar: 20 µm.

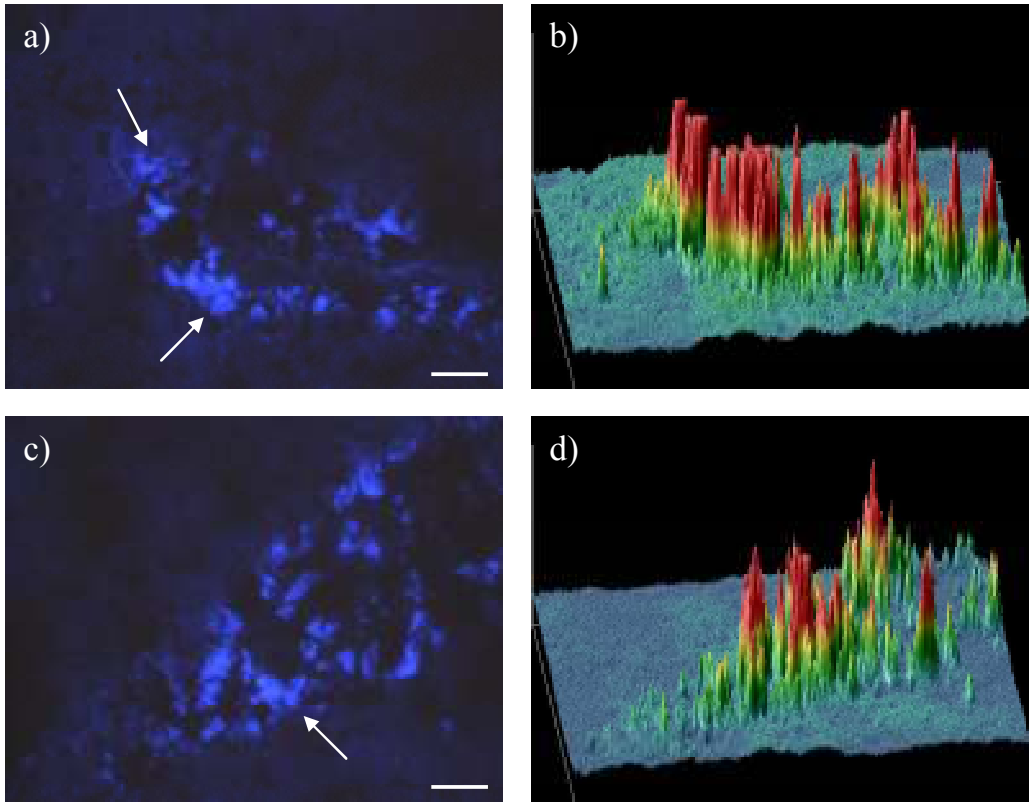

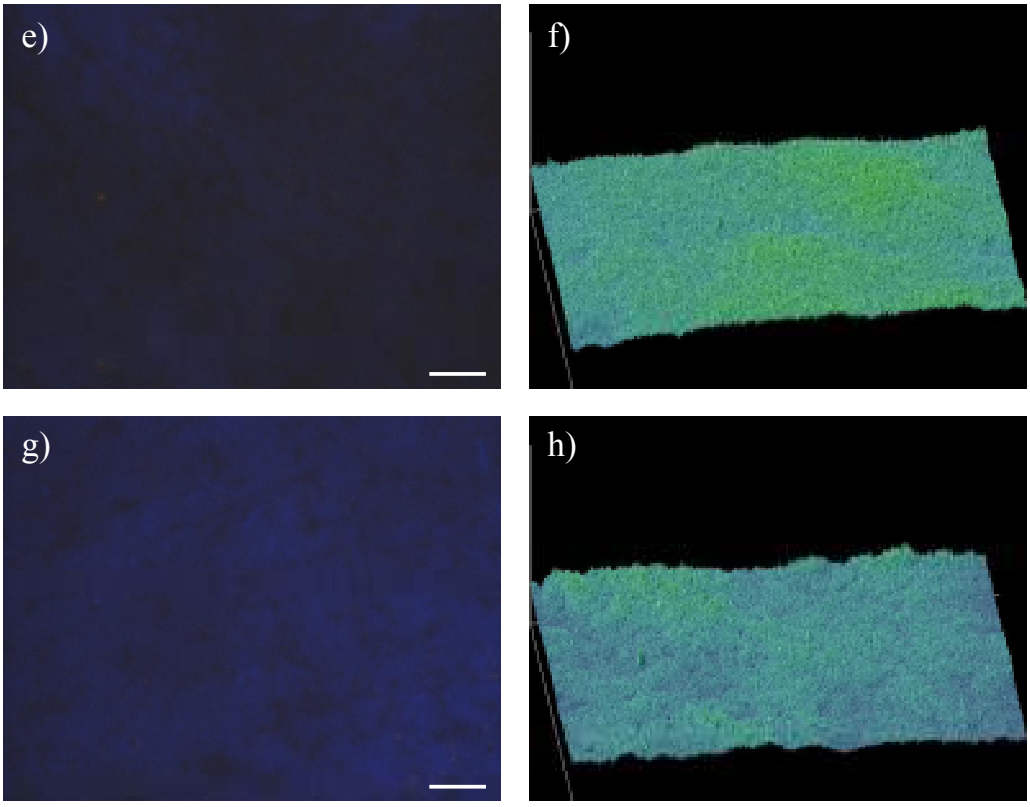

Figure 35 Fluorescent labelling of prion-associated amyloid deposits in ME7-scrapie infected brain [n=6; images a), b), c) & d)] and naïve brain sections [n=6; images e), f), g) & h)] utilising a BTA-1 concentration of 50 nM with an exposure time of 45 mins. Images a), c), e) & g) demonstrate EDIC/EF images with b), d), f) & h) displaying the corresponding surface plot. Arrows indicate areas of prion-associated amyloid deposition. Scale bar: 20 μm.

7.3.2. Screening of Thiazole Analogues for the Ability to Detect Amyloid in ME7 Scrapie-Infected Tissue

Each analogue was assessed for their ability to fluorescently label prion-associated amyloid in hippocampal sections of ME7-scrapie brain tissue. Amyloid was clearly visible in these sections following staining with both Thioflavin T and BTA-1 (Figure 36). Assessment was carried out in triplicate using the previously optimised protocols established for BTA-1 and Thioflavin T. Selection of the most suitable protocol was based on the structural relationship of the compound to either precursor.

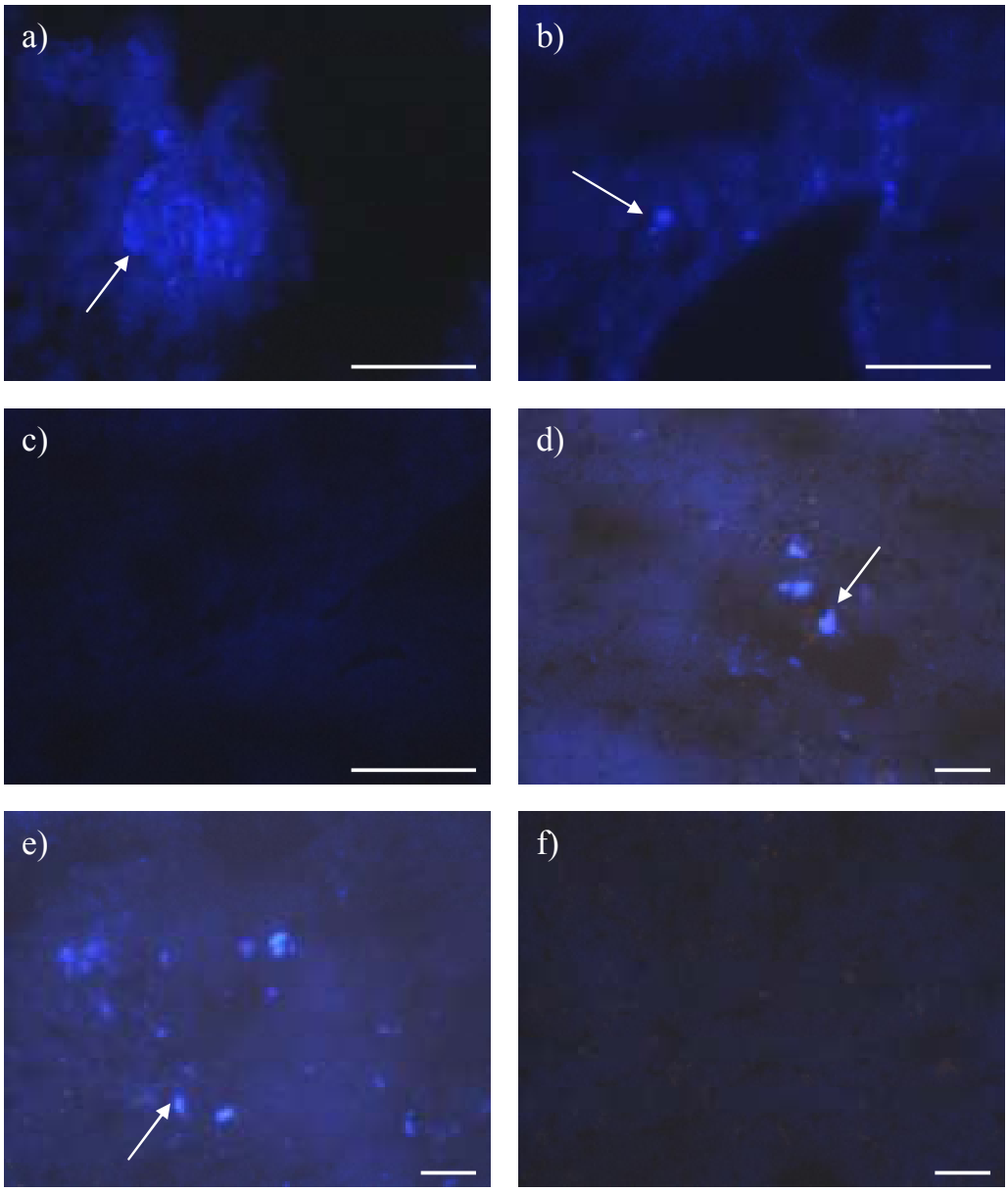

Figure 36 Prion-associated amyloid deposits in ME7 [a), b), d) & e)] and naïve brain [c) & f)] sections fluorescently labelled with Thioflavin T [n=6; images a), b) & c)] and BTA-1 [n=6; images d), e) & f)]. Arrows indicate prion-associated amyloid deposition.
Scale bar: 20 μm

Each BTA-1 analogue was evaluated at both 100 nM and 50 nM working concentrations. An arbitrary score was attributed to each analogue by four volunteers as a measure of the compounds ability to bind to and identify amyloid from naïve brain tissue relative to their structural precursor in regions of the brain known to display large concentrations of plaque deposition (Table 11 and Figure 37). Representative images of several of the analogues applied to ME7 scrapie-infected tissue are shown in Figure 38.

Table 12 Mean scores attributed to BTA-1 and Thioflavin T analogues assessing their ability to fluorescently label prion-associated amyloid.

BTA-1 analogues		Thioflavin T analogues	
Chemistry	Assessment scores[a]	Chemistry	Assessment scores[b]
BTA-1	✓✓✓✓✓	Thioflavin T	✓✓✓✓✓
28c	✓	30a*	✓
31d	✓	31a	x
28d	✓✓✓✓	31b	✓
30b	x	31c	✓
33b	x	33a*	x
33c	✓	29e*	✓✓
33d	x	28a	x
42b	x	28b*	x
41h	x	29d*	x
43	x	29b*	x
42c	x	29g	✓
42a	✓	29h*	x
41c	✓	29f	x
41e	x	29c*	✓
41a	✓		
41d	x		
41g	x		
41f	x		
41i	x		
44	✓		
41b	x		

[a]Response to 340 – 380 nm excitation. [b]Response to 405 – 455 nm excitation. [*]indicates analogue was incompletely soluble in 0.1 M HCl

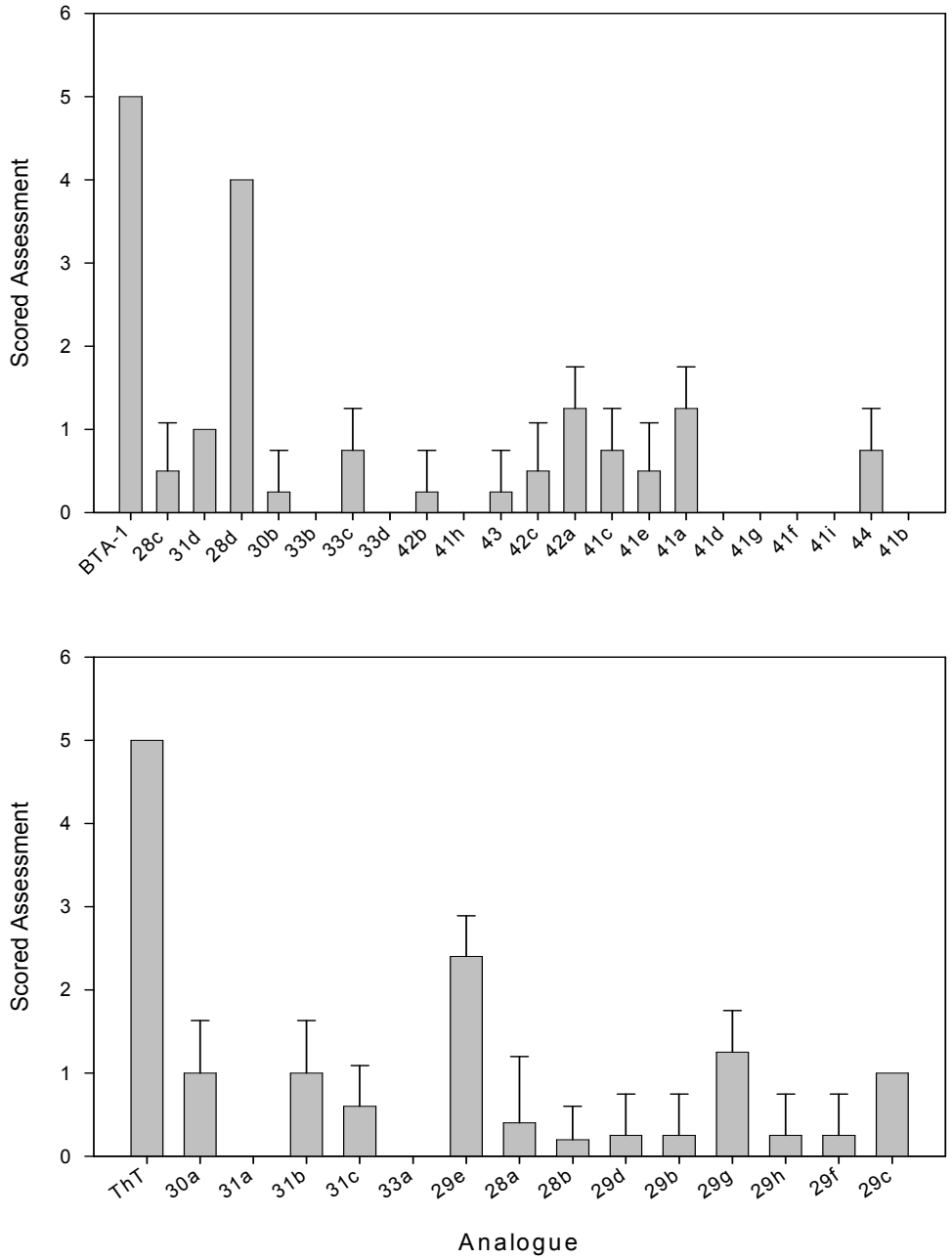

Figure 37 Graphical representation of the scored assessment of each thiazole analogue relative to their precursor upon staining of ME7 scrapie brain tissue sections (n=3/analogue). A score of 0 is equivalent to x and 5 = ✓✓✓✓✓.

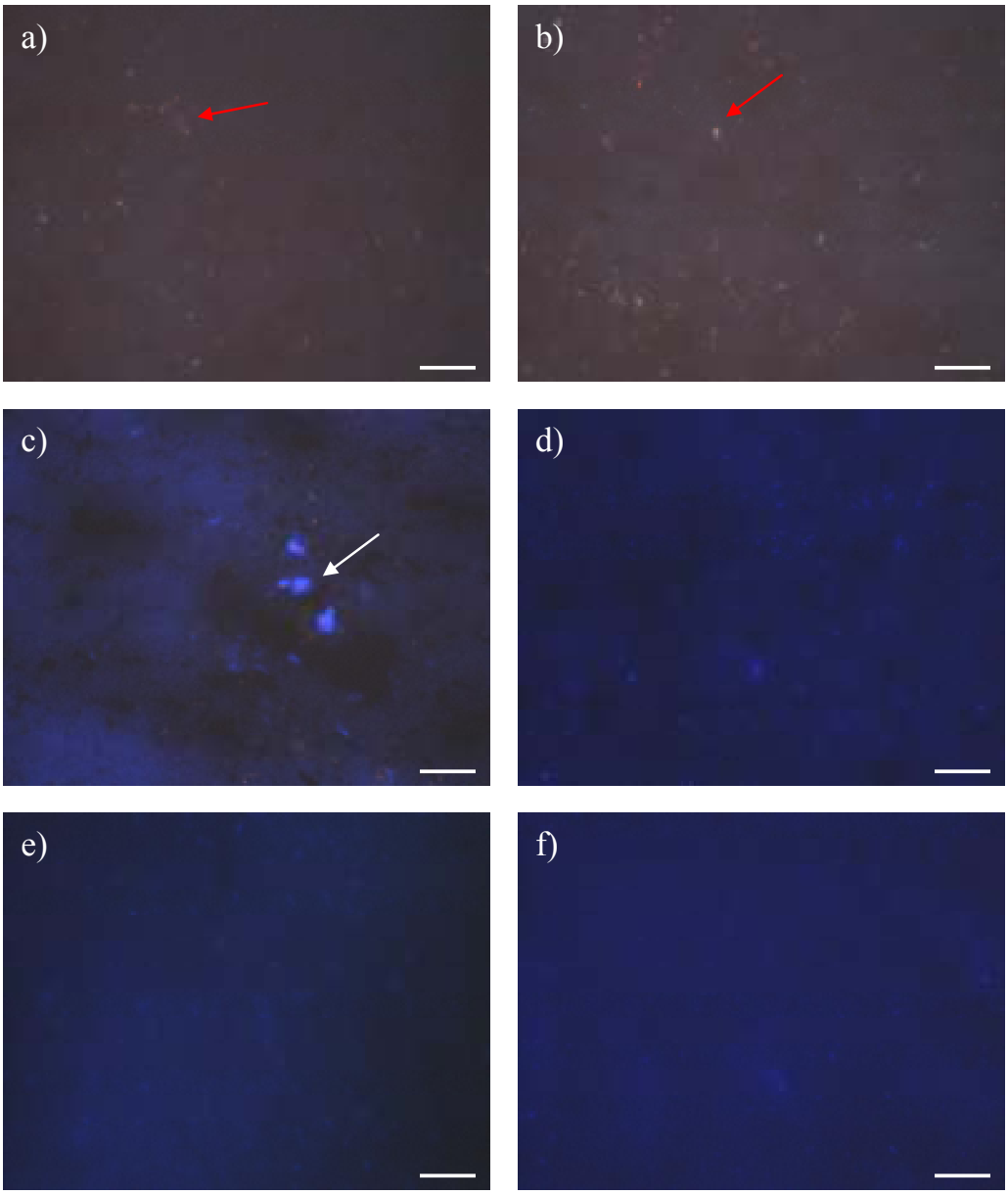

Figure 38 Representative photomicrographs of ME7 scrapie-infected brain sections (n=3/analogue) fluorescently labelled with the thiazole analogues: a) 41d, b) 41g, c) 28d, d) 29e, e) 31b & f) 31a. White arrow indicate positive staining of prion amyloid in a tissue section. Red arrows indicate autofluorescent lipofucin. Scale bar: 20 µm.

Screening of the thiazole analogues identified a Thioflavin T and BTA-1 derivative, designated 29e and 28d, respectively, as compounds of interest. Comparison with naïve brain sections stained in parallel with ME7 tissue confirmed the remaining compounds as being ineffective amyloid fluorophores. Faint autofluorescent lipofucin, visible as gold and blue deposits approximately 2 µm in diameter under BTA-1 and Thioflavin T EDIC/EF filters, respectively, was identified in both scrapie-infected and naïve brain sections (Figure 38). Further tissue section staining was performed using 29e and 28d analogues relative to

their precursors. This permitted the exclusion of the Thioflavin T analogue 29e for subsequent analysis based on poor reproducibility of initial results, potentially due to its incomplete solubilisation in HCl (Table 11). Conversely, the analogue 2-(4'-Dimethylaminophenyl)-6-methyloxybenzothiazole or 28d demonstrated intense fluorescence upon binding to deposits morphologically similar to prion-associated amyloid plaques at both 100 nM and 50 nM working concentrations.

7.3.3. Analysis of the Binding Sensitivity of BTA-1 and 28d Using Immunohistochemistry

To further assess the binding sensitivity of BTA-1 and 28d, both fluorophores were used to fluorescently label prion-associated amyloid in 263K scrapie-infected tissue sections. Their fluorescent signal upon binding to prion amyloid was overlaid with the primary antibody 6H4, recognising the prion protein amino acids 144 – 152, to confirm binding sensitivity. Negative controls performed in parallel with 263K scrapie-infected tissue sections confirmed the loss of PrP^c through the three step degradation process (data not shown).

Co-localisation of fluorescent signal from both BTA-1 and 28d was observed. Moreover, the fluorescent signal from both fluorophores was demonstrated to overlap with that of both diffuse and more concentrated prion-associated amyloid identified by 6H4 (Figure 39).

7.3.4. Analysis of 28d Binding Specificity Using EDIC/EF

Analysis of 28d binding specificity was performed. Positive, amyloid plaque-bound fluorescence of both BTA-1 and 28d (n=10/compound) was analysed against the fluorescence upon binding to naïve brain tissue. Amyloid plaques of similar dimensions were selected and analysis performed at a constant exposure. A high signal to background ratio corresponded to a greater difference between positive, amyloid-bound and background fluorescence. Consequently, a degree of specificity for each compound can be calculated.

Data obtained suggest that 28d demonstrates a greater specificity for prion-associated amyloid relative to BTA-1 as a result of a larger difference between fluorescently labelled prion-associated amyloid plaques and naïve brain tissue (Figure 40). Statistical analysis suggests a significant difference between the two data means ($P = 0.0015$) at the 95% confidence level.

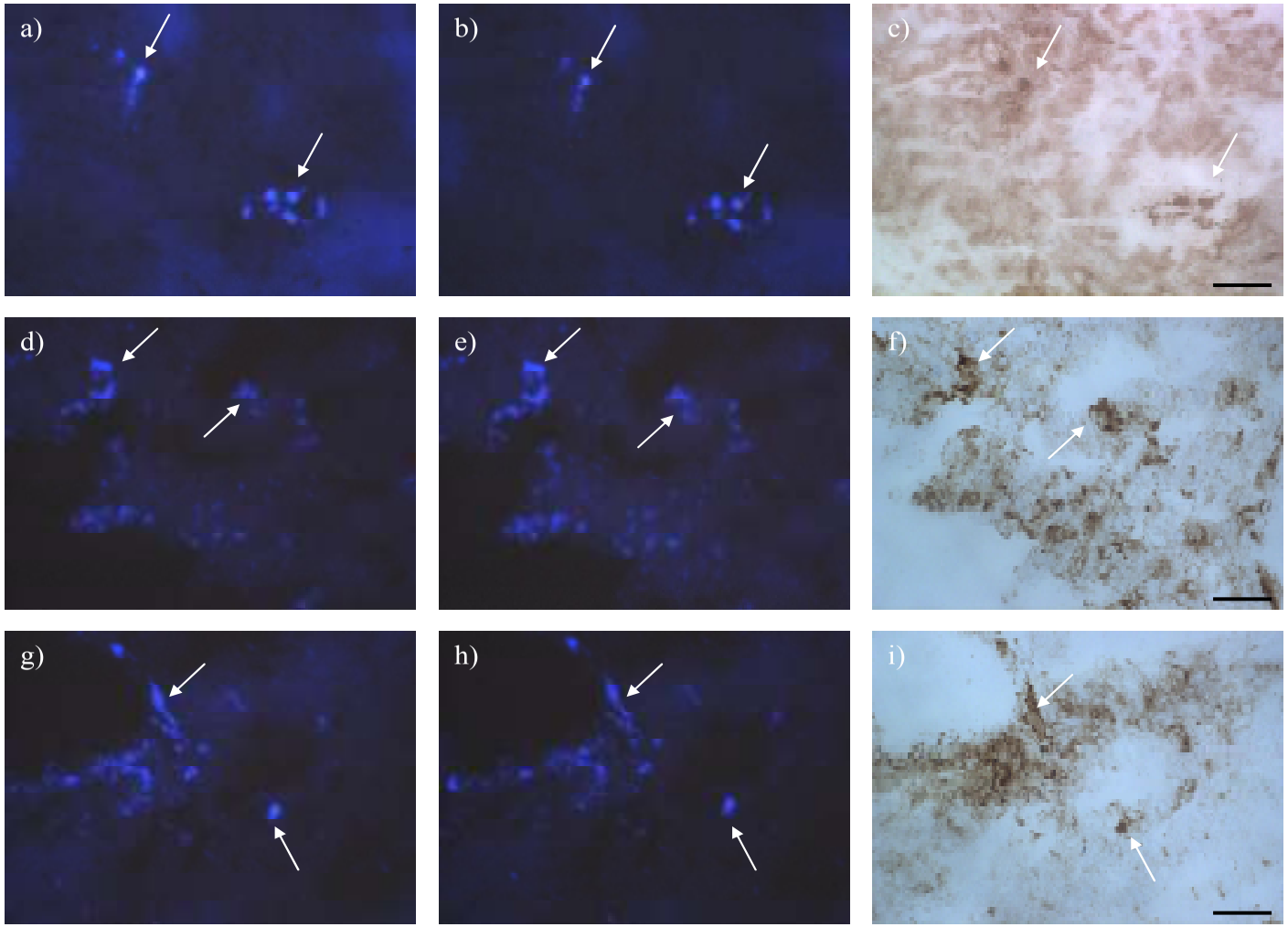

Figure 39 Photomicrographs indicating the association of fluorescent signal from the staining of prion-associated amyloid in 263K scrapie-infected brain (n=6 sections) with BTA-1 [a), d) & g)] and 28d [b), e), h)] with immunohistochemistry performed using the prion protein primary antibody 6H4 [c), f), i)]. Scale bar: 20 µm.

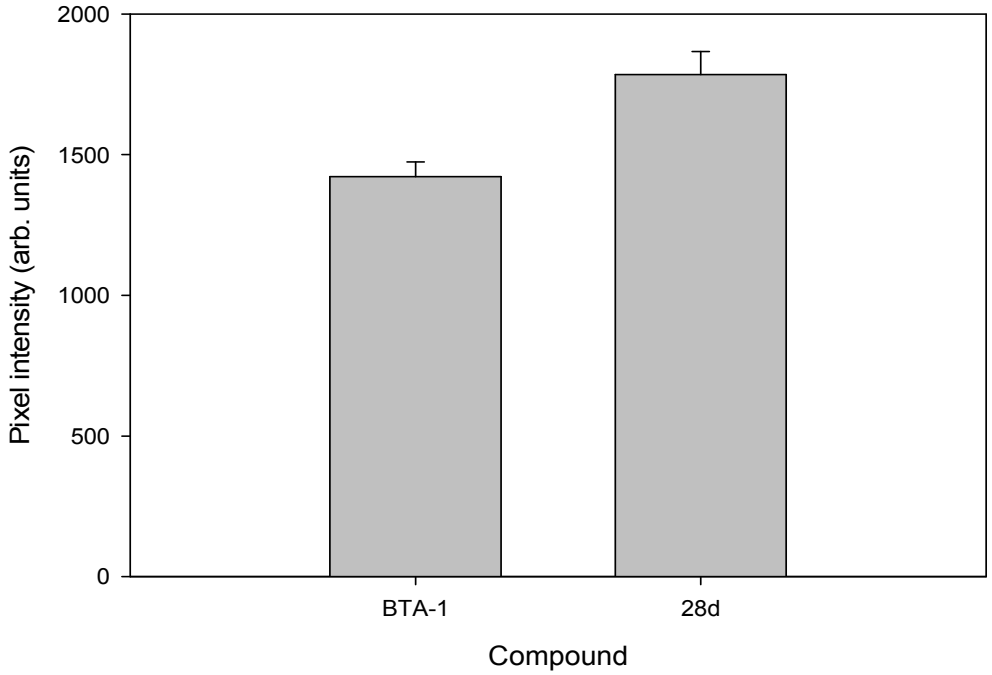

Figure 40 Ratio of prion amyloid-bound positive signal (n=10 amyloid plaques/staining procedure) to naïve tissue-bound background intensity of the thiazole fluorophores BTA-1 and 28d.

7.3.5. Analysis of the Rate of Photobleaching of 28d Against BTA-1

The rate of fluorescent signal loss or photobleaching was analysed. Amyloid plaques of similar dimensions were fluorescently labelled with either BTA-1 or 28d and the signal intensity was plotted at 10 sec intervals over a 10 min time course. A constant exposure was utilised throughout the experiment.

Data suggest a significant increase in amyloid-bound fluorescent signal stability relative to BTA-1 (Figure 41). The rate of fluorescent signal loss was markedly slower from amyloid plaques labelled with 28d comparative to BTA-1. At a time interval of 100 sec, 28d demonstrated an average signal intensity of 151.5 ± 3.4 relative to 96.7 ± 2.3 for BTA-1 at the same time period. This variation was demonstrated as statistically significant ($P = 0.00177$) at the 100 sec interval. However, at all time intervals, the plotted course of photobleaching was significantly different with an increased mean pixel intensity of amyloid-bound 28d relative to BTA-1.

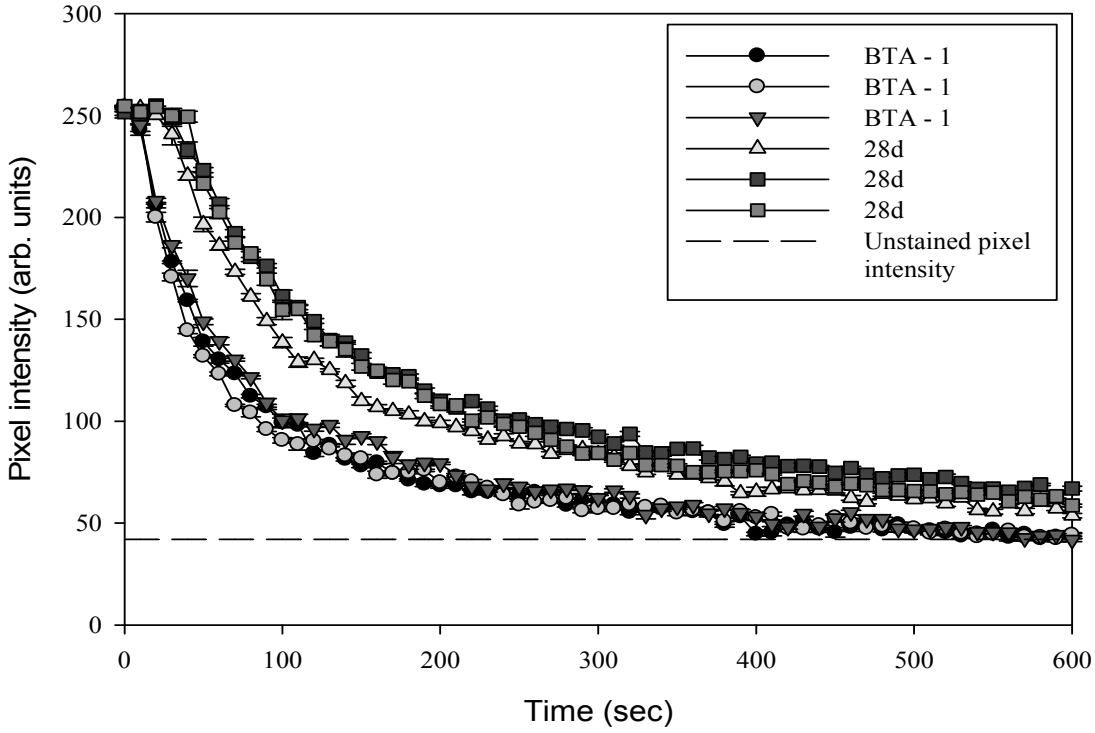

Figure 41 Loss of fluorescent signal intensity over a 10 minute time course for prion-associated amyloid plaques (n=3/staining procedure) fluorescently labelled with either 28d or BTA-1.

Significantly, both compounds displayed a comparable sigmoid pattern of fluorescent degradation. Critically, however, 28d demonstrates a much greater initial stability to signal degradation than BTA-1, resulting in a decreased overall rate of photobleaching. The fluorescent signal of 28d bound to amyloid is maintained at a constant level until approximately 40 sec, at which point the average fluorescent signal intensity of BTA-1 has decreased to 157.9 ± 2.02.

7.4. DISCUSSION

The amyloid flurophore 2-(4'-Methylaminophenyl) Benzothiazole or BTA-1 is a derivative of Thioflavin T. Studies have indicated that it possesses a high affinity for amyloid with high specificity towards amyloid plaques and neurofibrillary tangles in post-mortem Alzheimer brain tissue and selectively binds amyloid in both murine and several human TSE

strains (Ishikawa *et al.*, 2004; Klunk *et al.*, 2001; Klunk *et al.*, 2003). Absence of the positive charge from the quaternary heterocylic nitrogen of the benzothiazolium group also results in efficient brain entry and passage through the blood brain barrier, unlike Thioflavin T. Consequently, BTA-1, when radio-labelled with the positron-emitting radionuclide carbon 11 (^{11}C), represents a high quality tracer candidate for *in vivo* PET imaging (Klunk *et al.*, 2003; Mathis *et al.*, 2002; Neumaier *et al.*, 2007). Furthermore, derivatives of BTA-1, such as N-Methyl-^{11}C-2-(4'-methylamino-phenyl)-6-hydroxy-benzothiazole (^{11}C-6-OH-BTA-1; also known as "Pittsburgh Compound-B" or ^{11}C-PIB), have also demonstrated promising *in vivo* PET results in Alzheimer's disease (Butters *et al.*, 2008; Drzezga *et al.*, 2008; Ng *et al.*, 2007; Scheinin *et al.*, 2007). Further studies into amyloid detection using compounds such as BTA-1 and ^{11}C-PIB may aid in the early diagnosis of Alzheimer's disease, which is consequently critical for treatment considerations and disease management. In prion disease, amyloid fluorophores such as BTA-1 also possess the capacity to inhibit PrP^{res} formation in cellular models of TSE (Ishikawa *et al.*, 2004). Whilst BTA-1 had no effect on disease course in 263K or Rocky Mountain Laboratory (RML) *in vivo* rodent models, intravenous injection of 1 mg of the Congo red derivative (*trans*, *trans*),-1-Bromo-2,5-bis-(3-hydroxycarbonyl-4-hydroxy)styrylbenzene (BSB) prolonged the incubation period in RML mice by 14 %. These data suggest that amyloid imaging probes may provide significant advances in *in vitro* and *in vivo* detection, in addition to therapeutic benefits in prion diseases and the amyloidoses.

This study assessed the ability of thirty-five analogues of Thioflavin T and BTA-1 to fluorescently label prion-associated amyloid *in vitro* using the previously optimised protocol for their precursor. Initial study of the thiazole analogues was constrained by the total volume of each compound synthesised. However, the BTA-1 analogue 2-(4'-Dimethylaminophenyl)-6-methyloxybenzothiazol or 28d was selected for further evaluation based on the compounds ability to identify amyloid in ME7 scrapie-infected brain tissue. Structurally, 28d can be separated from BTA-1 due to the addition of a methoxyl group on the first ring and a methyl group, replacing a hydrogen atom, on the amine group (Figure 42). Interestingly, 28d also shares structural similarities with ^{11}C-PIB (Ng *et al.*, 2007).

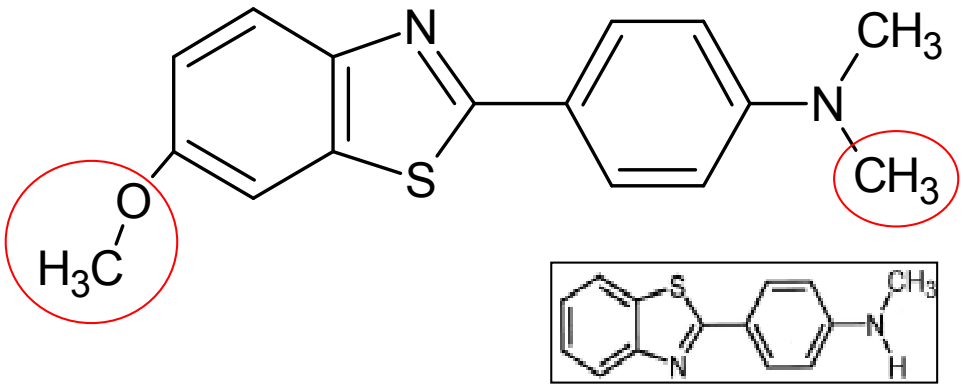

Figure 42 Chemical structure of 28d relative to BTA-1 (inset). Red circles indicate structural changes associated with 28d relative to BTA-1.

Common to the thiazole compounds, 28d possesses an intact three ring structure. No functionality was observed in compounds where the three ring structure was disturbed such as 30b or 31d, the latter possessing an identical empirical formula to 28d but structurally lacking a complete second ring. Compounds such as 28d, ^{11}C-PIB and BTA-1 lack the positive charge of the quaternary heterocyclic nitrogen observed in Thioflavin T. Therefore, it can be assumed that loss of this charge is beneficial to the compound in terms of sensitivity and/or specificity, or at least has no positive effect in addition to permitting greater blood brain barrier permeability as previously described. Moreover, compounds displaying a greater structural divergence from that of BTA-1 were ineffective. The structural similarities between 28d and ^{11}C-PIB suggest optimisation of the thiazole group of fluorescent amyloid-labelling compounds is likely to lie close to that of BTA-1. As such, 28d may represent an optimised chemical structure for the thiazoles.

Further analysis of 28d was performed to confirm the sensitivity of BTA-1 and 28d for amyloid. Positive fluorescent staining was overlayed with immunohistochemical labelled PrP^{res} using the primary antibody 6H4. A strong association was observed between 28d and BTA-1 fluorescence. Moreover, intense fluorescent signal, clearly distinguishable from surrounding tissue, strongly correlated with diffuse and concentrated PrP^{res} deposition as identified by 6H4. This suggests that the alteration in chemical structure of 28d from its precursor BTA-1 had no effect on the labelling of PrP^{res}. Data also demonstrate several advantageous features of 28d over its precursor. Firstly, positive, PrP^{res} fluorescence intensity was assessed relative to naïve tissue signal for both BTA-1 and 28d as a measure of compound specificity. The analogue 28d demonstrated a significantly greater difference in positively bound fluorescence compared with background fluorescence. Although this appeared to be a

result of a reduction in background fluorescence rather than an increase in binding to amyloid, it is not clear whether this difference may be due to a reduction in binding to naïve tissue or as a result of a lower degree of fluorescence upon attachment compared to BTA-1. Moreover, 28d also demonstrated greater signal stability relative to BTA-1. An important issue with regards to thiazole staining is the rate of signal degeneration which can be a major disadvantage compared to immunohistochemistry. With respect to its precursor Thioflavin T, BTA-1 is less stable under fluorescent light and any thiazole synthesis should aim to develop compounds with a slower rate of photobleaching. Conversely, 28d demonstrated a slower rate of fluorescent signal degradation over a 10 minute time course. At a 4 min time interval, the fluorescent signal of BTA-1 bound to PrP^{res} was indistinguishable from background fluorescence in contrast to 28d which was clearly visible. Critically, both BTA-1 and 28d display a weakening of signal through a similar path with an initial resistance to signal degeneration followed by a rapid loss of signal intensity which eventually begins to plateau after 3 minutes. However, 28d benefits from an increased stability when first exposed to fluorescent light which slows the time course of fluorescent signal degradation.

The implications for the identification of a novel thiazole compound capable of sensitively and specifically labelling prion-associated amyloid range beyond *in vitro* identification and the prion diseases. Similarities in the morphology of amyloid fibrils and the universal high β-sheet content common to all amyloid means that fluorophores are applicable and transferable between many of the amyloidoses such as prion, Alzheimer's, Parkinson's and Huntington's disease, unlike immunohistochemical techniques (Merlini & Bellotti, 2003). Moreover, techniques such as PET utilise amyloid fluorophores for *in vivo* detection in Alzheimer's disease and may be applicable to other diseases where amyloid deposition is a common event in the CNS or extraneural tissues. Data also suggest a potential therapeutic application for thiazole analogues (Ishikawa *et al.*, 2004; Ishikawa *et al.*, 2006). Unfortunately, evaluation of potential therapeutic benefit was beyond the scope of this study despite initial aims to perform such experiments. However, crucially, 28d represents a highly promising compound which may further enhance both *in vitro* and *in vivo* detection of amyloid disease. Preliminary evaluation suggests 28d to be both highly sensitive and specific for prion-associated amyloid and a more stable fluorophore, relative to BTA-1. Further tests are required to establish binding affinity data, brain permeability and toxicity. However, 28d represents a novel compound with potential as a therapeutic and *in vivo* imaging probe, in addition to increasing *in vitro* amyloid detection which may better correlate with infectivity in prion disease.

CHAPTER 8

FINAL DISCUSSION AND FUTURE WORK

This project was undertaken in order to improve methods of instrument decontamination in light of the risk of iatrogenic transmission of CJD to patients undergoing surgical procedures. Specifically, this project aimed to assess current decontamination procedures rather than the development of novel technologies or chemistries. It remained critical throughout this work that results and conclusions, as a consequence of these studies, were both applicable and translational to prion decontamination in an SSD setting.

An evaluation of current hospital decontamination procedures suggested that a significant concentration of proteinaceous contamination was accumulating on surgical instruments over their life cycle. Previous studies have also demonstrated significant residual contamination on surgical devices at the point of use (Lipscomb *et al.*, 2006a; Lipscomb *et al.*, 2006b; Murdoch et al., 2006; Smith *et al.*, 2005). However, these studies did not evaluate the effectiveness of the preceding decontamination process which is the most likely rationale for heavily soiled instruments. In this case, the cleaning and sterilisation procedure was confirmed as highly effective suggesting that instrument surface integrity is critical to the success of decontamination. As such it is clear that a standardised instrument life cycle must be employed across all SSDs whereby instruments of a certain age are withdrawn from circulation prior to the accumulation of significant levels of surface damage and contamination. This would significantly decrease the risk to a patient undergoing surgery due to instrument breakage or heavy soiling. However, this study also identified an exogenous source of proteinaceous instrument contamination other than that acquired during surgery. Handling by staff within the clean room during instrument inspection was demonstrated to apply significant concentrations of protein onto the surface of surgical instruments, which is then fixed to the surface through high temperature autoclave treatment (Howlin *et al*., 2009; Appendix B). Whilst this protein is unlikely to cause a direct risk to patient health itself, it will have an impact on the efficiency of subsequent decontamination processes over time. Critically, this work strongly suggests that gloves must be employed throughout all SSDs for staff handling instruments in order to remove this source of unnecessary contamination.

For the laboratory assessment of prion decontamination Chapter 4 utilised simulated washer-disinfector cycles. The data generated highlights the importance of the analysis of entire decontamination cycles rather than individual chemistries (Howlin *et al*., 2010; Appendix C). Whilst infectivity assays were not available for the study, this new protocol for the analysis of decontamination techniques can be utilised with the animal bioassay as it employs the same carrier surface as standard methods for the evaluation of prion infectivity (Fichet *et al*., 2004; Fichet *et al.*, 2007b; Fichet *et al*., 2007c; Jackson *et al.*, 2005; Peretz *et*

al., 2006). Moreover, it suggests that current decontamination methods, combined with the prevention of soil drying, represent the best safe-guard against iatrogenic CJD transmission, which is in agreement with other reports (Fichet *et al*., 2007a). However, stringent validation procedures are required and it is proposed that these utilise rapid and highly sensitive techniques, such as EDIC/EF analysis, rather than current methods, such as the Ninhydrin tests, which are clearly too insensitive (Lipscomb *et al.*, 2006a).

As a consequence of the association of instrument surface scarring with protein contamination, it was proposed that infectivity assays should better represent a worst-case scenario of surface contamination. Consequently, stainless steel wires were degraded with sodium hydroxide treatment prior to inoculation and implantation into the rodent host. This produced a surface which was demonstrated to be heavily scarred and damaged relative to standard stainless steel wires, adding to reports on the poor compatibility of WHO recommended guidelines with stainless steel instruments (Brown *et al*., 2005). Analysis of the degree of surface attachment of a 10 % (w/v) scrapie-infected brain homogenate by EDIC/EF and the dual stain method suggested a significantly higher concentration of non-amyloid, proteinaceous contamination bound to the degraded surface, compared with standard wires. Critically, therefore, this adjusted carrier surface does indeed represent a worst-case scenario of surface contamination. This is important, as the wire implant model can not reproduce the complexity of an instrument surface. As such, the more difficult surface contamination and removal is made for a decontamination process, the more translational the conclusions about the efficacy of a given chemistry are for the SSDs. It is hoped that advances in cell culture techniques may permit more complex surfaces to be introduced into infectivity studies (Edgeworth *et al*. 2009). However, this draw back in the methodology of the animal bioassay is counter-acted by the fact that the wires are left *in situ*, embedded in the CNS of the rodents throughout the experiment which may last up to a year, therefore prolonging the exposure surrounding tissue to the potentially infected surface. This is in contrast to the relatively brief contact patient tissues have with instruments during surgery and, consequently, prion material bound to the wire surface can be confirmed as fully inactivated or removed. Interestingly, initial results suggest that a degraded surface may possess the capacity to extend disease incubation time. Previous data on the reproducibility of this animal model argue against an inherent variability in the test method (Fichet *et al*., 2007c). It is possible that the extended incubation time is a consequence of the increase in surrounding proteinaceous contamination, thereby reducing contact of the infectious agent to surrounding host tissues. Whilst the prolonged incubation period was only statistically significant in one case, it can be assumed

that this may be a consequence of either the lack of complexity of the wire surface or potentially that the extent of the initial degradation of the surface was not sufficient to exert maximal effects. It is proposed that subsequent experiments be undertaken to confirm these initial findings, whereby the wire surface is exposed to multiple treatments with sodium hydroxide to observe whether further degradation can extend incubation periods.

In order to improve methods of prion decontamination, this project also aimed to critically assess the assays used to evaluate and confirm the efficacy of prion inactivation and removal. Routinely, these involve identification of PrP^{res} by Western blot and infectivity using the animal bioassay. The newly developed EDIC/EF dual stain to identify both total protein and prion-associated amyloid as a disease marker has demonstrated increased sensitivity relative to Western blot in both this project and published studies (Hervè *et al*., 2009; Lipscomb *et al*., 2007a). However, uncertainty over the size and nature of the infectious agent in prion diseases creates significant doubt over the validity of methods used to identify and evaluate decontamination processes. Sufficient data exists to suggest that infectivity associates with mature amyloid, PrP^{res} and smaller β-oligomers to varying degrees (Castilla *et al.*, 2005a; Novitskaya *et al.*, 2007; Redecke *et al.*, 2007; Silveira *et al.*, 2005). This project represents the first assessment of the identification methods used to assess prion decontamination techniques, as well as the first correlation of the EDIC/EF dual stain with infectivity. Surface Western blots demonstrated, not only a reduced sensitivity relative to EDIC/EF amyloid detection, but also poor correlation with infectivity, which has also been demonstrated in other studies (Fichet *et al*., 2004). Importantly, whilst the EDIC/EF dual stain displayed increased sensitivity for prion identification, relative to both surface and suspension Western blot, only the Western blots carried out in suspension demonstrated a 100 % correlation with infectious disease. Consequently, whilst EDIC/EF detection of amyloid is more sensitive that Western blot detection of PrP^{res}, the latter method is more specific for infectious disease. However, given the capacity of Thioflavin T to detect oligomeric molecules in both prion and Alzheimer's Disease it is likely that a significant degree of infectivity resides within these protein sub-species (Maezawa *et al.*, 2008; Simoneau *et al.*, 2007).

Given the close association of suspension Western blots with infectivity, further evaluation was performed to identify a correlation between structural alteration in PrP^{res} with infectivity. Primary antibodies were targetted to the N- and C-terminals of the prion protein, the OR region, with several directed to the central core of the prion protein; one encompassing Helix 1 which has previously been identified as a potentially important structure in the prion conversion process (Vorberg *et al.*, 2001). However, none of the six epitopes demonstrated

any link with infectious disease. This could be due to several reasons. Firstly, the decontamination process may have removed or modified the antibody binding epitope. Secondly, smaller structural changes may be sufficient to remove the capacity of the prion protein to transmit disease. Both the NaOH and Alkaline 1 treatment rendered both the OR region and central core residues PK-sensitive which may also affect the ability of the protein to transmit disease. Thirdly, it can not be excluded that infectivity resides within another epitope or, potentially, a smaller oligomeric PrP molecule undetected by Western blot analysis. However, it is clear that both EDIC/EF detection of amyloid and Western blot identification of PrP^{res} are not sufficient to confirm removal of the infectious agent alone and that they must be performed in combination with animal bioassays.

The final chapter of this project focused on the evaluation of other amyloid fluorophores in an effort to improve the sensitivity and specificity of EDIC/EF dual stain, and therefore improve *in situ* detection of prions. Previous reports have demonstrated the increased sensitivity of BTA-1 relative to its precursor Thioflavin T (Mathis *et al*., 2002; Mathis *et al*., 2003). A BTA-1 protocol for the fluorescent detection of prion-associated amyloid has been optimised. Moreover, this project has isolated an entirely novel fluorphore, designated 28d, which demonstrates enhanced specificity and a slower rate of photobleaching relative to BTA-1. Work is underway to develop an EDIC/EF dual stain incorporating both BTA-1 or 28d to improve the sensitivity of detection. However, additional work is required to further evaluate this novel compound. In addition to improving the *in vitro* and *in situ* detection of amyloid using fluorescent microscope techniques, these compounds have the capacity to replace existing compounds such as Thioflavin T in fibril formation studies and enhance *in vivo* PET imaging thereby improving their sensitivity. Moreover, amyloid flurophores have also been demonstrated to posses therapeutic effects in prion disease (Ishikawa *et al.*, 2004). It is hoped that 28d can be evaluated in future studies to assess its potential therapeutic effect to attenuate the onset of clinical symptoms upon treatment at several time points post-infection.

REFERENCES

Adams, D. H. & Edgar, W. M. (1978). Transmission of agent of Creutzfeldt-Jakob disease. *Br Med J* **1**, 987.

Adler, V., Zeiler, B., Kryukov, V., Kascsak, R., Rubenstein, R. & Grossman, A. (2003). Small, highly structured RNAs participate in the conversion of human recombinant PrP(Sen) to PrP(Res) in vitro. *J Mol Biol* **332**, 47-57.

Aguzzi, A. & Heppner F.L. (2000). Pathogenesis of prion diseases: A progress report. *Cell Death Differ* **7**, 889-902.

Aguzzi, A. & Polymenidou, M. (2004). Mammalian prion biology: One century of evolving concepts. *Cell* **116**, 313-327.

Aguzzi, A. (2006). Prion diseases of humans and farm animals: epidemiology, genetics, and pathogenesis. *J Neurochem* **97**, 1726-1739.

Alper, T., Cramp, W. A., Haig, D. A. & Clarke, M. C. (1967). Does the agent of scrapie replicate without nucleic acid? *Nature* **214**, 764-766.

Anderson, M., Bocharova, O. V., Makarava, N., Breydo, L., Salnikov, V. V. & Baskakov, I. V. (2006). Polymorphism and ultrastructural organization of prion protein amyloid fibrils: an insight from high resolution atomic force microscopy. *J Mol Biol* **358**, 580-596.

Andreoletti, O., Berthon, P., Marc, D., Sarradin, P., Grosclaude, J., van, K. L., Schelcher, F., Elsen, J. M. & Lantier, F. (2000). Early accumulation of PrP(Sc) in gut-associated lymphoid and nervous tissues of susceptible sheep from a Romanov flock with natural scrapie. *J Gen Virol* **81**, 3115-3126.

Angers, R. C., Browning, S. R., Seward, T. S., Sigurdson, C. J., Miller, M. W., Hoover, E. A. & Telling, G. C. (2006). Prions in skeletal muscles of deer with chronic wasting disease. *Science* **311**, 1117.

Arakawa, K., Nagara, H., Itoyama, Y., Doh-ura, K., Tomokane, N., Tateishi, J. & Goto, I. (1991). Clustering of three cases of Creutzfeldt-Jakob disease near Fukuoka City, Japan. *Acta Neurol Scand* **84**, 445-447.

Armitage, W. J., Tullo, A. B. & Ironside, J. W. (2009). Risk of Creutzfeldt-Jakob disease transmission by ocular surgery and tissue transplantation. *Eye*, doi:10.1038/eye.2008.381

Arnold, J. E., Tipler, C., Laszlo, L., Hope, J., Landon, M. & Mayer, R. J. (1995). The abnormal isoform of the prion protein accumulates in late-endosome-like organelles in scrapie-infected mouse brain. *J Pathol* **176**, 403-411.

arra-Mehrpour, M., Arrabal, S., Jalil, A., Pinson, X., Gaudin, C., Pietu, G., Pitaval, A., Ripoche, H., Eloit, M., Dormont, D. & Chouaib, S. (2004). Prion protein prevents human breast carcinoma cell line from tumor necrosis factor alpha-induced cell death. *Cancer Res* **64**, 719-727.

Asante, E. A., Linehan, J. M., Gowland, I., Joiner, S., Fox, K., Cooper, S., Osiguwa, O., Gorry, M., Welch, J., Houghton, R., Desbruslais, M., Brandner, S., Wadsworth, J. D. & Collinge, J. (2006). Dissociation of pathological and molecular phenotype of variant Creutzfeldt-Jakob disease in transgenic human prion protein 129 heterozygous mice. *Proc Natl Acad Sci U S A* **103**, 10759-10764.

Baeten, L. A., Powers, B. E., Jewell, J. E., Spraker, T. R. & Miller, M. W. (2007). A natural case of chronic wasting disease in a free-ranging moose (Alces alces shirasi). *J Wildl Dis* **43**, 309-314.

Ballerini, C., Gourdain, P., Bachy, V., Blanchard, N., Levavasseur, E., Gregoire, S., Fontes, P., Aucouturier, P., Hivroz, C. & Carnaud, C. (2006). Functional implication of cellular prion protein in antigen-driven interactions between T cells and dendritic cells. *J Immunol* **176**, 7254-7262.

Ban, T., Hamada, D., Hasegawa, K., Naiki, H. & Goto, Y. (2003). Direct observation of amyloid fibril growth monitored by Thioflavin T fluorescence. *J Biol Chem* **278**, 16462-16465.

Barret, A., Tagliavini, F., Forloni, G., Bate, C., Salmona, M., Colombo, L., De Luigi, A., Limido, L., Suardi, S., Rossi, G., Auvre, F., Adjou, K. T., Sales, N., Williams, A., Lasmezas, C. & Deslys, J. P. (2003). Evaluation of Quinacrine treatment for prion diseases. *J Virol* **77**, 8462-8469.

Barron, R. M., Campbell, S. L., King, D., Bellon, A., Chapman, K. E., Williamson, R. A. & Manson, J. C. (2007). High titres of TSE infectivity associated with extremely low levels of PrPSc in vivo. *J Biol Chem* **282**, 35878-86.

Bartz, J. C., Dejoia, C., Tucker, T., Kincaid, A. E. & Bessen, R. A. (2005). Extraneural prion neuroinvasion without lymphoreticular system infection. *J Virol* **79**, 11858-11863.

Baskakov, I. V. (2007a). Branched chain mechanism of polymerization and ultrastructure of prion protein amyloid fibrils. *FEBS J* **274**, 3756-3765.

Baskakov, I. V. (2007b). The reconstitution of mammalian prion infectivity de novo. *FEBS J* **274**, 576-587.

Baskakov, I. V., Legname, G., Baldwin, M. A., Prusiner, S. B. & Cohen, F. E. (2002a). Pathway complexity of prion protein assembly into amyloid. *J Biol Chem* **277**, 21140-21148.

Baskakov, I. V., Legname, G., Gryczynski, Z. & Prusiner, S. B. (2004). The peculiar nature of unfolding of the human prion protein. *Protein Sci* **13**, 586-595.

Baskakov, I. V., Legname, G., Prusiner, S. B. & Cohen, F. E. (2001). Folding of prion protein to its native alpha-helical conformation is under kinetic control. *J Biol Chem* **276**, 19687-19690.

Baskakov, I. V., Legname, G., Baldwin, M. A., Prusiner, S. B. & Cohen, F. E. (2002b). Pathway complexity of prion protein assembly into amyloid. *J Biol Chem* **277**, 21140-21148.

Basler, K., Oesch, B., Scott, M., Westaway, D., Walchli, M., Groth, D. F., McKinley, M. P., Prusiner, S. B. & Weissmann, C. (1986). Scrapie and cellular PrP isoforms are encoded by the same chromosomal gene. *Cell* **46**, 417-428.

Bate, C., Salmona, M., Diomede, L. & Williams, A. (2004). Squalestatin cures prion-infected neurons and protects against prion neurotoxicity. *J Biol Chem* **279**, 14983-14990.

Baumann, F., Tolnay, M., Brabeck, C., Pahnke, J., Kloz, U., Niemann, H. H., Heikenwalder, M., Rulicke, T., Burkle, A. & Aguzzi, A. (2007). Lethal recessive myelin toxicity of prion protein lacking its central domain. *EMBO J* **26**, 538-547.

Belay, E. D., Maddox, R. A., Williams, E. S., Miller, M. W., Gambetti, P. & Schonberger, L. B. (2004). Chronic wasting disease and potential transmission to humans. *Emerg Infect Dis* **10**, 977-984.

Belay, E. D. (1999). Transmissible spongiform encephalopathies in humans. *Annual Review of Microbiology* **53**, 283-314.

Belt, P. B., Muileman, I. H., Schreuder, B. E., Bos-de, R. J., Gielkens, A. L. & Smits, M. A. (1995). Identification of five allelic variants of the sheep PrP gene and their association with natural scrapie. *J Gen Virol* **76**, 509-517.

Benestad, S. L., Arsac, J. N., Goldmann, W. & Noremark, M. (2008). Atypical/Nor98 scrapie: properties of the agent, genetics, and epidemiology. *Vet Res* **39**, 19.

Benestad, S. L., Sarradin, P., Thu, B., Schonheit, J., Tranulis, M. A. & Bratberg, B. (2003). Cases of scrapie with unusual features in Norway and designation of a new type, Nor98. *Vet Rec* **153**, 202-208.

Berggren, K., Steinberg, T. H., Lauber, W. M., Carroll, J. A., Lopez, M. F., Chernokalskaya, E., Zieske, L., Diwu, Z., Haugland, R. P. & Patton, W. F. (1999). A luminescent ruthenium complex for ultrasensitive detection of proteins immobilized on membrane supports. *Anal Biochem* **276**, 129-143.

Beringue, V., Herzog, L., Reine, F., Le, D. A., Casalone, C., Vilotte, J. L. & Laude, H. (2008a). Transmission of atypical bovine prions to mice transgenic for human prion protein. *Emerg Infect Dis* **14**, 1898-1901.

Beringue, V., Vilotte, J. L. & Laude, H. (2008b). Prion agent diversity and species barrier. *Vet Res* **39**, 47.

Berman, P. H., Davidson, G. S. & Becker, L. E. (1988). Progressive neurological deterioration in a 14-year-old girl. *Pediatr Neurosci* **14**, 42-49.

Bernoulli, C., Siegfried, J., Baumgartner, G., Regli, F., Rabinowicz, T., Gajdusek, D. C. & Gibbs, C. J., Jr. (1977). Danger of accidental person-to-person transmission of Creutzfeldt-Jakob disease by surgery. *Lancet* **1**, 478-479.

Bessen, R. A., Raymond, G. J. & Caughey, B. (1997). In situ formation of protease-resistant prion protein in transmissible spongiform encephalopathy-infected brain slices. *J Biol Chem* **272**, 15227-15231.

Biacabe, A. G., Laplanche, J. L., Ryder, S. & Baron, T. (2004). Distinct molecular phenotypes in bovine prion diseases. *EMBO Rep* **5**, 110-115.

Bishop, M. T., Hart, P., Aitchison, L., Baybutt, H. N., Plinston, C., Thomson, V., Tuzi, N. L., Head, M. W., Ironside, J. W., Will, R. G. & Manson, J. C. (2006). Predicting susceptibility and incubation time of human-to-human transmission of vCJD. *Lancet Neurol* **5**, 393-398.

Blattler, T., Brandner, S., Raeber, A. J., Klein, M. A., Voigtlander, T., Weissmann, C. & Aguzzi, A. (1997). PrP-expressing tissue required for transfer of scrapie infectivity from spleen to brain. *Nature* **389**, 69-73.

Bocharova, O. V., Breydo, L., Parfenov, A. S., Salnikov, V. V. & Baskakov, I. V. (2005a). In vitro conversion of full-length mammalian prion protein produces amyloid form with physical properties of PrP(Sc). *J Mol Biol* **346**, 645-659.

Bocharova, O. V., Breydo, L., Salnikov, V. V. & Baskakov, I. V. (2005b). Copper(II) inhibits in vitro conversion of prion protein into amyloid fibrils. *Biochemistry* **44**, 6776-6787.

Borchelt, D. R., Taraboulos, A. & Prusiner, S. B. (1992) . Evidence for synthesis of scrapie prion proteins in the endocytic pathway. *J Biol Chem* **267**, 16188-16199.

Bounhar, Y., Zhang, Y., Goodyer, C. G. & LeBlanc, A. (2001). Prion protein protects human neurons against Bax-mediated apoptosis. *J Biol Chem* **276**, 39145-39149.

Bourvis, N., Boelle, P. Y., Cesbron, J. Y. & Valleron, A. J. (2007). Risk assessment of transmission of sporadic creutzfeldt-jakob disease in endodontic practice in absence of adequate prion inactivation. *PLoS ONE* **2**, e1330.

Brandner, S., Isenmann, S., Raeber, A., Fischer, M., Sailer, A., Kobayashi, Y., Marino, S., Weissmann, C. & Aguzzi, A. (1996). Normal host prion protein necessary for scrapie-induced neurotoxicity. *Nature* **379**, 339-343.

Brandner, S., Whitfield, J., Boone, K., Puwa, A., O'Malley, C., Linehan, J. M., Joiner, S., Scaravilli, F., Calder, I., Alpers, P., Wadsworth, J. D. & Collinge, J. (2008). Central and peripheral pathology of kuru: pathological analysis of a recent case and comparison with other forms of human prion disease. *Philos Trans R Soc Lond B Biol Sci* **363**, 3755-3763.

Breydo, L., Sun, Y., Makarava, N., Lee, C. I., Novitskaia, V., Bocharova, O., Kao, J. P. & Baskakov, I. V. (2007). Nonpolar substitution at the C-terminus of the prion protein, a mimic of the glycosylphosphatidylinositol anchor, partially impairs amyloid fibril formation. *Biochemistry* **46**, 852-861.

Brown S.A, Merritt K, Woods T.O & Busick D.N (2005). Effects on instruments of the World Health Organization - recommended protocols for decontamination after possible exposure to Transmissible Spongiform Encephalopathy - contaminated tissue. *J Biomed Mater Res B Appl Biomater* **72**, 186-190.

Brown, D. R., Nicholas, R. S. & Canevari, L. (2002). Lack of prion protein expression results in a neuronal phenotype sensitive to stress. *J Neurosci Res* **67**, 211-224.

Brown, D. R., Schulz-Schaeffer, W. J., Schmidt, B. & Kretzschmar, H. A. (1997). Prion protein-deficient cells show altered response to oxidative stress due to decreased SOD-1 activity. *Exp Neurol* **146**, 104-112.

Brown, K. L., Stewart, K., Ritchie, D. L., Mabbott, N. A., Williams, A., Fraser, H., Morrison, W. I. & Bruce, M. E. (1999). Scrapie replication in lymphoid tissues depends on prion protein-expressing follicular dendritic cells. *Nat Med* **5**, 1308-1312.

Brown, P. (1990). Transmissible spongiform encephalopathies in humans: kuru, Creutzfeldt-Jakob disease and Gerstmann-Straussler-Scheinker disease. *Can J Vet Res* **54**, 38-41.

Brown, P., Cathala, F., Labauge, R., Pages, M., Alary, J. C. & Baron, H. (1985). Epidemiologic implications of Creutzfeldt-Jakob disease in a 19 year-old girl. *Eur J Epidemiol* **1**, 42-47.

Brown, P., McShane, L. M., Zanusso, G. & Detwile, L. (2006). On the question of sporadic or atypical bovine spongiform encephalopathy and Creutzfeldt-Jakob disease. *Emerg Infect Dis* **12**, 1816-1821.

Brown, P., Rau, E. H., Johnson, B. K., Bacote, A. E., Gibbs, C. J., Jr. & Gajdusek, D. C. (2000). New studies on the heat resistance of hamster-adapted scrapie agent: threshold survival after ashing at 600 degrees C suggests an inorganic template of replication. *Proc Natl Acad Sci U S A* **97**, 3418-3421.

Brown, S. A., Merritt, K., Woods, T. O. & Busick, D. N. (2005). Effects on instruments of the World Health Organization--recommended protocols for decontamination after possible exposure to transmissible spongiform encephalopathy-contaminated tissue. *J Biomed Mater Res B Appl Biomater* **72**, 186-190.

Bruce, M. E. (2003). TSE strain variation. *Br Med Bull* **66**, 99-108.

Bruce, M. E., McConnell, I., Will, R. G. & Ironside, J. W. (2001). Detection of variant Creutzfeldt-Jakob disease infectivity in extraneural tissues. *Lancet* **358**, 208-209.

Bruce, M. E., Nonno, R., Foster, J., Goldmann, W., Di, B. M., Esposito, E., Benestad, S. L., Hunter, N. & Agrimi, U. (2007). Nor98-like sheep scrapie in the United Kingdom in 1989. *Vet Rec* **160**, 665-666.

Bruce, M. E., Will, R. G., Ironside, J. W., McConnell, I., Drummond, D., Suttie, A., McCardle, L., Chree, A., Hope, J., Birkett, C., Cousens, S., Fraser, H. & Bostock, C. J. (1997). Transmissions to mice indicate that 'new variant' CJD is caused by the BSE agent. *Nature* **389**, 498-501.

Budka, H., Dormont, D., Kretzschmar, H., Pocchiari, M. & van, D. C. (2002). BSE and variant Creutzfeldt-Jakob disease: never say never. *Acta Neuropathol* **103**, 627-628.

Bueler, H., Aguzzi, A., Sailer, A., Greiner, R. A., Autenried, P., Aguet, M. & Weissmann, C. (1993). Mice devoid of PrP are resistant to scrapie. *Cell* **73**, 1339-1347.

Bueler, H., Fischer, M., Lang, Y., Bluethmann, H., Lipp, H. P., DeArmond, S. J., Prusiner, S. B., Aguet, M. & Weissmann, C. (1992). Normal development and behaviour of mice lacking the neuronal cell-surface PrP protein. *Nature* **356**, 577-582.

Burthem, J., Urban, B., Pain, A. & Roberts, D. J. (2001). The normal cellular prion protein is strongly expressed by myeloid dendritic cells. *Blood* **98**, 3733-3738.

Buschmann, A., Biacabe, A. G., Ziegler, U., Bencsik, A., Madec, J. Y., Erhardt, G., Luhken, G., Baron, T. & Groschup, M. H. (2004). Atypical scrapie cases in Germany and France are identified by discrepant reaction patterns in BSE rapid tests. *J Virol Methods* **117**, 27-36.

Butters, M. A., Klunk, W. E., Mathis, C. A., Price, J. C., Ziolko, S. K., Hoge, J. A., Tsopelas, N. D., Lopresti, B. J., Reynolds, C. F., III, DeKosky, S. T. & Meltzer, C. C. (2008). Imaging Alzheimer pathology in late-life depression with PET and Pittsburgh Compound-B. *Alzheimer Dis Assoc Disord* **22**, 261-268.

Capobianco, R., Casalone, C., Suardi, S., Mangieri, M., Miccolo, C., Limido, L., Catania, M., Rossi, G., Di, F. G., Giaccone, G., Bruzzone, M. G., Minati, L., Corona, C., Acutis, P., Gelmetti, D., Lombardi, G., Groschup, M. H., Buschmann, A., Zanusso, G., Monaco, S., Caramelli, M. & Tagliavini, F. (2007). Conversion of the BASE prion strain into the BSE strain: the origin of BSE? *PLoS Pathog* **3**, e31.

Carp, R. I. (1982). Transmission of scrapie by oral route: effect of gingival scarification. *Lancet* **1**, 170-171.

Casalone, C., Zanusso, G., Acutis, P., Ferrari, S., Capucci, L., Tagliavini, F., Monaco, S. & Caramelli, M. (2004). Identification of a second bovine amyloidotic spongiform encephalopathy: molecular similarities with sporadic Creutzfeldt-Jakob disease. *Proc Natl Acad Sci U S A* **101**, 3065-3070.

Castilla, J., Saa, P., Hetz, C. & Soto, C. (2005a). In vitro generation of infectious scrapie prions. *Cell* **121**, 195-206.

Castilla, J., Saa, P. & Soto, C. (2005b). Detection of prions in blood. *Nat Med* **11**, 982-985.

Cattaneo, E., Rigamonti, D., Goffredo, D., Zuccato, C., Squitieri, F. & Sipione, S. (2001). Loss of normal huntingtin function: new developments in Huntington's disease research. *Trends Neurosci* **24**, 182-188.

Caughey, B., Kocisko, D. A., Raymond, G. J. & Lansbury, P. T., Jr. (1995). Aggregates of scrapie-associated prion protein induce the cell-free conversion of protease-sensitive prion protein to the protease-resistant state. *Chem Biol* **2**, 807-817.

Caughey, B. & Lansbury, P. T. (2003). Protofibrils, pores, fibrils, and neurodegeneration: separating the responsible protein aggregates from the innocent bystanders. *Annu Rev Neurosci* **26**, 267-298.

Caughey, B., Raymond, G. J. & Bessen, R. A. (1998). Strain-dependent differences in beta-sheet conformations of abnormal prion protein. *J Biol Chem* **273**, 32230-32235.

Caughey, B., Raymond, G. J., Ernst, D. & Race, R. E. (1991). N-terminal truncation of the scrapie-associated form of PrP by lysosomal protease(s): implications regarding the site of conversion of PrP to the protease-resistant state. *J Virol* **65**, 6597-6603.

Centers for Disease Control (1985). Fatal degenerative neurologic disease in patients who received pituitary-derived human growth hormone. *MMWR Morb Mortal Wkly Rep* **34**, 359-60.

Centers for Disease Control (1987). Rapidly progressive dementia in a patient who received a cadaveric dura mater graft. *MMWR Morb Mortal Wkly Rep* **36**, 49-50.

Chesebro, B., Trifilo, M., Race, R., Meade-White, K., Teng, C., LaCasse, R., Raymond, L., Favara, C., Baron, G., Priola, S., Caughey, B., Masliah, E. & Oldstone, M. (2005). Anchorless prion protein results in infectious amyloid disease without clinical scrapie. *Science* **308**, 1435-1439.

Chiti, F., Taddei, N., Bucciantini, M., White, P., Ramponi, G. & Dobson, C. M. (2000). Mutational analysis of the propensity for amyloid formation by a globular protein. *EMBO J* **19**, 1441-1449.

Chiti, F., Webster, P., Taddei, N., Clark, A., Stefani, M., Ramponi, G. & Dobson, C. M. (1999). Designing conditions for in vitro formation of amyloid protofilaments and fibrils. *Proc Natl Acad Sci U S A* **96**, 3590-3594.

Choi, C. J., Anantharam, V., Saetveit, N. J., Houk, R. S., Kanthasamy, A. & Kanthasamy, A. G. (2007). Normal cellular prion protein protects against manganese-induced oxidative stress and apoptotic cell death. *Toxicol Sci* **98**, 495-509.

Clarke, P. & Ghani, A. C. (2005). Projections of the future course of the primary vCJD epidemic in the UK: inclusion of subclinical infection and the possibility of wider genetic susceptibility. *J R Soc Interface* **2**, 19-31.

Cleary, J. P., Walsh, D. M., Hofmeister, J. J., Shankar, G. M., Kuskowski, M. A., Selkoe, D. J. & Ashe, K. H. (2005). Natural oligomers of the amyloid-beta protein specifically disrupt cognitive function. *Nat Neurosci* **8**, 79-84.

Cochius, J. I., Burns, R. J., Blumbergs, P. C., Mack, K. & Alderman, C. P. (1990). Creutzfeldt-Jakob disease in a recipient of human pituitary-derived gonadotrophin. *Aust N Z J Med* **20**, 592-593.

Cochius, J. I., Hyman, N. & Esiri, M. M. (1992). Creutzfeldt-Jakob disease in a recipient of human pituitary-derived gonadotrophin: a second case. *J Neurol Neurosurg Psychiatry* **55**, 1094-1095.

Cohen, F. E., Pan, K. M., Huang, Z., Baldwin, M., Fletterick, R. J. & Prusiner, S. B. (1994). Structural clues to prion replication. *Science* **264**, 530-531.

Coitinho, A. S., Roesler, R., Martins, V. R., Brentani, R. R. & Izquierdo, I. (2003). Cellular prion protein ablation impairs behavior as a function of age. *Neuroreport* **14**, 1375-1379.

Colby, D. W., Zhang, Q., Wang, S., Groth, D., Legname, G., Riesner, D. & Prusiner, S. B. (2007). Prion detection by an amyloid seeding assay. *Proc Natl Acad Sci U S A* **104**, 20914-20919.

Colling, S. B., Collinge, J. & Jefferys, J. G. (1996). Hippocampal slices from prion protein null mice: disrupted Ca(2+)-activated K+ currents. *Neurosci Lett* **209**, 49-52.

Colling, S. B., Khana, M., Collinge, J. & Jefferys, J. G. (1997). Mossy fibre reorganization in the hippocampus of prion protein null mice. *Brain Res* **755**, 28-35.

Collinge, J. (1997). Human prion diseases and bovine spongiform encephalopathy (BSE). *Hum Mol Genet* **6**, 1699-1705.

Collinge, J. (2005). Molecular neurology of prion disease. *J Neurol Neurosurg Psychiatry* **76**, 906-919.

Collinge, J., Palmer, M. S., Sidle, K. C., Gowland, I., Medori, R., Ironside, J. & Lantos, P. (1995). Transmission of fatal familial insomnia to laboratory animals. *Lancet* **346**, 569-570.

Collinge, J., Sidle, K. C., Meads, J., Ironside, J. & Hill, A. F. (1996). Molecular analysis of prion strain variation and the aetiology of 'new variant' CJD. *Nature* **383**, 685-690.

Collinge, J., Whitfield, J., McKintosh, E., Beck, J., Mead, S., Thomas, D. J. & Alpers, M. P. (2006). Kuru in the 21st century--an acquired human prion disease with very long incubation periods. *Lancet* **367**, 2068-2074.

Collinge, J. (1999). Variant Creutzfeldt-Jakob disease. *The Lancet* **354**, 317-323.

Collinge, J. (2001). Prion disease of humans and animals: their causes and molecular basis. *Annual Review of Neuroscience* **24**, 519-550.

Collins, S. J., Lawson, V. A. & Masters, C. L. (2004a). Transmissible spongiform encephalopathies. *The Lancet* **363**, 51-61.

Collins, S. R., Douglass, A., Vale, R. D. & Weissman, J. S. (2004b). Mechanism of prion propagation: amyloid growth occurs by monomer addition. *PLoS Biol* **2**, e321.

Comoy, E. E., Casalone, C., Lescoutra-Etchegaray, N., Zanusso, G., Freire, S., Marce, D., Auvre, F., Ruchoux, M. M., Ferrari, S., Monaco, S., Sales, N., Caramelli, M., Leboulch, P., Brown, P., Lasmezas, C. I. & Deslys, J. P. (2008). Atypical BSE (BASE) transmitted from asymptomatic aging cattle to a primate. *PLoS ONE* **3**, e3017.

Cordeiro, Y., Kraineva, J., Gomes, M. P., Lopes, M. H., Martins, V. R., Lima, L. M., Foguel, D., Winter, R. & Silva, J. L. (2005). The amino-terminal PrP domain is crucial to modulate prion misfolding and aggregation. *Biophys J* **89**, 2667-2676.

Cordeiro, Y., Machado, F., Juliano, L., Juliano, M. A., Brentani, R. R., Foguel, D. & Silva, J. L. (2001). DNA converts cellular prion protein into the beta-sheet conformation and inhibits prion peptide aggregation. *J Biol Chem* **276**, 49400-49409.

Criado, J. R., Sanchez-Alavez, M., Conti, B., Giacchino, J. L., Wills, D. N., Henriksen, S. J., Race, R., Manson, J. C., Chesebro, B. & Oldstone, M. B. (2005). Mice devoid of prion protein have cognitive deficits that are rescued by reconstitution of PrP in neurons. *Neurobiol Dis* **19**, 255-265.

Critchley, P., Kazlauskaite, J., Eason, R. & Pinheiro, T. J. (2004). Binding of prion proteins to lipid membranes. *Biochem Biophys Res Commun* **313**, 559-567.

Cunningham, C., Deacon, R., Wells, H., Boche, D., Waters, S., Diniz, C. P., Scott, H., Rawlins, J. N. & Perry, V. H. (2003). Synaptic changes characterize early behavioural signs in the ME7 model of murine prion disease. *Eur J Neurosci* **17**, 2147-2155.

Cunningham, C., Wilcockson, D. C., Boche, D. & Perry, V. H. (2005). Comparison of inflammatory and acute-phase responses in the brain and peripheral organs of the ME7 model of prion disease. *J Virol* **79**, 5174-5184.

da Costa, C. A., Ancolio, K. & Checler, F. (2000). Wild-type but not Parkinson's disease-related ala-53 --> Thr mutant alpha -synuclein protects neuronal cells from apoptotic stimuli. *J Biol Chem* **275**, 24065-24069.

Dagleish, M. P., Martin, S., Steele, P., Finlayson, J., Siso, S., Hamilton, S., Chianini, F., Reid, H. W., Gonzalez, L. & Jeffrey, M. (2008). Experimental transmission of bovine spongiform encephalopathy to European red deer (Cervus elaphus elaphus). *BMC Vet Res* **4**, 17.

Darghal, N., Garnier-Suillerot, A. & Salerno, M. (2006). Mechanism of thioflavin T accumulation inside cells overexpressing P-glycoprotein or multidrug resistance-associated protein: role of lipophilicity and positive charge. *Biochem Biophys Res Commun* **343**, 623-629.

Davanipour, Z., Alter, M., Sobel, E., Asher, D. & Gajdusek, D. C. (1985). Creutzfeldt-Jakob disease: possible medical risk factors. *Neurology* **35**, 1483-1486.

de Almeida, C. J., Chiarini, L. B., da Silva, J. P., PM, E. S., Martins, M. A. & Linden, R. (2005). The cellular prion protein modulates phagocytosis and inflammatory response. *J Leukoc Biol* **77**, 238-246.

de Bruijn A.C.P & van Drongelen A.W. (2005). EN ISO 15883: A great standard for not so great test soils! *Zentral Sterilisation* **13**, 334-336.

De, G. L., Selvaggini, C., Ghibaudi, E., Diomede, L., Bugiani, O., Forloni, G., Tagliavini, F. & Salmona, M. (1994). Conformational polymorphism of the amyloidogenic and neurotoxic peptide homologous to residues 106-126 of the prion protein. *J Biol Chem* **269**, 7859-7862.

DeArmond, S. J. & Prusiner, S. B. (1995). Etiology and pathogenesis of prion diseases. *Am J Pathol* **146**, 785-811.

DeArmond, S. J., Qiu, Y., Sanchez, H., Spilman, P. R., Ninchak-Casey, A., Alonso, D. & Daggett, V. (1999). PrPc glycoform heterogeneity as a function of brain region: implications for selective targeting of neurons by prion strains. *J Neuropathol Exp Neurol* **58**, 1000-1009.

DeArmond, S. J., Sanchez, H., Yehiely, F., Qiu, Y., Ninchak-Casey, A., Daggett, V., Camerino, A. P., Cayetano, J., Rogers, M., Groth, D., Torchia, M., Tremblay, P.,

Scott, M. R., Cohen, F. E. & Prusiner, S. B. (1997). Selective neuronal targeting in prion disease. *Neuron* **19**, 1337-1348.

DeArmond, S. J. (2004). Discovering the mechanisms of neurodegeneration in prion diseases. *Neurochemical Research* **29**, 1979-1998.

DeBosschere, H., Roels, S., Benestad, S. L. & Vanopdenbosch, E. (2004). Scrapie case similar to Nor98 diagnosed in Belgium via active surveillance. *Vet Rec* **155**, 707-708.

Del, P. P., Weiss, A., Bertsch, U., Renner, C., Mentler, M., Grantner, K., Fiorino, F., Meyer-Klaucke, W., Moroder, L., Kretzschmar, H. A. & Parak, F. G. (2007). The configuration of the Cu2+ binding region in full-length human prion protein. *Eur Biophys J* **36**, 239-252.

Deleault, N. R., Lucassen, R. W. & Supattapone, S. (2003). RNA molecules stimulate prion protein conversion. *Nature* **425**, 717-720.

DeMarco, M. L. & Daggett, V. (2005). Local environmental effects on the structure of the prion protein. *Comptes Rendus Biologies* **328**, 847-862.

Dima, R. I. & Thirumalai, D. (2004). Probing the instabilities in the dynamics of helical fragments from mouse PrPC. *Proc Natl Acad Sci U S A* **101**, 15335-15340.

Dodelet, V. C. & Cashman, N. R. (1998). Prion protein expression in human leukocyte differentiation. *Blood* **91**, 1556-1561.

Dong, C. F., Shi, S., Wang, X. F., An, R., Li, P., Chen, J. M., Wang, X., Wang, G. R., Shan, B., Zhang, B. Y., Han, J. & Dong, X. P. (2008). The N-terminus of PrP is responsible for interacting with tubulin and fCJD related PrP mutants possess stronger inhibitive effect on microtubule assembly in vitro. *Arch Biochem Biophys* **470**, 83-92.

Drzezga, A., Grimmer, T., Henriksen, G., Stangier, I., Perneczky, R., ehl-Schmid, J., Mathis, C. A., Klunk, W. E., Price, J., DeKosky, S., Wester, H. J., Schwaiger, M. & Kurz, A. (2008). Imaging of amyloid plaques and cerebral glucose metabolism in semantic dementia and Alzheimer's disease. *Neuroimage* **39**, 619-633.

Duffy, P., Wolf, J., Collins, G., DeVoe, A. G., Streeten, B. & Cowen, D. (1974). Letter: Possible person-to-person transmission of Creutzfeldt-Jakob disease. *N Engl J Med* **290**, 692-693.

Dupiereux, I., Falisse-Poirrier, N., Zorzi, W., Watt, N. T., Thellin, O., Zorzi, D., Pierard, O., Hooper, N. M., Heinen, E. & Elmoualij, B. (2008). Protective effect of prion protein via the N-terminal region in mediating a protective effect on paraquat-induced oxidative injury in neuronal cells. *J Neurosci Res* **86**, 653-659.

Dupiereux, I., Zorzi, W., Rachidi, W., Zorzi, D., Pierard, O., Lhereux, B., Heinen, E. & Elmoualij, B. (2006). Study on the toxic mechanism of prion protein peptide 106-126 in neuronal and non neuronal cells. *J Neurosci Res* **84**, 637-46.

Edgeworth, J. A., Jackson, G. S., Clarke, A. R., Weissmann, C. & Collinge, J. (2009). Highly sensitive, quantitative cell-based assay for prions adsorbed to solid surfaces. *Proc Natl Acad Sci U S A* **106**, 3479-3483.

Elsen, J. M., Amigues, Y., Schelcher, F., Ducrocq, V., Andreoletti, O., Eychenne, F., Khang, J. V., Poivey, J. P., Lantier, F. & Laplanche, J. L. (1999). Genetic susceptibility and transmission factors in scrapie: detailed analysis of an epidemic in a closed flock of Romanov. *Arch Virol* **144**, 431-445.

Ena, J. (2005). Prions: Who Should Worry about Them? *Archives of Medical Research* **36**, 622-627.

Epstein, V., Pointing, S. & Halfacre, S. (2005). Atypical scrapie in the Falkland Islands. *Vet Rec* **157**, 667-668.

Everest, S. J., Thorne, L., Barnicle, D. A., Edwards, J. C., Elliott, H., Jackman, R. & Hope, J. (2006). Atypical prion protein in sheep brain collected during the British scrapie-surveillance programme. *J Gen Virol* **87**, 471-477.

Felten, S. Y., Felten, D. L., Bellinger, D. L., Carlson, S. L., Ackerman, K. D., Madden, K. S., Olschowka, J. A. & Livnat, S. (1988). Noradrenergic sympathetic innervation of lymphoid organs. *Prog Allergy* **43**, 14-36.

Fernie, K., Steele, P. J., Taylor, D. M. & Somerville, R. A. (2007). Comparative studies on the thermostability of five strains of transmissible-spongiform-encephalopathy agent. *Biotechnol Appl Biochem* **47**, 175-183.

Ferrer, I. (2002). Synaptic pathology and cell death in the cerebellum in Creutzfeldt-Jakob disease. *Cerebellum* **1**, 213-222.

Fichet, G., Comoy, E., Duval, C., Antloga, K., Dehen, C., Charbonnier, A., McDonnell, G., Brown, P., Ida Lasmezas, C. & Deslys, J. P. (2004). Novel methods for disinfection of prion-contaminated medical devices. *The Lancet* **364**, 521-526.

Fichet, G., Harrison, J. & McDonnell, G. (2007a). Reduction of the risk of prion transmission on surgical devices with effective cleaning processes. *Zentral Sterilisation* **15**, 418-437.

Fichet, G., Antloga, K., Comoy, E., Deslys, J. P. & McDonnell, G. (2007b). Prion inactivation using a new gaseous hydrogen peroxide sterilisation process. *J Hosp Infect* **67**, 278-286.

Fichet, G., Comoy, E., Dehen, C., Challier, L., Antloga, K., Deslys, J. P. & McDonnell, G. (2007c). Investigations of a prion infectivity assay to evaluate methods of decontamination. *J Microbiol Methods* **70**, 511-518.

Fischer, M., Rulicke, T., Raeber, A., Sailer, A., Moser, M., Oesch, B., Brandner, S., Aguzzi, A. & Weissmann, C. (1996). Prion protein (PrP) with amino-proximal deletions restoring susceptibility of PrP knockout mice to scrapie. *EMBO J* **15**, 1255-1264.

Flechsig, E., Hegyi, I., Enari, M., Schwarz, P., Collinge, J. & Weissmann, C. (2001). Transmission of scrapie by steel-surface-bound prions. *Mol Med* **7**, 679-684.

Forloni, G., Angeretti, N., Chiesa, R., Monzani, E., Salmona, M., Bugiani, O. & Tagliavini, F. (1993). Neurotoxicity of a prion protein fragment. *Nature* **362**, 543-546.

Foster, J. D., Hope, J., McConnell, I., Bruce, M. & Fraser, H. (1994). Transmission of bovine spongiform encephalopathy to sheep, goats, and mice. *Ann N Y Acad Sci* **724**, 300-303.

Fournier, J. G., Escaig-Haye, F. & Grigoriev, V. (2000). Ultrastructural localization of prion proteins: physiological and pathological implications. *Microsc Res Tech* **50**, 76-88.

Frankenfield, K. N., Powers, E. T. & Kelly, J. W. (2005). Influence of the N-terminal domain on the aggregation properties of the prion protein. *Protein Sci* **14**, 2154-2166.

Gabizon, R., McKinley, M. P., Groth, D., Westaway, D., DeArmond, S. J., Carlson, G. A. & Prusiner, S. B. (1989). Immunoaffinity purification and neutralization of scrapie prions. *Prog Clin Biol Res* **317**, 583-600.

Gacia, M., Safranow, K., Styczynska, M., Jakubowska, K., Peplonska, B., Chodakowska-Zebrowska, M., Przekop, I., Slowik, A., Golanska, E., Hulas-Bigoszewska, K., Chlubek, D., Religa, D., Zekanowski, C. & Barcikowska, M. (2006). Prion protein gene M129 allele is a risk factor for Alzheimer's disease. *J Neural Transm* **113**, 1747-51.

Gajdusek D.C & Zigas V (1957). Degenerative disease of the central nervous system in New Guinea; the endemic occurrence of kuru in the native population. *N Engl J Med* **257**, 974-978.

Gajdusek, D. C., Gibbs, C. J. & Alpers, M. (1966). Experimental transmission of a Kuru-like syndrome to chimpanzees. *Nature* **209**, 794-796.

Gajdusek, D. C., Gibbs, C. J., Jr. & Alpers, M. (1967). Transmission and passage of experimenal "kuru" to chimpanzees. *Science* **155**, 212-214.

Gambetti, P., Dong, Z., Yuan, J., Xiao, X., Zheng, M., Alshekhlee, A., Castellani, R., Cohen, M., Barria, M. A., Gonzalez-Romero, D., Belay, E. D., Schonberger, L. B., Marder, K., Harris, C., Burke, J. R., Montine, T., Wisniewski, T., Dickson, D. W., Soto, C., Hulette, C. M., Mastrianni, J. A., Kong, Q. & Zou, W. Q. (2008). A novel human disease with abnormal prion protein sensitive to protease. *Ann Neurol* **63**, 697-708.

Gambetti, P., Parchi, P., Petersen, R. B., Chen, S. G. & Lugaresi, E. (1995). Fatal familial insomnia and familial Creutzfeldt-Jakob disease: clinical, pathological and molecular features. *Brain Pathol* **5**, 43-51.

Gasset, M., Baldwin, M. A., Lloyd, D. H., Gabriel, J. M., Holtzman, D. M., Cohen, F., Fletterick, R. & Prusiner, S. B. (1992). Predicted alpha-helical regions of the prion protein when synthesized as peptides form amyloid. *Proc Natl Acad Sci U S A* **89**, 10940-10944.

Gavier-Widen, D., Noremark, M., Benestad, S., Simmons, M., Renstrom, L., Bratberg, B., Elvander, M. & af Segerstad, C. H. (2004). Recognition of the Nor98 variant of scrapie in the Swedish sheep population. *J Vet Diagn Invest* **16**, 562-567.

Gibbs, C. J., Jr., Asher, D. M., Kobrine, A., Amyx, H. L., Sulima, M. P. & Gajdusek, D. C. (1994). Transmission of Creutzfeldt-Jakob disease to a chimpanzee by electrodes contaminated during neurosurgery. *J Neurol Neurosurg Psychiatry* **57**, 757-758.

Giles, K., Glidden, D. V., Beckwith, R., Seoanes, R., Peretz, D., DeArmond, S. J. & Prusiner, S. B. (2008). Resistance of bovine spongiform encephalopathy (BSE) prions to inactivation. *PLoS Pathog* **4**, e1000206.

Glatzel, M., Abela, E., Maissen, M. & Aguzzi, A. (2003). Extraneural pathologic prion protein in sporadic Creutzfeldt-Jakob disease. *N Engl J Med* **349**, 1812-1820.

Glatzel, M., Heppner, F. L., Albers, K. M. & Aguzzi, A. (2001). Sympathetic innervation of lymphoreticular organs is rate limiting for prion neuroinvasion. *Neuron* **31**, 25-34.

Glockshuber, R., Hornemann, S., Billeter, M., Riek, R., Wider, G. & Wuthrich, K. (1998). Prion protein structural features indicate possible relations to signal peptidases. *FEBS Lett* **426**, 291-296.

Goldmann, W. (2008). PrP genetics in ruminant transmissible spongiform encephalopathies. *Vet Res* **39**, 30.

Goldmann, W., Hunter, N., Foster, J. D., Salbaum, J. M., Beyreuther, K. & Hope, J. (1990). Two alleles of a neural protein gene linked to scrapie in sheep. *Proc Natl Acad Sci U S A* **87**, 2476-2480.

Govaerts, C., Wille, H., Prusiner, S. B. & Cohen, F. E. (2004). Evidence for assembly of prions with left-handed beta-helices into trimers. *Proc Natl Acad Sci U S A* **101**, 8342-8347.

Graner, E., Mercadante, A. F., Zanata, S. M., Forlenza, O. V., Cabral, A. L., Veiga, S. S., Juliano, M. A., Roesler, R., Walz, R., Minetti, A., Izquierdo, I., Martins, V. R. & Brentani, R. R. (2000). Cellular prion protein binds laminin and mediates neuritogenesis. *Brain Res Mol Brain Res* **76**, 85-92.

Groenning, M., Norrman, M., Flink, J. M., van de, W. M., Bukrinsky, J. T., Schluckebier, G. & Frokjaer, S. (2007). Binding mode of Thioflavin T in insulin amyloid fibrils. *J Struct Biol* **159**, 483-497.

Gross, M., Wilkins, D. K., Pitkeathly, M. C., Chung, E. W., Higham, C., Clark, A. & Dobson, C. M. (1999). Formation of amyloid fibrils by peptides derived from the bacterial cold shock protein CspB. *Protein Sci* **8**, 1350-1357.

Guenther, K., Deacon, R. M., Perry, V. H. & Rawlins, J. N. (2001). Early behavioural changes in scrapie-affected mice and the influence of dapsone. *Eur J Neurosci* **14**, 401-409.

Guijarro, J. I., Sunde, M., Jones, J. A., Campbell, I. D. & Dobson, C. M. (1998). Amyloid fibril formation by an SH3 domain. *Proc Natl Acad Sci U S A* **95**, 4224-4228.

Haigh, C. L. & Brown, D. R. (2006). Prion protein reduces both oxidative and non-oxidative copper toxicity. *J Neurochem* **98**, 677-89.

Hainfellner, J. A., Brantner-Inthaler, S., Cervenakova, L., Brown, P., Kitamoto, T., Tateishi, J., Diringer, H., Liberski, P. P., Regele, H., Feucht, M. (1995). The original Gerstmann-Straussler-Scheinker family of Austria: divergent clinicopathological phenotypes but constant PrP genotype. *Brain Pathol* **5**, 201-211.

Haire, L. F., Whyte, S. M., Vasisht, N., Gill, A. C., Verma, C., Dodson, E. J., Dodson, G. G. & Bayley, P. M. (2004). The crystal structure of the globular domain of sheep prion protein. *J Mol Biol* **336**, 1175-1183.

Haley, N. J., Seelig, D. M., Zabel, M. D., Telling, G. C. & Hoover, E. A. (2009). Detection of CWD prions in urine and saliva of deer by transgenic mouse bioassay. *PLoS ONE* **4**, e4848.

Hamir, A. N., Kunkle, R. A., Cutlip, R. C., Miller, J. M., O'Rourke, K. I., Williams, E. S., Miller, M. W., Stack, M. J., Chaplin, M. J. & Richt, J. A. (2005). Experimental transmission of chronic wasting disease agent from mule deer to cattle by the intracerebral route. *J Vet Diagn Invest* **17**, 276-281.

Hamir, A. N., Kunkle, R. A., Cutlip, R. C., Miller, J. M., Williams, E. S. & Richt, J. A. (2006). Transmission of chronic wasting disease of mule deer to Suffolk sheep following intracerebral inoculation. *J Vet Diagn Invest* **18**, 558-565.

Hamir, A. N., Miller, J. M., Kunkle, R. A., Hall, S. M. & Richt, J. A. (2007). Susceptibility of cattle to first-passage intracerebral inoculation with chronic wasting disease agent from white-tailed deer. *Vet Pathol* **44**, 487-493.

Hammersmith K. M., Cohen E. J., Rapuano C. J. & Laibson P. R. (2004). Creutzfeldt-Jakob disease following corneal transplantation. *Cornea* **23**, 406-408.

Harries-Jones, R., Knight, R., Will, R. G., Cousens, S., Smith, P. G. & Matthews, W. B. (1988). Creutzfeldt-Jakob disease in England and Wales, 1980-1984: a case-control study of potential risk factors. *J Neurol Neurosurg Psychiatry* **51**, 1113-1119.

Harris, D. A. (1999). Cellular biology of prion diseases. *Clin Microbiol Rev* **12**, 429-444.

Harris, D. A. & True, H. L. (2006). New insights into prion structure and toxicity. *Neuron* **50**, 353-357.

Head, M. W., Ritchie, D., Smith, N., McLoughlin, V., Nailon, W., Samad, S., Masson, S., Bishop, M., McCardle, L. & Ironside, J. W. (2004). Peripheral tissue involvement in sporadic, iatrogenic, and variant Creutzfeldt-Jakob disease: an immunohistochemical, quantitative, and biochemical study. *Am J Pathol* **164**, 143-153.

Heikenwalder, M., Zeller, N., Seeger, H., Prinz, M., Klohn, P. C., Schwarz, P., Ruddle, N. H., Weissmann, C. & Aguzzi, A. (2005). Chronic lymphocytic inflammation specifies the organ tropism of prions. *Science* **307**, 1107-1110.

Heinen, E., Bosseloir, A. & Bouzahzah, F. (1995). Follicular dendritic cells: origin and function. *Curr Top Microbiol Immunol* **201**, 15-47.

Heppner, F. L., Christ, A. D., Klein, M. A., Prinz, M., Fried, M., Kraehenbuhl, J. P. & Aguzzi, A. (2001). Transepithelial prion transport by M cells. *Nat Med* **7**, 976-977.

Hervé R, Collin, R., Pinchin, H., Secker T & Keevil, C. W. (2009). A rapid dual staining procedure for the quatitative discrimination of prion amyloid from tissues reveals how interactions between amyloid and lipids in tissue homogenates may hinder the detection of prions. *J Microbiol Methods* **77**, 90-7.

Hill, A. F., Butterworth, R. J., Joiner, S., Jackson, G., Rossor, M. N., Thomas, D. J., Frosh, A., Tolley, N., Bell, J. E., Spencer, M., King, A., al-Sarraj, S., Ironside, J. W., Lantos, P. L. & Collinge, J. (1999). Investigation of variant Creutzfeldt-Jakob disease and other human prion diseases with tonsil biopsy samples. *Lancet* **353**, 183-189.

Hill, A. F., Desbruslais, M., Joiner, S., Sidle, K. C., Gowland, I., Collinge, J., Doey, L. J. & Lantos, P. (1997). The same prion strain causes vCJD and BSE. *Nature* **389**, 448-50, 526.

Hill, A. F., Joiner, S., Linehan, J., Desbruslais, M., Lantos, P. L. & Collinge, J. (2000). Species-barrier-independent prion replication in apparently resistant species. *Proc Natl Acad Sci U S A* **97**, 10248-10253.

Hilton, D. A., Ghani, A. C., Conyers, L., Edwards, P., McCardle, L., Ritchie, D., Penney, M., Hegazy, D. & Ironside, J. W. (2004). Prevalence of lymphoreticular prion protein accumulation in UK tissue samples. *J Pathol* **203**, 733-739.

Hosszu, L. L. P., Wells, M. A., Jackson, G. S., Jones, S., Batchelor, M., Clarke, A. R., Craven, C. J., Waltho, J. P. & Collinge, J. (2005). Definable equilibrium states in the folding of human prion protein. *Biochemistry* **44**, 16649-16657.

Houston, F., Goldmann, W., Chong, A., Jeffrey, M., Gonzalez, L., Foster, J., Parnham, D. & Hunter, N. (2003). Prion diseases: BSE in sheep bred for resistance to infection. *Nature* **423**, 498.

Howlin, R. P., Harrison, J., Secker, T. & Keevil, C. W. (2009). Acquisition of proteinaceous contamination through the hanlding of surgical instruments by hospital staff in sterile service departments. *J Inf Prev* **10**, 106-111.

Howlin, R.P., Khammo, N., Secker, T., McDonnell, G. & Keevil, C.W. (2010). Application of a fluorescent dual stain to assess decontamination of tissue protein and prion amyloid from surgical stainless steel during simulated washer-disinfector cycles. *J Hosp Infect.* In press.

Hutter, G., Heppner, F. L. & Aguzzi, A. (2003). No superoxide dismutase activity of cellular prion protein in vivo. *Biol Chem* **384**, 1279-1285.

Ingrosso, L., Pisani, F. & Pocchiari, M. (1999). Transmission of the 263K scrapie strain by the dental route. *J Gen Virol* **80**, 3043-3047.

Ironside, J. W., Bishop, M. T., Connolly, K., Hegazy, D., Lowrie, S., Le, G. M., Ritchie, D. L., McCardle, L. M. & Hilton, D. A. (2006). Variant Creutzfeldt-Jakob disease:

prion protein genotype analysis of positive appendix tissue samples from a retrospective prevalence study. *BMJ* **332**, 1186-1188.

Isaacs, J. D., Jackson, G. S. & Altmann, D. M. (2006). The role of the cellular prion protein in the immune system. *Clin Exp Immunol* **146**, 1-8.

Ishikawa, K., Kudo, Y., Nishida, N., Suemoto, T., Sawada, T., Iwaki, T. & Doh-ura, K. (2006). Styrylbenzoazole derivatives for imaging of prion plaques and treatment of transmissible spongiform encephalopathies. *J Neurochem* **99**, 198-205.

Ishikawa, K., Doh-ura, K., Kudo, Y., Nishida, N., Murakami-Kubo, I., Ando, Y., Sawada, T. & Iwaki, T. (2004). Amyloid imaging probes are useful for detection of prion plaques and treatment of transmissible spongiform encephalopathies. *J Gen Virol* **85**, 1785-1790.

Ishikura, N., Clever, J. L., Bouzamondo-Bernstein, E., Samayoa, E., Prusiner, S. B., Huang, E. J. & DeArmond, S. J. (2005). Notch-1 activation and dendritic atrophy in prion disease. *PNAS* **102**, 886-891.

Jackson, G. S., McKintosh, E., Flechsig, E., Prodromidou, K., Hirsch, P., Linehan, J., Brandner, S., Clarke, A. R., Weissmann, C. & Collinge, J. (2005). An enzyme-detergent method for effective prion decontamination of surgical steel. *J Gen Virol* **86**, 869-878.

Jamieson, E., Jeffrey, M., Ironside, J. W. & Fraser, J. R. (2001). Apoptosis and dendritic dysfunction precede prion protein accumulation in 87V scrapie. *Neuroreport* **12**, 2147-2153.

Jarrett, J. T. & Lansbury, P. T., Jr. (1993). Seeding "one-dimensional crystallization" of amyloid: a pathogenic mechanism in Alzheimer's disease and scrapie? *Cell* **73**, 1055-1058.

Jeffrey, M., Gonzalez, L., Espenes, A., Press, C. M., Martin, S., Chaplin, M., Davis, L., Landsverk, T., MacAldowie, C., Eaton, S. & McGovern, G. (2006). Transportation of prion protein across the intestinal mucosa of scrapie-susceptible and scrapie-resistant sheep. *J Pathol* **209**, 4-14.

Jeffrey, M., Martin, S., Thomson, J. R., Dingwall, W. S., Begara-McGorum, I. & Gonzalez, L. (2001a). Onset and distribution of tissue prp accumulation in scrapie-affected suffolk sheep as demonstrated by sequential necropsies and tonsillar biopsies. *J Comp Pathol* **125**, 48-57.

Jeffrey, M., Ryder, S., Martin, S., Hawkins, S. A., Terry, L., Berthelin-Baker, C. & Bellworthy, S. J. (2001b). Oral inoculation of sheep with the agent of bovine spongiform encephalopathy (BSE). 1. Onset and distribution of disease-specific PrP accumulation in brain and viscera. *J Comp Pathol* **124**, 280-289.

Jennelle, C. S., Samuel, M. D., Nolden, C. A., Keane, D. P., Barr, D. J., Johnson, C., Vanderloo, J. P., Aiken, J. M., Hamir, A. N. & Hoover, E. A. (2009). Surveillance for transmissible spongiform encephalopathy in scavengers of white-tailed deer carcasses in the chronic wasting disease area of Wisconsin. *J Toxicol Environ Health A* **72**, 1018-1024.

Jimenez, J. L., Nettleton, E. J., Bouchard, M., Robinson, C. V., Dobson, C. M. & Saibil, H. R. (2002). The protofilament structure of insulin amyloid fibrils. *Proc Natl Acad Sci U S A* **99**, 9196-9201.

Jimenez, J. L., Tennent, G., Pepys, M. & Saibil, H. R. (2001). Structural diversity of ex vivo amyloid fibrils studied by cryo-electron microscopy. *J Mol Biol* **311**, 241-247.

Jobling, M. F., Stewart, L. R., White, A. R., McLean, C., Friedhuber, A., Maher, F., Beyreuther, K., Masters, C. L., Barrow, C. J., Collins, S. J. & Cappai, R. (1999). The hydrophobic core sequence modulates the neurotoxic and secondary structure properties of the prion peptide 106-126. *J Neurochem* **73**, 1557-1565.

Johnson, C., Johnson, J., Vanderloo, J. P., Keane, D., Aiken, J. M. & McKenzie, D. (2006). Prion protein polymorphisms in white-tailed deer influence susceptibility to chronic wasting disease. *J Gen Virol* **87**, 2109-2114.

Kaneko, K., Vey, M., Scott, M., Pilkuhn, S., Cohen, F. E. & Prusiner, S. B. (1997). COOH-terminal sequence of the cellular prion protein directs subcellular trafficking and controls conversion into the scrapie isoform. *Proc Natl Acad Sci U S A* **94**, 2333-2338.

Kayed, R., Head, E., Thompson, J. L., McIntire, T. M., Milton, S. C., Cotman, C. W. & Glabe, C. G. (2003). Common structure of soluble amyloid oligomers implies common mechanism of pathogenesis. *Science* **300**, 486-489.

Keane, D. P., Barr, D. J., Bochsler, P. N., Hall, S. M., Gidlewski, T., O'Rourke, K. I., Spraker, T. R. & Samuel, M. D. (2008). Chronic wasting disease in a Wisconsin white-tailed deer farm. *J Vet Diagn Invest* **20**, 698-703.

Keeler, N., Schonberger, L. B., Belay, E. D., Sehulster, L., Turabelidze, G. & Sejvar, J. J. (2006). Investigation of a possible iatrogenic case of creutzfeldt-jakob disease after a neurosurgical procedure. *Infect Control Hosp Epidemiol* **27**, 1352-1357.

Keevil, C. W. (2003). Rapid detection of biofilms and adherent pathogens using scanning confocal laser microscopy and episcopic differential interference contrast microscopy. *Water Sci Technol* **47**, 105-116.

Khosravani, H., Zhang, Y., Tsutsui, S., Hameed, S., Altier, C., Hamid, J., Chen, L., Villemaire, M., Ali, Z., Jirik, F. R. & Zamponi, G. W. (2008). Prion protein attenuates excitotoxicity by inhibiting NMDA receptors. *J Cell Biol* **181**, 551-565.

Khurana, R., Coleman, C., Ionescu-Zanetti, C., Carter, S. A., Krishna, V., Grover, R. K., Roy, R. & Singh, S. (2005). Mechanism of Thioflavin T binding to amyloid fibrils. *Journal of Structural Biology* **151**, 229-238.

Kim, T. Y., Shon, H. J., Joo, Y. S., Mun, U. K., Kang, K. S. & Lee, Y. S. (2005). Additional cases of Chronic Wasting Disease in imported deer in Korea. *J Vet Med Sci* **67**, 753-759.

Kimberlin, R. H. & Walker, C. (1977). Characteristics of a short incubation model of scrapie in the golden hamster. *J Gen Virol* **34**, 295-304.

Kimberlin, R. H. & Walker, C. A. (1988). Pathogenesis of experimental scrapie. *Ciba Found Symp* **135**, 37-62.

Kirkitadze, M. D., Bitan, G. & Teplow, D. B. (2002). Paradigm shifts in Alzheimer's disease and other neurodegenerative disorders: the emerging role of oligomeric assemblies. *J Neurosci Res* **69**, 567-577.

Kitamoto, T., Muramoto, T., Mohri, S., Doh-ura, K. & Tateishi, J. (1991). Abnormal isoform of prion protein accumulates in follicular dendritic cells in mice with Creutzfeldt-Jakob disease. *J Virol* **65**, 6292-6295.

Klamt, F., Dal-Pizzol, F., Conte da Frota ML JR, Walz, R., Andrades, M. E., da Silva, E. G., Brentani, R. R., Izquierdo, I. & Fonseca Moreira, J. C. (2001). Imbalance of antioxidant defense in mice lacking cellular prion protein. *Free Radic Biol Med* **30**, 1137-1144.

Klein, M. A., Frigg, R., Flechsig, E., Raeber, A. J., Kalinke, U., Bluethmann, H., Bootz, F., Suter, M., Zinkernagel, R. M. & Aguzzi, A. (1997). A crucial role for B cells in neuroinvasive scrapie. *Nature* **390**, 687-690.

Klein, M. A., Frigg, R., Raeber, A. J., Flechsig, E., Hegyi, I., Zinkernagel, R. M., Weissmann, C. & Aguzzi, A. (1998). PrP expression in B lymphocytes is not required for prion neuroinvasion. *Nat Med* **4**, 1429-1433.

Klein, M. A., Kaeser, P. S., Schwarz, P., Weyd, H., Xenarios, I., Zinkernagel, R. M., Carroll, M. C., Verbeek, J. S., Botto, M., Walport, M. J., Molina, H., Kalinke, U., cha-Orbea, H. & Aguzzi, A. (2001). Complement facilitates early prion pathogenesis. *Nat Med* **7**, 488-492.

Klingeborn, M., Wik, L., Simonsson, M., Renstrom, L. H., Ottinger, T. & Linne, T. (2006). Characterization of proteinase K-resistant N- and C-terminally truncated PrP in Nor98 atypical scrapie. *J Gen Virol* **87**, 1751-1760.

Klunk, W. E., Wang, Y., Huang, G. f., Debnath, M. L., Holt, D. P. & Mathis, C. A. (2001). Uncharged thioflavin-T derivatives bind to amyloid-beta protein with high affinity and readily enter the brain. *Life Sciences* **69**, 1471-1484.

Klunk, W. E., Wang, Y., Huang, G. f., Debnath, M. L., Holt, D. P., Shao, L., Hamilton, R. L., Ikonomovic, M. D., DeKosky, S. T. & Mathis, C. A. (2003). The binding of 2-(4'-Methylaminophenyl)Benzothiazole to postmortem brain homogenates is dominated by the amyloid component. *J Neurosci* **23**, 2086-2092.

Kocisko, D. A., Come, J. H., Priola, S. A., Chesebro, B., Raymond, G. J., Lansbury, P. T. & Caughey, B. (1994). Cell-free formation of protease-resistant prion protein. *Nature* **370**, 471-474.

Kocisko, D. A., Lansbury, P. T., Jr. & Caughey, B. (1996). Partial unfolding and refolding of scrapie-associated prion protein: evidence for a critical 16-kDa C-terminal domain. *Biochemistry* **35**, 13434-13442.

Kocisko, D. A., Priola, S. A., Raymond, G. J., Chesebro, B., Lansbury, P. T., Jr. & Caughey, B. (1995). Species specificity in the cell-free conversion of prion protein to

protease-resistant forms: a model for the scrapie species barrier. *Proc Natl Acad Sci U S A* **92**, 3923-3927.

Kondo, K. & Kuroiwa, Y. (1982). A case control study of Creutzfeldt-Jakob disease: association with physical injuries. *Ann Neurol* **11**, 377-381.

Kong, Q., Huang, S., Zou, W., Vanegas, D., Wang, M., Wu, D., Yuan, J., Zheng, M., Bai, H., Deng, H., Chen, K., Jenny, A. L., O'Rourke, K., Belay, E. D., Schonberger, L. B., Petersen, R. B., Sy, M. S., Chen, S. G. & Gambetti, P. (2005). Chronic wasting disease of elk: transmissibility to humans examined by transgenic mouse models. *J Neurosci* **25**, 7944-7949.

Kong, Q., Zheng, M., Casalone, C., Qing, L., Huang, S., Chakraborty, B., Wang, P., Chen, F., Cali, I., Corona, C., Martucci, F., Iulini, B., Acutis, P., Wang, L., Liang, J., Wang, M., Li, X., Monaco, S., Zanusso, G., Zou, W. Q., Caramelli, M. & Gambetti, P. (2008). Evaluation of the human transmission risk of an atypical bovine spongiform encephalopathy prion strain. *J Virol* **82**, 3697-3701.

Krebs, M. R. H., Bromley, E. H. C. & Donald, A. M. (2005). The binding of Thioflavin-T to amyloid fibrils: localisation and implications. *Journal of Structural Biology* **149**, 30-37.

Kubler, E., Oesch, B. & Raeber, A. J. (2003). Diagnosis of prion diseases. *Br Med Bull* **66**, 267-279.

Kuczius, T. & Groschup, M. H. (1999). Differences in proteinase K resistance and neuronal deposition of abnormal prion proteins characterize bovine spongiform encephalopathy (BSE) and scrapie strains. *Mol Med* **5**, 406-418.

Kulczycki, J., Jedrzejowska, H., Gajkowski, K., Tarnowska-Dziduszko, E. & Lojkowska, W. (1991). Creutzfeldt-Jakob disease in young people. *Eur J Epidemiol* **7**, 501-504.

Kurschner, C. & Morgan, J. I. (1995). The cellular prion protein (PrP) selectively binds to Bcl-2 in the yeast two-hybrid system. *Brain Res Mol Brain Res* **30**, 165-168.

Kuwahara, C., Takeuchi, A. M., Nishimura, T., Haraguchi, K., Kubosaki, A., Matsumoto, Y., Saeki, K., Matsumoto, Y., Yokoyama, T., Itohara, S. & Onodera, T. (1999). Prions prevent neuronal cell-line death. *Nature* **400**, 225-226.

Ladogana, A., Puopolo, M., Croes, E. A., Budka, H., Jarius, C., Collins, S., Klug, G. M., Sutcliffe, T., Giulivi, A., Alperovitch, A., asnerie-Laupretre, N., Brandel, J.-P., Poser, S., Kretzschmar, H., Rietveld, I., Mitrova, E., Cuesta, J. d. P., Martinez-Martin, P., Glatzel, M., Aguzzi, A., Knight, R., Ward, H., Pocchiari, M., van Duijn, C. M., Will, R. G. & Zerr, I. (2005). Mortality from Creutzfeldt-Jakob disease and related disorders in Europe, Australia, and Canada. *Neurology* **64**, 1586-1591.

Lasmezas, C. I., Deslys, J. P., Robain, O., Jaegly, A., Beringue, V., Peyrin, J. M., Fournier, J. G., Hauw, J. J., Rossier, J. & Dormont, D. (1997). Transmission of the BSE agent to mice in the absence of detectable abnormal prion protein. *Science* **275**, 402-405.

Lawson, V. A., Priola, S. A., Wehrly, K. & Chesebro, B. (2001). N-terminal truncation of prion protein affects both formation and conformation of abnormal protease-resistant prion protein generated in vitro. *J Biol Chem* **276**, 35265-35271.

Leffers K. W., Wille H, Stohr J, Junger E, Prusiner, S. B. & Reisner D (2005). Assembly of natural and recombinant prion protein into fibrils. *Biol Chem* **386**, 569-580.

Legname, G., Baskakov, I. V., Nguyen, H. O., Riesner, D., Cohen, F. E., DeArmond, S. J. & Prusiner, S. B. (2004). Synthetic mammalian prions. *Science* **305**, 673-676.

Legname, G., Nguyen, H. O., Baskakov, I. V., Cohen, F. E., DeArmond, S. J. & Prusiner, S. B. (2005). Strain-specified characteristics of mouse synthetic prions. *Proc Natl Acad Sci U S A* **102**, 2168-2173.

Legname, G., Nguyen, H. O., Peretz, D., Cohen, F. E., DeArmond, S. J. & Prusiner, S. B. (2006). Continuum of prion protein structures enciphers a multitude of prion isolate-specified phenotypes. *Proc Natl Acad Sci U S A* **103**, 19105-19110.

Lehmann, S., Pastore, M., Rogez-Kreuz, C., Richard, M., Belondrade, M., Rauwel, G., Durand, F., Yousfi, R., Criquelion, J., Clayette, P. & Perret-Liaudet, A. (2009). New hospital disinfection processes for both conventional and prion infectious agents compatible with thermosensitive medical equipment. *J Hosp Infect* **72**, 342-350.

Lemmer, K., Mielke, M., Kratzel, C., Joncic, M., Oezel, M., Pauli, G. & Beekes, M. (2008). Decontamination of surgical instruments from prions. II. In vivo findings with a model system for testing the removal of scrapie infectivity from steel surfaces. *J Gen Virol* **89**, 348-358.

Lemmer, K., Mielke, M., Pauli, G. & Beekes, M. (2004). Decontamination of surgical instruments from prion proteins: in vitro studies on the detachment, destabilization and degradation of PrPSc bound to steel surfaces. *J Gen Virol* **85**, 3805-3816.

Lesne, S., Koh, M. T., Kotilinek, L., Kayed, R., Glabe, C. G., Yang, A., Gallagher, M. & Ashe, K. H. (2006). A specific amyloid-beta protein assembly in the brain impairs memory. *Nature* **440**, 352-357.

Lewis, P. A., Properzi, F., Prodromidou, K., Clarke, A. R., Collinge, J. & Jackson, G. S. (2006a). Removal of the glycosylphosphatidylinositol anchor from PrP(Sc) by cathepsin D does not reduce prion infectivity. *Biochem J* **395**, 443-448.

Lewis, P. A., Tattum, M. H., Jones, S., Bhelt, D., Batchelor, M., Clarke, A. R., Collinge, J. & Jackson, G. S. (2006b). Codon 129 polymorphism of the human prion protein influences the kinetics of amyloid formation. *J Gen Virol* **87**, 2443-2449.

Li, A., Barmada, S. J., Roth, K. A. & Harris, D. A. (2007a). N-terminally deleted forms of the prion protein activate both Bax-dependent and Bax-independent neurotoxic pathways. *J Neurosci* **27**, 852-859.

Li, A., Christensen, H. M., Stewart, L. R., Roth, K. A., Chiesa, R. & Harris, D. A. (2007b). Neonatal lethality in transgenic mice expressing prion protein with a deletion of residues 105-125. *EMBO J* **26**, 548-558.

Li, A. & Harris, D. A. (2005). Mammalian prion protein suppresses Bax-induced cell death in yeast. *J Biol Chem* **280**, 17430-17434.

Li, R., Liu, D., Zanusso, G., Liu, T., Fayen, J. D., Huang, J. H., Petersen, R. B., Gambetti, P. & Sy, M. S. (2001). The expression and potential function of cellular prion protein in human lymphocytes. *Cell Immunol* **207**, 49-58.

Liberski, P. P. (2004). Amyloid plaques in transmissible spongiform encephalopathies (prion diseases). *Folia Neuropathol* **42**, 109-119.

Liberski, P. P. & Brown, P. (2004). Kuru: a half-opened window onto the landscape of neurodegenerative diseases. *Folia Neuropathol* **42**, 3-14.

Liberski, P. P. & Budka, H. (1995). Ultrastructural pathology of Gerstmann-Straussler-Scheinker disease. *Ultrastruct Pathol* **19**, 23-36.

Lipscomb, I. P., Herve, R., Harris, K., Pinchin, H., Collin, R. & Keevil, C. W. (2007a). Amyloid-specific fluorophores for the rapid, sensitive in situ detection of prion contamination on surgical instruments. *J Gen Virol* **88**, 2619-2626.

Lipscomb, I. P., Pinchin, H., Collin, R. & Keevil, C. W. (2007b). Effect of drying time, ambient temperature and pre-soaks on prion-infected tissue contamination levels on surgical stainless steel: concerns over prolonged transportation of instruments from theatre to central sterile service departments. *J Hosp Infect* **65**, 72-77.

Lipscomb, I. P., Sihota, A. K. & Keevil, C. W. (2007c). Comparison between visual analysis and microscope assessment of surgical instrument cleanliness from sterile service departments. *J Hosp Infect* **68**, 52-8.

Lipscomb, I. P., Pinchin, H. E., Collin, R., Harris, K. & Keevil, C. W. (2006a). The sensitivity of approved Ninhydrin and Biuret tests in the assessment of protein contamination on surgical steel as an aid to prevent iatrogenic prion transmission. *J Hosp Infect* **64**, 288-92

Lipscomb, I. P., Sihota, A. K., Botham, M., Harris, K. L. & Keevil, C. W. (2006b). Rapid method for the sensitive detection of protein contamination on surgical instruments. *Journal of Hospital Infection* **62**, 141-148.

Lipscomb, I. P., Sihota, A. K. & Keevil, C. W. (2006c). Comparative study of surgical instruments from sterile service departments for the presence of residual Gram - negative endotoxin and proteinaceous deposits. *J Clin Microbiol* **44**, 3728-33.

Lipscomb, I. P., Sihota, A. K. & Keevil, C. W. (2006d). Diathermy forceps and pencils: reservoirs for protein and prion contamination? *J Hosp Infect* **64**, 193-4.

Liu, T., Li, R., Wong, B. S., Liu, D., Pan, T., Petersen, R. B., Gambetti, P. & Sy, M. S. (2001). Normal cellular prior protein is preferentially expressed on subpopulations of murine hemopoietic cells. *J Immunol* **166**, 3733-3742.

Llewelyn, C. A., Hewitt, P. E., Knight, R. S. G., Amar, K., Cousens, S., Mackenzie, J. & Will, R. G. (2004). Possible transmission of variant Creutzfeldt-Jakob disease by blood transfusion. *The Lancet* **363**, 417-421.

Lockhart, A., Ye, L., Judd, D. B., Merritt, A. T., Lowe, P. N., Morgenstern, J. L., Hong, G., Gee, A. D. & Brown, J. (2005). Evidence for the presence of three distinct binding sites for the thioflavin T class of Alzheimer's disease PET imaging agents on beta-amyloid peptide fibrils. *J Biol Chem* **280**, 7677-7684.

Lowe, A. H., Bagg, J., Burke, F. J., MacKenzie, D. & McHugh, S. (2002). A study of blood contamination of Siqveland matrix bands. *Br Dent J* **192**, 43-45.

Luhr, K. M., Low, P., Taraboulos, A., Bergman, T. & Kristensson, K. (2009). Prion adsorption to stainless steel is promoted by nickel and molybdenum. *J Gen Virol* doi:10.1099/vir.0.012302-0.

Ma, J. & Lindquist, S. (2002). Conversion of PrP to a self-perpetuating PrPSc-like conformation in the cytosol. *Science* **298**, 1785-1788.

Mabbott, N. A., Brown, K. L., Manson, J. & Bruce, M. E. (1997). T-lymphocyte activation and the cellular form of the prion protein. *Immunology* **92**, 161-165.

Mabbott, N. A., Bruce, M. E., Botto, M., Walport, M. J. & Pepys, M. B. (2001). Temporary depletion of complement component C3 or genetic deficiency of C1q significantly delays onset of scrapie. *Nat Med* **7**, 485-487.

Mabbott, N. A., Mackay, F., Minns, F. & Bruce, M. E. (2000a). Temporary inactivation of follicular dendritic cells delays neuroinvasion of scrapie. *Nat Med* **6**, 719-720.

Mabbott, N. A., Williams, A., Farquhar, C. F., Pasparakis, M., Kollias, G. & Bruce, M. E. (2000b). Tumor necrosis factor alpha-deficient, but not interleukin-6-deficient, mice resist peripheral infection with scrapie. *J Virol* **74**, 3338-3344.

Maezawa, I., Hong, H. S., Liu, R., Wu, C. Y., Cheng, R. H., Kung, M. P., Kung, H. F., Lam, K. S., Oddo, S., Laferla, F. M. & Jin, L. W. (2008). Congo red and Thioflavin-T analogs detect Abeta oligomers. *J Neurochem* **104**, 457-468.

Mahal, S. P., Baker, C. A., Demczyk, C. A., Smith, E. W., Julius, C. & Weissmann, C. (2007). Prion strain discrimination in cell culture: The cell panel assay. *PNAS* **104**, 20908-20913.

Maheshwar, A., De, M. & Browning, S. T. (2003). Reusable versus disposable instruments in tonsillectomy: a comparative study of outcomes. *Int J Clin Pract* **57**, 579-583.

Mahillo-Fernandez, I., de Pedro-Cuesta, J., Bleda, M. J., Cruz, M., Molbak, K., Laursen, H., Falkenhorst, G., Martinez-Martin, P. & Siden, A. (2008). Surgery and risk of sporadic Creutzfeldt-Jakob disease in Denmark and Sweden: registry-based case-control studies. *Neuroepidemiology* **31**, 229-240.

Mallucci, G., Dickinson, A., Linehan, J., Klohn, P. C., Brandner, S. & Collinge, J. (2003). Depleting neuronal PrP in prion infection prevents disease and reverses spongiosis. *Science* **302**, 871-874.

Mallucci, G. R., Ratte, S., Asante, E. A., Linehan, J., Gowland, I., Jefferys, J. G. & Collinge, J. (2002). Post-natal knockout of prion protein alters hippocampal CA1 properties, but does not result in neurodegeneration. *EMBO J* **21**, 202-210.

Mallucci, G. R., White, M. D., Farmer, M., Dickinson, A., Khatun, H., Powell, A. D., Brandner, S., Jefferys, J. G. & Collinge, J. (2007). Targeting cellular prion protein reverses early cognitive deficits and neurophysiological dysfunction in prion-infected mice. *Neuron* **53**, 325-335.

Manson, J. C., Cancellotti, E., Hart, P., Bishop, M. T. & Barron, R. M. (2006). The transmissible spongiform encephalopathies: emerging and declining epidemics. *Biochem Soc Trans* **34**, 1155-1158.

Manson, J. C., Hope, J., Clarke, A. R., Johnston, A., Black, C. & MacLeod, N. (1995). PrP gene dosage and long term potentiation. *Neurodegeneration* **4**, 113-114.

Manuelidis, L., Fritch, W. & Xi, Y. G. (1997). Evolution of a strain of CJD that induces BSE-like plaques. *Science* **277**, 94-98.

Manuelidis, L., Liu, Y. & Mullins, B. (2009). Strain-specific viral properties of variant Creutzfeldt-Jakob disease (vCJD) are encoded by the agent and not by host prion protein. *J Cell Biochem* **106**, 220-231.

Martinez-Lage, J. F., Rabano, A., Bermejo, J., Martinez Perez, M., Guerrero, M. C., Contreras, M. A. & Lunar, A. (2005). Creutzfeldt-Jakob disease acquired via a dural graft: failure of therapy with quinacrine and chlorpromazine. *Surgical Neurology* **64**, 542-545.

Martins, V. R., Linden, R., Prado, M. A., Walz, R., Sakamoto, A. C., Izquierdo, I. & Brentani, R. R. (2002). Cellular prion protein: on the road for functions. *FEBS Lett* **512**, 25-28.

Martins, V. R. & Brentani, R. R. (2002). The biology of the cellular prion protein. *Neurochemistry International* **41**, 353-355.

Mathiason, C. K., Hays, S. A., Powers, J., Hayes-Klug, J., Langenberg, J., Dahmes, S. J., Osborn, D. A., Miller, K. V., Warren, R. J., Mason, G. L. & Hoover, E. A. (2009). Infectious prions in pre-clinical deer and transmission of chronic wasting disease solely by environmental exposure. *PLoS ONE* **4**, e5916.

Mathis, C. A., Wang, Y., Holt, D. P., Huang, G. F., Debnath, M. L. & Klunk, W. E. (2003). Synthesis and evaluation of 11C-Labeled 6-Substituted 2-Arylbenzothiazoles as amyloid imaging agents. *J Med Chem* **46**, 2740-2754.

Mathis, C. A., Bacskai, B. J., Kajdasz, S. T., McLellan, M. E., Frosch, M. P., Hyman, B. T., Holt, D. P., Wang, Y., Huang, G. f., Debnath, M. L. & Klunk, W. E. (2002). A lipophilic Thioflavin-T derivative for positron emission tomography (PET) imaging of amyloid in brain. *Bioorganic & Medicinal Chemistry Letters* **12**, 295-298.

Mayer, R. J., Landon, M., Laszlo, L., Lennox, G. & Lowe, J. (1992). Protein processing in lysosomes: the new therapeutic target in neurodegenerative disease. *Lancet* **340**, 156-159.

McBride, P. A. & Beekes, M. (1999). Pathological PrP is abundant in sympathetic and sensory ganglia of hamsters fed with scrapie. *Neurosci Lett* **265**, 135-138.

McDonnell, G. & Burke P (2003). The challenge of prion decontamination. *Clin Infect Dis* **36**, 1152-1154.

McDonnell, G. (2008). Prion disease transmission: can we apply standard precautions to prevent or reduce risks? *J Perioper Pract* **18**, 298-304.

McKinley, M. P., Bolton, D. C. & Prusiner, S. B. (1983). A protease-resistant protein is a structural component of the scrapie prion. *Cell* **35**, 57-62.

McKinley, M. P., Meyer, R. K., Kenaga, L., Rahbar, F., Cotter, R., Serban, A. & Prusiner, S. B. (1991a). Scrapie prion rod formation in vitro requires both detergent extraction and limited proteolysis. *J Virol* **65**, 1340-1351.

McKinley, M. P., Taraboulos, A., Kenaga, L., Serban, D., Stieber, A., DeArmond, S. J., Prusiner, S. B. & Gonatas, N. (1991b). Ultrastructural localization of scrapie prion proteins in cytoplasmic vesicles of infected cultured cells. *Lab Invest* **65**, 622-630.

McLean, C. A. (2008). Review. The neuropathology of kuru and variant Creutzfeldt-Jakob disease. *Philos Trans R Soc Lond B Biol Sci* **363**, 3685-3687.

McLennan, N. F., Brennan, P. M., McNeill, A., Davies, I., Fotheringham, A., Rennison, K. A., Ritchie, D., Brannan, F., Head, M. W., Ironside, J. W., Williams, A. & Bell, J. E. (2004). Prion protein accumulation and neuroprotection in hypoxic brain damage. *Am J Pathol* **165**, 227-235.

Merlini, G. & Bellotti, V. (2003). Molecular mechanisms of amyloidosis. *N Engl J Med* **349**, 583-596.

Meyer, N., Rosenbaum, V., Schmidt, B., Gilles, K., Mirenda, C., Groth, D., Prusiner, S. B. & Riesner, D. (1991). Search for a putative scrapie genome in purified prion fractions reveals a paucity of nucleic acids. *J Gen Virol* **72**, 37-49.

Miele, G., Jeffrey, M., Turnbull, D., Manson, J. & Clinton, M. (2002). Ablation of cellular prion protein expression affects mitochondrial numbers and morphology. *Biochem Biophys Res Commun* **291**, 372-377.

Mitteregger, G., Vosko, M., Krebs, B., Xiang, W., Kohlmannsperger, V., Nolting, S., Hamann, G. F. & Kretzschmar, H. A. (2007) . The role of the octarepeat region in neuroprotective function of the cellular prion protein. *Brain Pathol* **17**, 174-183.

Mody, I. & MacDonald, J. F. (1995). NMDA receptor-dependent excitotoxicity: the role of intracellular Ca2+ release. *Trends Pharmacol Sci* **16**, 356-359.

Monreal, J., Collins, G. H., Masters, C. L., Fisher, C. M., Kim, R. C., Gibbs, C. J., Jr. & Gajdusek, D. C. (1981). Creutzfeldt-Jakob disease in an adolescent. *J Neurol Sci* **52**, 341-350.

Montrasio, F., Frigg, R., Glatzel, M., Klein, M. A., Mackay, F., Aguzzi, A. & Weissmann, C. (2000). Impaired prion replication in spleens of mice lacking functional follicular dendritic cells. *Science* **288**, 1257-1259.

Moore R.A, Vorberg I & Priola S.A (2005). Species barriers in prion diseases - brief review. *Arch Virol Suppl* **19**, 187-202.

Mouillet-Richard, S., Ermonval, M., Chebassier, C., Laplanche, J. L., Lehmann, S., Launay, J. M. & Kellermann, O. (2000). Signal transduction through prion protein. *Science* **289**, 1925-1928.

Muramoto, T., Scott, M., Cohen, F. E. & Prusiner, S. B. (1996). Recombinant scrapie-like prion protein of 106 amino acids is soluble. *Proc Natl Acad Sci U S A* **93**, 15457-15462.

Murdoch, H., Taylor, D., Dickinson, J., Walker, J. T., Perrett, D., Raven, N. D. & Sutton, J. M. (2006). Surface decontamination of surgical instruments: an ongoing dilemma. *J Hosp Infect* **63**, 432-8.

Murray, K., Ritchie, D. L., Bruce, M., Young, C. A., Doran, M., Ironside, J. W. & Will, R. G. (2008). Sporadic Creutzfeldt-Jakob disease in two adolescents. *J Neurol Neurosurg Psychiatry* **79**, 14-18.

Neumaier, B., Deisenhofer, S., Furst, D., von Arnim, C. A., Thees, S., Buck, A. K., Glatting, G., Landwehrmeyer, G. B., Krause, B. J., Muller, H. D., Sommer, C., Reske, S. N. & Mottaghy, F. M. (2007). Radiosynthesis and evaluation of [11C]BTA-1 and [11C]3'-Me-BTA-1 as potential radiotracers for in vivo imaging of beta-amyloid plaques. *Nuklearmedizin* **46**, 271-280.

Neutra, M. R., Frey, A. & Kraehenbuhl, J. P. (1996). Epithelial M cells: gateways for mucosal infection and immunization. *Cell* **86**, 345-348.

Ng, S., Villemagne, V. L., Berlangieri, S., Lee, S. T., Cherk, M., Gong, S. J., Ackermann, U., Saunder, T., Tochon-Danguy, H., Jones, G., Smith, C., O'Keefe, G., Masters, C. L. & Rowe, C. C. (2007). Visual assessment versus quantitative assessment of 11C-PIB PET and 18F-FDG PET for detection of Alzheimer's disease. *J Nucl Med* **48**, 547-552.

Nix, P. (2003). Prions and disposable surgical instruments. *Int J Clin Pract* **57**, 678-680.

Norstrom, E. M. & Mastrianni, J. A. (2006). The charge structure of Helix 1 in the prion protein regulates conversion to pathogenic PrPSc. *J Virol* **80**, 8521-8529.

Novitskaya, V., Makarava, N., Bellon, A., Bocharova, O. V., Bronstein, I. B., Williamson, R. A. & Baskakov, I. V. (2006). Probing the conformation of the prion protein within a single amyloid fibril using a novel immunoconformational assay. *J Biol Chem* **281**, 15536-45.

Novitskaya, V., Makarava, N., Sylvester, I., Bronstein, I. B. & Baskakov, I. V. (2007). Amyloid fibrils of mammalian prion protein induce axonal degeneration in NTERA2-derived terminally differentiated neurons. *J Neurochem* **102**, 398-407.

Onnasch, H., Gunn, H. M., Bradshaw, B. J., Benestad, S. L. & Bassett, H. F. (2004). Two Irish cases of scrapie resembling Nor98. *Vet Rec* **155**, 636-637.

Orge, L., Galo, A., Machado, C., Lima, C., Ochoa, C., Silva, J., Ramos, M. & Simas, J. P. (2004). Identification of putative atypical scrapie in sheep in Portugal. *J Gen Virol* **85**, 3487-3491.

Pan, K. M., Baldwin, M., Nguyen, J., Gasset, M., Serban, A., Groth, D., Mehlhorn, I., Huang, Z., Fletterick, R. J., Cohen, F. E. & . (1993). Conversion of alpha-helices into beta-sheets features in the formation of the scrapie prion proteins. *Proc Natl Acad Sci U S A* **90**, 10962-10966.

Peden, A. H., Head, M. W., Diane, L. R., Jeanne, E. B. & James, W. I. (2004). Preclinical vCJD after blood transfusion in a PRNP codon 129 heterozygous patient. *The Lancet* **364**, 527-529.

Peden, A. H., Ritchie, D. L., Head, M. W. & Ironside, J. W. (2006). Detection and localization of PrPSc in the skeletal muscle of patients with variant, iatrogenic, and sporadic forms of Creutzfeldt-Jakob Disease. *Am J Pathol* **168**, 927-935.

Peretz, D., Williamson, R. A., Legname, G., Matsunaga, Y., Vergara, J., Burton, D. R., DeArmond, S. J., Prusiner, S. B. & Scott, M. R. (2002). A change in the conformation of prions accompanies the emergence of a new prion strain. *Neuron* **34**, 921-932.

Peretz, D., Supattapone, S., Giles, K., Vergara, J., Freyman, Y., Lessard, P., Safar, J. G., Glidden, D. V., McCulloch, C., Nguyen, H. O., Scott, M., DeArmond, S. J. & Prusiner, S. B. (2006). Inactivation of prions by acidic Sodium Dodecyl Sulfate. *J Virol* **80**, 322-331.

Petzold, G. C., Westner, I., Bohner, G., Einhaupl, K. M., Kretzschmar, H. A. & Valdueza, J. M. (2004). False-positive pulvinar sign on MRI in sporadic Creutzfeldt-Jakob disease. *Neurology* **62**, 1235-1236.

Pham, N., Yin, S., Yu, S., Wong, P., Kang, S. C., Li, C. & Sy, M. S. (2008). Normal cellular prion protein with a methionine at position 129 has a more exposed helix 1 and is more prone to aggregate. *Biochem Biophys Res Commun* **368**, 875-881.

Piccardo, P., Manson, J. C., King, D., Ghetti, B. & Barron, R. M. (2007). Accumulation of prion protein in the brain that is not associated with transmissible disease. *Proc Natl Acad Sci U S A* **104**, 4712-4717.

Pilon, J. L., Nash, P. B., Arver, T., Hoglund, D. & Vercauteren, K. C. (2009). Feasibility of infectious prion digestion using mild conditions and commercial subtilisin. *J Virol Methods* **161**, 168-172.

Pinheiro, T. J. (2006). The role of rafts in the fibrillization and aggregation of prions. *Chem Phys Lipids* **141**, 66-71.

Poser, C. M. (2002). Notes on the history of the prion diseases. Part I. *Clinical Neurology and Neurosurgery* **104**, 1-9.

Post, K., Pitschke, M., Schafer, O., Wille, H., Appel, T. R., Kirsch, D., Mehlhorn, I., Serban, H., Prusiner, S. B. & Riesner, D. (1998). Rapid acquisition of beta-sheet structure in the prion protein prior to multimer formation. *Biol Chem* **379**, 1307-1317.

Preusser, M., Strobel, T., Gelpi, E., Eiler, M., Broessner, G., Schmutzhard, E. & Budka, H. (2006). Alzheimer-type neuropathology in a 28 year old patient with iatrogenic Creutzfeldt-Jakob disease after dural grafting. *J Neurol Neurosurg Psychiatry* **77**, 413-416.

Prinz, M., Heikenwalder, M., Junt, T., Schwarz, P., Glatzel, M., Heppner, F. L., Fu, Y. X., Lipp, M. & Aguzzi, A. (2003). Positioning of follicular dendritic cells within the spleen controls prion neuroinvasion. *Nature* **425**, 957-962.

Prinz, M., Montrasio, F., Klein, M. A., Schwarz, P., Priller, J., Odermatt, B., Pfeffer, K. & Aguzzi, A. (2002). Lymph nodal prion replication and neuroinvasion in mice devoid of follicular dendritic cells. *Proc Natl Acad Sci U S A* **99**, 919-924.

Prusiner, S. B. (1982). Novel proteinaceous infectious particles cause scrapie. *Science* **216**, 136-144.

Prusiner, S. B. (1986). Prions are novel infectious pathogens causing scrapie and Creutzfeldt-Jakob disease. *Bioessays* **5**, 281-286.

Prusiner, S. B. (1998). Prions. *PNAS* **95**, 13363-13383.

Prusiner, S. B., Groth, D., Serban, A., Koehler, R., Foster, D., Torchia, M., Burton, D., Yang, S. L. & DeArmond, S. J. (1993). Ablation of the prion protein (PrP) gene in mice prevents scrapie and facilitates production of anti-PrP antibodies. *Proc Natl Acad Sci U S A* **90**, 10608-10612.

Prusiner, S. B., McKinley, M. P., Bowman, K. A., Bolton, D. C., Bendheim, P. E., Groth, D. F. & Glenner, G. G. (1983). Scrapie prions aggregate to form amyloid-like birefringent rods. *Cell* **35**, 349-358.

Race, B., Meade-White, K., Race, R. & Chesebro, B. (2009). Prion infectivity in fat of deer with chronic wasting disease. *J Virol* **83**, 9608-9610.

Race, R. E., Raines, A., Raymond, G. J., Caughey, B. & Chesebro, B. (2001). Long-term subclinical carrier state precedes scrapie replication and adaptation in a resistant species: analogies to bovine spongiform encephalopathy and variant Creutzfeldt-Jakob disease in humans. *J Virol* **75**, 10106-10112.

Race, R. E. & Raymond, G. J. (2004). Inactivation of transmissible spongiform encephalopathy (prion) agents by environ LpH. *J Virol* **78**, 2164-2165.

Ramirez-Alvarado, M., Merkel, J. S. & Regan, L. (2000). A systematic exploration of the influence of the protein stability on amyloid fibril formation in vitro. *Proc Natl Acad Sci U S A* **97**, 8979-8984.

Ransjo, U., Engstrom, L., Hakansson, P., Ledel, T., Lindgren, L., Lindqvist, A. L., Marcusson, E. & Rudback, K. (2001). A test for cleaning and disinfection processes in a washer-disinfector. *APMIS* **109**, 299-304.

Raymond, G. J., Bossers, A., Raymond, L. D., O'Rourke, K. I., McHolland, L. E., Bryant, P. K., III, Miller, M. W., Williams, E. S., Smits, M. & Caughey, B. (2000).

Evidence of a molecular barrier limiting susceptibility of humans, cattle and sheep to chronic wasting disease. *EMBO J* **19**, 4425-4430.

Re, F., Sesana, S., Barbiroli, A., Bonomi, F., Cazzaniga, E., Lonati, E., Bulbarelli, A. & Masserini, M. (2008). Prion protein structure is affected by pH-dependent interaction with membranes: a study in a model system. *FEBS Lett* **582**, 215-220.

Redecke, L., von, B. M., Clos, J., Konarev, P. V., Svergun, D. I., Fittschen, U. E., Broekaert, J. A., Bruns, O., Georgieva, D., Mandelkow, E., Genov, N. & Betzel, C. (2007). Structural characterization of beta-sheeted oligomers formed on the pathway of oxidative prion protein aggregation in vitro. *J Struct Biol* **157**, 308-320.

Reed, L. J. & Muench, H. (1938). A simple method of estimating fifty per cent endpoints. *Am J Epidemiol* **27**, 493-497.

Rial, D., Duarte, F. S., Xikota, J. C., Schmitz, A. E., Dafre, A. L., Figueiredo, C. P., Walz, R. & Prediger, R. D. (2009). Cellular prion protein modulates age-related behavioral and neurochemical alterations in mice. *Neuroscience* doi:10.1016/j.neuroscience. 2009.09.005.

Rogers, M., Yehiely, F., Scott, M. & Prusiner, S. B. (1993). Conversion of truncated and elongated prion proteins into the scrapie isoform in cultured cells. *Proc Natl Acad Sci U S A* **90**, 3182-3186.

Ronga, L., Tizzano, B., Palladino, P., Ragone, R., Urso, E., Maffia, M., Ruvo, M., Benedetti, E. & Rossi, F. (2006). The prion protein: Structural features and related toxic peptides. *Chem Biol Drug Des* **68**, 139-147.

Roostaee, A., Cote, S. & Roucou, X. (2009). Aggregation and amyloid fibril formation induced by chemical dimerization of recombinant prion protein in physiological-like conditions. *J Biol Chem* doi:10.1074/jbc.M109.057950.

Ross, C. A., Poirier, M. A., Wanker, E. E. & Amzel, M. (2003). Polyglutamine fibrillogenesis: the pathway unfolds. *Proc Natl Acad Sci U S A* **100**, 1-3.

Rubinsztein, D. C. (2002). Lessons from animal models of Huntington's disease. *Trends Genet* **18**, 202-209.

Saa, P., Castilla, J. & Soto, C. (2006a). Presymptomatic detection of prions in blood. *Science* **313**, 92-94.

Saa, P., Castilla, J. & Soto, C. (2006b). Ultra-efficient replication of infectious prions by automated protein misfolding cyclic amplification. *J Biol Chem* **281**, 35245-52.

Safar, J., Wille, H., Itri, V., Groth, D., Serban, H., Torchia, M., Cohen, F. E. & Prusiner, S. B. (1998). Eight prion strains have PrP(Sc) molecules with different conformations. *Nat Med* **4**, 1157-1165.

Safar, J. G., Lessard, P., Tamguney, G., Freyman, Y., Deering, C., Letessier, F., DeArmond, S. J. & Prusiner, S. B. (2008). Transmission and detection of prions in feces. *J Infect Dis* **198**, 81-89.

Safar, J. G., Kellings, K., Serban, A., Groth, D., Cleaver, J. E., Prusiner, S. B. & Riesner, D. (2005). Search for a prion-specific nucleic acid. *J Virol* **79**, 10796-10806.

Sailer, A., Bueler, H., Fischer, M., Aguzzi, A. & Weissmann, C. (1994). No propagation of prions in mice devoid of PrP. *Cell* **77**, 967-968.

Sakudo, A., Wu, G., Onodera, T. & Ikuta, K. (2008). Octapeptide repeat region of prion protein (PrP) is required at an early stage for production of abnormal prion protein in PrP-deficient neuronal cell line. *Biochem Biophys Res Commun* **365**, 164-169.

Sales, N., Rodolfo, K., Hassig, R., Faucheux, B., Di, G. L. & Moya, K. L. (1998). Cellular prion protein localization in rodent and primate brain. *Eur J Neurosci* **10**, 2464-2471.

Santuccione, A., Sytnyk, V., Leshchyns'ka, I. & Schachner, M. (2005). Prion protein recruits its neuronal receptor NCAM to lipid rafts to activate p59fyn and to enhance neurite outgrowth. *J Cell Biol* **169**, 341-354.

Sato T (2003). Infectious prion disease: CJD with dura mater transplantation. *Rinsho Shinkeigaku* **43**, 870-872.

Scheinin, N. M., Tolvanen, T. K., Wilson, I. A., Arponen, E. M., Nagren, K. A. & Rinne, J. O. (2007). Biodistribution and radiation dosimetry of the amyloid imaging agent 11C-PIB in humans. *J Nucl Med* **48**, 128-133.

Schettler, E., Steinbach, F., Eschenbacher-Kaps, I., Gerst, K., Muessdoerffer, F., Risch, K., Streich, W. J. & Frolich, K. (2006). Surveillance for prion disease in cervids, Germany. *Emerg Infect Dis* **12**, 319-322.

Schiffer, N. W., Broadley, S. A., Hirschberger, T., Tavan, P., Kretzschmar, H. A., Giese, A., Haass, C., Hartl, F. U. & Schmid, B. (2007). Identification of anti-prion compounds as efficient inhibitors of polyglutamine protein aggregation in a zebrafish model. *J Biol Chem* **282**, 9195-9203.

Scott, M. R., Foster, D., Mirenda, C., Serban, D., Coufal, F., Walchli, M., Torchia, M., Groth, D., Carlson, G., DeArmond, S. J. & . (1989). Transgenic mice expressing hamster prion protein produce species-specific scrapie infectivity and amyloid plaques. *Cell* **59**, 847-857.

Scott, M. R., Groth, D., Tatzelt, J., Torchia, M., Tremblay, P., DeArmond, S. J. & Prusiner, S. B. (1997). Propagation of prion strains through specific conformers of the prion protein. *J Virol* **71**, 9032-9044.

Scott, M. R., Will, R., Ironside, J., Nguyen, H. O., Tremblay, P., DeArmond, S. J. & Prusiner, S. B. (1999). Compelling transgenetic evidence for transmission of bovine spongiform encephalopathy prions to humans. *Proc Natl Acad Sci U S A* **96**, 15137-15142.

Scott, M. D. (2006). Inactivation of prion proteins via covalent grafting with methoxypoly(ethylene glycol). *Medical Hypotheses* **66**, 387-393.

Sehulster, L. M. (2004). Prion inactivation and medical instrument reprocessing: challenges facing healthcare facilities. *Infect Control Hosp Epidemiol* **25**, 276-279.

Seidel, B., Thomzig, A., Buschmann, A., Groschup, M. H., Peters, R., Beekes, M. & Terytze, K. (2007). Scrapie agent (Strain 263K) can transmit disease via the oral route after persistence in soil over years. *PLoS ONE* **2**, e435.

Seuberlich, T., Botteron, C., Benestad, S. L., Brunisholz, H., Wyss, R., Kihm, U., Schwermer, H., Friess, M., Nicolier, A., Heim, D. & Zurbriggen, A. (2007). Atypical scrapie in a Swiss goat and implications for transmissible spongiform encephalopathy surveillance. *J Vet Diagn Invest* **19**, 2-8.

Shinde, A., Kunieda, T., Kinoshita, Y., Wate, R., Nakano, S., Ito, H., Yamada, M., Kitamoto, T., Nakamura, Y., Matsumoto, S. & Kusaka, H. (2009). The first Japanese patient with variant Creutzfeldt-Jakob disease (vCJD). *Neuropathology* doi:10.1111/j.1440-1789.2009.01006.

Shyu, W. C., Lin, S. Z., Chiang, M. F., Ding, D. C., Li, K. W., Chen, S. F., Yang, H. I. & Li, H. (2005). Overexpression of PrPC by adenovirus-mediated gene targeting reduces ischemic injury in a stroke rat model. *J Neurosci* **25**, 8967-8977.

Sigurdson, C. J., Williams, E. S., Miller, M. W., Spraker, T. R., O'Rourke, K. I. & Hoover, E. A. (1999). Oral transmission and early lymphoid tropism of chronic wasting disease PrPres in mule deer fawns (Odocoileus hemionus). *J Gen Virol* **80**, 2757-2764.

Silveira, J. R., Raymond, G. J., Hughson, A. G., Race, R. E., Sim, V. L., Hayes, S. F. & Caughey, B. (2005). The most infectious prion protein particles. *Nature* **437**, 257-261.

Simoneau, S., Rezaei, H., Sales, N., Kaiser-Schulz, G., Lefebvre-Roque, M., Vidal, C., Fournier, J. G., Comte, J., Wopfner, F., Grosclaude, J., Schatzl, H. & Lasmezas, C. I. (2007). In vitro and in vivo neurotoxicity of prion protein oligomers. *PLoS Pathog* **3**, e125.

Smith, A., Letters, S., Lange, A., Perrett, D., McHugh, S. & Bagg, J. (2005). Residual protein levels on reprocessed dental instruments. *J Hosp Infect* **61**, 237-241.

Smith, P. G. & Bradley, R. (2003). Bovine spongiform encephalopathy (BSE) and its epidemiology. *Br Med Bull* **66**, 185-198.

Solassol, J., Arlotto, M. & Lehmann, S. (2004). Detection of prion after decontamination procedures: comparative study of standard Western blot, filter retention and scrapie-cell assay. *Journal of Hospital Infection* **57**, 156-161.

Solforosi, L., Criado, J. R., McGavern, D. B., Wirz, S., Sanchez-Alavez, M., Sugama, S., DeGiorgio, L. A., Volpe, B. T., Wiseman, E., Abalos, G., Masliah, E., Gilden, D., Oldstone, M. B., Conti, B. & Williamson, R. A. (2004). Cross-linking cellular prion protein triggers neuronal apoptosis in vivo. *Science* **303**, 1514-1516.

Somerville, R. A., Birkett, C. R., Farquhar, C. F., Hunter, N., Goldmann, W., Dornan, J., Grover, D., Hennion, R. M., Percy, C., Foster, J. & Jeffrey, M. (1997). Immunodetection of PrPSc in spleens of some scrapie-infected sheep but not BSE-infected cows. *J Gen Virol* **78**, 2389-2396.

Sorgato, M. C. & Bertoli, A. (2006). Physiopathologic implications of the structural and functional domains of the prion protein. *Ital J Biochem* **55**, 222-231.

Spencer, M. D., Knight, R. S. & Will, R. G. (2002). First hundred cases of variant Creutzfeldt-Jakob disease: retrospective case note review of early psychiatric and neurological features. *BMJ* **324**, 1479-1482.

Spraker, T. R., Miller, M. W., Williams, E. S., Getzy, D. M., Adrian, W. J., Schoonveld, G. G., Spowart, R. A., O'Rourke, K. I., Miller, J. M. & Merz, P. A. (1997). Spongiform encephalopathy in free-ranging mule deer (Odocoileus hemionus), white-tailed deer (Odocoileus virginianus) and Rocky Mountain elk (Cervus elaphus nelsoni) in northcentral Colorado. *J Wildl Dis* **33**, 1-6.

Spudich, A., Frigg, R., Kilic, E., Kilic, U., Oesch, B., Raeber, A., Bassetti, C. L. & Hermann, D. M. (2005). Aggravation of ischemic brain injury by prion protein deficiency: role of ERK-1/-2 and STAT-1. *Neurobiol Dis* **20**, 442-449.

Stohr, J., Weinmann, N., Wille, H., Kaimann, T., Nagel-Steger, L., Birkmann, E., Panza, G., Prusiner, S. B., Eigen, M. & Riesner, D. (2008). Mechanisms of prion protein assembly into amyloid. *Proc Natl Acad Sci U S A* **105**, 2409-2414.

Sun, Y., Breydo, L., Makarava, N., Yang, Q., Bocharova, O. V. & Baskakov, I. V. (2007). Site-specific conformational studies of PrP amyloid fibrils revealed two cooperative folding domains within amyloid structure. *J Biol Chem* **282**, 9090-7.

Sun, Y., Makarava, N., Lee, C. I., Laksanalamai, P., Robb, F. T. & Baskakov, I. V. (2008). Conformational stability of PrP amyloid fibrils controls their smallest possible fragment size. *J Mol Biol* **376**, 1155-1167.

Tagliavini, F., Prelli, F., Verga, L., Giaccone, G., Sarma, R., Gorevic, P., Ghetti, B., Passerini, F., Ghibaudi, E., Forloni, G. & . (1993). Synthetic peptides homologous to prion protein residues 106-147 form amyloid-like fibrils in vitro. *Proc Natl Acad Sci U S A* **90**, 9678-9682.

Tanaka, M., Collins, S. R., Toyama, B. H. & Weissman, J. S. (2006). The physical basis of how prion conformations determine strain phenotypes. *Nature* **442**, 585-9.

Taraboulos, A., Raeber, A. J., Borchelt, D. R., Serban, D. & Prusiner, S. B. (1992). Synthesis and trafficking of prion proteins in cultured cells. *Mol Biol Cell* **3**, 851-863.

Taraboulos, A., Scott, M., Semenov, A., Avrahami, D., Laszlo, L., Prusiner, S. B. & Avraham, D. (1995). Cholesterol depletion and modification of COOH-terminal targeting sequence of the prion protein inhibit formation of the scrapie isoform. *J Cell Biol* **129**, 121-132.

Taraboulos, A., Serban, D. & Prusiner, S. B. (1990). Scrapie prion proteins accumulate in the cytoplasm of persistently infected cultured cells. *J Cell Biol* **110**, 2117-2132.

Taylor, D. M. (2000). Inactivation of transmissible degenerative encephalopathy agents: A review. *Vet J* **159**, 10-17.

Taylor, D. M. (2004). Practical aspects of decontamination of the unconventional transmissible agents that cause sporadic and variant Creutzfeldt-Jakob disease and other similar human diseases. *Ig Sanita Pubbl* **60**, 141-150.

Taylor, D. M., Woodgate, S. J., Fleetwood, A. J. & Cawthorne, R. J. G. (1997). Effect of rendering procedures on the scrapie agent. *Vet Rec* **141**, 643-649.

Taylor, D. M., Woodgate, S. L. & Atkinson, M. J. (1995). Inactivation of the bovine spongiform encephalopathy agent by rendering procedures. *Vet Rec* **137**, 605-610.

Taylor, D. R. & Hooper, N. M. (2006). The prion protein and lipid rafts (Review). *Mol Membr Biol* **23**, 89-99.

Taylor, D. R., Watt, N. T., Perera, W. S. & Hooper, N. M. (2005). Assigning functions to distinct regions of the N-terminus of the prion protein that are involved in its copper-stimulated, clathrin-dependent endocytosis. *J Cell Sci* **118**, 5141-5153.

Telling, G. C., Haga, T., Torchia, M., Tremblay, P., DeArmond, S. J. & Prusiner, S. B. (1996). Interactions between wild-type and mutant prion proteins modulate neurodegeneration in transgenic mice. *Genes Dev* **10**, 1736-1750.

Telling, G. C., Scott, M., Mastrianni, J., Gabizon, R., Torchia, M., Cohen, F. E., DeArmond, S. J. & Prusiner, S. B. (1995). Prion propagation in mice expressing human and chimeric PrP transgenes implicates the interaction of cellular PrP with another protein. *Cell* **83**, 79-90.

Terry, L. A., Marsh, S., Ryder, S. J., Hawkins, S. A., Wells, G. A. & Spencer, Y. I. (2003). Detection of disease-specific PrP in the distal ileum of cattle exposed orally to the agent of bovine spongiform encephalopathy. *Vet Rec* **152**, 387-392.

Terry, L. A., Howells, L., Hawthorn, J., Edwards, J. C., Moore, S. J., Bellworthy, S. J., Simmons, H., Lizano, S., Estey, L., Leathers, V. & Everest, S. J. (2009). Detection of PrPsc in blood from sheep infected with scrapie and bovine spongiform encephalopathy. *J Virol* doi:0:JVI.00311-09.

Thackray, A. M., Klein, M. A., Aguzzi, A. & Bujdoso, R. (2002). Chronic subclinical prion disease induced by low-dose inoculum. *J Virol* **76**, 2510-2517.

Thadani, V., Penar, P. L., Partington, J., Kalb, R., Janssen, R., Schonberger, L. B., Rabkin, C. S. & Prichard, J. W. (1988). Creutzfeldt-Jakob disease probably acquired from a cadaveric dura mater graft. Case report. *J Neurosurg* **69**, 766-769.

Thirumalai, D., Klimov, D. K. & Dima, R. I. (2003). Emerging ideas on the molecular basis of protein and peptide aggregation. *Curr Opin Struct Biol* **13**, 146-159.

Tizzano, B., Palladino, P., De, C. A., Marasco, D., Rossi, F., Benedetti, E., Pedone, C., Ragone, R. & Ruvo, M. (2005). The human prion protein alpha2 helix: a thermodynamic study of its conformational preferences. *Proteins* **59**, 72-79.

Tobler, I., Gaus, S. E., Deboer, T., Achermann, P., Fischer, M., Rulicke, T., Moser, M., Oesch, B., McBride, P. A. & Manson, J. C. (1996). Altered circadian activity rhythms and sleep in mice devoid of prion protein. *Nature* **380**, 639-642.

Trifilo, M. J., Yajima, T., Gu, Y., Dalton, N., Peterson, K. L., Race, R. E., Meade-White, K., Portis, J. L., Masliah, E., Knowlton, K. U., Chesebro, B. & Oldstone, M. B. (2006). Prion-induced amyloid heart disease with high blood infectivity in transgenic mice. *Science* **313**, 94-97.

Tsutsui, S., Hahn, J. N., Johnson, T. A., Ali, Z. & Jirik, F. R. (2008). Absence of the cellular prion protein exacerbates and prolongs neuroinflammation in experimental autoimmune encephalomyelitis. *Am J Pathol* **173**, 1029-1041.

Turk, E., Teplow, D. B., Hood, L. E. & Prusiner, S. B. (1988). Purification and properties of the cellular and scrapie hamster prion proteins. *Eur J Biochem* **176**, 21-30.

van Keulen, L. J., Vromans, M. E. & van Zijderveld, F. G. (2002). Early and late pathogenesis of natural scrapie infection in sheep. *APMIS* **110**, 23-32.

Vassar, P. S. & Culling, C. F. (1959). Fluorescent stains, with special reference to amyloid and connective tissues. *Arch Pathol* **68**, 487-498.

Vorberg, I., Chan, K. & Priola, S. A. (2001). Deletion of beta-strand and alpha-helix secondary structure in normal prion protein inhibits formation of its protease-resistant isoform. *J Virol* **75**, 10024-10032.

Voropai E.S., Samtsov M.P., Kaplevskii K.N., Maskevich A. A., Stepuro V. I., Povarova O. I., Kuznetsova I. M., Turoverov K. K., Fink A. L. & Uverskii V. N. (2003). Spectral properties of Thioflavin T and its complexes with amyloid fibrils. *J Appl Spectros* **70**, 868-874.

Wadsworth, J. D., Joiner, S., Fox, K., Linehan, J. M., Desbruslais, M., Brandner, S., Asante, E. A. & Collinge, J. (2007). Prion infectivity in variant Creutzfeldt-Jakob disease rectum. *Gut* **56**, 90-94.

Wadsworth, J. D., Joiner, S., Hill, A. F., Campbell, T. A., Desbruslais, M., Luthert, P. J. & Collinge, J. (2001). Tissue distribution of protease resistant prion protein in variant Creutzfeldt-Jakob disease using a highly sensitive immunoblotting assay. *Lancet* **358**, 171-180.

Wadsworth, J. D., Joiner, S., Linehan, J. M., Asante, E. A., Brandner, S. & Collinge, J. (2008a). The origin of the prion agent of kuru: molecular and biological strain typing. *Philos Trans R Soc Lond B Biol Sci* **363**, 3747-3753.

Wadsworth, J. D., Joiner, S., Linehan, J. M., Desbruslais, M., Fox, K., Cooper, S., Cronier, S., Asante, E. A., Mead, S., Brandner, S., Hill, A. F. & Collinge, J. (2008b). Kuru prions and sporadic Creutzfeldt-Jakob disease prions have equivalent transmission properties in transgenic and wild-type mice. *Proc Natl Acad Sci U S A* **105**, 3885-3890.

Wallis, J. P., Wells, A. W., Matthews, J. N. & Chapman, C. E. (2004). Long-term survival after blood transfusion: a population based study in the North of England. *Transfusion* **44**, 1025-1032.

Walz, R., Amaral, O. B., Rockenbach, I. C., Roesler, R., Izquierdo, I., Cavalheiro, E. A., Martins, V. R. & Brentani, R. R. (1999). Increased sensitivity to seizures in mice lacking cellular prion protein. *Epilepsia* **40**, 1679-1682.

Ward, H. J., Everington, D., Croes, E. A., Alperovitch, A., asnerie-Laupretre, N., Zerr, I., Poser, S. & van Duijn, C. M. (2002). Sporadic Creutzfeldt-Jakob disease and surgery: a case-control study using community controls. *Neurology* **59**, 543-548.

Ward, H. J. & Knight, R. S. (2008). Surgery and risk of sporadic Creutzfeldt-Jakob disease. *Neuroepidemiology* **31**, 241-242.

Watarai, M., Kim, S., Erdenebaatar, J., Makino, S., Horiuchi, M., Shirahata, T., Sakaguchi, S. & Katamine, S. (2003). Cellular prion protein promotes Brucella infection into macrophages. *J Exp Med* **198**, 5-17.

Watzlawik, J., Skora, L., Frense, D., Griesinger, C., Zweckstetter, M., Schulz-Schaeffer, W. J. & Kramer, M. L. (2006). Prion protein Helix1 promotes aggregation but is not converted into beta-sheet. *J Biol Chem* **281**, 30242-30250.

Webb, T. E., Pal, S., Siddique, D., Heaney, D. C., Linehan, J. M., Wadsworth, J. D., Joiner, S., Beck, J., Wroe, S. J., Stevenson, V., Brandner, S., Mead, S. & Collinge, J. (2008). First report of Creutzfeldt-Jakob disease occurring in 2 siblings unexplained by PRNP mutation. *J Neuropathol Exp Neurol* **67**, 838-841.

Weise, J., Crome, O., Sandau, R., Schulz-Schaeffer, W., Bahr, M. & Zerr, I. (2004). Upregulation of cellular prion protein (PrPc) after focal cerebral ischemia and influence of lesion severity. *Neurosci Lett* **372**, 146-150.

Weise, J., Sandau, R., Schwarting, S., Crome, O., Wrede, A., Schulz-Schaeffer, W., Zerr, I. & Bahr, M. (2006). Deletion of cellular prion protein results in reduced Akt activation, enhanced postischemic caspase-3 activation, and exacerbation of ischemic brain injury. *Stroke* **37**, 1296-1300.

Weissmann, C. (2004). The state of the prion. *Nat Rev Microbiol* **2**, 861-871.

Weissmann, C., Bueler, H., Fischer, M., Sailer, A., Aguzzi, A. & Aguet, M. (1994). PrP-deficient mice are resistant to scrapie. *Ann N Y Acad Sci* **724**, 235-240.

Wells, G. A., Scott, A. C., Johnson, C. T., Gunning, R. F., Hancock, R. D., Jeffrey, M., Dawson, M. & Bradley, R. (1987). A novel progressive spongiform encephalopathy in cattle. *Vet Rec* **121**, 419-420.

Wells, G. A., Spiropoulos, J., Hawkins, S. A. & Ryder, S. J. (2005). Pathogenesis of experimental bovine spongiform encephalopathy: preclinical infectivity in tonsil and observations on the distribution of lingual tonsil in slaughtered cattle. *Vet Rec* **156**, 401-407.

Westergard, L., Christensen, H. M. & Harris, D. A. (2007). The cellular prion protein (PrP(C)): its physiological function and role in disease. *Biochim Biophys Acta* **1772**, 629-644.

Whitfield, J. T., Pako, W. H., Collinge, J. & Alpers, M. P. (2008). Mortuary rites of the South Fore and kuru. *Philos Trans R Soc Lond B Biol Sci* **363**, 3721-3724.

Whittal, R. M., Ball, H. L., Cohen, F. E., Burlingame, A. L., Prusiner, S. B. & Baldwin, M. A. (2000). Copper binding to octarepeat peptides of the prion protein monitored by mass spectrometry. *Protein Sci* **9**, 332-343.

Wientjens, D. P., Davanipour, Z., Hofman, A., Kondo, K., Matthews, W. B., Will, R. G. & van Duijn, C. M. (1996). Risk factors for Creutzfeldt-Jakob disease: a reanalysis of case-control studies. *Neurology* **46**, 1287-1291.

Wildegger, G., Liemann, S. & Glockshuber, R. (1999). Extremely rapid folding of the C-terminal domain of the prion protein without kinetic intermediates. *Nat Struct Biol* **6**, 550-553.

Wilesmith, J. W., Ryan, J. B. & Atkinson, M. J. (1991). Bovine spongiform encephalopathy: epidemiological studies on the origin. *Vet Rec* **128**, 199-203.

Wilesmith, J. W., Wells, G. A., Cranwell, M. P. & Ryan, J. B. (1988). Bovine spongiform encephalopathy: epidemiological studies. *Vet Rec* **123**, 638-644.

Will, R. G. (2003). Acquired prion disease: iatrogenic CJD, variant CJD, kuru. *Br Med Bull* **66**, 255-265.

Will, R. G., Ironside, J. W., Zeidler, M., Cousens, S. N., Estibeiro, K., Alperovitch, A., Poser, S., Pocchiari, M., Hofman, A. & Smith, P. G. (1996). A new variant of Creutzfeldt-Jakob disease in the UK. *Lancet* **347**, 921-925.

Wille, H., Michelitsch, M. D., Guenebaut, V., Supattapone, S., Serban, A., Cohen, F. E., Agard, D. A. & Prusiner, S. B. (2002). Structural studies of the scrapie prion protein by electron crystallography. *Proc Natl Acad Sci U S A* **99**, 3563-3568.

Wong, B. S., Liu, T., Li, R., Pan, T., Petersen, R. B., Smith, M. A., Gambetti, P., Perry, G., Manson, J. C., Brown, D. R. & Sy, M. S. (2001). Increased levels of oxidative stress markers detected in the brains of mice devoid of prion protein. *J Neurochem* **76**, 565-572.

Yan, Z. X., Stitz, L., Heeg, P., Pfaff, E. & Roth, K. (2004). Infectivity of prion protein bound to stainless steel wires: a model for testing decontamination procedures for transmissible spongiform encephalopathies. *Infect Control Hosp Epidemiol* **25**, 280-283.

Yao, H. L., Han, J., Gao, J. M., Zhang, J., Zhang, B. Y., Guo, Y. J., Nie, K., Gao, C., Wang, X. F. & Dong, X. P. (2005). Comparative study of the effects of several chemical and physical treatments on the activity of protease resistance and infectivity of scrapie strain 263K. *J Vet Med B Infect Dis Vet Public Health* **52**, 437-443.

Zahn, R., Liu, A., Luhrs, T., Riek, R., von Schroetter, C., Lopez Garcia, F., Billeter, M., Calzolai, L., Wider, G. & Wuthrich, K. (2000). NMR solution structure of the human prion protein. *PNAS* **97**, 145-150.

Zanusso, G., Farinazzo, A., Prelli, F., Fiorini, M., Gelati, M., Ferrari, S., Righetti, P. G., Rizzuto, N., Frangione, B. & Monaco, S. (2004). Identification of distinct N-terminal truncated forms of prion protein in different Creutzfeldt-Jakob Disease subtypes. *J Biol Chem* **279**, 38936-38942.

Zeitlin, S., Liu, J. P., Chapman, D. L., Papaioannou, V. E. & Efstratiadis, A. (1995). Increased apoptosis and early embryonic lethality in mice nullizygous for the Huntington's disease gene homologue. *Nat Genet* **11**, 155-163.

Zerr, I., Brandel, J. P., Masullo, C., Wientjens, D., de, S. R., Zeidler, M., Granieri, E., Sampaolo, S., van, D. C., asnerie-Laupretre, N., Will, R. & Poser, S. (2000). European surveillance on Creutzfeldt-Jakob disease: a case-control study for medical risk factors. *J Clin Epidemiol* **53**, 747-754.

Zhang, C. C., Steele, A. D., Lindquist, S. & Lodish, H. F. (2006). Prion protein is expressed on long-term repopulating hematopoietic stem cells and is important for their self-renewal. *PNAS* **103**, 2184-2189.

Zidar, J., Pirc, E. T., Hodoscek, M. & Bukovec, P. (2008). Copper(II) ion binding to cellular prion protein. *J Chem Inf Model* **48**, 283-287.

Zobeley E., Flechsig E., Cozzio A., Enari M., & Weissmann C. (1999). Infectivity of scrapie prions bound to a stainless steel surface. *Mol Med* **5**, 240-243.

PUBLISHED REPORTS AND BOOKS

Department of Health: NHS Estates (2001). A review of the decontamination of surgical instruments in the NHS in England.

Department of Health. (2003). "Assessment to be carried out before surgery and/or endoscopy to identify patients with, or at an increased risk of, CJD or vCJD" (Annex J of ACDP TSE Working Group guidance)

Health Protection Agency. (2007). Health Protection Agency: Weekly Report. **1** (50)

Health Technical Memorandum (HTM) 2030 (1997). Washer-disinfectors. Validation and verification.

Khammo N. & McDonnell, G. (2006). Trouble shooting problems associated with cleaning, disinfection and sterilisation of medical devices. IDSC: Official Reference Book, 115-26

Medical Research Council. (2006). UK strategy for research and development on human and animal health aspects of transmissible spongiform encephalopathies 2005-2008.

NHS (2006) "Patient safety and reduction of the risk of transmission of Creutzfeldt-Jakob disease (CJD) via interventional procedures".

SEAC (2005). SEAC minutes of 86th meeting.

World Health Organization (2006). WHO guidelines on tissue infectivity distribution in transmissible spongiform encephalopathies.

WEBPAGES

www.cjd.ed.ac.uk/figures

www.hpa.org.uk.vCJDpresurgicalassessment

www.oie.int/eng/info/en_esbru

APPENDIX A

OVERVIEW OF THE ROUTES OF SYSNTHESIS AND CHEMICAL STRUCTURES OF THIOFLAVIN T AND BTA-1 ANALOGUES

Two general routes of synthesis were utilized in this study. The choice of method was influenced by the availability of starting materials and the desired final product. The first of these is shown in Figure 43 and the resultant products shown in Table 12.

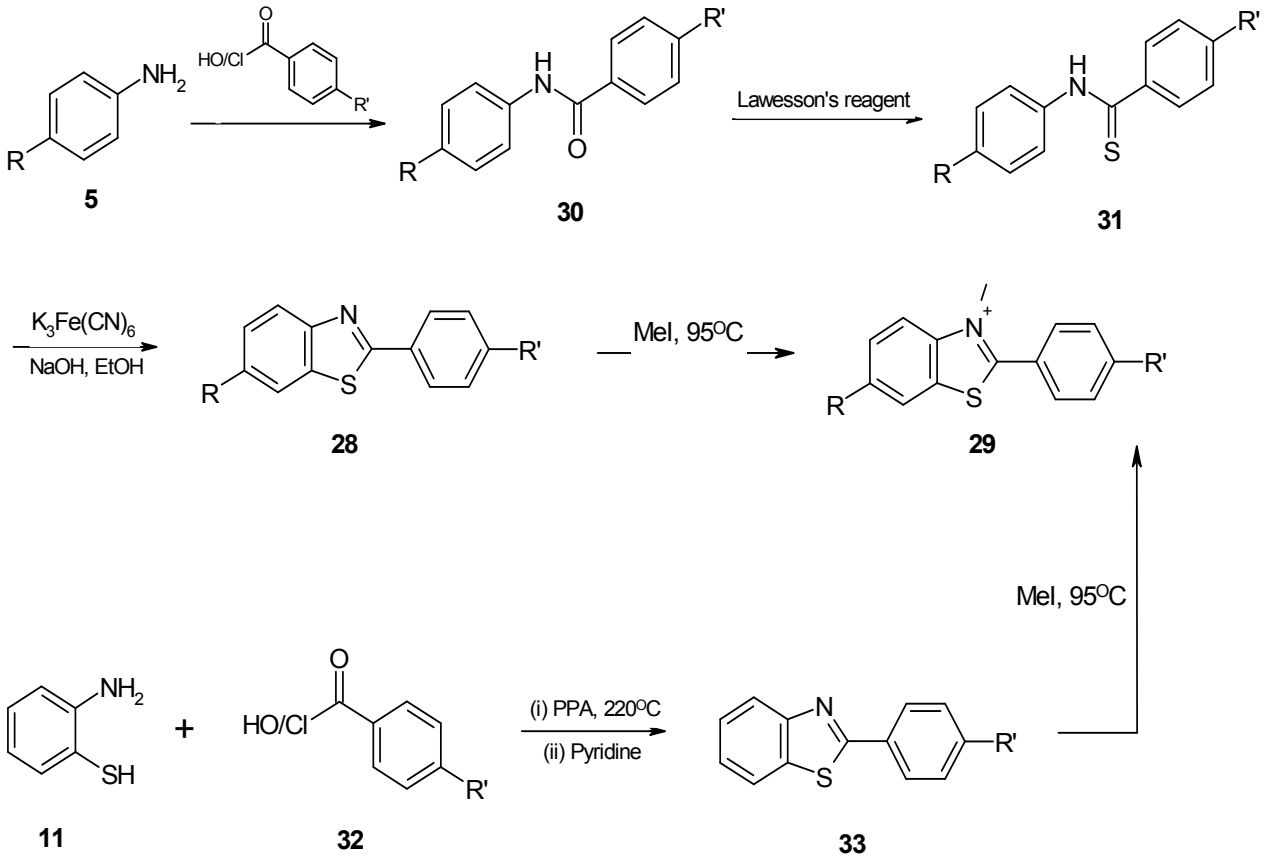

Figure 43 Route utilised in the synthesis of thiazole analogues

Table 13 Melting point and yield for thiazole analogues and several intermediary precursors synthesised by the route described in Figure 43.

Compound	R	R'	Melting point (°C)	Yield (%)
30a [α]	CH_3	$N(CH_3)_2$	152-153	84
30b [α]	CH_3	OCH_3	142-146	68
30c [α]	CH_3	Br	-	89
30d [α]	OCH_3	$N(CH_3)_2$	178-179	66
31a [β]	CH_3	$N(CH_3)_2$	-	38
31b [γ]	CH_3	OCH_3	-	77
31c [δ]	CH_3	Br	180-185	90
31d [δ]	OCH_3	$N(CH_3)_2$	-	87
28a [α]	CH_3	$N(CH_3)_2$	202-204	82
28b [α]	CH_3	OCH_3	161-165	68
28c [α]	CH_3	Br	194-197	63
28d [α]	OCH_3	$N(CH_3)_2$	168-171	46
33a [α]	H	$N(CH_3)_2$	170-172	75
33b [α]	H	OCH_3	100-102	62
33c [α]	H	Br	110-113	51
33d [α]	Br	H	110-113	56
29b [ε]	CH_3	OCH_3	207-208	76
29c [ε]	CH_3	Br	212-213	37
29d [ε]	OCH_3	$N(CH_3)_2$	179-180	29
29e [ε]	H	$N(CH_3)_2$	+250	78
29f [ε]	H	OCH_3	186-189	68
29g [ε]	H	Br	204-207	27
29h [ε]	Br	H	204-207	35

α = recrystallised from hot MeOH.; β = columned in EtoAc/Hex (30%).; γ = pure product precipitated from solution.; δ = product precipitated from solution.; ε = recrystallised from hot $CHCl_3$.

In addition, the synthesis of a series of compounds was performed by an alternative route using the method demonstrated in Figure 44 and the products are listed in Table 13. Here, the chain between the second and third aromatic ring was varied, introducing a variety of chemical groups.

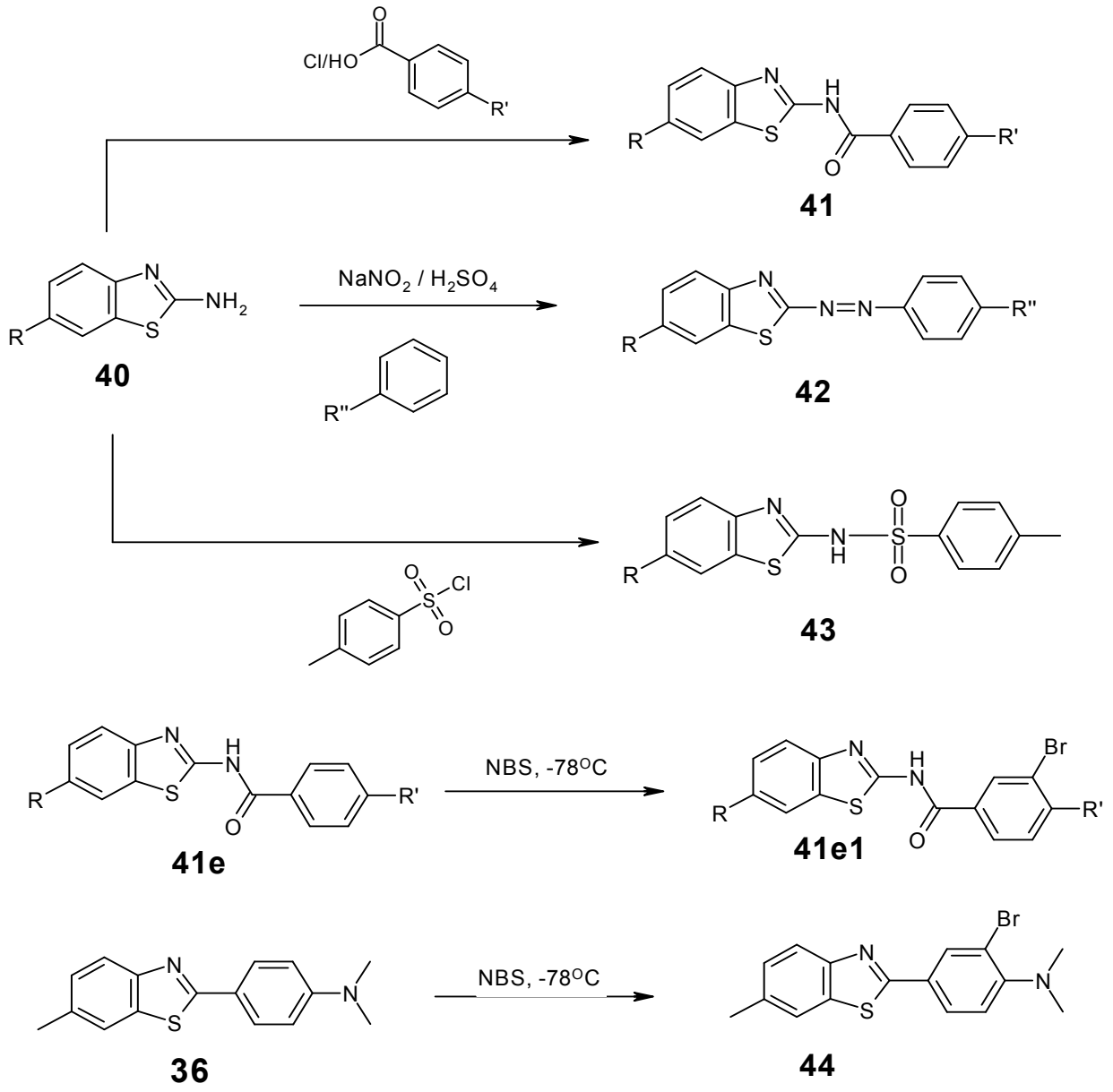

Figure 44 An additional route for the synthesis of a series of thiazole analogues

Table 14 Compound and corresponding melting points of thiazole analogues and intermediary precursors synthesised by the route described in Figure 44.

Compound	R	R'	R''	Melting point (^{o}C)
41a	CH_3	$N(CH_3)_2$	H	182-188
41b	CH_3	Br	H	+250
41c	$O(CH_3)$	$N(CH_3)_2$	H	186-193
41d	H	$N(CH_3)_2$	H	207-208
41e	CH_3	$N(CH_3)_2$	Br	160-167
41f	H	Br	H	227-230
41g	H	OCH_3	H	156-160
41h	-	-	-	128
41i	CH_3	OCH_3	H	206-210
42a	H	$N(CH_3)_2$	H	-
42b	CH_3	NH_2	H	+250
42c	OCH_3	$N(CH_3)_2$	H	207-208
42d	H	40	H	118-120
43	CH_3	$S(O)_2Ph$	H	+250
44	CH_3	$N(CH_3)_2$	Br	121-122

All reactions proceeded as predicted with the exception of one which generated an unexpected compound. The coupling of 40 (see Figure 44) to dimethyamino benzoic acid using benzotriazol-1-yl-oxytripyrrolidinophosphonium hexafluorophosphate (PyBOP) as a coupling reagent resulted in the synthesis of 41h possibly due to the strong affinity between the two compounds (Figure 45).

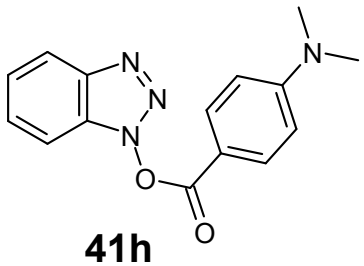

41h

Figure 45 Product from attempted coupling of dimethylamino benzoic acid and amino benzothiazole using PyBOP.

APPENDIX B

Journal of Infection Prevention

http://bji.sagepub.com

Acquisition of proteinaceous contamination through the handling of surgical instruments by hospital staff in sterile service departments

RP Howlin, J. Harrison, T. Secker and CW Keevil

Journal of Infection Prevention 2009; 10; 106
DOI: 10.1177/1757177409105073

The online version of this article can be found at:
http://bji.sagepub.com/cgi/content/abstract/10/3/106

Published by:
SAGE
http://www.sagepublications.com

On behalf of:
BJIC
Infection Prevention Society

Additional services and information for *Journal of Infection Prevention* can be found at:

Email Alerts: http://bji.sagepub.com/cgi/alerts

Subscriptions: http://bji.sagepub.com/subscriptions

Reprints: http://www.sagepub.com/journalsReprints.nav

Permissions: http://www.sagepub.co.uk/journalsPermissions.nav

Citations http://bji.sagepub.com/cgi/content/refs/10/3/106

Downloaded from http://bji.sagepub.com at University of Southampton on May 14, 2009

JIP

Acquisition of proteinaceous contamination through the handling of surgical instruments by hospital staff in sterile service departments

Howlin RP[1*], Harrison J[2], Secker T[1], Keevil CW[1]

1. Environmental Healthcare Unit, School of Biological Sciences, University of Southampton, UK. Email: rph@soton.ac.uk
2. Basingstoke & North Hampshire Hospital, Aldermaston Road, Basingstoke, UK.
*Corresponding author

Accepted for publication: 19 February 2009
Key words: Decontamination, sterile service departments, surgical instruments, episcopic differential interference contrast/epi-fluorescence microscopy, SYPRO Ruby

Abstract

Using Episcopic Differential Interference Contrast (EDIC) microscopy, this study has investigated the potential reapplication of proteinaceous contamination onto surgical instruments following a washer-disinfector cycle through the handling of staff within the clean room. The deposition of 0.51 ng/mm^2 of protein onto surgical grade stainless steel by one finger print alone has been demonstrated. Moreover, using a previously described contamination index, a 5 to 10-fold increase in protein present on surgical instruments was noted following handling by clean-room staff under current departmental practices, relative to instruments handled by staff wearing gloves. While unlikely to pose a direct risk to patient health, subsequent sterilisation will fix protein to an instrument surface thereby decreasing the effectiveness of further decontamination cycles. Current guidelines make no recommendations surrounding the use of gloves by staff working within the clean room. However it is clear that this matter must be reviewed to limit the unnecessary transference of protein to surgical instruments.

Introduction

The effective implementation of decontamination procedures within sterile service departments (SSDs) is crucial in order to render reuseable surgical instruments safe for both patients and hospital staff. The build up of organic material such as tissue and bodily fluids through inefficient instrument reprocessing can decrease the effectiveness of subsequent disinfection and sterilisation procedures (Ransjo et al, 2001). Other solutions such as iodine and saline can also discolour and corrode stainless steel if allowed to dry for any length of time (Khammo and McDonnell, 2006).

The inherent risks to a patient's health during surgical procedures increase when preceded by poor and/or ineffective decontamination processes. Bloodborne pathogens such as the hepatitis B virus (HBV) represent a particular concern for both medical and dental practices (Lowe et al, 2002). The risk of iatrogenic transmission of the variant form of Creutzfeldt-Jakob disease (vCJD) via neurosurgical procedures creates further problems for SSDs because of the resistance of the causative prion protein to standard sterilisation methods (Gibbs Jr et al, 1994). Arguably, the threat of iatrogenic CJD has, in several ways, been beneficial to SSDs in the United Kingdom. Concerns surrounding the theoretical transmission of vCJD to patients resulted in a commissioned report from the Department of Health highlighting areas of improvement in decontamination standards, and a subsequent £200 million investment from the UK government to improve facilities and standards (NHS Estates, 2001). However, several subsequent studies have once again raised concerns over the effectiveness of current decontamination procedures and highlighted instances where instruments at the point of use demonstrated considerable residual soiling. In one study, a McIvor gag, Draffin rod and Yankaur sucker displayed 1.028 mg, 1.286 mg and 2.228 mg of extractable protein respectively at the point of instrument use (Murdoch et al, 2006). In a further examination of surgical instruments, large concentrations of in situ proteinaceous contamination (0.42–4.2 µg/mm^2), in addition to general bioburden, were visualised at the ends of diathermy forceps and pencils, instruments routinely used to cauterise vessels or dissect tissues, and general surgical devices (Lipscomb et al, 2006a,b).

Using previously described Episcopic Differential Interference/Epi-fluorescence (EDIC/EF) microscopy (Keevil, 2003; Lipscomb et al, 2006c) we are able to visualise both proteinaceous and non-proteinaceous contaminants in situ without the need for elution of soiling from the instrument surface, which can decrease the sensitivity of detection. Rather, the sensitivity of EDIC/EF microscopy is in fact influenced by the choice of fluorescent stain. SYPRO Ruby is a luminescent metal chelate stain incorporating ruthenium into an organic complex with the capacity to fluorescently label proteins. A previous

Peer reviewed paper

© Infection Prevention Society 2009
SAGE Publications
10.1177/175717740910507

Downloaded from http://jip.sagepub.com at University of Southampton on May 14, 2009

study has demonstrated a detection sensitivity of 0.25–1 ng protein/mm² on polyvinylidene fluoride (PVDF) membranes (Berggren et al, 1999). However, coupled with EDIC/EF microscopy, SYPRO Ruby has been shown to be able to detect levels of <400 pg/mm² of protein on surgical grade stainless steel (Lipscomb et al, 2006c). This technique has led to the proposal and subsequent application of a contamination index able to sensitively and rapidly assess instrument contamination levels as a function of particulate size and area coverage (Lipscomb et al, 2006c; Lipscomb et al, 2008).

In this study we have utilised EDIC/EF microscopy coupled with SYPRO Ruby to further evaluate the effectiveness of SSD decontamination procedures, specifically the risk of unnecessary transference of proteinaceous contamination following cleaning through instrument handling by department staff. The transference of protein by a single finger print onto a PVDF membrane as detected by SYPRO Ruby has been shown previously (Berggren et al, 1999) although this has not subsequently been demonstrated on stainless steel. Importantly, handling of the instruments following a washer-disinfector cycle is performed in a clean room prior to sterilisation, typically in high temperature and pressure autoclaves. As a result, any contamination applied within the clean room is likely to be encrusted onto the instrument due to the sterilisation process and decrease the effectiveness of subsequent decontamination due to the tenacity of the heat-sterilised material to withstand removal.

Methods

Stainless steel tokens

In order to determine the potential for protein transference by hand onto stainless steel, surgical grade 316L stainless steel tokens (25 mm×75 mm; Advanced Alloys Ltd, Eastleigh, UK) were initially cleaned by swabbing in 100% acetone followed by a soak in acetone for 5 min in order to remove grease and lipid deposits. Subsequently, the tokens were rinsed in filtered distilled water for 2×5 min followed by immersion autoclaving in distilled water at 121°C for 20 min. The tokens were allowed to cool at room temperature before drying overnight at 37°C.

Surface contamination

The impact of a single thumb print by a bare hand on proteinaceous contamination was investigated on stainless steel tokens (n=6). Contamination via a single thumb print from a hand wearing standard nitrile laboratory gloves was also assessed (n=6). To compare the amount of protein transferred by one thumb print with that of normal handling and manipulation by bare and gloved hands, tokens (n=6) were each contaminated with 10 thumb prints. Twelve tokens were used as untouched controls. Following staining, 20 random fields of view were imaged from each token and analysed for SYPRO Ruby fluorescently labelled protein.

Staining

Staining was performed as described previously (Lipscomb et al, 2008) by the application of 100% SYPRO Ruby (Invitrogen) for 15 min in the dark. This was followed by three rinses in nanopure water (18.2 MΩ, pH 7) and visualisation using EDIC/EF microscopy (excitation 465–495 nm, DM 505, emission 605–635 nm). Image capture was performed using a CCD camera (Roper Industries, UK) with Image Pro Plus software (MediaCybernetics) for data quantification and analysis.

Surgical instruments

Two new sets of surgical instruments were recovered after 10 surgical procedures and confirmed to possess similarly low levels of proteinaceous contamination. Each set included plain dissecting forceps, scissors angled on flat, hagar dilator, straight mosquito forceps, curved mosquito forceps, and curved dunhill artery forceps. Following a subsequent cleaning cycle in the SSD washer-disinfector unit, staff in the clean room were instructed to handle one instrument set with bare hands as per normal SSD operating procedures carrying out a visual inspection of each instrument. The other instrument set was handled in an identical way by staff wearing standard latex gloves. Each instrument set was then sterilised via high temperature and pressure autoclave treatment and taken for staining.

Analysis was performed using a previously published contamination index which uses an increasing scale from 1–4 taking into account surface coverage as well as particulate height and width to rapidly assess proteinaceous contamination of a surface (Lipscomb et al, 2006c, 2008). Twenty areas displaying representative instrument contamination were photographed from four separate areas of the instrument surface – the handle, arm, joint and tip/blade. In a blind study, using comparative photomicrographs of the contamination index, five volunteers allocated scores accordingly for each of the images. Each of the four areas of each instrument was then given a mean contamination index value. Statistical analysis was carried out using t-tests to compare data means.

Results

Protein contamination by hand

Using a known amount of protein stained with SYPRO Ruby as a standard reference we were able to estimate the amount of protein transferred onto stainless steel through handling (Figure 1). One thumb print was able to transfer 0.51 ng/mm² of protein. Handling, as mimicked by 10 thumb prints to the surface of the token, corresponded to a mean level of proteinaceous contamination of 0.67 ng/mm². Statistical analysis showed that there was no significant difference between the mean amount of protein observed following a single thumb print and handling of the tokens with bare hands ($p=0.24$). Importantly, <0.06 pg/mm² was detected on the surface of the token following a thumb print by a gloved hand. This amount was not statistically different from the amount of protein observed on clean, untouched control tokens ($p=0.195$).

Surgical instruments

Assessment of proteinaceous contamination via the contamination index is displayed for each individual instrument as well as instrument sample regions in Figure 3. Each instrument handled by staff wearing gloves displayed a statistically significant decrease in the mean contamination index score ($p=0.0$ for five of the six instruments, $p=0.012$ for straight mosquito forceps). For five of the instruments analysed, this difference corresponded to an approximate one index score less than corresponding instruments handled with bare hands. Representative photomicrographs of protein deposits taken in situ on the surface demonstrate the increased level of contamination of instruments handled by bare hands (Figure 4). Instruments handled with gloved hands showed much lower amounts of protein contamination, despite the surfaces appearing heavily scarred and pitted due to repeated cleaning cycles. Interestingly, many of the protein deposits visualised on the instruments showed similarities in size and estimated protein amount with those observed on the stainless steel tokens (~15 μm diameter, 9.71 pg±0.8).

Isolation of the contamination index scores by sample region also demonstrates statistically significant differences between the two handling conditions (inside hinge and arm: $p=0.0$, blade/tip and outside hinge: $p=<4\times10^{-7}$). An increase in index score by a factor of one was observed on the outside hinge joint and arm sampling regions of the instrument handled by bare hands. The difference in score was less pronounced from inside the hinge joint and the blade/tip sampling regions, although significant proteinaceous contamination was

Peer reviewed paper

Downloaded from http://ipi.sagepub.com at University of Southampton on May 14, 2009

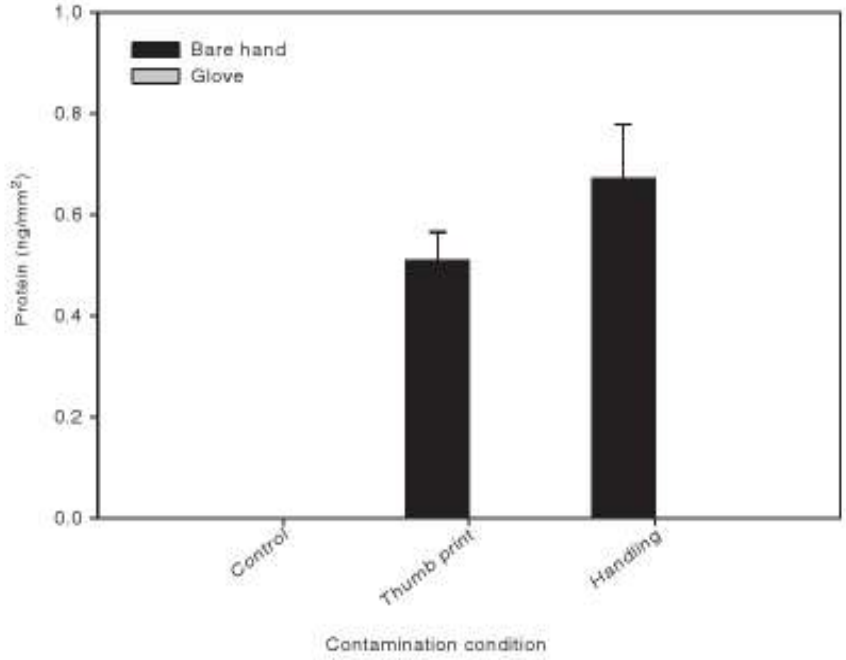

Figure 1. Mean levels of proteinaceous contamination observed on stainless steel tokens following a thumb print and handling by both a bare hand and a gloved hand

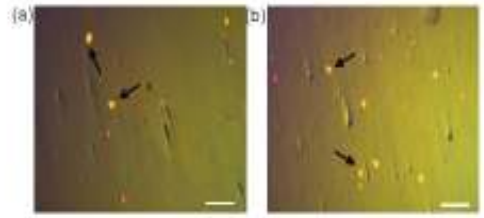

Figure 2. Representative photomicrographs of the surface of stainless steel tokens following contamination with bare hands via: a) single thumb print, and b) handling. Arrows indicate several proteinaceous deposits. Scale bars: 100 µm

observed in these sampling regions relative to instruments handled with gloves.

Discussion

Decontamination is an amalgamation of practices used to render a reuseable item safe for further use for both patients and staff (NHS Estates, 2003). The life-cycle of a surgical instrument begins upon purchase, through both cleaning and disinfection to sterilisation and use. For efficient decontamination, high standards must be set and implemented at all stages of the life-cycle in order to minimise the risk of transmitting infection to a patient during surgical procedures. These high standards must involve the application of effective pre-cleaning procedures, such as the prevention of drying of soil onto instruments, which has been shown to decrease the effectiveness of subsequent cleaning (Upscomb et al, 2007) as well as damage and discolour stainless steel devices (Khammo and McDonnell, 2006). Upon reaching the cleaning stage, it is crucial that an effective washer-disinfector cycle is employed. Failure of a validated washer-disinfector cycle to efficiently remove soiling from the device is likely to be amplified as an instrument ages. Damage and scarring through everyday use creates a surface with a greater resistance to decontamination, and the subsequent build-up of soiling over time is likely to lead to ineffectual sterilisation with a consequent increase in risk to the patient.

Perhaps unsurprisingly, the majority of focus into the effectiveness of SSD practice centres on two main stages of an instrument life-cycle: instrument treatment immediately after use in surgical theatre and the effectiveness of various cleaning chemistries at the removal of general bioburden and pathogens. However the process of handling and cleanliness evaluation within the clean room has the potential to reinstate contamination onto instruments after cleaning if not properly controlled.

As such, we investigated the influence of current clean-room practices in the handling of devices without gloves and the possibility for the transference of protein from hands to stainless steel instruments using EDIC/EF microscopy and SYPRO Ruby, a highly sensitive protein stain. We were able to determine that a single finger print could apply an estimated 0.51 ng/mm^2 of protein to a stainless steel token. This figure did not increase significantly following mimicked handling of the token, whereby 0.67 ng/mm^2 was observed, demonstrating that one finger print can introduce substantial amounts of protein onto stainless steel. Importantly, the use of standard laboratory nitrile gloves resulted in a significant reduction in the amount of protein applied to the token following a thumb print and none following mimicked handling. The former displayed an observed protein amount of less than 0.06 pg/mm^2, which was not statistically significant when compared to untouched controls. This level of protein detection once again displays the increased sensitivity of the EDIC/EF microscopy method with the application of the SYPRO Ruby protein stain when compared with the sensitivity of currently recommended Ninhydrin and Biuret tests for instrument cleanliness (9.25 µg and 6.7 µg protein, respectively) (Upscomb et al, 2006d).

With the application of a previously proposed contamination index, we were able to determine whether handling in the clean room may contribute to observed levels of protein on surgical instruments within current SSD working procedures. Using the contamination index we observed an increase in index by a factor of one on the majority of instruments relative to those handled by staff wearing gloves. This corresponds to an increase in field of view coverage from 1–2% to

Peer reviewed paper

Downloaded from http://ipi.sagepub.com at University of Southampton on May 14, 2009

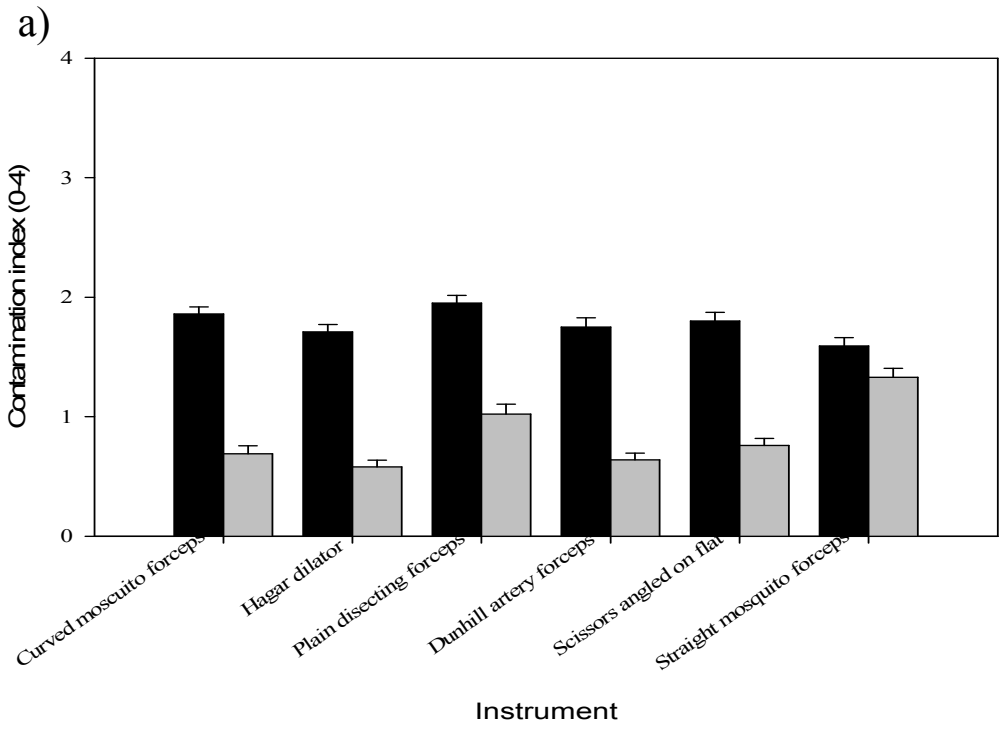

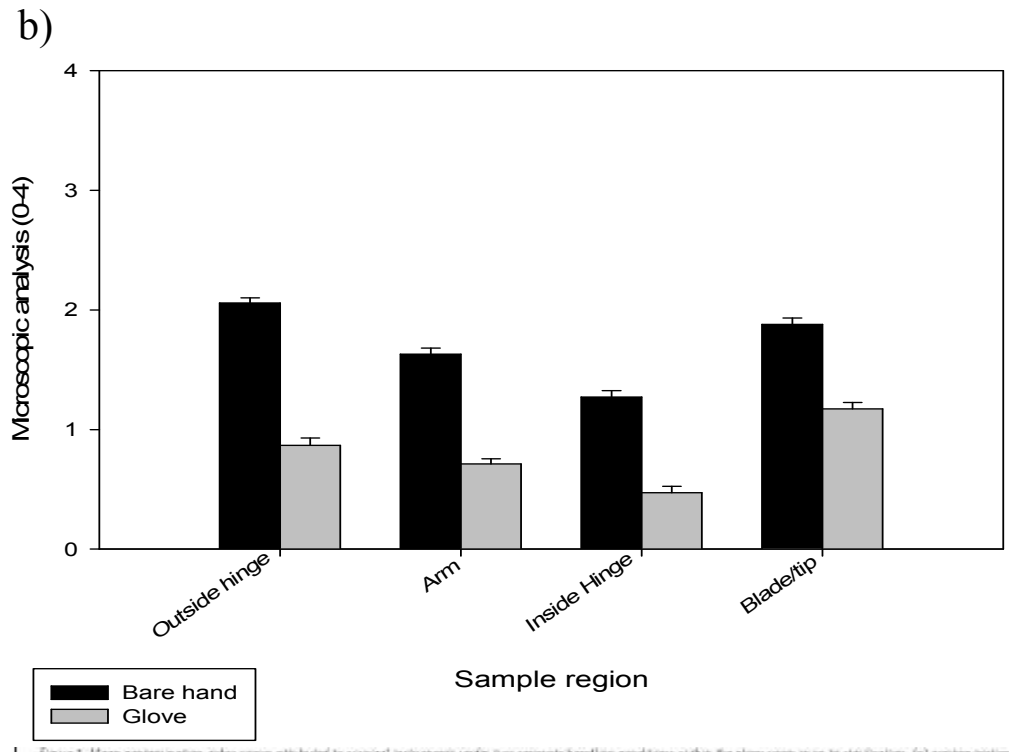

Figure 3. Mean contamination index scores attributed to surgical instruments under two separate handling conditions within the clean room prior to sterilisation. (a) contamination index expressed as variations between instruments within a single set. (b) regional variation of mean contamination index scores for all six instruments.

5–10% following handling with bare hands, representing a 5 to 10-fold increase in proteinaceous contamination.

Microbial flora known to reside on the skin include *Staphylococcus aureus* and *Staphylococcus epidermis*, as well as *Corynebacterium diphtheria* among others (Cogen et al, 2008). However, stringent hand washing procedures and subsequent sterilisation in high heat and pressure autoclaves are likely to negate the risk of bacterial contamination.

Nevertheless, high temperature autoclave procedures identical to those used for sterilisation in SSDs will encrust proteinaceous contamination onto stainless steel. Drying alone at room temperature has been shown to greatly decrease the effectiveness of cleaning (Lipscomb et al, 2007). Assuming that subsequent sterilisation results in the fixation of 100% or 75% of the amount of protein estimated to be transferred by a single finger print, following 50 decontamination cycles,

Peer reviewed paper

Downloaded from http://ipi.sagepub.com at University of Southampton on May 14, 2009

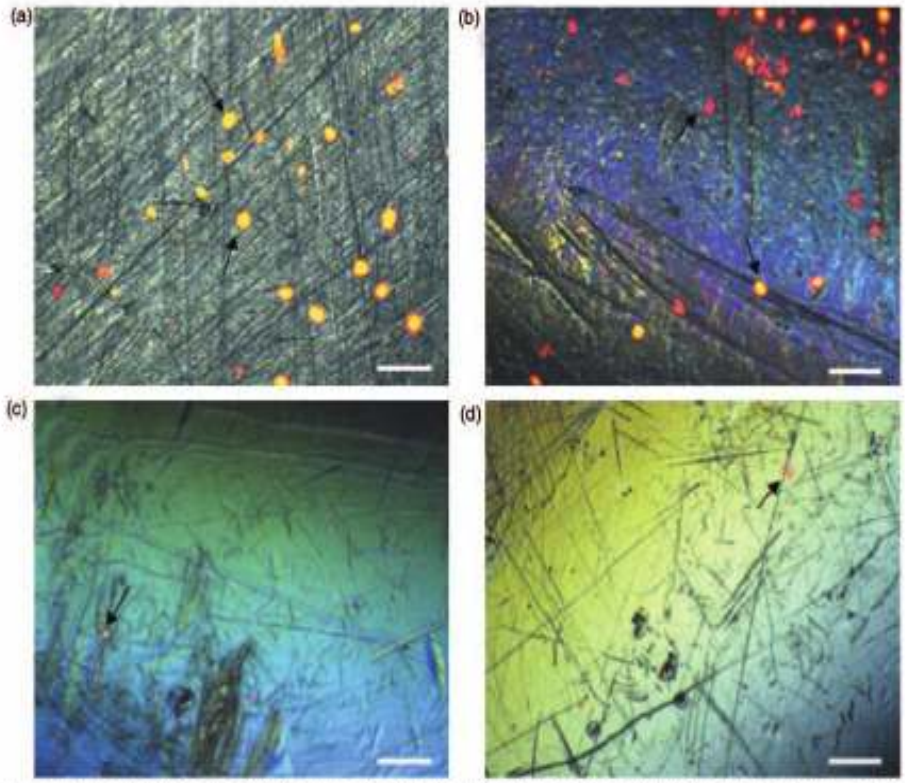

Figure 4 Representative photomicrographs taken using EDI/DIF microscopy of surgical instruments following handling with bare hands: (a) and (b) and gloved hands: (c) and (d) within the clean room prior to sterilisation. Arrows indicate several proteinaceous deposits. Scale bars: 100 µm

25.5–19 ng/mm^2 of protein, respectively, will be present on an instrument as a result of current clean-room handling guidelines. While unlikely to pose a direct risk to patient health, protein acquired via handling over time, in addition to that from ineffective decontamination, will add to the bioburden of an instrument and help to decrease the effectiveness of successive cleaning and sterilisation cycles. This will subsequently increase the risk to patient health over an instrument life-cycle as levels of fixed contamination rise. Current SSD operating guidelines make no recommendations about the handling of instruments, which have already undergone decontamination and cleaning, by staff working within the clean room. This study suggests that these guidelines must be reviewed. The implementation of gloves for use by SSD staff working within the clean room will ensure that the acquisition of soiling following cleaning is significantly reduced.

Acknowledgements

The authors would like to acknowledge the staff at the North Hampshire & Basingstoke hospital sterile service department for their help with this study and J Warner, H Pinchin, B Collin and A Sihota at the Environmental Healthcare Unit, University of Southampton for their contribution with instrument analysis. This work was funded by the Biotechnology and Biological Sciences Research Council (BBSRC: BBS/S/M/2005/12416) and STERIS Ltd.

References

Berggren K, Steinberg TH, Lauber WM, Carroll JA, Lopez MF, Chernokalskaya E, Zieske L, Diwu Z, Haugland RP, Patton WF (1999) A luminescent ruthenium complex for ultrasensitive detection of proteins immobilized on membrane supports. *Analytical Biochemistry* **276(2)**: 129–45.

Cogen AL, Nizet V, Gallo RL (2008) Skin microbiota: a source of disease or defence? *British Journal of Dermatology* **158(3)**: 442–55.

Gibbs Jr CJ, Asher DM, Kobrine A, Amyx HL, Sulima MP, Gajdusek DC (1994) Transmission of Creutzfeldt-Jakob disease to a chimpanzee by electrodes contaminated during neurosurgery. *Journal of Neurology, Neurosurgery and Psychiatry* **57(6)**: 757–8.

Keevil CW (2003) Rapid detection of biofilms and adherent pathogens using scanning confocal laser microscopy and episcopic differential interference contrast microscopy. *Water Science and Technology* **(5)**: 105–18.

Khammo N, McDonnell G (2006) *Trouble shooting problems associated with cleaning, disinfection and sterilisation of medical devices*. IDSc Official Reference Book. Institute of Decontamination Services: Rathgate, 115–26.

Lipscomb IP, Sihota AK, Keevil CW (2006a) Diathermy forceps and pencils: reservoirs for protein and prion contamination? *Journal of Hospital Infection* **64(2)**: 193–4.

Lipscomb IP, Sihota AK, Keevil CW (2006b) Comparative study of surgical instruments from sterile service departments for the presence of residual Gram-negative endotoxin and proteinaceous deposits. *Journal of Clinical Microbiology* **44(10)**: 3728–33.

Lipscomb IP, Sihota AK, Botham M, Harris KL, Keevil CW (2006c) Rapid method for the sensitive detection of protein contamination on surgical instruments. *Journal of Hospital Infection* **62(2)**: 141–8.

Peer reviewed paper

Downloaded from http://ipi.sagepub.com at University of Southampton on May 14, 2009

Peer reviewed paper

Lipscomb IP, Pinchin HE, Collin R, Harris K, Keevil CW. (2006d) The sensitivity of approved Ninhydrin and Biuret tests in the assessment of protein contamination on surgical steel as an aid to prevent iatrogenic prion transmission. *Journal of Hospital Infection* **64(3)**: 288–92.

Lipscomb IP, Pinchin H, Collin R, Keevil CW. (2007) Effect of drying time, ambient temperature and pre-soaks on prion-infected tissue contamination levels on surgical stainless steel: concerns over prolonged transportation of instruments from theatre to central sterile service departments. *Journal of Hospital Infection* **65(1)**: 72–7.

Lipscomb IP, Sihota AK, Keevil CW. (2008) Comparison between visual analysis and microscope assessment of surgical instrument cleanliness from sterile service departments. *Journal of Hospital Infection* **68(1)**: 52–8.

Lowe PH, Bagg J, Burke FJ, MacKenzie D, McHugh S. (2002) A study of blood contamination of Sigveland matrix bands. *British Dental Journal* **192(1)**: 43–5.

Murdoch H, Taylor D, Dickinson J, Walker JT, Perrett D, Raven ND, Sutton JM. (2006) Surface decontamination of surgical instruments: an ongoing dilemma. *Journal of Hospital Infection* **63(4)**: 412–8.

NHS Estates. (2001) *A review of the decontamination of surgical instruments in the NHS in England*. Department of Health: London.

NHS Estates. (2003) *A guide to the decontamination of reusable surgical instruments*. Department of Health: London.

Ransjo U, Engstrom L, Hakansson P, Ledel T, Lindgren L, Lindqvist AL, Marcusson E, Rudback K. (2001) A test for cleaning and disinfection processes in a washer-disinfector. *APMIS* **109(4)**: 299–304.

Downloaded from http://jip.sagepub.com at University of Southampton on May 14, 2009

APPENDIX C

Editorial Manager(tm) for Journal of Hospital Infection
Manuscript Draft

Manuscript Number: JHI-D-09-00429R1

Title: Application of a fluorescent dual stain to assess decontamination of tissue protein and prion amyloid from surgical stainless steel during simulated washer-disinfector cycles

Article Type: Original Article

Corresponding Author: Mr Robert Paul Howlin, BSc Biomedical Sciences

Corresponding Author's Institution: University of Southampton

First Author: Robert Paul Howlin, BSc Biomedical Sciences

Order of Authors: Robert Paul Howlin, BSc Biomedical Sciences; Nancy Khammo, PhD; Thomas Secker, BSc; Gerry McDonnell, PhD; Charles W Keevil, Professor

Manuscript Region of Origin: United Kingdom

Abstract: Current World Health Organisation guidelines pertaining to the reprocessing of surgical instruments in the face of potential iatrogenic transmission of Creutzfeldt-Jakob disease (iCJD) are incompatible for the vast majority of devices. This has led to the advent of a range of new decontamination measures. However, even without the implementation of these new procedures, the incidence of proven iCJD through surgery remains low. In this study, existing decontamination processes in sterile service departments have been evaluated using simulated washer-disinfector cycles on surgical grade stainless steel wires inoculated with ME7 scrapie homogenate. The consequence of varying the soil drying times and choice of cycle pre-treatment on prion removal were evaluated. Assessment of residual contamination at each cycle phase was carried out with the application of a sensitive fluorescent staining procedure to identify both total protein and prion-associated amyloid. The study confirmed that immediate reprocessing following contamination was beneficial during the pre-treatment phase with either an enzymatic and pre-soak wetting agent. However, final total protein levels at the end of the cycles were not significantly different to those where the soil was allowed to dry. In addition, cycles involving a pre-treatment with either an enzymatic cleaner or pre-soak, whether the soil was allowed to dry or not, showed complete removal of detectable prion amyloid. The results suggest that current decontamination procedures, combined with immediate processing of surgical instruments, have the potential to be highly effective alone at reducing the risk of surgical transmission of CJD.

Application of a fluorescent dual stain to assess decontamination of tissue protein and prion amyloid from surgical stainless steel during simulated washer-disinfector cycles

Howlin R.P[1*], *Khammo N*[2], *Secker T*[1], *McDonnell G*[2], *Keevil C.W*[1].

[1]Environmental Healthcare Unit, School of Biological Sciences, University of Southampton, U.K.

[2]STERIS Ltd, Viables, Basingstoke, U.K.

*corresponding author: Environmental Healthcare Unit, School of Biological Sciences, University of Southampton, Bassett Crescent East, Southampton, SO16 7PX, U.K.

Tel. ++44 (0) 2380592034, Fax. ++44 (0) 23594459

email: rph@soton.ac.uk

Running title: Dual stain to assess prion decontamination

SUMMARY

Current World Health Organisation guidelines pertaining to the reprocessing of surgical instruments in the face of potential iatrogenic transmission of Creutzfeldt-Jakob disease (iCJD) are incompatible for the vast majority of devices. This has led to the advent of a range of new decontamination measures. However, even without the implementation of these new procedures, the incidence of proven iCJD through surgery remains low. In this study, existing decontamination processes in sterile service departments have been evaluated using simulated washer-disinfector cycles on surgical grade stainless steel wires inoculated with ME7 scrapie homogenate. The consequence of varying the soil drying times and choice of cycle pre-treatment on prion removal were evaluated. Assessment of residual contamination at each cycle phase was carried out with the application of a sensitive fluorescent staining procedure to identify both total protein and prion-associated amyloid. The study confirmed that immediate reprocessing following contamination was beneficial during the pre-treatment phase with either an enzymatic and pre-soak wetting agent. However, final total protein levels at the end of the cycles were not significantly different to those where the soil was allowed to dry. In addition, cycles involving a pre-treatment with either an enzymatic cleaner or pre-soak, whether the soil was allowed to dry or not, showed complete removal of detectable prion amyloid. The results suggest that current decontamination procedures, combined with immediate processing of surgical instruments, have the potential to be highly effective alone at reducing the risk of surgical transmission of CJD.

Keywords: Amyloid; Decontamination; Iatrogenic CJD; Instruments; Prion.

INTRODUCTION

The nature of the infectious agent in transmissible spongiform encephalopathies (TSEs) creates a significant challenge for decontamination practices. Standard methods for the disinfection of bacteria and viruses, such as germicidal light, glutaraldehyde, formaldehyde and alcohol possess a negligible effect on the inactivation of TSE agents.[1] Furthermore, prion extracts from crude brain tissue of scrapie-infected hamsters can withstand temperatures of up to 600 ºC and remain infective.[2]

Infectivity has been shown to associate avidly with stainless steel with the iatrogenic spread of prions via surgical instruments a proven route of disease transmission.[3-5] Moreover, although the disease targets the central nervous system, studies into the pathophysiology of disease and investigations into the organ distribution of the protease resistant form of the prion protein (PrP^{res}) have identified extraneural deposition in a wide range of tissues in both the variant and sporadic forms of CJD. Among these, PrP^{res} is readily detected in lymphoid tissues including the spleen and tonsil,[6] in addition to rectal tissue,[7] skeletal muscle[8] and blood.[9] Hamster oral tissue preparations have also demonstrated transmissible scrapie.[10] This is coupled with the potential for asymptomatic carriers of disease which has been demonstrated in animal models[11] and clinically in humans[9] with the potential for induction by low-dose inoculum,[12] such as may be encountered in extra-neural surgery.

To reduce transmission of these agents, the World Health Organisation recommends extended steam sterilization and/or chemical treatment involving 1 M sodium hydroxide or 20,000 ppm sodium hypochlorite for the treatment of high-risk re-useable instruments. However, these treatments are incompatible with the majority of surgical instruments,

especially devices containing gum, plastic, joints or electronic components.[13] In addition, efforts to implement single use instruments in non-emergency tonsillectomies and adenoidectomies to manage the risk of iCJD in the UK resulted in an increase in postoperative haemorrhaging to 7.8 – 12 % of patients compared with 1 % observed with reusable instruments.[14,15] However, single use instruments remain in circulation in some UK hospital sterile service departments (SSDs).[16] As such, improved methods of decontamination have been assessed that are compatible for use on re-useable surgical instruments. Several studies have presented significant data for various enzymatic[17] and chemical[18,19] compounds which are able to remove and/or inactivate infectivity from stainless steel surfaces. However, unlike previously published scientific studies, the decontamination of surgical instruments within hospital SSDs is typically an amalgamation of several treatments or chemistries.[20] The potential influence of an individual chemistry on infectivity was demonstrated whereby disease transmission in the animal bioassay was increased following a combined enzymatic and autoclave treatment compared to an autoclave treatment alone.[21] As such, for the assessment of chemistries to be relevant to decontamination practices, they must be analysed within the context of the various pre-cleaning and validated cleaning steps to assure the safety of such practices.

MATERIALS AND METHODS

Contamination of wires

Surgical grade 316L stainless steel wires (Orminston Wire Ltd; 5·0 mm length × 0·16 mm diameter) were cleaned by ultrasonication in a 2 % (v/v) Triton X-100 solution for 15 min. The wires were then treated to three separate 2 min sonications in deionised water followed by immersion autoclaving in deionised water for 20 min at 121 °C and

then dried at 37 °C for 1 h. Six wires were removed using sterilised forceps at this stage to confirm the cleanliness of the surface preparation process.

Female C57BL/6J mice injected with 1 µl of 10 % (w/v) ME7-infected brain homogenate into the dorsal hippocampus were sacrificed between 19 – 21 weeks post-inoculation. The ME7-scrapie strain was selected due to high PrP^{res} accumulation in the CNS of infected C57BL/6J mice and increased resistance to proteolytic degradation relative to other rodent scrapie strains.[22] Wires were contaminated by immersion in either 10 % (w/v) ME7-scrapie brain homogenate, normal brain homogenate (NBH) as negative controls or nanopure water (Thermo Scientific Barnstead NANOpure water purification system) as experimental controls for 1 h at room temperature. Wires were then dried for 16 h at room temperature or immediately subjected to decontamination.

Decontamination

Contaminated wires were subject to simulated decontamination steps under laboratory conditions. Each chemical agent was heated to operating temperature prior to wire exposure. Cycles began with a pre-treatment stage involving either an enzymatic [Klenzyme, STERIS Ltd; 0.8 % (v/v) in deionised water, 5 min at room temperature] or a pre-soak transport gel designed to prevent the soil drying (PRE-Klenz, STERIS Ltd; 5 min at room temperature). As a comparison, a cycle was incorporated which did not involve pre-treatment. The wires were then transferred into deionised water, as a rinse step, at room temperature for 1 min. At this stage, wires (n = 7) were removed and left to dry at room temperature over night. The remaining wires were then immersed in the main wash alkaline detergent [HAMO 100, STERIS Ltd; 0.8 % (v/v), 7 min at 45 °C] and rinsed at 45 °C. Wires (n=7) were removed and left to dry overnight, with the remaining

wires subjected to disinfection at 90 °C in deionised water for 1 min. Each cycle was performed in autoclaved glass vials in a Reactor Station Heat Block (Fisher, UK) with sterile magnetic stirrers to allow for gentle mixing.

Fluorescent microscopy

To fluorescently label and track general tissue protein and prion-associated amyloid removal from the wires, a previously described protocol was used.[23] Briefly, fluorescent detection of prion-associated amyloid was permitted using Thioflavin T, which was then counter-stained with SYPRO Ruby to indiscriminately identify total protein. Using a protein concentration as a standard, quantification of wire-bound protein was determined. As previously described, amyloid concentration was estimated as a function of total protein and Thioflavin T positive signal on ME7 scrapie wires was normalised against non-specific fluorescent signal on corresponding NBH wires.[23] Visualisation was performed using EDIC/EF microscopy.[23]

Western blot analysis

Samples of brain homogenate were added in a ratio of 1:4 to pre-warmed chemistry. Analysis of the pre-soak transport gel was not possible due to the viscosity of the product. Exposure of the enzymatic was carried out at a concentration of 0.8 % (v/v) at room temperature for 5 min. The alkaline detergent was added at 0.4 % (v/v) and 0.8 % (v/v) at 45 °C for 7 min. The samples were then placed on ice to cool followed by centrifugation to pellet. The supernatant was discarded and the pellet resuspended in phosphate buffered saline.

Samples were treated with or without proteinase K (PK) for 1 h at 37°C and loaded onto a 12% (v/v) polyacrylamide gel (Bio-rad; brain homogenate equivalent to 50 µg per well). Following separation, proteins were transferred onto a PVDF membrane and PrP was detected using the mouse monoclonal antibody SAF 60 (1/5000 concentration) raised against hamster PrP codon 142–160. This was followed by addition of a horseradish peroxidase-conjugated anti-mouse IgG secondary antibody (GE Healthcare; 1/5000 concentration) for 1 h. Immunoreactive bands were visualized using enhanced chemiluminescence (ECL, Amersham Biosciences).

RESULTS

The effect of the enzymatic pre-treatment and alkali detergent on naïve PrP, PrP^{res} and its associated protease resistance was determined by Western blot (Figure 1). The enzymatic pre-treatment (which contains proteases) reduced the total detectable protein, however PrP^{res} (indicated by resistance to 200 µg/ml of PK) demonstrated only a small reduction in overall signal relative to untreated controls. Treatment with the alkaline detergent (ingredients including potassium hydroxide) resulted in degradation of PrP^{res} and sensitisation to PK, which was evident under exposure at the lowest concentration (0.4 % v/v).

A dual staining procedure to distinguish general protein contamination and prion-associated amyloid on surfaces was applied to wires following decontamination. Dual stain analysis of non-contaminated control wires confirmed the cleanliness of the surface prior to contamination (data not shown). Analysis of experimental control wires contaminated with nanopure water throughout each cycle phase allowed an overall cut-

off value of 0.001 ng/mm^2 to be established. Consequently, wire-bound contamination below this cut-off was not considered significant and the wires were assessed as clean.

Comparison of variations in pre-treatment and soil drying time were assessed under alkali exposure conditions of 7 min at 0.8 % (v/v) concentration (Figure 2 & 3). Importantly, wires allowed to continue into the disinfection stage of the cycle demonstrated an increase in non-specific background signal in several cycles, as observed in Figure 2a and 2b. Consequently, analysis of residual amyloid levels was performed following alkaline washing. The enzymatic pre-treatment was the most effective in terms of both total protein (Figure 2) and amyloid (Figure 3) removal with a reduction of approximately 2 logs in comparison to the pre-soak under conditions where soil had been allowed to dry. Following immediate processing after contamination, the enzymatic pre-treatment was a further 1 log more efficient at removal of amyloid. In cycles where a pre-soak treatment was used, immediate processing of the wires following contamination resulted in a 2 log and 1 log reduction in total protein and amyloid respectively compared to dried soil wires.

Following alkaline treatment in a cycle beginning with the active enzymatic pre-treatment, total protein and prion-associated amyloid concentrations were reduced below the experimental cut-off value of 0.001 ng/mm^2 irrespective of whether the soil had been allowed to dry or not. Conversely, under either drying condition, residual total protein, as identified by SYPRO Ruby, was detected following alkaline treatment in cycles initiated with either the pre-soak or no pre-treatment with the exception of one cycle (Figure 2b; NBH-contaminated, no pre-treatment wire cohort). However, there was no statistically significant difference in either ME7 or NBH total protein levels following alkaline

cleaning between wires processed immediately or those dried for 16 h prior to decontamination (pre-soak: ME7 P = 0.427, NBH P = 0.268; no pre-treatment: ME7 P = 0.179, NBH P = 0.061 using a T-test to compare data means).

With respect of prion-associated amyloid, alkaline cleaning subsequent to a pre-soak pre-treatment was able to completely remove detectable amyloid from the wires which were immediately processed (Figure 3). Residual prion-associated amyloid following alkaline treatment on wires initially dried for 16 h was not significantly different from the experimental cut-off (P = 0.97). Critically, cycles which did not incorporate a pre-treatment step displayed an estimated 0.03 ng/mm^2 of residual prion amyloid on wires following drying of soil and treatment with the alkaline detergent. Similar to the two other pre-treatment conditions, immediate processing of the wires following contamination resulted in complete removal of prion-associated amyloid through treatment with the alkaline detergent alone.

Importantly, correlation of EDIC/EF detection of prion-associated amyloid (Figure 3) with the Western blot (Figure 1) suggests a relative increase in sensitivity of the staining procedure. Both the Western blot and EDIC/EF detection method were capable of identifying residual PrP^{res} following treatment with the enzymatic pre-treatment. However, PrP^{res} signal by Western blot is almost completely removed following alkaline treatment, in contrast to EDIC/EF detection of prion-associated amyloid (Figure 3; no pre-treatment).

DISCUSSION

The emerging pathophysiology of the infectious agent in prion disease suggests that iatrogenic transmission of CJD via surgical instruments should pose a greater risk to patient health than has currently been documented. Nevertheless, concerns remain over the lack of world-wide accepted methods for prion inactivation and reports persist over possible iatrogenic cases of CJD after neurosurgical procedures.[24] In the UK, for example, there have been 317 documented incidents of potential iatrogenic exposure to CJD from surgery between 1 January 2000 and 30 June 2007 where instruments potentially contaminated with the infectious agent have been subsequently re-used on further patients.[25] However, of these, only 17 incidents were considered to be of serious danger of exposure to CJD with a further 72 considered "at risk".

Utilisation of existing cleaning chemistries used for manual or automated cleaning cycles in this study has confirmed previous reports on the reduced sensitivity of the Western blot technique relative to EDIC/EF combined with Thioflavin T.[23,26] The removal or disruption of antibody binding epitopes, in addition to altered solubility of PrP^{res} following treatment, is likely to account significantly for this loss of sensitivity which procedures such as the EDIC/EF dual stain technique are not affected by. This study represents the first application and critical assessment of the EDIC/EF dual stain method for the evaluation of decontamination procedures for which it was designed. Importantly however, under conditions used to assess decontamination, this study established an experiment cut-off of 0.001 ng/mm^2, 1 log lower than the picogram maximal level of detection previously described.[23,26] Moreover, following heat-treatment, an increase in background fluorescence of negative control wires was observed suggesting limitations of this method under high temperature conditions where protein structural modification

can occur. Both EDIC/EF and Western blot methods were able to confirm residual PrP^{res} following enzymatic exposure. Immunoblotting suggests that the enzymatic treatment had no obvious effect on the structure of PrP^{res}, with the reduction in amyloid observed using Thioflavin T a result of removal from the wires rather than degradation. Previously published *in vivo* data under identical wire preparation and disinfection conditions on the highly proteolytically-stable 263K scrapie strain demonstrated transmission of disease in all rodent test subjects following treatment with the same enzymatic chemistry.[18,27] Both the dual stain and Western blot procedures confirmed the presence of PrP^{res} in solution and bound to stainless steel following treatment with the main-wash alkaline detergent, although at varying sensitivities. However, the immunoblot assay suggests a sensitisation of residual PrP^{res} to protease degradation following treatment. No transmissible disease in the 263K animal model under 7 min exposure at 0.8 % (v/v) was observed in another study.[19] Given the variable proteolytic sensitivity associated with different strains, a direct correlation between the dual stain, Western blot and infectivity is on going and may provide interesting insights into the role of amyloid and PrP^{res} in infectious disease under decontamination conditions.

This study utilised stainless steel wires as a carrier surface. Whilst it is acknowledged that these do not represent the complexity of a surgical instrument, interesting observations on the impact of decontamination cycle conditions were observed. Analysis of simulated decontamination cycles via the EDIC/EF dual stain method suggested that, predictably, the enzymatic chemistry used in this study was the most effective pre-treatment. Importantly, the data indicated that it is during the pre-treatment stage where the effects of soil drying time are most prevalent. The enzymatic pre-treatment tested was 1 log more effective at removal of prion-associated amyloid following immediate processing

relative to dried soil. Moreover, following drying of the soil, addition of the pre-soak transport gel had little effect on protein removal and no significant effect on *in situ* amyloid. This is not surprising as the recommended use of this product is following immediate contamination in order to prevent soil drying. As such, immediate immersion in the pre-soak gel following contamination resulted in a 1 log reduction in amyloid and 2 log in total protein through a water rinse alone.

However, when taken in context of the end product of the entire cycle, soil drying time had no effect on the efficacy of cycles which incorporated pre-treatments. Concentrations of total protein demonstrated no statistically significant difference between drying conditions. Moreover, prion-associated amyloid levels were removed to levels below, or not significantly different from the experimental cut-off. Even in cycles without a pre-treatment, total protein levels were not significantly different between drying conditions. This implies that the subsequent alkaline wash used in this cycle was sufficiently effective to account for an unsuccessful or lack of a pre-treatment in terms of protein removal in all cycles and, with respect to prion-associated amyloid, in those cycles with pre-treatments. This data also highlights the need to assess decontamination in the context of an entire cycle rather than individual treatments.

Critically, it is important to note that cycles with no pre-treatment following drying of the soil were the least effective in terms of amyloid removal. A concentration of 0.03 ng/mm^2 prion-associated amyloid was detected *in situ* on the wires. However, even in the absence of a pre-treatment, immediate processing of the wires following contamination resulted in complete removal of prion-associated amyloid.

This study has, for the first time, assessed prion decontamination techniques within the context of typical reprocessing conditions in an SSD. It has demonstrated that not only the chemistry type but also the various decontamination steps involved can have a profound effect on the overall outcome of instrument decontamination. Moreover, the data also demonstrate that whilst immediate processing was clearly beneficial in all cycles, even with soil drying particular cycles were capable of significant, and in some cases complete, reduction in both total protein and prion-associated amyloid. As a result, current decontamination processes, with validated chemical formulations, combined with prevention of contaminant drying and/or immediate processing, are likely to provide a highly effective safe-guard against iatrogenic transmission of prions.

ACKNOWLEDGEMENTS

The primary antibody was provided Dr E. Comoy, CEA, Fontenay-aux-Roses. Homogenates were provided by Professor V. H. Perry, University of Southampton. This work was funded by the Biotechnology and Biological Sciences Research Council (BBSRC; BBS/S/M/2005/12416) and STERIS Ltd.

REFERENCES

1. McDonnell G, Burke P. The challenge of prion decontamination. *Clin Infect Dis* 2003; **36**:1152-1154.

2. Brown P, Rau EH, Johnson BK, Bacote AE, Gibbs CJ Jr, Gajdusek DC. New studies on the heat resistance of hamster-adapted scrapie agent: threshold survival after ashing at 600 degrees C suggests an inorganic template of replication. *Proc Natl Acad Sci U S A* 2000; **97**: 3418-3421.

3. Flechsig E, Hegyi I, Enari M, Schwarz P, Collinge J, Weissmann C. 2001. Transmission of scrapie by steel-surface-bound prions. Mol Med. 7: 679-684.

4. Bernoulli C, Siegfried J, Baumgartner G *et al*. Danger of accidental person-to-person transmission of Creutzfeldt-Jakob disease by surgery. *Lancet* 1977; **1**: 478-479.

5. Gibbs CJ Jr, Asher DM, Kobrine A, Amyx HL, Sulima MP, Gajdusek DC. Transmission of Creutzfeldt-Jakob disease to a chimpanzee by electrodes contaminated during neurosurgery. *J Neurol Neurosurg Psychiatry* 1994; **57**: 757-758.

6. Bruce ME, McConnell I, Will, RG, Ironside JW. Detection of variant Creutzfeldt-Jakob disease infectivity in extraneural tissues. *Lancet* 2001; **358**: 208-209.

7. Wadsworth JD, Joiner S, Fox K *et al*.. Prion infectivity in variant Creutzfeldt-Jakob disease rectum. *Gut* 2007; **56**: 90-94.

8. Peden AH., Ritchie DL, Head MW, Ironside JW. Detection and Localization of PrP^{sc} in the Skeletal Muscle of Patients with Variant, Iatrogenic, and Sporadic Forms of Creutzfeldt-Jakob Disease. *Am J Pathol* 2006; **168**: 927-935.

9. Peden AH, Head MW, Diane LR, Jeanne EB, James WI. Preclinical vCJD after blood transfusion in a PRNP codon 129 heterozygous patient. *Lancet* 2004; **364**: 527-529.

10. Ingrosso L, Pisani F, Pocchiari M. Transmission of the 263K scrapie strain by the dental route. *J Gen Virol* 1999; **80**: 3043-3047.

11. Race R, Raines A, Raymond GJ, Caughey B, Chesebro B. Long-term subclinical carrier state precedes scrapie replication and adaptation in a resistant species: analogies to bovine spongiform encephalopathy and variant Creutzfeldt-Jakob disease in humans. *J Virol* 2001; **75**: 10106-10112.

12. Thackray AM, Klein MA, Aguzzi A, Bujdoso R. Chronic subclinical prion disease induced by low-dose inoculum. *J Virol* 2002; **76**: 2510-2517.

13. Brown SA, Merritt K, Woods TO, Busick DN. Effects on instruments of the World Health Organization--recommended protocols for decontamination after possible exposure to transmissible spongiform encephalopathy-contaminated tissue. *J Biomed Mater Res B Appl Biomater* 2005; **72**: 186-190.

14. Maheshwar A, De M, Browning ST. Reusable versus disposable instruments in tonsillectomy: a comparative study of outcomes. *Int J Clin Pract* 2003; **57**: 579-583.

15. Nix P. Prions and disposable surgical instruments. *Int J Clin Pract* 2003; **57**: 678-680.

16. Tomkinson A, Phillips P, Scott JB *et al*. A laboratory and clinical evaluation of single-use instruments for tonsil and adenoid surgery. *Clin Otolaryngol* 2005; **30**: 135-42.

17. Jackson GS, McKintosh E, Flechsig E *et al*. An enzyme-detergent method for effective prion decontamination of surgical steel. *J Gen Virol* 2005; **86**: 869-878.

18. Fichet G, Comoy E, Duval C et al. Novel methods for disinfection of prion-contaminated medical devices. *Lancet* 2004; **364**: 521-526.

19. Fichet G, Comoy E, Dehen C *et al*. Investigations of a prion infectivity assay to evaluate methods of decontamination. *J Microbiol Methods* 2007; **70**: 511-518.

20. Khammo N & McDonnell G. Trouble shooting problems associated with cleaning, disinfection and sterilisation of medical devices. *IDSc: Official Reference Book* 2006; 115-126.

21. Yan ZX, Stitz L, Heeg P, Pfaff E, Roth K. Infectivity of prion protein bound to stainless steel wires: a model for testing decontamination procedures for transmissible spongiform encephalopathies. *Infect Control Hosp Epidemiol* 2004; **25**: 280-283.

22. Kuczius T, Groschup MH. Differences in proteinase K resistance and neuronal deposition of abnormal prion proteins characterize bovine spongiform encephalopathy (BSE) and scrapie strains. *Mol Med* 1999; **5**: 406-418.

23. Hervé R, Collin R, Pinchin HE, Secker T, Keevil CW. A rapid dual staining procedure for the quatitative discrimination of prion amyloid from tissues reveals how interactions between amyloid and lipids in tissue homogenates may hinder the detection of prions. *J Microbiol Methods* 2009; **77**: 90-97

24. Keeler N, Schonberger LB, Belay ED, Sehulster L, Turabelidze G, Sejvar JJ. Investigation of a possible iatrogenic case of Creutzfeldt-Jakob disease after a neurosurgical procedure. *Infect Control Hosp Epidemiol* 2006; **27**: 1352-1357.

25. Health Protection Agency. Health Protection Agency: Weekly Report. 2007; **1** (50)

26. Lipscomb IP, Hervé R, Harris K, Pinchin H, Collin R, Keevil CW. Amyloid-specific fluorophores for the rapid, sensitive *in situ* detection of prion contamination on surgical instruments. *J Gen Virol* 2007; **88**: 2619-2626.

27. Fernie K, Steele PJ, Taylor DM, Somerville RA. Comparative studies on the thermostability of five strains of transmissible-spongiform-encephalopathy agent. *Biotechnol Appl Biochem* 2007; **47**: 175-183.

FIGURES

Figure 1

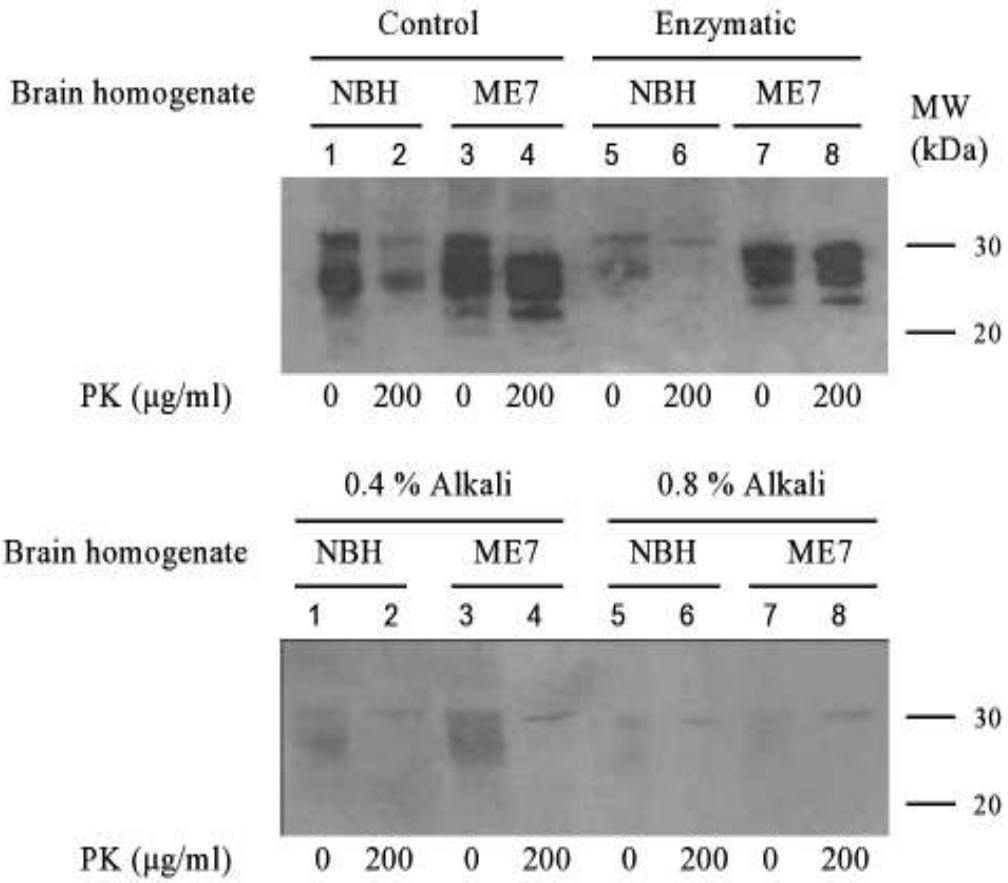

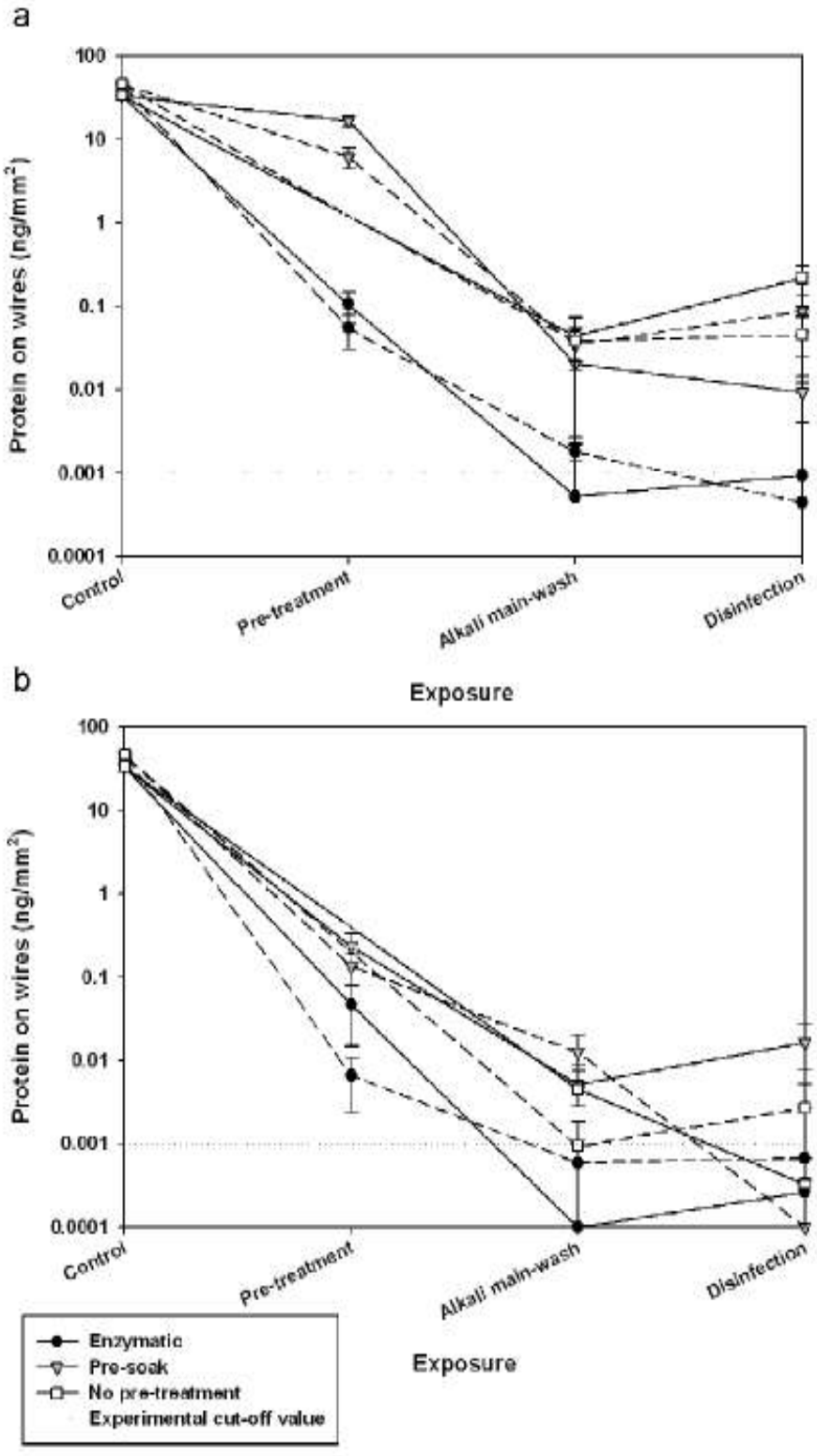

448

449

450 **Figure 3**

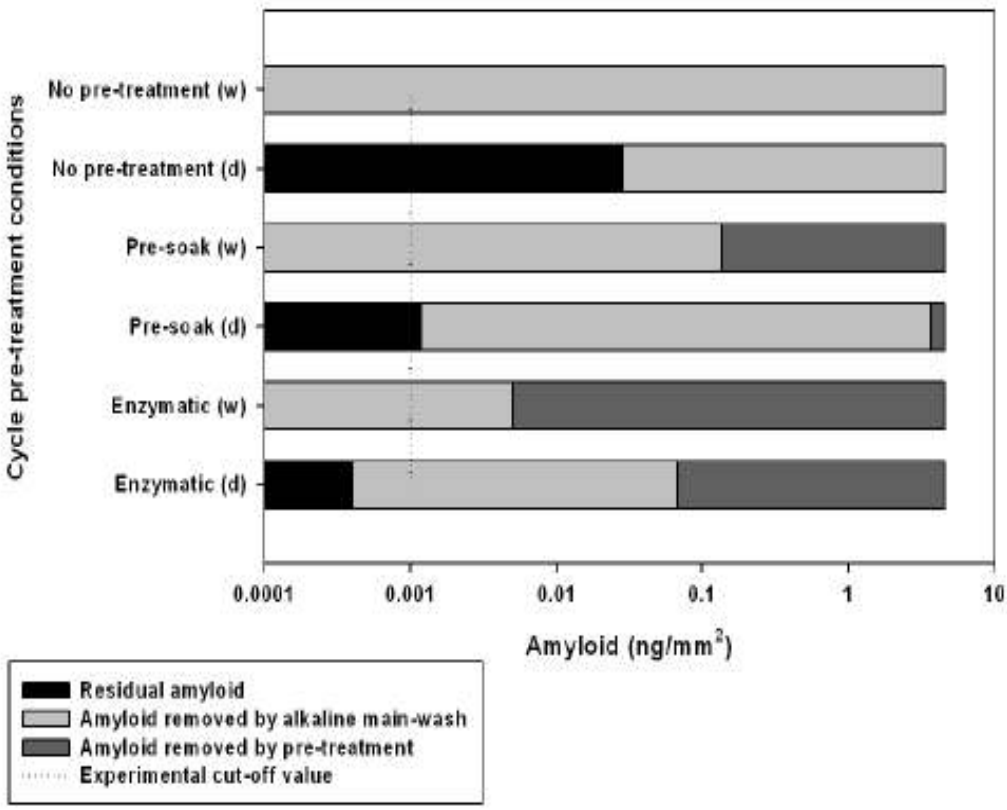

FIGURE LEGENDS

Figure 1 Western blot analysis demonstrating the effectiveness of PrP^{res} degradation. Treatment of NBH and ME7 scrapie brain homogenate was undertaken with an enzymatic pre-treatment or alkaline detergent relative to untreated control homogenate, with and without proteinase K (PK). All lanes correspond to the analysis of 50 µg of brain equivalent.

Figure 2 Tracking of total protein and prion-associated amyloid through typical decontamination cycles with variations in pre-treatment involving either an enzymatic cleaner, a pre-soak or in the absence of any pre-treatment. Exposure of the alkaline detergent was carried out for 7 min at 0.8 % in all cycles. a) Removal of total protein from wires where the soil was allowed to dry for 16 h before decontamination. b) Removal of total protein from wires where decontamination was initiated immediately following contamination. Solid lines represent ME7-scrapie contaminated wires; dashed lines represent NBH contaminated wires.

Figure 3 Mean residual amyloid on wires following different stages of a washer-disinfector cycle where decontamination was carried out following drying of soil for 16 h (d) or immediately post-contamination (w).